



VNIVERSITAT DE VALÈNCIA

DOCTORAL THESIS
Programa de Biomedicina y Biotecnología

Paving the crossroad of biorefinery

Author:
Christian Abendroth

Supervisor:
Dr. Manuel Porcar

*A thesis submitted in fulfillment of the requirements
for the degree of Doctor of Philosophy*

in the

Facultat de Ciències Biològiques
Departament de Bioquímica i Biologia Molecular
Universitat de València

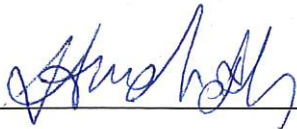
November the 27th, 2017

Declaration of Authorship

I, Christian Abendroth, declare that this thesis entitled, "Paving the crossroad of biorefinery" and the work presented in it are my own. I hereby confirm that:

- This work was done while in candidature for a research degree at this University.
- Where any part of this thesis has previously been submitted for a degree or any other qualification at this University or any other institution, this has been clearly stated.
- Where I have consulted the published work of others, this is always clearly attributed.
- Where I have quoted from the work of others, the source is always given.
- I have acknowledged all main sources of help.
- Where the thesis is based on work done by myself jointly with others, I have made clear exactly what was done by others and what I have contributed myself.

Signed: _____



Date: _____

Valencia, 12/17/17

“Everything is everywhere, but, the environment selects.”

Lourens G.M. Baas Becking

El Dr. MANUEL PORCAR MIRALLES, Investigador contratado Doctor de la Universitat de València (Instituto de Biología Integrativa de Sistemas (I2SysBio), Universitat de València) y la Dra. NURIA PARICIO ORTIZ, Profesora Titular de Genética de la Universitat de València:


AUTORIZAN la presentación de la memoria titulada "Paving the Crossroad of Biorefinery" y CERTIFICAN que los resultados que incluye fueron obtenidos bajo la dirección de Dr. MANUEL PORCAR MIRALLES en el Instituto Cavanilles de Biodiversidad Biología Evolutiva , en el Robert Boyle Institute y en el Instituto de Biología Integrativa de Sistemas (I2SysBio) para CHRISTIAN MATTHIAS ABENDROTH. Y para que conste, firman el siguiente certificado.

Valencia, 8/11/2017
Lugar, Fecha



Dr. Manuel Porcar (Director)

Valencia, 8/11/2017
Lugar, Fecha



Dra. Nuria Paricio Ortiz (Tutora)

Acknowledgements

My experimental work during this thesis was performed in the Biotechnology and Synthetic Biology laboratory of Dr. Manuel Porcar (University of Valencia, Spain), as well as in the Robert Boyle Institute and the company Bio H2 Umwelt GmbH in Jena (Germany). I am very grateful for the patience of all my superiors and for the opportunity to manage my own timetable, which made this international collaboration possible in the first place.

I especially want to thank my thesis director, Dr. Manuel Porcar. Throughout the last four years he always has been open, creative, a supportive mentor and good motivator. He is a great writer and he taught me a great deal in terms of making experimental data suitable for publication. He gave me considerable freedom to develop my own ideas and helped me to realise them. He always had useful suggestions for connecting topics from the different research facilities I was involved in, and he taught me how to successfully build scientific research projects. Finally, he had much valuable advice about how to structure my thesis in several subtopics. He was the best thesis director anyone could wish for.

In this academic context, I also want to thank Dr. Thomas Günther from the Eurofins Company and Dr. Michael Klocke from the Leibniz Institute for Agricultural Engineering and Bioeconomy for their academic

supervision during my time in Germany.

An extraordinary thanks goes to Olaf Luschig. He is truly an expert on the anaerobic digestion-based economy and always motivated me to widen my view on the economic situation of the anaerobic digestion field. Besides this, he taught me all I know about project funding and helped me with the project management that was needed to gain funding for most of the experiments during this thesis. In this context, I also want to thank Christoph Bürger for proofreading research proposals and for his many great ideas for improving them.

Throughout my research, I have benefited from the substantial support of many researchers and employees from the various research facilities and I thank you all, especially Cristina Vilanova, Claudia Simeonov, Kristie Tanner and Sarah Hahnke. You all helped me a great deal with experimental designs, bioinformatics and proofreading and I am very grateful for that.

Finally, I want to thank my family and my friends. You always helped me to overcome difficult times. I am exceptionally grateful to my wife Johana Abendroth. Spending half of my time away from her in Valencia was challenging for both of us. But, still, she always motivated me, supported my dreams and was a very good listener.

Contents

Acknowledgements	vii
Introduction	1
Industrial microbiomes	1
Economic perspectives of anaerobic digestion	2
Microbiomes from anaerobic digestion	3
Robustness of anaerobic microbiomes	4
The role of anaerobic digestion in biorefinery	5
Objectives	11
Chapter 1: Characterisation of biogas-producing facilities in Germany	13
Publication 1	14
Chapter 2: Holistic characterization of two-stage digestion	29
Publication 2	30
Chapter 3: Using robust microorganisms for new industrial approaches	49
Publication 3	50
Publication 4	66
Publication 5	73
Chapter 4: New taxa with foreseeable roles in biorefinery	83
Publication 6	84
Publication 7	87
Publication 8	90
General Results and Discussion	103
Microbial markers to evaluate anaerobic process performance	103
Paving the crossroad of bio-refinery	106
Robustness of methanogenic and acidifying microbiomes	108
Conclusions	117
Resumen en castellano	119
Resumen global de la temática	119
Resultados principales	123
Conclusiones	135
A Original publication reprints	141
B Supplementary material	195
C Metrics	221

List of Figures

1	The central role of anaerobic digestion for biorefinery	1
2	Number of biogas plants in Europe	2
3	The four phases of anaerobic digestion	3
4	Structure of the thesis	6
5	Sampling of anaerobic digesters in Thuringia	16
6	3D plots of chemical parameters from anaerobic digesters in Thuringia	18
7	Bacterial profiles of anaerobic digester plants in Thuringia	19
8	Archaeal profiles of anaerobic digester plants in Thuringia	21
9	Holistic two stage characterization - Overview	33
10	Holistic two stage characterization - Chemical data	34
11	Holistic two stage characterization - Bacterial Community	36
12	Holistic two stage characterization - Archaeal Community	38
13	Holistic two stage characterization - Proteomic profile evolution	39
14	Holistic two stage characterization - Proteomic differences between 37 and 55 °C	40
15	MTC - Schematic drawing	55
16	MTC - Time course of broth and room temperature	58
17	MTC - Typical performance without TE-Power Probe	59
18	MTC - Heat yield due to yeast growth for different MTC configurations	61
19	MTC - Electricity production	62
20	Characterisation of acidification of chicken manure	68
21	Long-term batch digestion of chicken manure at an initial concentration of 10 g/L VS	69
22	Analysis of the gas-production during batch acidification of chicken manure	70
23	Experimental set-up to investigate the influence of heat-shocks on anaerobic microbiomes	75
24	Experimental timeline of heat-shock experiments	76
25	Chemical analysis of heat-shock experiments	78
26	Microbiome composition of heat-shocked samples	79
27	SEM and microbial composition of sauna and dishwasher samples . . .	94
28	Lipolytic activity of strains isolated from sauna and dishwasher samples	96
29	Surface graphs of lypolytic activities of the five selected strains from sauna and dishwasher samples	98
30	Comparison of methanogenic microbiomes at mesophilic temperatures	103
31	Hypothetic methanogenic markers of anaerobic digestion conditions .	104
32	Hypothetic bacterial markers of anaerobic digestion conditions	106
33	Hypothetical industrial flowchart for anaerobic digestion of chicken manure	109
34	Stability of microbiomes from methane-producing digesters against bioaugmentation	111
35	Microbial robustness of high-strength liquor against mild heat-shocks	113
36	<i>El papel central de la digestión anaerobia en la biorrefinería</i>	120

37	<i>Estructura de la presente tesis doctoral</i>	122
38	<i>Comparación de microbiomas metanógenos a temperaturas mesofílicas</i>	123
39	<i>Marcadores metanógenos hipotéticos</i>	125
40	<i>Marcadores bacteriales hipotéticos</i>	126
41	<i>Diagrama de flujo de un proceso hipotético de digestión anaerobia de elevadas concentraciones de estiércol de gallina (EG)</i>	129
42	<i>Estabilidad de los microbiomas de digestores productores de metano</i>	132
43	<i>Robustez microbiana de hidrolizado ante choques térmicos suaves</i>	134

List of Tables

1	Overview of sampled digesters in Thuringia	17
2	Nomenclature used in MTC modelling.	54
3	Chemical characteristics of dried CM (mean \pm standard deviation). . .	68

List of Abbreviations

ABC	Ammonium bicarbonate buffer
ACN	Acrylonitrile
CBM	Carbohydrate-binding domain
CD	Co-digester
CM	Chicken manure
COD	Chemical oxygen demand
CSTR	Continuous stirred tank reactor
DTT	Dithiothreitol
DE	Germany
DMSO	Dimethyl sulfoxide
DNA	Deoxyribonucleic acid
EEG	Erneuerbares Energie Gesetz - German law for renewable energies
FA	Formic acid
g	Gravitational acceleration
GmbH	Gesellschaft mit beschränkter Haftung - Company with limited liability
LB	Leachbed
LC	Liquid chromatography
LTD.	Limited
MS	Mass spectroscopy
MTC	Microbial Thermoelectric Cell
N	Total nitrogen content
PBS	Phosphate-Buffered Saline
PCA	Principal component analysis
PCR	Polymerase chain reaction
PGM	Personal genome machine
PTS	Phosphotransferase system
rDNA	Ribosomal DNA
RT	Room temperature
SS	Sewage sludge
TCA	Trichloroacetic Acid
TFA	Trifluoroacetic acid
TEAB	Triethylammonium bicarbonate buffer
TOC	Total organic carbon
TS	Total solids
TVFA	Total volatile fatty acids
VDI	Association of German Engineers
VS	Volatile solids

Introduction

Industrial microbiomes

Since the beginning of industrialisation in the 18th century mankind opened step by step a window into industrial microbiology. New emerging industries created new microbial niches and many of them were characterized by chemical stress or high temperature. Microorganisms able to degrade industrial pollutants such as biphenyl, organochlorine pesticides, dioxins/furans [1], petroleum [2], organohalide [3] and many more were reported. Some bacteria have even been reported to resist to several harsh conditions at the same time. For example, it has been described that *Acidocella aromatica* is able to uptake the irritant element Vanadium at low pH

levels down to 2 [4]. Such works indicate the very high microbial adaptability, which allows them to grow on hostile places, like solar panels [5], coffee machines [6] or even in places with high radiation like Chernobyl [7].

The ability of microorganisms to grow in extreme environments is especially interesting for applied microbiologists, as those places are promising sources of industrially applicable enzymes and microorganisms [8]. Examples of such potential are a thermostable esterase from the bacterium *Thermus thermophilus* [9], a cold-active and solvent-tolerant lipase from *Stenotrophomonas maltophilia* [10] or a thermoalkalophilic esterase from *Geobacillus* sp. [11].

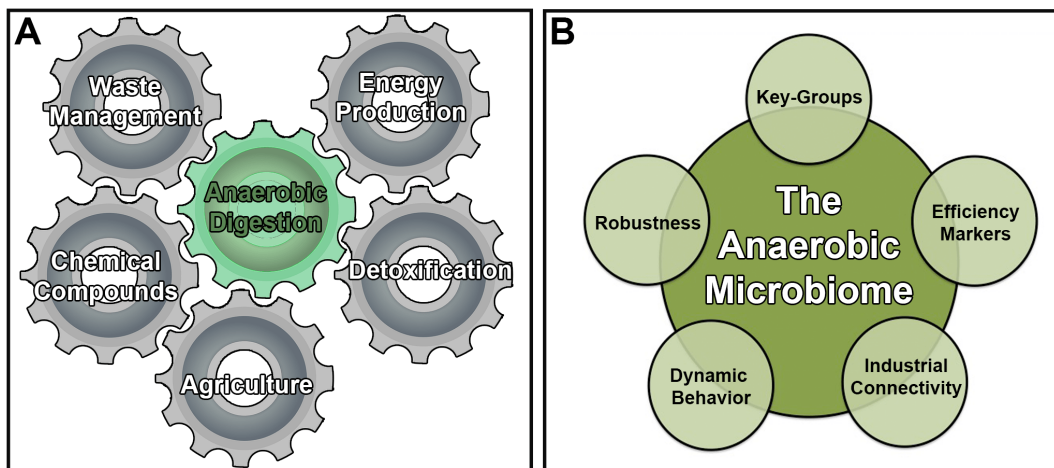


FIGURE 1: The central role of anaerobic digestion for biorefinery: Anaerobic digestion is a multifunctional technology that allows linking of multiple industrial fields (A). The key for this multifunctionality is a highly diverse and robust microbiome and therefore, a better understanding of anaerobic microbiomes is one of the main goals of this thesis (B).

Another industrial habitat that, due to the recent worldwide energy crisis, has become a topic of high interest is anaerobic sludge from water treatment or codigestion. Anaerobic digestion (AD) is a process that leads to methane formation, which in turn can be burnt to produce energy. AD processes are very comprehensive and allow manifold treatments, profitable usage of uncountable waste sources and complex crosslinking with different fields of industry and biorefinery (Fig. 1A). Furthermore, the underlying biocenosis proves to be highly dynamic, robust and is a promising source of new industrially interesting microorganisms. However, the dynamic and robust behaviour of anaerobic digestion processes are not fully understood yet. Therefore, one

of the main goals of this PhD thesis was to shed light on the robustness and dynamic behaviour of microbiomes from anaerobic digestion processes (Fig. 1B).

Economic perspectives of anaerobic digestion

The number of European biogas plants is continuously increasing (Fig. 2) [12]. In 2014, the European Biogas Association (EBA) counted 17,240 biogas plants in Europe. Most of them (10,786) were located in Germany. However, due to recent changes in the German law for renewable energies, the economic situation of the biogas market is very unstable.

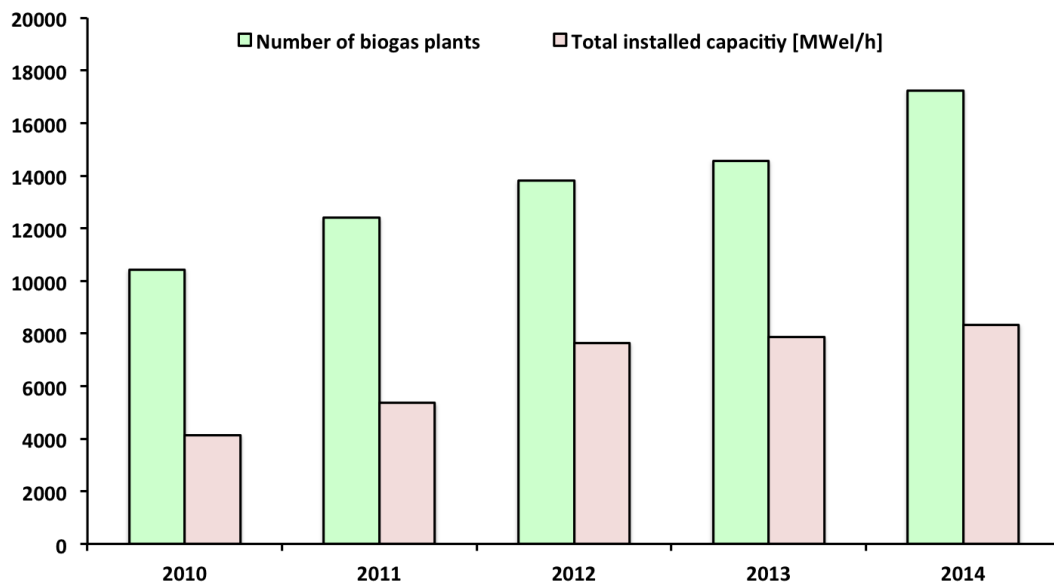


FIGURE 2: “Number of biogas plants and total installed capacity in Europe 2010–2014” [adapted from 12]

Biogas plants that were built before 2014 are protected by a provision, which is made to safeguard existing standards for 20 years. During this time, those plants have important subventions, which allow them to sell each kWh at

prices up to 0.2€.

Biogas plants that were built after 2014 are not protected by this provision. Those plants have to sell their biogas or their generated energy according to the conditions listed in the last version

of the renewable energy law, from 2017, where less profit is granted. In order to stabilize the market situation and to make new digester plants more competitive, improved technology is needed. One way to achieve this relies on a better understanding of anaerobic microbiomes.

Microbiomes from anaerobic digestion

Anaerobic digestion (AD) occurs in four phases: hydrolysis, acidogenesis,

acetogenesis and methanogenesis (Fig. 3). During hydrolysis, degradation of proteins, lipids, carbohydrates and cellulose takes place. Resulting fatty acids, amino acids and sugars are transformed during acidogenesis into volatile fatty acids (VFA) and alcohols, which are eventually degraded to acetate, H_2 and CO_2 , in a process called acetogenesis. Finally, hydrogenotrophic and acetotrophic methanogens use acetate, H_2 and CO_2 for methane formation [13, 14] (Figure 3).

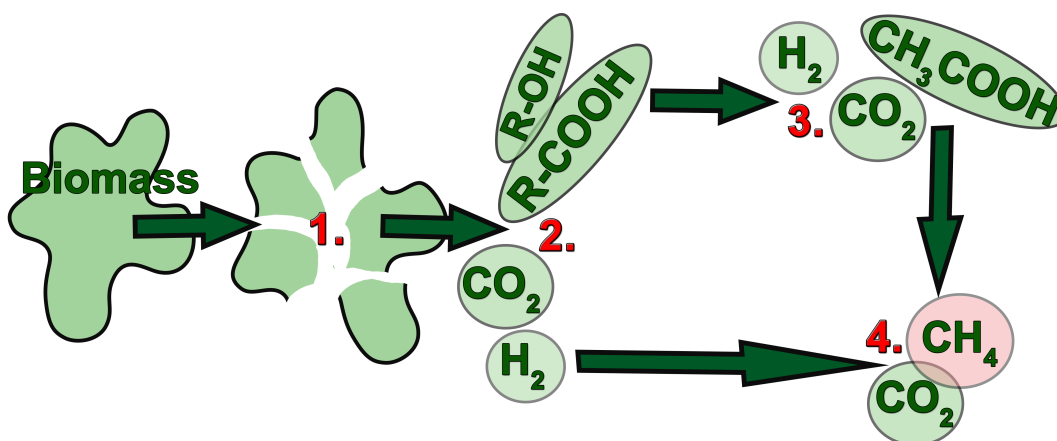


FIGURE 3: The four phases of anaerobic digestion: (1) Biomass is hydrolysed and transformed into smaller molecules (hydrolysis); (2) During acidogenesis, the hydrolysed biomass becomes organic acids, alcohols, hydrogen and carbon dioxide; (3) acetogenesis takes place, where mainly acetic acid, hydrogen and carbon dioxide are formed; (4) Finally, these substances are used for methane formation (methanogenesis).

Research on AD processes has been carried out for more than one century already, since the works from Söhngen (1906)[15] or Coolhas (1928)[16]; however, further work remains to be done to fully understand anaerobic microbiomes, as many involved microorganisms and their specific functions are still unknown. Researchers are still struggling with many details like for example syntrophic acetate oxidation [17, 18] or the influence of certain VFAs on microbial behaviour. To give here

an example: it has been recently shown that compared to propionate, acetate improves phosphorus accumulation into aerobic granular sludge [19]. In general, the microbial diversity in anaerobic digestion is especially high at mesophilic temperatures [20] and new species are discovered regularly from anaerobic sludges [21, 22, 23]. Based on 16S-rRNA gene high-throughput amplicon sequencing, high numbers of unclassified species have been described [24]. The lack of knowledge about

many bacterial species from anaerobic digesters complicates the analysis of microbiomes at lower taxonomic levels. Therefore, studies on bacteria from AD processes are often restricted to the analysis of higher taxonomic levels. This is the case in studies from Goux et al. [25] and Lebhuhn et al. [26], where high abundances of Firmicutes and Bacteroidetes were described. In contrast, the archaeal community of AD processes is much better characterized, as sequences can usually be classified at the genus or even species level [27]. The incomplete knowledge about bacterial communities in AD processes suggests that there is a great potential for the future of biorefinery. In a recent work, over 100 strains of cellulose-degrading bacteria were isolated from an agricultural biogas plant [28]. In another work, a new methanotrophic species belonging to the genus *Methylocaldum*, which might allow effective methanol production, was isolated from digestate [29]. AD sludge is also a promising source for lipase- and protease-producing bacteria. Recently, a novel cold-adapted family VIII esterase was discovered in biogas slurry [30]. Also recently, a new strain of *Bacillus subtilis* (IND19), which allows simultaneous production of carboxy methylcellulose and protease, was discovered in cow dung [31]. Taken together, these works indicate that anaerobic sludge from different AD-processes contains highly diverse microbiomes with tremendous industrial potential, which are worth to be investigated. This is in concordance with other works that already highlighted the importance of anaerobic digestion for biotechnological applications during the 90s [32, 33].

Robustness of anaerobic microbiomes

The robust and dynamic behaviour of AD processes was studied during the 80s. For example, the microbial capability to degrade organic compounds in anaerobic digesters at high salt concentrations was detected in 1988. In that work, it was shown that salt concentrations up to 3–4 M allow acidogenesis, but inhibit methane-producing archaea [34]. AD sludge from such harsh fermentation conditions is an excellent source of biotechnologically relevant strains. For example, in 2013, a thermoactive and salt tolerant α -amylase was isolated from a thermophilic digester plant [35]. It has further been demonstrated that microbiomes from AD processes are able to resist high nitrogen concentrations. Nitrogen is well known for its inhibitory effect, and is abundant in several substrates used in anaerobic digestion. One example is manure from chicken farming. Researchers have been investigating this substrate and its inhibitory effect on microbiomes for several decades [36, 37]. To overcome inhibitory effects caused by high ammonia concentrations, researchers described ammonia-stripping processes [38], but also pointed out that repeated batch-cultures might allow slow adaptation of the underlying sludge biocenosis to high levels of ammonia [39]. For methanisation under high ammonia levels, syntrophic acetate oxidising bacteria and hydrogenotrophic archaea seem to play an important role [40, 41, 22]. Besides the resistance to high ammonia levels, SAOBs show high resistance to other toxics too, which allows anaerobic treatment of substances like oxytetracycline. In contrast to SAOBs, acetoclastic methanogens seem to be negatively affected by high levels of oxytetracycline [42]. Other toxicants, which were successfully treated, based

on anaerobic digestion, are for example Coumarin [43], chloroform [44] and dichloromethane [45]. In Summary, microbiomes from anaerobic digestion processes prove to be very robust, which in turn allows implementation of anaerobic digestion into concepts from waste treatment and bioremediation.

The role of anaerobic digestion in biorefinery

Methane, being the main product of AD-processes, has already a promising role in biorefinery. Besides its role as energy source, it can be used to grow methanotrophs, which are a viable source of proteins that can be used as food supplement. Moreover, methanotrophs are a promising source of several other products, since they accumulate osmolytes (e.g. ectoine or sucrose), phospholipids, biopolymers and enzymes [46]. However, anaerobic digestion is not only restricted to methane production.

The liquid effluent of biogas plants, due to its high content of nitrogen and phosphorus, can be used as fertilizer and allows effective production of algae [47, 48]. Besides this, separated fibres from anaerobic plant degradation can be used for saccharification to produce sugars and lignin, which eventually can be used for production of propionic acid, lactic acid, succinic acid, diols, butanol, ethanol, carbon fibres and biopolymers. Via thermochemical processes, lignin can also be used for production of heat, electricity, syngas and phenolic compounds. And finally, solid fibres can be transformed via pyrolysis and hydrothermal processes into bio-oil or biochar [48, 49].

Production of bio-products through anaerobic digestion is especially interesting, as it allows valorisation of multiple waste sources, as for example

mixed microalgae [50], pulp and paper sludge [51] or municipal waste [52]. Anaerobic fermentation of multiple wastes also allows degradation of multiple pollutants, as for example phenols [53] or paraffin [54].

With the perspective of using anaerobic digestion for a synergistic interconnection of multiple biorefinery processes, a fragmentation of AD-processes in two process stages becomes an interesting possibility. Since the 80s, scientists have described the possibility of separating hydrolysis and acidogenesis from acetogenesis and methanogenesis [55, 56, 57]. Low levels of pH and high concentration of volatile fatty acids (VFA) allow an inhibition of methanogenesis [58]. In turn, inhibition of methanogenesis leads to accumulation of interesting VFAs, like for example acetic-, lactic-, propionic- and butyric acid. VFAs are interesting products as they can be applied as platform chemicals in multiple chemical reactions [59], even though the extraction of those acids is still very challenging [60]. And finally, inhibition of methanogenesis allows production of hydrogen too [61]. The manifold application possibilities of separated acidification stages from anaerobic digesters might help to synergistically link different fields of biorefinery. However, to reach that aim, a deeper knowledge on microbial diversity and the robustness of anaerobic microbiomes appears necessary. Therefore, the presented PhD-thesis was designed to shed light on the dynamic and robust behaviour of microbiomes from anaerobic digestion. In the frame of this thesis it was further aimed to define key-microbiomes of anaerobic digestion processes, to highlight the importance of separated acidification stages, and to find new strains with potential application in the industry (Fig. 3).

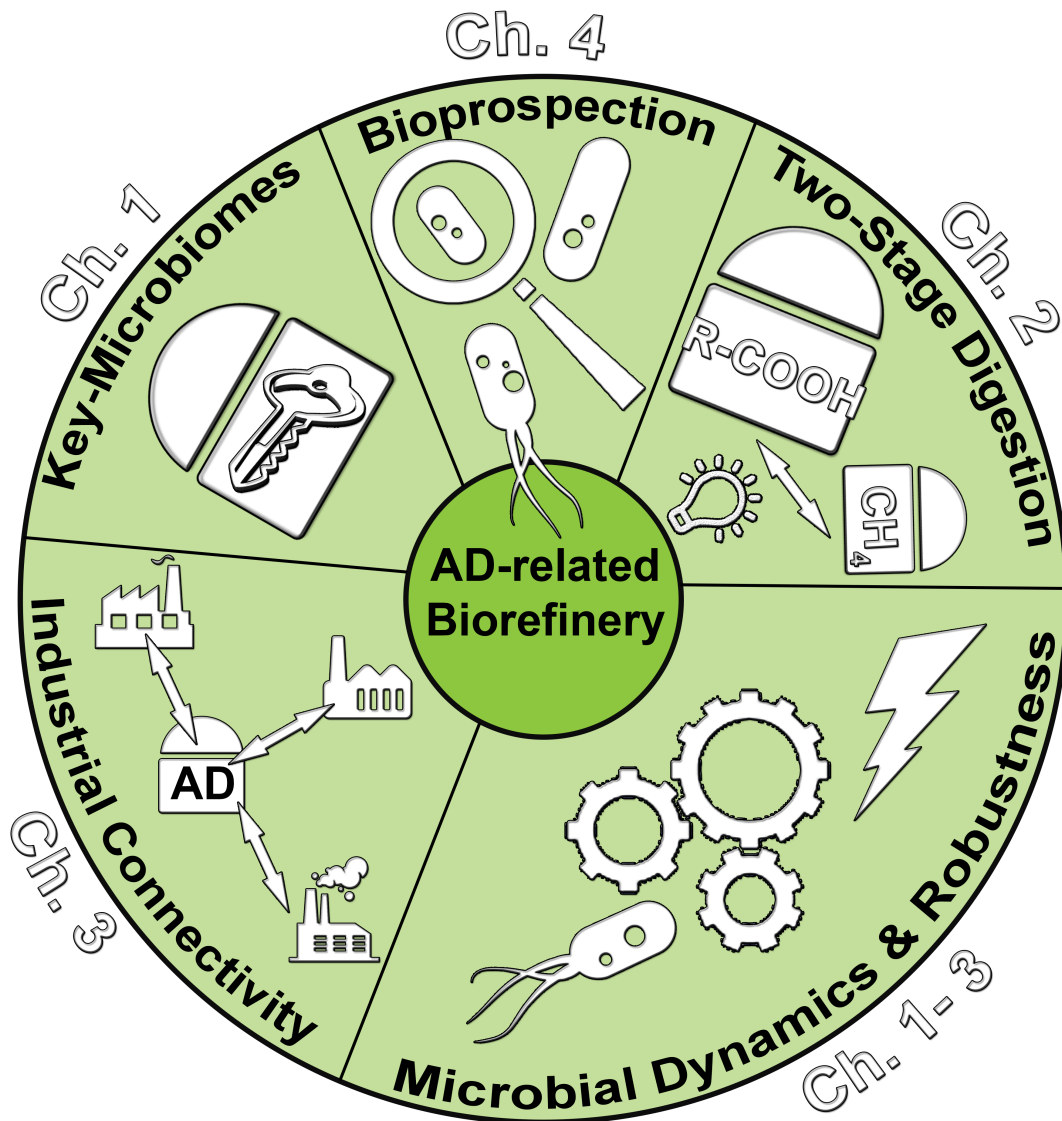


FIGURE 4: Structure of the thesis: Looking forward to a future, where industrial biorefinery is synergistically interconnected and uses anaerobic digestion (AD) as crosspoint. Based on this idea, this thesis is focussed on the shown topics. Corresponding chapters are indicated at the outer circle.

References

1. Chakraborty J, Das S. Molecular perspectives and recent advances in microbial remediation of persistent organic pollutants. *Environ Sci Pollut Res Int.* 2016;17:16883–16903.
2. Haghollahi A, Fazaelpoor MH, Schaffie M. The effect of soil type on the bioremediation of petroleum contaminated soils. *J Environ Manage.* 2016;180:197–201.
3. Jugder BE, Ertan H, Bohl S, Lee M, Marquis CP, Manefield M; 2016. Organohalide Respiring Bacteria and Reductive Dehalogenases: Key Tools in Organohalide Bioremediation. *Front Microbiol.* 2016;7:249. doi: 10.3389/fmicb.2016.00249.
4. Okibe N, Maki M, Nakayama D, Sasaki K; 2016. Microbial recovery of vanadium by the acidophilic bacterium, *Acidocella aromatica*. *Biotechnol Lett.* 2016;38:1475–81.
5. Dorado-Morales P, Vilanova C, Peretó J, Codoñer FM, Ramón D, Porcar M. A highly

- diverse, desert-like microbial biocenosis on solar panels in a Mediterranean city. *Sci Rep.* 2016;6:29235. doi: 10.1038/srep29235.
6. Vilanova C, Iglesias A, Porcar M. The coffee-machine bacteriome: biodiversity and colonisation of the wasted coffee tray leach. *Sci Rep.* 2015;5:17163, doi: 10.1038/srep17163.
7. Niedrée B, Berns AE, Vereecken H, Burauel P. Do Chernobyl-like contaminations with (137)Cs and (90)Sr affect the microbial community, the fungal biomass and the composition of soil organic matter in soil? *J Environ Radioact.* 2013;118:21–9.
8. Preiss L, Hicks DB, Suzuki S, Meier T, Krulwich TA. Alkaliphilic Bacteria with Impact on Industrial Applications, Concepts of Early Life Forms, and Bioenergetics of ATP Synthesis. *Front Bioeng Biotechnol.* 2015;3:75. doi: 10.3389/fbioe.2015.00075.
9. Leis B, Angelov A, Mientus M, Li H, Pham VT, Lauinger B, Bongen P, Pietruszka J, Gonçalves LG, Santos H, Liebl W. (2015). Identification of novel esterase-activity enzymes from hot environments by use of the host bacterium *Thermus thermophilus*. *Front Microbiol.* 2015 Apr 8;6:275. doi: 10.3389/fmicb.2015.00275.
10. Li M, Yang L, Xu G, Wu J. Screening, purification and characterization of a novel cold-active and organic solvent-tolerant lipase from *Stenotrophomonas maltophilia* CGMCC 4254. *Bioresour Technol.* 2013;148:114–120.
11. Tekedar HC, Sanli-Mohamed G. Molecular cloning, over expression and characterization of thermoalkalophilic esterases isolated from *Geobacillus* sp. *Extremophiles.* 2011;2:203–211.
12. <http://biomassmagazine.com/articles/12857/european-biogas-association-releases-biogas-biomethane-report>
13. Ferry JG. Methane from Acetate. *Jour. Bacteriol.* 1992;174:5489–5495.
14. Haarstrick A, Hempel DC, Ostermann L, Ahrens H, Dinkler D. Modelling of the biodegradation of organic matter in municipal landfills. *Waste Manag Res.* 2001;19:320–331.
15. Söhngen HL. Het Ontstaan en Verdwijnen van Waterstoff onder den invloed van het organische Leven. 1906; Dissertation, Delft.
16. Coolhas, C. Zur Kenntnis der Dissimilation Fettsaurer. *Centr. Bakt. II.* 1928;75:161–170.
17. Müller B, Sun L, Schnürer A. First insights into the syntrophic acetate-oxidizing bacteria – a genetic study. *Microbiologyopen.* 2013;1:35–53.
18. Beckmann S, Welte C, Li X, Oo YM, Kroeninger L, Heo Y, Zhang M, Ribeiro D, Lee M, Bhadbhade M, Marjo CE, Seidel J, Deppenmeier U, Manefield M. Novel phenazine crystals enable direct electron transfer to methanogens in anaerobic digestion by redox potential modulation, *Energy Environ Sci.* 2016;9:644–655.
19. Cai W, Huang W, Li H, Sun B, Xiao H, Zhang Z, Lei Z. Acetate favors more phosphorus accumulation into aerobic granular sludge than propionate during the treatment of synthetic fermentation liquor. *Bioresour Technol.* 2016;214:596–603.
20. Gagliano MC, Braguglia CM, Gallipoli A, Gianico A, Rossetti S. Microbial diversity in innovative mesophilic/thermophilic temperature-phased anaerobic digestion of sludge. *Environ Sci Pollut Res Int.* 2015;22:7339–7348.
21. Zhang YZ, Fang MX, Zhang WW, Li TT, Wu M, Zhu XF. *Salimesophilobacter vulgaris* gen. nov., sp. nov., an anaerobic bacterium isolated from paper-mill wastewater. *Int J Syst Evol Microbiol.* 2013;63:1317–1322.
22. Müller B, Sun L, Westerholm M, Schnürer A. Bacterial community composition and fhs profiles of low? and high? ammonia biogas digesters reveal novel syntrophic acetate?oxidising bacteria. *Biotechnol Biofuels.* 2016;9:48. doi: 10.1186/s13068-016-0454-9.
23. Hahnke S, Langer T, Koeck D, Klocke M. Description of *Proteiniphilum saccharofermentans* sp. nov., *Petrimonas mucosa* sp. nov. and *Fermentimonas caenicola* gen. nov., sp. nov. isolated from mesophilic lab-scale biogas reactors and emended description of the genus *Proteiniphilum*. *International Journal of Systematic and Evolutionary Microbiology.* 2016;66:1466–1475.
24. Maus I, Koeck DE, Cibis KG, Hahnke S, Kim YS, Langer T, Kreubel J, Erhard M, Bremges A, Off S, Stolze Y, Jaenicke S, Goesmann A, Sczyrba A, Scherer P, König H, Schwarz WH, Zverlov VV, Liebl W, Pühler A, Schlüter A, Klocke M. Unraveling the microbiome of a thermophilic biogas

- plant by metagenome and metatranscriptome analysis complemented by characterization of bacterial and archaeal isolates. *Biotechnol Biofuels*. 2016;9:171. doi 10.1186/s13068-016-0581-3.
25. Goux X, Calusinska M, Lemaigre S, Marynowska M, Klocke M, Udelhoven T, Benizri E, Delfosse P. Microbial community dynamics in replicate anaerobic digesters exposed sequentially to increasing organic loading rate, acidosis, and process recovery. *Biotechnol Biofuels*. 2015;8:122. doi: 10.1186/s13068-015-0309-9.
26. Lebuhn M, Hanreich A, Klocke M, Schlüter A, Bauer C, Pérez CM. Towards molecular biomarkers for biogas production from lignocellulose-rich substrates. *Anaerobe*. 2014;10–21.
27. Heeg K, Pohl M, Sontag M, Mumme J, Klocke M, Nettmann E. Microbial communities involved in biogas production from wheat straw as the sole substrate within a two-phase solid-state anaerobic digestion. *Syst Appl Microbiol*. 2014;37:590–600.
28. Poszytek K, Ciezkowska M, Sklodowska A, Drewniak L; Microbial Consortium with High Cellulolytic Activity (MCHCA) for Enhanced Biogas Production. *Front Microbiol*. 2016;7:324. doi: 10.3389/fmicb.2016.00324.
29. Sheets JP, Ge X, Li YF, Yu Z, Li Y. Biological conversion of biogas to methanol using methanotrophs isolated from solid-state anaerobic digestate. *Bioresour Technol*. 2016;201: 50–57.
30. Cheng X, Wang X, Qiu T, Yuan M, Sun J, Gao J. Molecular cloning and characterization of a novel cold-adapted family VIII esterase from a biogas slurry metagenomic library. *J Microbiol Biotechnol*. 2014;24:1484–1489.
31. Vijayaraghavan P, Arun A, Al-Dhabi NA, Vincent SG, Arasu MV, Choi KC. Novel *Bacillus subtilis* IND19 cell factory for the simultaneous production of carboxy methyl cellulase and protease using cow dung substrate in solid-substrate fermentation. *Biotechnol Biofuels*. 2016;9:73. doi: 10.1186/s13068-016-0481-6.
32. Morris JG. Obligately anaerobic bacteria in biotechnology. *Appl Biochem Biotechnol*. 1994;48:75–106.
33. Wallace RJ. Ruminant Microbiology, Biotechnology, and Ruminant Nutrition: Progress and Problems. *J Anim. Sci*. 1994;72:2992–3003.
34. Oren A. Anaerobic degradation of organic compounds at high salt concentrations. *Antonie Van Leeuwenhoek*. 1988;54:267–277.
35. Jabbour D, Sorger A, Sahm K, Antranikian G. A highly thermoactive and salt-tolerant α -amylase isolated from a pilot-plant biogas reactor. *Appl Microbiol Biotechnol*. 2013;97:2971–2978.
36. Webb AR and Hawkes FR. The anaerobic digestion of poultry manure: Variation of gas yield with influent concentration and ammonium-nitrogen levels. *Agricultural Wastes*. 1985;14:135–156.
37. Bujoczek G, Oleszkiewicz J, Sparling R, Cenkowskic S. High solid anaerobic digestion of chicken manure. *J Agr Eng Res*. 2000;76:51–60.
38. Abouelenien F, Fujiwara W, Namba Y, Kosseva M, Nishio N, Nakashimada Y. Improved methane fermentation of chicken manure via ammonia removal by biogas recycle. *Bioresour Technol*. 2010;101: 6368–6373.
39. Abouelenien F, Nakashimada Y, Nishio N. Dry mesophilic fermentation of chicken manure for production of methane by repeated batch culture. *J Biosci Bioeng*. 2009;107:293–295.
40. Westerholm M, Levén L, Schnürer A. Bioaugmentation of Syntrophic Acetate-Oxidizing Culture in Biogas Reactors Exposed to Increasing Levels of Ammonia. *Appl Environ Microbiol*. 2012;78:7619–7625.
41. Wang H, Fotidis IA, Angelidaki I. Ammonia effect on hydrogenotrophic methanogens and syntrophic acetate-oxidizing bacteria. *FEMS Microbiol Ecol*. 2015; doi: 10.1093/femsec/fiv130.
42. Turker G, Aydin S, Akyol Ç, Yenigun O, Ince O, Ince B. Changes in microbial community structures due to varying operational conditions in the anaerobic digestion of oxytetracycline-medicated cow manure. *Appl Microbiol Biotechnol*. 2016 100, 6469–6479.
43. Popp D, Schrader S, Kleinstaub S, Harms H, Sträuber H; 2015. Biogas production from coumarin-rich plants—inhibition by coumarin and recovery

- by adaptation of the bacterial community. *FEMS Microbiol.* doi: 10.1093/femsec/fiv103.
44. McCormick ML, Adriaens P. Carbon tetrachloride transformation on the surface of nanoscale biogenic magnetite particles. *Environ Sci Technol.* 2004;38:1045–1053.
45. Justicia-Leon SD, Ritalahti KM, Mack EE, Löffler FE. Dichloromethane Fermentation by a *Dehalobacter* sp. in an Enrichment Culture Derived from Pristine River Sediment. *Appl Environ Microbiol.* 2012;78:1288–1291.
46. Strong PJ, Kalyuzhnaya M, Silverman J, Clarke WP. A methanotroph-based biorefinery: Potential scenarios for generating multiple products from a single fermentation. *Bioresour Technol.* 2016;215:314–323.
47. Cheng J, Ye Q, Xu J, Yang Z, Zhou J, Cen K. Improving pollutants removal by microalgae *Chlorella* PY-ZU1 with 15% CO₂ from undiluted anaerobic digestion effluent of food wastes with ozonation pretreatment. *Bioresour Technol.* 2016;216:273–279.
48. Sawatdeenarunat C, Nguyen D, Surendra KC, Shrestha S, Rajendran K, Oechsner H, Xie L, Khanal SK. Anaerobic biorefinery: Current status, challenges, and opportunities. *Bioresour Technol.* 2016;215:304–313.
49. Fabbri D, Torri C; 2016. Linking pyrolysis and anaerobic digestion (Py-AD) for the conversion of lignocellulosic biomass. *Curr Opin Biotechnol.* 2016;38:167–73.
50. Daelman MR, Sorokin D, Kruse O, van Loosdrecht MC, Strous M. Haloalkaline Bioconversions for Methane Production from Microalgae Grown on Sunlight. *Trends Biotechnol.* 2016;3:450–457.
51. Gottumukkala LD, Haigh K, Collard FX, van Rensburg E, Görgens J; 2016. Opportunities and prospects of biorefinery-based valorisation of pulp and paper sludge. *Bioresour Technol.* 2016;215:37–49.
52. Chen P, Xie Q, Addy M, Zhou W, Liu Y, Wang Y, Cheng Y, Li K, Ruan R. Utilization of municipal solid and liquid wastes for bioenergy and bioproducts production. *Bioresour Technol.* 2016;215:163–172.
53. Poirier S, Bize A, Bureau C, Bouchez T, Chapleur O. Community shifts within anaerobic digestion microbiota facing phenol inhibition: Towards early warning microbial indicators? *Water Res.* 2016;100:296–305.
54. Wawrik B, Marks CR, Davidova IA, McNerny MJ, Pruitt S, Duncan K, Suflita JM, Callaghan AV; 2016. Methanogenic paraffin degradation proceeds via alkane addition to fumerate by *Smithella*? spp. mediated by a syntrophic coupling with hydrogenotrophic methanogens, *Environ Microbiol.* doi: 10.1111/1462-2920.13374.
55. Baccay RA, Hashimoto AG. Acidogenic and methanogenic fermentation of causticized straw. *Biotechnol Bioeng.* 1984;8:885–891.
56. Dinopoulou G, Rudd T, Lester JN. Anaerobic acidogenesis of a complex wastewater: I. The influence of operational parameters on reactor performance. *Biotechnol Bioeng.* 1988;31, 958–968.
57. Gijzen HJ, Zwart KB, Verhagen FJ, Vogels GP. High-Rate two-phase process for the anaerobic degradation of cellulose, employing rumen microorganisms for an efficient acidogenesis. *Biotechnol Bioeng.* 1988;31:418–425.
58. Demeyer D, Henderickx H, Van Nevel C. Influence of pH on fatty acid inhibition of methane production by mixed rumen bacteria. *Arch Int Physiol Biochim.* 1967 75:555–556.
59. Zhou M, Yan B, Wong JWC, Zhang Y. Enhanced volatile fatty acids production from anaerobic fermentation of food waste: A mini-review focusing on acidogenic metabolic pathways. *Bioresour Technol.* 2017; doi: 10.1016/j.biortech.2017.06.121.
60. Koutinas A, Kanellaki M, Bekatorou A, Kandyli P, Pissaridi K, Dima A, Boura K, Lappa K, Tsafarakidou P, Stergiou PY, Foukis A, Gkini OA, Papamichael EM. Economic evaluation of technology for a new generation biofuel production using wastes. *Bioresour Technol.* 2016;200:178–185.
61. Dareioti MA, Kornaros M. Anaerobic mesophilic co-digestion of ensiled sorghum, cheese whey and liquid cow manure in a two-stage CSTR system: Effect of hydraulic retention time, *Bioresour Technol.* 2014;175:553–562.

Objectives

The present thesis focuses on anaerobic digestion, more specifically on the dynamic behaviour of the underlying microbiomes and the role of anaerobic digestion for biorefinery. In the past decades, tremendous progress has been made on the field of anaerobic digestion. Innovative methods, especially high-throughput sequencing approaches, have allowed the study of biotechnologically-relevant biocenosis more deeply. However, the exact behaviour of the involved microbiomes under different conditions is still an unresolved topic. In order to shed light on the diversity, biological activity and robustness of microbial consortia responsible for biotechnologically relevant processes, the present PhD thesis has been designed in order to address the following objectives:

1.) Characterisation of biogas-producing facilities in Germany, in the widest study to date, aiming at the identification of common cores of microbial keyplayers linked to biogas production.

2.) Performing the first holistic characterization of two-stage digestion with an acid accumulating pretreatment step based on a multi-omics approach, including both metagenomics and proteomics.

3.) Exploring new applications of the anaerobic pretreatment of biomass, such as electricity production, pre-treatment of substrates that are difficult to digest and combined application of thermal pretreatment and microbial driven acidification.

4.) Identification of new microbial strains with foreseeable roles in anaerobic digestion and biorefinery.

Chapter 1: Characterisation of biogas-producing facilities in Germany

Summary: Only a fraction of the microbial species used for anaerobic digestion in biogas production plants are methanogenic archaea. We have analyzed the taxonomic profiles of eubacteria and archaea, a set of chemical key parameters, and biogas production in samples from nine production plants in seven facilities in Thuringia, Germany, including co-digesters, leach-bed, and sewage sludge treatment plants. A complex taxonomic composition was found for both eubacteria and archaea, both of which strongly correlated with digester type. Plant-degrading Firmicutes as well as Bacteroidetes dominated eubacteria profiles in high viscid co-digester sludge; whereas Bacteroidetes and Spirochaetes were the major phyla in leach-bed and sewage sludge digesters. *Methanoculleus* was the dominant archaea genus in co-digesters, whereas *Methanosarcina* and *Methanosaeta* were the most abundant methanogens in leachate from leach-bed and sewage sludge digesters, respectively.

Publication 1

Abendroth C, Vilanova C, Günther T, Luschnig O, Porcar M. Eubacteria and archaea communities in seven mesophilic anaerobic digester plants in Germany, *Biotechnol Biofuels*. 2015;8:87. doi: 10.1186/s13068-015-0271-6.



Publication 1

Eubacteria and archaea communities in seven mesophilic anaerobic digester plants in Germany

Christian Abendroth^{1,2}, Cristina Vilanova¹, Thomas Günther³, Olaf Luschnig^{2,4}, Manuel Porcar^{*1,5}

¹Cavanilles Institute of Biodiversity and Evolutionary Biology, Universitat de València, 46020 Valencia, Spain. ²Bio H2 Energy GmbH, Im Steinfeld 10, 07751 Jena, Germany. ³Eurofins Umwelt Ost GmbH, Löbstedter Straße 78, 07749 Jena, Germany. ⁴BioEnergie Verbund e.V., Im Steinfeld 10, 07751 Jena, Germany. ⁵Fundació General de la Universitat de València, València, Spain.

Abstract

Background: Only a fraction of the microbial species used for anaerobic digestion in biogas production plants are methanogenic archaea. We have analyzed the taxonomic profiles of eubacteria and archaea, a set of chemical key parameters, and biogas production in samples from nine production plants in seven facilities in Thuringia, Germany, including co-digesters, leach-bed, and sewage sludge treatment plants. Reactors were sampled twice, at a 1-week interval, and three biological replicates were taken in each case.

Results: A complex taxonomic composition was found for both eubacteria and archaea, both of which strongly correlated with digester type. Plant-degrading Firmicutes as well as Bacteroidetes dominated eubacteria profiles in high biogas-producing co-digesters; whereas Bacteroidetes and Spirochaetes were the major phyla in leach-bed and sewage sludge digesters. *Methanoculleus* was the dominant archaea genus in co-digesters, whereas *Methanosarcina* and *Methanosaeta* were the most abundant methanogens in leachate from leach-bed and sewage sludge digesters, respectively.

Conclusions: This is one of the most comprehensive characterizations of the microbial communities of biogas-producing facilities. Bacterial profiles exhibited very low variation within replicates, including those of semi-solid samples; and, in general, low variation in time. However, facility type correlated closely with the bacterial profile: each of the three reactor types exhibited a characteristic eubacteria and archaea profile. Digesters operated with solid feedstock, and high biogas production correlated with abundance of plant degraders (Firmicutes) and biofilm-forming methanogens (*Methanoculleus* spp.). By contrast, low biogas-producing sewage sludge treatment digesters correlated with high titers of volatile fatty acid-adapted *Methanosaeta* spp.

Background

Knowledge of the effects of greenhouse gases on the climate dates back to the 1970s, with CO₂ representing a key greenhouse gas [1]. Today, there is general assent on the urgent need to reduce greenhouse gases in order to mitigate climate change [2, 3]. One of the main strategies to meet this goal requires shifting from fossil to renewable energy sources. In fact, it is expected that by

2020, 20 % of total energy consumption in Europe will be covered by renewable energies [4].

Biomass is a very promising alternative energy source, in particular as a source of biogas. Indeed, almost 70 % of all renewable energies in Europe came from biomass management in 2010 [5], with Germany being a leader in the biomass-based bioeconomy. During recent years, as supported by the EEG (German law for renewable energies) [6], the number of biogas plants and biogas production has increased dramatically in Germany. For example, in 2012, 7200 biogas plants in Germany provided enough energy to power 5.3 million households [7]. Despite this success, the underlying microbial biocenoses of biogas-producing facilities are not yet fully understood, and the whole methanogenesis process is often referred to as a “black box” even in some of the recent literature [7–9]. In the last decades, substantial efforts have been undertaken to shed light on the microbial communities involved in the anaerobic digestion process, as deduced by 16S-rDNA sequencing [10–13], *mcrA* gene-based analysis [14, 15], or metagenomic approaches [16, 17]. Different microbial profiles have been reported for biogas production plants fed with different types of biomass. For example, the microbial diversity in a completely stirred digester fed with fodder beet silage as a monosubstrate is reported to be particularly rich in Clostridiales, Deltaproteobacteria, Bacilli, and Bacteroidetes [18]. Other studies describe the effect of biowaste sludge maturation on the microbial profile within a thermophilic digester, which contained mainly Clostridia [19]; while the microbial communities in lab-scale reactors fed with casein, starch, and cream are particularly abundant in Firmicutes and Bacteroidetes [20]. Given these reports, we could say that microbial profiles of anaerobic digesters are, to some extent, specific

for each biogas reactor/biomass type. This raises the question whether a common core of microbial key players does exist for anaerobic digesters in general. It is indeed possible to find common microbial actors when higher taxonomic levels are compared. For instance, it is known how methanogenic archaea (genus *Methanosaeta*) dominates environments with low acetate, while increasing amounts of inhibiting substances (like volatile fatty acids or hydrogen sulfide) foster *Methanosarcina* spp. growth [21]. Under thermophilic conditions, *Methanosarcina* spp. proves more frequent than *Methanosaeta* spp. Regarding eubacteria, the phyla Firmicutes and Bacteroidetes play an important role in anaerobic digestion [13, 22] and within Firmicutes, the class Clostridia is the most abundant group [18, 23]. Regarding bacteria, and similarly to methanogens stressed above, eubacterial profiles of anaerobic co-digesters and from the anaerobic stage of sewage plants are typically different [13].

In the present work, we have performed a holistic analysis of seven different digesters at two distinct time points (2 · 9 reactors, sampled within 1 week) from Thuringia, Germany (Fig. 5; Table 1). The digesters corresponded to three different configurations: completely mixed and continuously stirred single-stage tank reactors for sewage sludge digestion (SS); leach-bed digesters operating discontinuously in batches (LB); and a two-stage system consisting of a vertical plug flow reactor followed by an upright continuously stirred tank digester and a final digestate storage tank (hereafter referred to as CD, standing for co-digester). With the exception of the digestate storage tank, which was operated at room temperature (RT), all facilities were operated at mesophilic temperature. The analysis included chemical characterization and

biogas measurement of the samples and the determination of the archaea and eubacteria taxonomic profiles by 16S amplicons sequencing on three replicates of each reactor/time. Our results reveal that microbial profiles were strongly dependent on reactor type and moderately dependent on the facility/particular reactor sampled. We

also found that profiles were stable in time and exhibited a low degree of variation within the three replicates analyzed. Globally, the 54 subsamples sequenced are the most comprehensive microbial characterization of biogas communities performed to date.

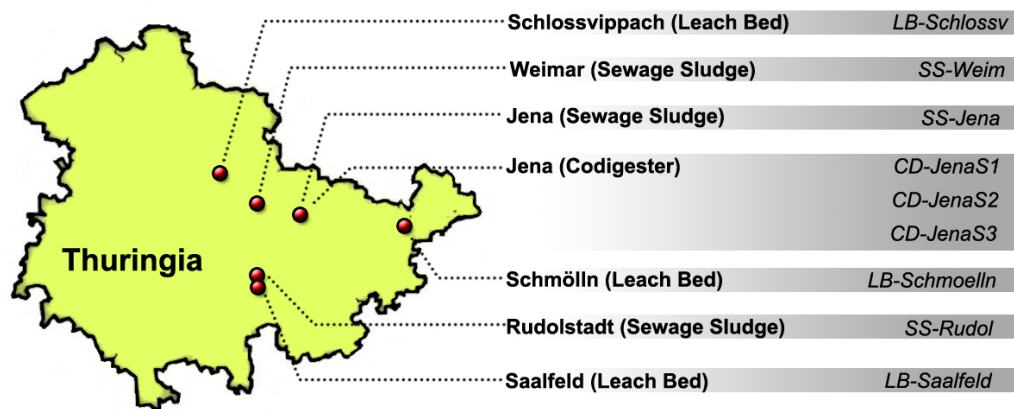


FIGURE 5: Sampling of anaerobic digesters in Thuringia (Germany). Seven different facilities with a total of nine reactors were sampled in Schlossvippach, Weimar, Jena (two plants, one of them with three reactors), Schmölln, Rudolstadt, and Saalfeld. Sampling was repeated twice at a 1-week interval, and three replicates were processed (54 samples in total). CD three-stage plant, SS sewage plants, LB leach-bed reactors, S1 plug flow reactor, S2 continuous stirred tank reactor, S3 storage tank for digestion remnants.

Results and discussion

Chemical parameters

Eleven parameters were measured for each of the reactor samples: COD (chemical oxygen demand), TOC (total organic carbon), total nitrogen content (N), electrical conductivity, TVFA (total volatile fatty acids), TS (total solids), VS (volatile solids), pH, biogas yield, and concentrations of CH₄ and CO₂ (Additional file 1: Table S1). Biogas yields were obtained from lab-scale batch experiments, whereas all the other parameters originated from in situ measurements of digester samples. Batch experiments were

performed without adding substrates and obtained biogas yields depended only on the organic fraction within the sludge samples. After normalizing the data, successive combinations of three parameters (permutation) were plotted in a Gnuplot multiplot (Fig. 6). The resulting data matrix included biogas production but not methane and CO₂ concentration, in order to avoid redundancies. This resulted in three clearly defined clouds, each corresponding to one of the different digester facility types (Fig. 6a). SS and CD values were plotted in two opposed vertices of the plot, with LB located in an intermediate position.

TABLE 1: Overview of sampled digester types and input feeding based on descriptive data.

Sample	Digester type	Input materials	Plant configuration
LB-Schmölln	Leach-bed batch digester	Silage, straw, cow manure	Batch process (11 batches) Digester volume: 11·800 m ³ Leachate tank: 1000 m ³ Batch process duration: 26-29 d Gas production: 0.7 m ³ /m ³ ·d OLR: 1.3 Kg·VS/m ³ ·d
CD-Jena	two- stage digester (vertical plug flow reactor / stirred tank)	Silage, farm manure, Livestock farming waste	Two-stage process Stage 1 (plug flow): 790 m ³ Stage 2 (CSTR): 2000 m ³ Stage 3 (final storage tank): 3800 m ³ HRT: 87d Gas production: 1.2 m ³ /m ³ ·d OLR: 3.0 Kg·VS/m ³ ·d
SS-Jena	Completely mixed tank digester	Mono-digestion of municipal sewage sludge	Single stage process (2 digesters) Digester volume: 2·2000 m ³ HRT: 21d Gas production: 0.6 m ³ /m ³ ·d OLR: 1.8 Kg·VS/m ³ ·d
SS-Weimar	Completely mixed tank digester	Mono-digestion of municipal sewage sludge	Single stage process Digester volume: 3200 m ³ HRT: 29d Gas production: 0.6 m ³ /m ³ ·d OLR: 0.96 Kg·VS/m ³ ·d
LB-Schlossvippach	Leach-bed batch digester	Cow manure, straw, feed residues	Batch process (8 batches) Leachate tank: 1000 m ³ Digester volume: 8·330 m ³ Batch process duration: 32-35 d Gas production: 0.5 m ³ /m ³ ·d OLR: 2.1 Kg·VS/m ³ ·d
SS-Rudolstadt	Completely mixed tank digester	Co-digestion of municipal and industrial sewage sludge with seasonally available co-substrates (biodiesel waste)	Single stage process (2 digesters) Digester volume: 2·2000 m ³ HRT: 25d Gas production: 0.3 m ³ /m ³ ·d OLR: 0.54 Kg·VS/m ³ ·d
LB-Saalfeld	Leach-bed batch digester	Organic fraction of municipal solid waste	Batch process (9 batches) Digester volume: 9·826 m ³ Leachate tank: 1060 m ³ Batch process duration: 33 d Gas production: 0.7 m ³ /m ³ ·d OLR: 0.9 Kg·VS/m ³ ·d

Gas production is given in cubic meter of produced gas per cubic meter of sludge per day
HRT hydraulic retention time, CSTR continuous stirred-tank reactor, OLR organic loading rate

The yield of biogas produced is shown in Fig. 6b and the highest yields are plotted as a relatively small cloud (black dots) overlapping with the extremes of the CD cloud. As a general conclusion, parameter values were higher (corresponding in general with high nutrient contents) when biogas

production was highest. In a second statistical approach, this observation was verified by a principal component analysis (Additional file 2: Figure S1), where samples coming from the same type or reactor clustered together and notably differed from those from other reactor types.

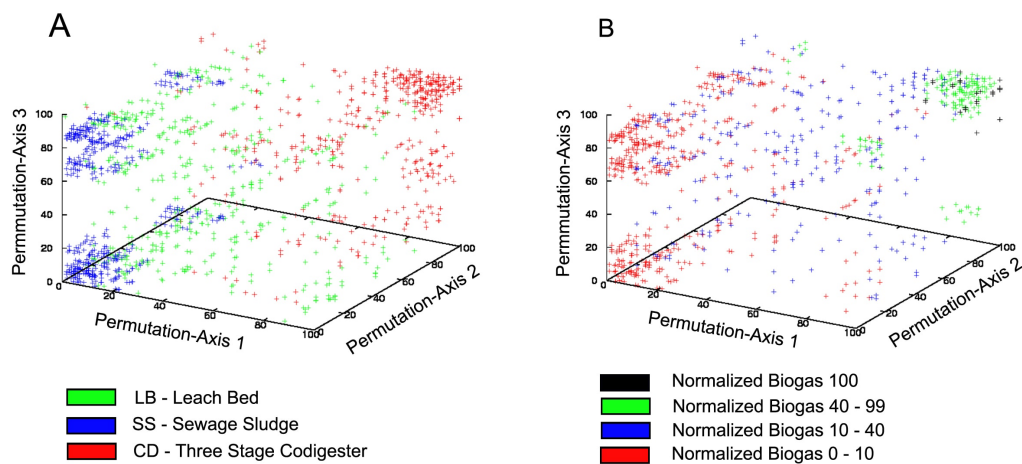


FIGURE 6: 3D plots of chemical parameters. COD, TOC, total nitrogen contents (N), conductivity, TVFA, TS, VS, pH, and produced volume of biogas are plotted in a 3D representation in which the permutation of all determined parameters define axis X, Y, and Z. The underlying biogas facilities are highlighted correspondingly (a). Plotting the parameters without the biogas yield and coloring the dots according to their biogas production rate gives the second plot (b).

Taxonomic composition of eubacteria

Eubacteria from all samples were identified by highthroughput sequencing as described in “Material and methods” section, and phylum-level results are shown in Fig. 7. There was little variation between replicates, clearly indicating that differences in taxonomic composition accounted for the differences found between reactors and time. Similarly, different sampling times resulted in very small variations in the taxonomic profile, being the taxonomic composition of each sample very constant after 1 week. Only in one case (LB reactor in Saalfeld) a substantial shift was detected in the amount of

Bacteroidetes and Spirochaetes after 1 week. The taxonomic composition of the samples correlated closely with reactor type. Indeed, three different profiles were observed, each corresponding to a particular facility type. CD samples were dominated by the phylum Firmicutes, with nearly 46–60 % of classified sequences assigned to Firmicutes in the first two stages and less than 20–32 % in the third stage (remnant storage); followed by Bacteroidetes, which proved mainly in the third stage, when it accounted for up to 73 % of the total identified taxa.

The three CD digesters contained low amounts of Synergistetes, and the remnant storage contained moderated amounts of Actinobacteria, Proteobacteria, Spirochaetes, and Tenericutes (Fig. 7a). The second facility type (LB) displayed a totally different microbial composition (Fig. 7b) with comparatively fewer Firmicutes reads (between 3 and 19 % of total sequences). The microbial LB communities were dominated by Spirochaetes (30 and 72 % of the total reads), along with Bacteroidetes

(11 and 47 %). The third phylum, Thermothogae, reached low to moderate frequencies in LB facilities in Schmölln and Saalfeld (between 2 and 19 %), and it was absent in the six replicates of Schlossvippach. Minor counts of Actinobacteria and Proteobacteria were also detected. The third profile was associated with the sewage sludge digesters (Fig. 7c). Although the SS facilities showed certain similarities compared to the LB facilities, the overall microbial composition differed from both CD and LB reactors.

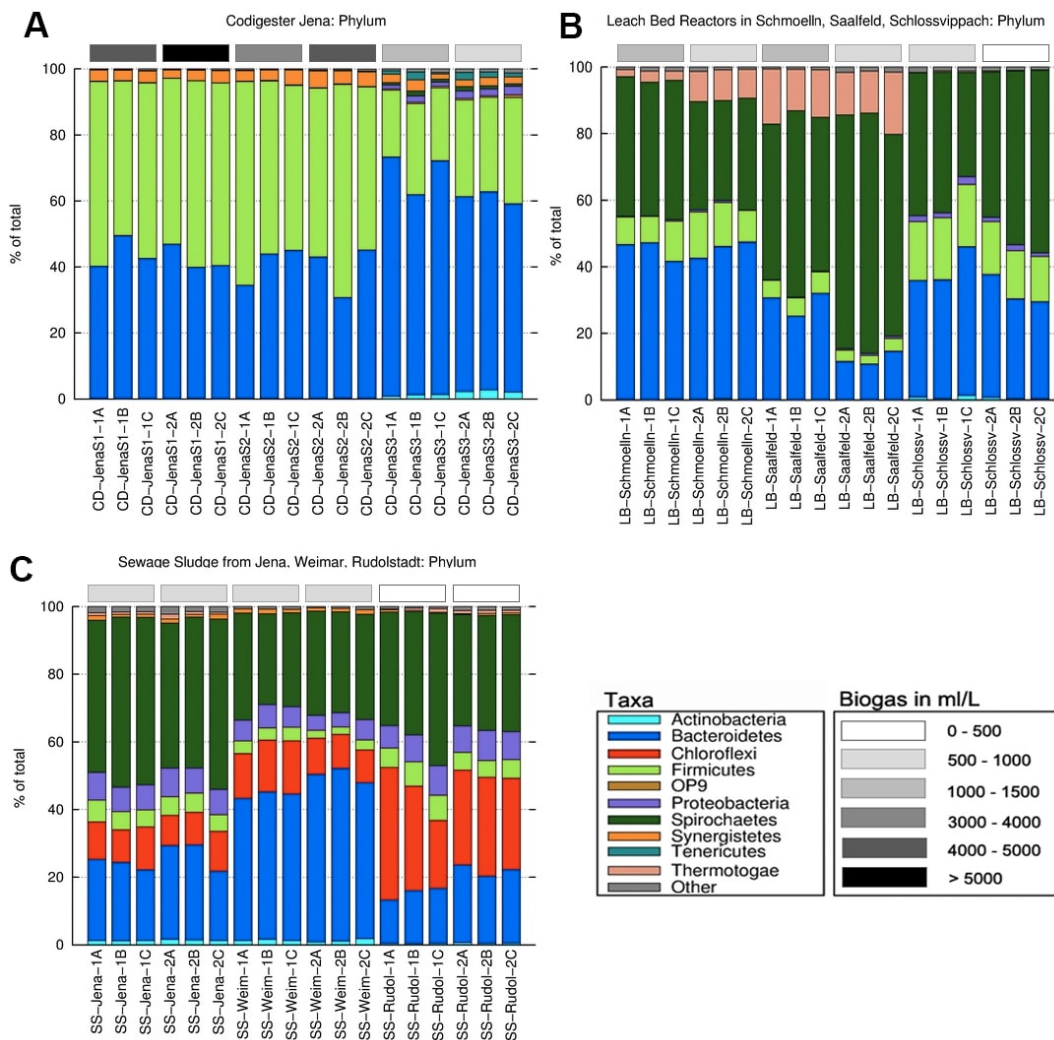


FIGURE 7: Bacterial profiles of the anaerobic digester plants analyzed. Taxonomic (phylum) composition of eubacteria populations in the reactors as deduced by 16S amplicons isolated and sequenced as described in “Material and methods” section. (a) Three-stage co-digester (CD) plant in Jena, (b) leach-bed reactors, and (c) sewage plants. The grey scale (top right) corresponds to biogas yield ranges as shown at the right.

In common with the LB samples, SS reactors contained high amounts of Bacteroidetes and Spirochaetes (Bacteroidetes between 13 and 51 %, Spirochaetes between 27 and 50 %). However, unlike the CD and LB facilities, SS reactors were particularly rich in Chloroflexi (9 and 39 %) and Proteobacteria (4–9 %). Besides the aforementioned taxa, small amounts of Actinobacteria, Synergistetes, and Thermotogae were also observed. Minor variations or sub-profiles of the three main biomass-associated profiles were detected. For example, two of the three Jena CD reactors were very similar, while the third one displayed higher eubacteria diversity. This might be due to the fact that the last stage (remnants) was kept at RT instead of mesophile temperatures. Although LB and SS samples corresponded to two main profiles, one location of each type (LB-Schlossvippach and SS-Rudolstadt) exhibited a characteristic presence/absence of one particular taxon: the former typically lacked Thermotogae, which was well represented in the other two LB plants; while SS Rudolstadt was particularly rich in Chloroflexi (Fig. 7b, c). The absence of Thermotogae in the LB reactor from Schlossvippach may be due to the fact that the solid phase is mainly heated up by the leachate (without extra heating in the solids storage-“garage”), which can lead to irregularities in temperature. In the Schlossvippach sample, it took more than 1 week to heat up a newly filled garage (Christoph Bürger and Kevin Lindner personal communication). In general, taxonomic eubacteria profiles strongly correlated with the biomass type. The differences observed between CD and SS reactors are in accordance with previous studies [13] describing an overall difference between sewage sludge and co-fermentation regarding the microbial profile. The high amount of Bacteroidetes and Firmicutes in CD

reactors is also consistent with previous reports [13, 18, 22, 24]. One reason for the abundance of Firmicutes could be the high content in TS derived from plant material (Additional file 1: Table S1), which probably fosters biofilm formation. Firmicutes have been described as main degraders of cellulolytic material [24] and are abundant in biofilms of water supply systems [25, 26]. LB and SS reactors, both containing liquid substrates, had high titers of the very mobile and efficient swimmer Spirochaete, described as able to swim in high viscous gel-like liquids, such as those found in LB reactors [27]. It has to be highlighted that the observed microbial profiles for the LB samples were only those from leachate, and that the solid fraction of LB systems might be rich in Firmicutes due to the high percentage of solids. The abundance of Chloroflexi in SS reactors has previously been reported. In fact, different Chloroflexi species have been found in more than 60 sewage reactors in different European countries based on FISH experiments [28] and also in other facilities around the world [29]. The prevalence of Proteobacteria and Bacteroidetes is in accordance with the work by Wang et al. [30] on the microbial profile of domestic sewage outfalls. The different taxonomic profiles we found correlated to biogas yield. For instance, the phylum Chloroflexi was detected in sewage plants, where very low biogas yields were measured. Also, Proteobacteria were only found in the plants with low biogas yields (digestate storage of the three-stage plant, Schlossvippach, and all sewage samples), while Firmicutes were particularly abundant in reactors with high biogas yields (CD samples). However, differences in biogas yield might also be a consequence of the concentration of TS, which is especially high in CD reactors.

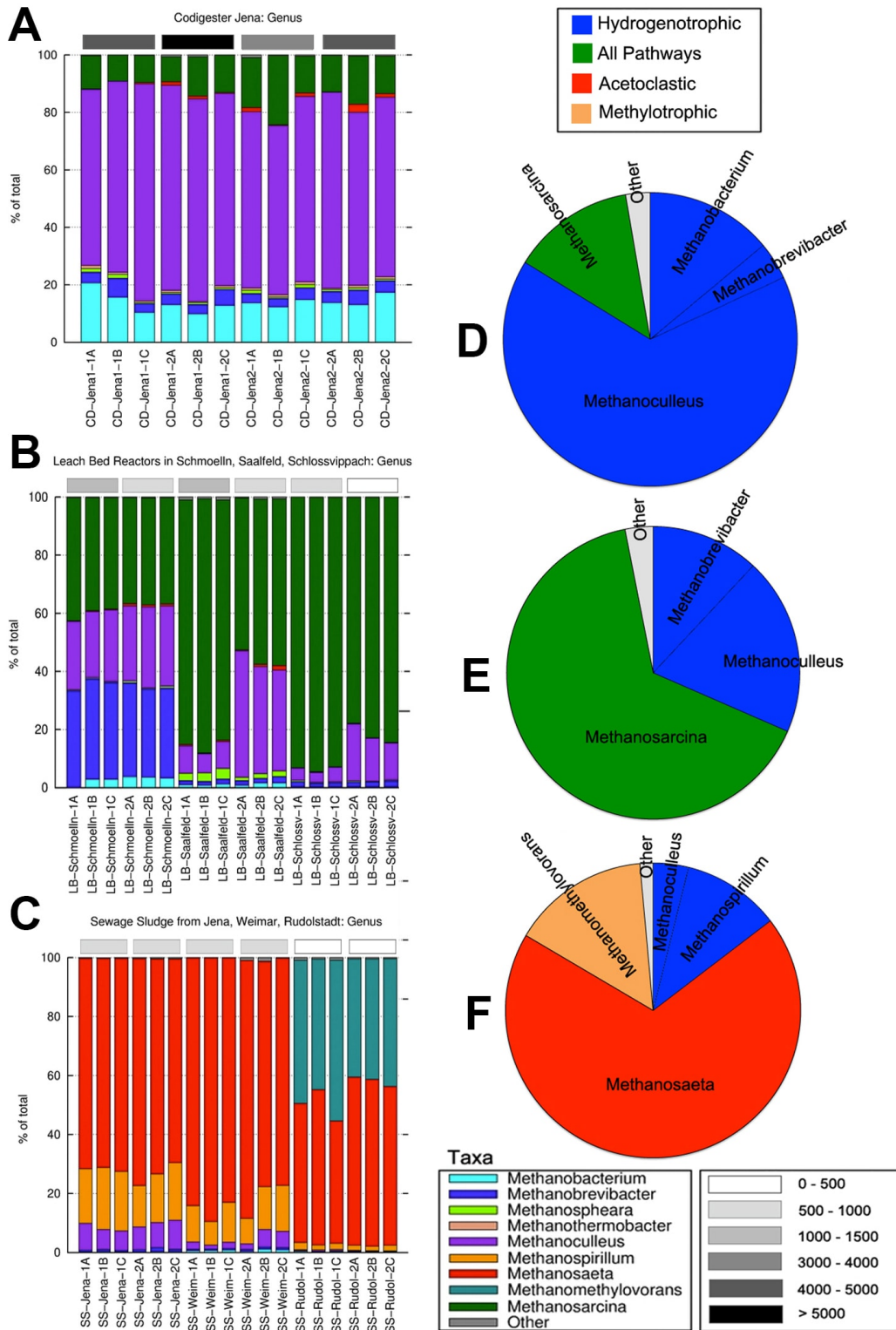


FIGURE 8: Taxonomic (genus) composition of archaea in the anaerobic digester plants. Taxonomic composition based on 16S archaea-specific amplicon sequences is shown. (a) The three-stage plant (CD) in Jena, (b) leach-bed reactors, and (c) sewage plants. The grey scale (top right) corresponds to biogas production values as in Fig. 7. Samples corresponding to the storage tank of the digestion remnants reactor (CD-Jena S3) are not shown as they failed to produce any amplicon with the selected oligonucleotides. Methanogenesis pathways are shown in (d) three stage plant, (e) leach-bed reactors, and (f) sewage plants.

In summary, our results are strongly consistent with previous reports demonstrating patchiness of the digesters in terms of the distribution of bacterial populations [31]. This strongly suggests ecological parameters (i.e. liquid/solid substrate or biomass type) are the key factors shaping microbial communities; but also reveal an important, albeit secondary, role of the facility/reactor on this mainly biomass-associated distribution of the taxonomic profiles.

Taxonomic composition of archaea

The taxonomic composition of the sampled reactors in terms of archaea contents is shown in Fig. 8. The data correspond to all but one reactor (three replicates and two time points), corresponding to the third stage of the Jena CD reactor, from which no archaeal DNA could be amplified. CD reactors were dominated by archaea belonging to the genus *Methanoculleus* (Fig. 8a), accounting for 59–76 % of all the sequences. A significant amount of *Methanosarcina* (9–24 %), *Methanobacterium* (10–21 %), and *Methanobrevibacter* (3–7 %) was detected, as well as infrequent genera such as *Methanosphaera*, *Methanothermobacter*, and *Methanosaeta*. In contrast, LB digesters were characterized by substantially smaller amounts of *Methanoculleus* (3–44 %); and by the abundance of *Methanosarcina* (37–95 %). One of the three LB-digesters showed a very high amount of *Methanobrevibacter* (31–35 %), whereas the other two reactors had very low amounts (1–2 %). Minor genera were *Methanobacterium*, *Methanosphaera*, and *Methanosaeta*. In the SS samples, *Methanosaeta* proved the most prevalent genus with a total number of reads between 42 and 88 % (Fig. 8c). While *Methanosaeta* was detected in high amounts in all the SS reactors, the frequency of other genera differed among SS digesters. The biogas

plant in Rudolstadt was very rich in *Methanomethylovorans* (40–55 %), while the other two SS reactors showed a relatively high amount of *Methanoculleus* (1–10 %) and *Methanospirillum* (8–21 %). As in the eubacteria profiles, three main taxonomic combinations were found to correlate with the three reactor types. The CD samples showed a strikingly similar profile independently on the replicate, reactor, or time sampled. LB and SS reactors did exhibit sub-profiles with no variation within replicates and dependent on the sampling time (Schlossvippach and Saalfeld) or on the location sampled (Rudolstadt). The two LB facilities from Schlossvippach and Saalfeld showed an increased amount of *Methanoculleus* after 1 week, while the amount of *Methanosarcina* decreased during this period. It is likely that genus *Methanoculleus* is more abundant in the solid fraction of these LB systems due to the high percentage of solids. Rudolstadt samples had the typical *Methanosaeta* abundance of SS reactors but were characterized by an exceptionally high frequency of *Methanomethylovorans*. The presence of *Methanosarcina* and *Methanoculleus* correlated to high yields of biogas, while low biogas yields correlated with higher amounts of *Methanosaeta*. Since methane production is solely due to the archaeal community and the different methanogenesis pathways are well known and genus-linked, we studied the expected methanogenesis pathways in each facility type according to the average taxonomic distribution (Fig. 8d–f). Interestingly, each facility type displayed a different combination of methanogenesis pathways. The CD reactors were very rich in archaea using the hydrogenotrophic pathway (Fig. 8d); LB reactors were dominated by *Methanosarcina* and thus with the ability to use all known pathways for methane production (Fig. 8e); and SS reactors were characterized by containing high rates of archaea using the acetoclastic

pathway for methane production (Fig. 8f).

The archaea composition we describe here for the different reactor types is generally in accordance with that reported in previous studies. The prevalence of *Methanoculleus* in CD reactors was also found in other works with classical anaerobic digesters [22, 32, 33]. Although other studies describe a prevalence of *Methanosarcina* in this reactor type [34], our data is in concordance with other works linking *Methanosarcina* to LB reactors [35, 36]. The differences in TS levels between CD and LB reactors might be the key factor explaining their differences in microbial composition. The TS content of LB reactors was much lower (Additional file 1: Table S1), so the surface available for the growth of biofilm-forming species, such as *Methanoculleus* [37], was limited compared to CD reactors. Indeed, previous reports have found a prevalence of *Methanoculleus* in the solid fraction of LB reactors [36, 38]. Additionally, a lower number of TS may hamper the formation of spatial syntrophic relationships between acetate-oxidizing bacteria and hydrogenotrophic methanogens such as *Methanoculleus*. This might lead to an increase in growth of acetoclastic methanogens such as *Methanosarcina*, able to directly metabolize acetate (Fig. 8d–f). These findings are in concordance with previous reports on the link between high content of TS and a high frequency of hydrogen using methanogens compared to acetoclastic methanogens [39–42].

The finding that *Methanosaeta* is the dominating genus in all SS digesters is consistent with other screenings [21, 43, 44]. However, the abundance of *Methanomethylovorans* in the SS digester in Rudolstadt might be connected to the presence of particularly high amounts of oil and alcohols such as methanol, since this particular digester

was supplemented with remnants from biodiesel production, and the prevalence of this organism has been reported in sewage sludge reactors supplemented with molasses alcohol wastewater [45]. The genus *Methanospirillum* was more abundant in the SS reactors in Jena and Weimar but not in Rudolstadt. This genus proved, along with *Methanolinea*, particularly abundant in a previous SS characterization [46], suggesting that *Methanospirillum* and *Methanosaeta* are two competing genera within the anaerobic digestion process of SS sludge.

Conclusions

The present work describes a holistic characterization of, to the best of our knowledge, the widest screening of biogas production facilities performed to date. We studied nine reactors, three replicates, and two time points (1-week interval) yielding 54 subsamples, the taxonomic diversity of which was determined for both archaea and eubacteria contents. Despite the heterogeneous nature of some of the samples (especially those from CD reactors), our data reveal a very small effect of inter-replicate variation. All our results suggest a strong link between reactor type and taxonomic profile (for both archaea and bacteria), as well as an additional, significant effect of the location/particular reactor on the microbial community. Additionally, the three reactor types yielded separate blocks when chemical parameters were plotted in 3D and a principal component analysis was performed. Taken together, our results confirm the tight link between digester type, chemical parameters, and microbial biocenoses and also support the existence of a very stable microbial core adapted to each reactor type. Furthermore, our study provides a strong dataset for future diagnostic strategies aiming to predict biogas production of mesophile reactors on the basis of their microbial composition.

Materials and methods

Sampling

Seven anaerobic reactors accounting for nine different reactors from Thuringia, Germany, were sampled twice at a 1-week interval. These biogas plants included codigesters, leach bed, and sewage sludge treatment plants (Fig. 5). Triplet samples from the first sampling time point were labelled as 1A, 1B, and 1C; whereas triplet samples from the second time point were labelled as 2A, 2B, and 2C.

An overview of the sampled digester types and input feedings is shown in Table 1. Additional file 1: Table S1 and Additional file 3: Table S2 show specific environmental chemical parameters regarding biogas production, biogas composition, and VFA spectrum. All sampled digester types were operated at mesophilic temperature (except the sampled storage chamber for digestion remnants, which was left at RT). For the chemical analysis, a total volume of 5 L was collected in buckets via a sampling port at each plant. The sampling procedure was similar for all plants and stages (SS plants, LB systems, and all the stages of the one-phase CD). In the case of the LB facilities, only leachate from the leach tank could be collected. Small amounts of sample were then transferred into Falcon tubes, which were directly frozen on dry ice to prevent further microbial growth or DNA degradation, and immediately sent on dry ice from Thuringia to Valencia (Spain) for DNA isolation and sequencing. The remaining sludge was transferred to the laboratory of Bio H2 Energy GmbH in Jena. From this sludge, 1.5 L was used for gas production analysis directly upon sampling. The remaining 3.5 L of sludge was aliquoted into smaller plastic boxes and stored at 20 °C for further analysis at Eurofins and Bio H2 companies.

Determination of biogas production

For each anaerobic sludge sample, 1.5 L was incubated in batch-experiments for 1 week at 37 °C. Incubation bottles (0.5 L) were filled with 0.5 L of sample (three bottles per sample without additional feeding), connected to a liquid displacement device (eudiometer, custom-built model calibrated by the German Eichamt), and the whole setup was flushed with nitrogen to ensure an anaerobic atmosphere. Biogas yield was measured as produced volume of biogas per volume of sludge sample [mL/L]. The concentration of CO₂ and CH₄ in the produced biogas was determined with the “Binder COMBIMASS GA-m” gas-measurement device (Binder, Germany).

Measurement of chemical parameters

Totals solids (TS), volatile solids (VS), chemical oxygen demand (COD), electrical conductivity, and total organic carbon (TOC) were determined according to German standard measurement methods [47]. Total nitrogen was determined as previously described (VDLUFA-Methodenbuch II, 3.5.2.7). The VFA spectrum was determined with a gas chromatograph (Shimadzu, Japan). The flame ionization detector was equipped with a DB.1701 column (Machery-Nagel/Germany).

DNA extraction from reactor samples

Three DNA samples were prepared from each sludge sample. In order to reduce the amount of inhibiting substances (especially humic acids), biomass was sedimented by centrifugation (5–10 min at 20,000 g for SS and LB samples, and 15 min at 20,000 g for CD samples) and washed several times with sterile PBS buffer until a clear supernatant was observed. DNA was isolated with the “PowerSoil DNA isolation KIT” (Mo Bio Laboratories, USA) following

the manufacturer's instructions. Long centrifugations were performed (5–10 min at 20,000 g for SS and LB samples, and 15 min at 20,000 g for CD samples) to ensure an almost complete removal of particles and cell fragments after the mechanical bead treatment. Finally, DNA quality was checked on a 0.8 % (w/v) agarose gel and quantified with Nanodrop-1000 Spectrophotometer (Thermo Scientific, Wilmington, DE, USA).

PCR amplification

In order to survey bacterial diversity, a 500-bp fragment of the V1-V3 hypervariable region of the 16S ribosomal RNA gene was PCR-amplified from all the samples with universal primers 28F (5'-GAG TTT GAT CNT GGC TCA G-3') and 519R (5'-GTN TTA CNG CGG CKG CTG-3'). In the case of archaea, primers Arch349F (5'-GYG CAS CAG KCG MGA AW-3') and Ar9r (5'- CCC GCC AAT TCC TTT AAG TTTC-3') were used to amplify a 578-bp fragment of the 16S region [48]. A short (10–12 nucleotides) barcode sequence was included at the 5' end of the oligonucleotides used as forward primers in order to assign sequences to samples after high-throughput sequencing. All the amplifications were performed under the following thermal cycling conditions: initial denaturing at 95 °C for 5 min, followed by 35 cycles of denaturing at 95 °C for 30 s, annealing at 54 °C (for both, bacteria and archaea) for 30 s, and extension at 72 °C for 1 min, finalized by a 10-min elongation at 72 °C. The resulting amplicons were checked on a 0.8 % (w/v) agarose gel and purified by precipitation with 3 M potassium acetate (pH = 5) and isopropanol. Pure amplicons were quantified with the Qubit 2.0 Fluorometer (Invitrogen, Carlsbad, CA, USA), and two equimolar pools of bacteria and archaea amplicons, respectively, were prepared from all the samples.

Ion torrent sequencing

Two sequencing libraries were constructed with 100 ng of the eubacteria and archaea amplicon pool, respectively, by the amplicon fusion method (Ion Plus Fragment Library Kit, MAN0006846, Life Technologies). Each library was quantified with the Agilent2100 Bioanalyzer (Agilent Technologies Inc, Palo Alto, CA, USA) prior to clonal amplification. Emulsion PCRs were carried out applying the Ion PGM Template OT2 400 kit as described in the user guide (MAN0007218, Revision 3.0 Life Technologies) provided by the manufacturer. Finally, the libraries were sequenced in an Ion 318 Chip v2 on a Personal Genome Machine (PGM) (IonTorrent™, Life Technologies) at Life Sequencing S.L. (Life Sequencing, Valencia, Spain), using the Ion PGM Sequencing 400 kit following the manufacturer's protocol (publication number MAN0007242, revision 2.0, Life Technologies). Sequence statistics are shown in Additional file 4: Table S3.

Sequence analysis and taxonomic classification

Raw sequences obtained from the sequencing center were processed with the MOTHUR software [49]. Short (<100 bp) and low-quality (<q15) reads were removed in a first step. The degenerated forward primer sequence was searched among the resulting sequences, and reads were discarded if either the primer (three mismatches allowed) or the barcode sequence was missing. Sequences were then split into groups based on barcode matches, and both primer and barcode sequences were trimmed. Finally, each resulting sequence was aligned to the ribosomal 16S reference Greengenes database and taxonomy was assigned based on nucleotide similarity with the k-mer algorithm. Assignments based on a similarity percentage lower than 70 % were not considered for further analysis.

Statistics

A principal component analysis (PCA) was performed using the Statgraphics software. Data from COD, TOC, total nitrogen contents (N), conductivity, TVFA, TS, VS, pH, and biogas corresponding to all samples were normalized, and two components explaining almost 90 % of the total variance were used for plotting. Row-stacked histograms, representing taxonomic profiles (Figs. 7 and 8), were prepared using Gnuplot and modified with Photoshop to insert grey bars representing intervals of biogas production. Pie charts (Fig. 8) were plotted in Excel. In order to plot all environmental chemical parameters in one diagram (Fig. 6), the `splot` and `multiplot` commands of Gnuplot were combined to plot the permutation of all normalized parameters (normalized to values between 0 and 100). Each combination with three chosen variables was plotted and overlaid with the other combinations using the Gnuplot `multiplot` command. Since nine parameters were measured (COD, TOC, total nitrogen contents, conductivity, TVFA, TS, VS, pH, and volume of biogas), 84 resulting combinations were overlaid in the plot (Fig. 6a).

Acknowledgements

We thank the German Federal Ministry of Economics and Technology (ZIM, grant 16KN017627) for supporting this work. We also thank the plant operators for providing samples and descriptive data (Table 1).

References

1. Damon PE, Kunen SM. Global cooling? *Science*. 1976;193:447–53.
2. Bagley JE, Miller J, Bernacchi CJ. Biophysical impacts of climate-smart agriculture in the midwest United States. *Plant Cell Environ*. 2014. doi:10.1111/pce.12485.
3. Scoma A, Rebecchi S, Bertin L, Fava F. High impact biowastes from South European agro-industries as feedstock for second-generation biorefineries. *Crit Rev Biotechnol*. 2014;1–15.
4. European Commission. Renewable energy road map renewable energies in the 21st century: building a more sustainable future. KOM (2006) 848 final. Brussels: European Commission; 2007.
5. Eurostat–database, source code ten00081 and ten00082. Primary production of renewable energy, 2000 and 2010. [http://epp.eurostat.ec.europa.eu/statistics_explained/index.php/File:Primary_production_of_renewable_energy,_2000_and_2010-fr.png]
6. BGBl (Bundesgesetzblatt) Teil 1. Gesetz zur Neuregelung des Rechts der Erneuerbaren Energien im Strombereich und zur Änderung damit zusammenhängender Vorschriften vom 25.10.2008, 2074–2100; 2008.
7. Rademacher A, Hanreich A, Bergmann I, Klocke M. Black-Box-Biogasreaktor–mikrobielle Gemeinschaften zur Biogas erzeugung. *BIOspektrum*. 2012;18:727–9.
8. Wiese J, König R. From a black-box to a glass-box system: the attempt towards a plant-wide automation concept for full-scale biogas plants. *Water Sci Technol*. 2009;60:321–7.
9. Koch C, Müller S, Harms H, Harnisch F. Microbiomes in bioenergy production: from analysis to management. *Curr Opin Biotechnol*. 2014;27:65–72.
10. Nettmann E, Bergmann I, Pramschüfer S, Mundt K, Plogsties V, Hermann C, et al. Polyphasic analyses of methanogenic archaeal communities in agricultural biogas plants. *Appl Environ Microbiol*. 2010;76:2540–8.
11. Jaenicke S, Ander C, Bekel T, Bisdorf R, Dröge M, Gartemann KH, et al. Comparative and joint analysis of two metagenomic datasets from a biogas fermenter obtained by 454-pyrosequencing. *PLoS One*. 2011;6:e14519.
12. Sträuber H, Schröder M, Kleinstaub S. Metabolic and microbial community dynamics during the hydrolytic and acidogenic fermentation in a leach-bed process. *Energy Sustain Soc*. 2012;2:13.
13. Sundberg C, Al-Soud WA, Larsson M,

- Alm E, Yekta SS, Svensson BH, et al. 454 pyrosequencing analyses of bacterial and archaeal richness in 21 full-scale biogas digesters. *FEMS Microbiol Ecol*. 2013;85:612–26.
14. Luton PE, Wayne JM, Sharp RJ, Riley PW. The *mcrA* gene as an alternative to 16S rRNA in the phylogenetic analysis of methanogen populations in landfill. *Microbiology*. 2002. p. 3521–30.
15. Nettmann E, Bergmann I, Mundt K, Linke B, Klocke M. Archaea diversity within a commercial biogas plant utilizing herbal biomass determined by 16S rDNA and *mcrA* analysis. *J Appl Microbiol*. 2008;105:1835–50.
16. Rademacher A, Zarzewski M, Schlüter A, Schönberg M, Szczepanowski R, Goesmann A, et al. Characterization of microbial biofilms in a thermophilic biogas system by high-throughput metagenome sequencing. *FEMS Microbiol Ecol*. 2012;79:785–99.
17. Solli L, Håvelsrud OE, Horn SJ, Rike AG. A metagenomic study of the microbial communities in four parallel biogas reactors. *Biotechnol Biofuels*. 2014;7:146.
18. Klocke M, Mähnert P, Mundt K, Souidi K, Linke B. Microbial community analysis of a biogas-producing completely stirred tank reactor fed continuously with fodder beet silage as mono-substrate. *Syst Appl Microbiol*. 2007;30:139–51.
19. Goberna M, Insam H, Franke-Whittle IH. Effect of biowaste sludge maturation on the diversity of thermophilic bacteria and archaea in an anaerobic reactor. *Appl Environ Microbiol*. 2009;75:2566–72.
20. Kampmann K, Raterin S, Kramer I, Schmidt M, Zerr W, Schnell S. Unexpected stability of Bacteroidetes and Firmicutes communities in laboratory biogas reactors fed with different defined substrates. *Appl Environ Microbiol*. 2012;78:2106–19.
21. Demirel B, Scherer P. The roles of acetotrophic and hydrogenotrophic methanogens during anaerobic conversion of biomass to methane: a review. *Rev Environ Sci Biotechnol*. 2008;7:173–90.
22. Ziganshin AM, Liebetreu J, Pröter J, Kleinstaub S. Microbial community structure and dynamics during anaerobic digestion of various agricultural waste materials. *Appl Microbiol Biotechnol*. 2013;97:5161–74.
23. Smith AM, Sharma D, Lappin-Scott H, Burton S, Huber DH. Microbial community structure of a pilot-scale thermophilic anaerobic digester treating poultry litter. *Appl Microbiol Biotechnol*. 2014;98:2321–34.
24. Hanreich A, Schimpf U, Zakrzewski M, Schlüter A, Benndorf D, Heyer R, et al. Metagenome and metaproteome analyses of microbial communities in mesophilic biogas-producing anaerobic batch fermentations indicate concerted plant carbohydrate degradation. *Syst Appl Microbiol*. 2013;36:330–8.
25. Luo J, Liang H, Yan L, Ma J, Yang Y, Li G. Microbial community structures in a closed raw water distribution system biofilm as revealed by 454-pyrosequencing analysis and the effect of microbial biofilm communities on raw water quality. *Bioresour Technol*. 2013;148:189–95.
26. Sun H, Shi B, Bai Y, Wang D. Bacterial community of biofilms developed under different water supply conditions in a distribution system. *Sci Total Environ*. 2014;472:99–107.
27. Li C, Motaleb A, Sal M, Goldstein SF, Charon NW. Spirochete periplasmic flagella and motility. *J Mol Microbiol Biotechnol*. 2000;2:345–54.
28. Kragelund C, Levantesi C, Borger A, Thelen K, Eikelboom D, Tandoi V, et al. Identity, abundance and ecophysiology of filamentous Chloroflexi species present in activated sludge treatment plants. *FEMS Microbiol Ecol*. 2007;59:671–82.
29. Björnsson L, Hugenholtz P, Tyson GW, Blackall LL, Hill R. Filamentous Chloroflexi (green non-sulfur bacteria) are abundant in wastewater treatment processes with biological nutrient. *Microbiology*. 2002;148(8):2309–18.
30. Wang ZH, Yang JQ, Zhang DJ, Zhou J, Zhang CD, Su XR, et al. Composition and structure of microbial communities associated with different domestic sewage outfalls. *Genet Mol Res*. 2014;13:7542–52.
31. Lee SH, Kang HJ, Lee YH, Lee TJ, Han K, Choi Y, et al. Monitoring bacterial community structure and variability in time scale in full-scale anaerobic digesters. *J Environ Monit*. 2012;14:1893–905.
32. Traversi D, Villa S, Acri M, Pietrangeli B, Degan R, Gilli G. The role of different

- methanogen groups evaluated by Real-Time qPCR as high-efficiency bioindicators of wet anaerobic co-digestion of organic waste. *AMB Express*. 2011;1:28.
33. Wirth R, Kovács E, Maróti G, Bagi Z, Rákhely G, Kovács KL. Characterization of a biogas-producing microbial community by short-read next generation DNA sequencing. *Biotechnol Biofuels*. 2012;5:41.
34. St. Pierre B, Wright AD. Metagenomic analysis of methanogen populations in three full-scale mesophilic anaerobic manure digesters operated on dairy farms in Vermont, USA. *Bioresour Technol*. 2013;138:277–84.
35. Klocke M, Nettmann E, Bergmann I, Mundt K, Souidi K, Mumme J, et al. Characterization of the methanogenic Archaea within two-phase biogas reactor systems operated with plant biomass. *Syst Appl Microbiol*. 2008;31:190–205.
36. Zhao H, Li J, Li J, Yuan X, Piao R, Zhu W, et al. Organic loading rate shock impact on operation and microbial communities in different anaerobic fixed-bed reactors. *Bioresour Technol*. 2013;140:211–9.
37. Weiß S, Lebhuhn M, Andrade D, Zankel A, Cardinale M, Birner-Gruenberger R, et al. Activated zeolite? suitable carriers for microorganisms in anaerobic digestion processes? *Appl Microbiol Biotechnol*. 2013;97:3225–38.
38. Zhang D, Li J, Guo P, Li P, Suo Y, Wang X, et al. Dynamic transition of microbial communities in response to acidification in fixed-bed anaerobic baffled reactors (FABR) of two different flow directions. *Bioresour Technol*. 2011;102:4703–11.
39. Ariesyady HD, Ito T, Okabe S. Functional bacterial and archaeal community structures of major trophic groups in a full-scale anaerobic sludge digester. *Water Res*. 2007;41:1554–68.
40. Montero B, García-Morales JL, Sales D, Solera R. Evolution of microorganisms in thermophilic-dry anaerobic digestion. *Bioresour Technol*. 2008;99:3233–43.
41. Montero B, García-Morales JL, Sales D, Solera R. Analysis of methanogenic activity in a thermophilic-dry anaerobic reactor: use of fluorescent in situ hybridization. *Waste Manag*. 2009;29:1144–51.
42. Zahedi S, Sales D, Romero LI, Solera R. Optimisation of single-phase dry-thermophilic anaerobic digestion under high organic loading rates of industrial municipal solid waste: Population dynamics. *Bioresour Technol*. 2013;146:109–17.
43. Nakakihara E, Ikemoto-Yamamoto R, Honda R, Ohtsuki S, Takano M, Suetsugu Y, et al. Effect of the addition of rice straw on microbial community in a sewage sludge digester. *Water Sci Technol*. 2014;70:819–27.
44. Li J, Zhang L, Ban Q, Jha AK, Xu Y. Diversity and distribution of methanogenic archaea in an anaerobic baffled reactor (ABR) treating sugar refinery wastewater. *J Microbiol Biotechnol*. 2013;23:137–43.
45. Shen P, Zhang J, Zhang J, Jiang C, Tang X, Li J, et al. Changes in microbial community structure in two anaerobic systems to treat bagasse spraying wastewater with and without addition of molasses alcohol wastewater. *Bioresour Technol*. 2013;131:333–40.
46. Kim J, Kim W, Lee C. Absolute dominance of hydrogenotrophic methanogens in full-scale anaerobic sewage sludge digesters. *J Environ Sci (China)*. 2013;25:2272–80.
47. German standard methods for the examination of water, wastewater and sludge. *Wiley-VCH*. 2013, Weinheim, Germany.
48. Klindworth A, Pruesse E, Schweer T, Peplies J, Quast C, Horn M, et al. Evaluation of general 16S ribosomal RNA gene PCR primers for classical and next-generation sequencing-based diversity studies. *Nucleic Acids Res*. 2013;41:e1.
49. Schloss PD, Westcott SL, Ryabin T, Hall JR, Hartmann M, Hollister EB, et al. Introducing MOTHUR: open-source, platform-independent, community supported software for describing and comparing microbial communities. *Appl Environ Microbiol*. 2009;75:7537–41.

Chapter 2: Holistic characterization of two-stage digestion

Summary: Presented results are the first multi-omics characterisation of a two-stage biogas production system. To assess the underlying fermentation process in more detail, a combination of high-throughput sequencing and proteomics on the acidification step of plant material (grass) at both mesophilic and thermophilic temperatures (37 and 55 °C, respectively) was applied. High-strength liquor from acidified grass biomass exhibited a low biodiversity, which differed greatly depending on temperature. It was dominated by Bacteroidetes and Firmicutes at 37 °C, and by Firmicutes and Proteobacteria at 55 °C. At the methane stage, *Methanosaeta*, *Methanomicrobium* and *Methanosarcina* proved to be highly sensitive to environmental changes as their abundance in the seed sludges dropped dramatically after transferring the seed sludges from the respective reactors into the experimental setup.

Further, an increase in Actinobacteria coincided with reduced biogas production at the end of the experiment. Over 1700 proteins were quantified from the first cycle of acidification samples using label-free quantitative proteome analysis and searching protein databases. The most abundant proteins included an almost complete set of glycolytic enzymes indicating that the microbial population is basically engaged in the degradation and catabolism of sugars. More differentially expressed proteins were found under mesophilic (120) than thermophilic (5) conditions. Metaproteome analyses only detected significant expression differences in mesophilic samples, whereas thermophilic samples showed more stable protein composition with an abundance of chaperones suggesting a role in protein stability under thermal stress.

Publication 2

Abendroth C, Simeonov C, Peretó J, Antúnez O, Gavidia R, Luschign O, Porcar M. From grass to gas: microbiome dynamics of grass biomass acidification under mesophilic and thermophilic temperatures, *Biotechnol Biofuels*. 2015;10:171. doi: 10.1186/s13068-017-0859-0.



Publication 2

From grass to gas: microbiome dynamics of grass biomass acidification under mesophilic and thermophilic temperatures

Christian Abendroth^{1,2,3}, Claudia Simeonov³, Juli Peretó^{1,2,4,7}, Oreto Antúnez⁵, Raquel Gavidia⁵, Olaf Luschnig⁶, Manuel Porcar^{*1,2,7,8}

¹Cavanilles Institute of Biodiversity and Evolutionary Biology, Universitat de València, C/ José Beltran 2, 46980 Paterna, Spain. ²Institute for Integrative Systems Biology (I2SysBio, Universitat de València-CSIC), C/ José Beltran 2, 46980 Paterna, Spain. ³ Robert Boyle Institut e.V., Im Steinfeld 10, 07751 Jena, Germany. ⁴Departament de Bioquímica i Biologia Molecular, Universitat de València, Paterna, Spain. ⁵Servei Central de Suport a la Investigació Experimental (SCSIE), Universitat de València-CSIC, Paterna, Spain. ⁶Bio H2 Energy GmbH, Im Steinfeld 10, 07751 Jena, Germany. ⁷Darwin Bioprospecting Excellence, S.L. Parc Científic Universitat de Valencia, C/ Catedrático Agustín Escardino Benlloch, 9, 46980 Paterna, València, Spain. ⁸Institute for Integrative Systems Biology (I2SysBio, Universitat de València-CSIC), Postal Code 22085, 46071 Paterna, València, Spain.

Abstract

Background: Separating acidification and methanogenic steps in anaerobic digestion processes can help to optimize the process and contribute to producing valuable sub-products such as methane, hydrogen and organic acids. However, the full potential of this technology has not been fully explored yet. To assess the underlying fermentation process in more detail, a combination of high-throughput sequencing and proteomics on the acidification step of plant material (grass) at both mesophilic and thermophilic temperatures (37 and 55 °C, respectively) was applied for the first time.

Results: High-strength liquor from acidified grass biomass exhibited a low biodiversity, which differed greatly depending on temperature. It was dominated by Bacteroidetes and Firmicutes at 37 °C, and by Firmicutes and Proteobacteria at 55 °C. At the methane stage, *Methanosaeta*,

Methanomicrobium and *Methanosarcina* proved to be highly sensitive to environmental changes as their abundance in the seed sludges dropped dramatically after transferring the seed sludges from the respective reactors into the experimental setup. Further, an increase in Actinobacteria coincided with reduced biogas production at the end of the experiment. Over 1700 proteins were quantified from the first cycle of acidification samples using label-free quantitative proteome analysis and searching protein databases. The most abundant proteins included an almost complete set of glycolytic enzymes indicating that the microbial population is basically engaged in the degradation and catabolism of sugars. Differences in protein abundances clearly separated samples into two clusters corresponding to culture temperature. More differentially expressed proteins were found under mesophilic (120) than thermophilic (5) conditions.

Conclusions: Our results are the first multi-omics characterisation of a two-stage biogas production system with separated acidification and suggest that screening approaches targeting specific taxa such as *Methanosaeta*, *Methanomicrobium* and *Methanosarcina* could be useful diagnostic tools as indicators of environmental changes such as temperature or oxidative stress or, as in the case of Actinobacteria, they could be used as a proxy of the gas production potential of anaerobic digesters. Metaproteome analyses only detected significant expression differences in mesophilic samples, whereas thermophilic samples showed more stable protein composition with an abundance of chaperones suggesting a role in protein stability under thermal stress.

Background

Anaerobic digestion is a promising technology for biofuel production, and has been the object of research for over 100 years [1, 2]. The anaerobic digestion process consists of four stages: hydrolysis, acidogenesis, acetogenesis and methanogenesis. During the first three stages, hydrogen and acetate are formed as intermediary products, which are then converted into methane and carbon dioxide during methanogenesis [3]. Countless works have been published characterizing those stages or comparing different substrates for co-digestion and reactor configurations. Furthermore, substantial efforts have been made in recent decades to shed light on the underlying microbial biocoenosis of anaerobic digestion processes. The first determinations of taxonomic profiles appeared in the 90 s [4, 5], when 16S-rDNA data from anaerobic sludges were investigated. More recently, high-throughput approaches like 16S-rDNA sequencing or metagenomics have been applied [2, 6-8], as well as proteome analyses [9, 10].

However, most of the aforementioned work focused on reactor configurations, where acidogenesis and methanogenesis occur, combined in the same reactor stage. It is well-known since the 80 s that the process can be split into multistage processes, in such a way that hydrolysis/acidogenesis occurs separately from acetogenesis/ methanogenesis [11, 12]. Although it may be difficult to fully separate the underlying microbial processes (for example nitrogen-rich substrates seem to cause methanogenic contaminations in the acid-producing step [13]), improved biogas production has been reported using a separated setup. For example, in 1988 authors described a rumen-derived microbial community optimally fermenting cellulose in a separated acidification step [14]. Others report that some practices such as shock loading (high loads of substrate that cause accumulation of volatile fatty acids, VFA) increase hydrogen formation at pH < 6.5 [15]. As pH values between 4 and 6.5 are common during acidification [16–18] and methanogenesis is inhibited at either low pH or high VFA concentration [19], this renders hydrogen production in the acidification stage as a valuable sub-product in addition to the methane [20]. Additionally, a high concentration of acetic acid is known to improve chemical hydrolysis [21]. Even though hydrogen production in seed sludges with diverse microbiomes is highly unpredictable, a few previous reports have explored the possible production of hydrogen [22–24], by, for example, immobilization of hydrogen-producing bacteria [23, 24].

Separated acidification has been proposed as the best technology to produce organic acids like lactic, butyric and acetic acid, even though it is still complicated to extract organic acids from the fermentation process [25]. The benefits of separated acidification cannot be fully explored without a deeper knowledge of the underlying

microbial communities. Currently, such knowledge is very fragmentary. For example, it is known that fermentation of 52.85 g/L of rice straw at 39.23 °C and pH 10.0 leads to an increase in the families Ruminococcaceae, Bacteroidaceae, Porphyromonadaceae and Lachnospiraceae [26]; or that the acidification of alginate correlates with high titres of *Bacteroides*- and *Clostridium*-related microorganisms [27]. Proteomics has been used to study standard, one-step digestion plants without separated acidification [9, 10, 28], but there are no detailed proteomics studies of a separated acidification stage to date. In order to bridge this gap and to finely characterize one of the most important phases of the biogas production process, the dynamic behaviour of grass acidification processes at mesophilic and thermophilic temperatures (37 and 55 °C, respectively) was monitored through both proteomics and 16S-rDNA analysis. The efficient use of lignocellulosic biomass as a feedstock is an active research area of high interest [30]. In the present work grass was chosen because of its potential as a renewable energy source [29].

Results and discussion

16S-rDNA-based analysis on high-strength liquor from grass acidification

Mechanically ground mixed grass (Graminidae) was acidified in three subsequent batch reactions under anaerobic conditions at mesophilic and thermophilic temperatures (Fig. 9). pH was automatically adjusted to 5.5 to prevent it dropping below that value. Acidification occurred in tap water as a result of microbial activity. The second and third batch received 5 % Inoculum from the previous batch. Samples for VFA analysis were taken daily and every two days for 16S-rDNA amplicon sequencing. The

mixed grass microbiome was analysed prior to entering acidification reactors, and it proved rich in Cyanobacteria- and Proteobacteria-related taxa. Upon transference into the reactors, the taxonomic profile rapidly switched to the one dominated by members of the phylum Firmicutes. This happened under both mesophilic and thermophilic conditions (Fig. 9).

After just two days, hardly any Proteobacteria and Cyanobacteria remained. As often occurs with 16S-rDNA-based analyses of plant material, cyanobacteria-related sequences may correlate to plant chloroplasts. On day four, most of the Firmicutes were suppressed by Bacteroidetes at mesophilic temperatures, while the proportion of Firmicutes remained high at 55 °C. The acidification process was repeated three times in a row and Bacteroidetes were also the dominating phylum at mesophilic temperatures. At thermophile temperatures the dominant phylum was Firmicutes, although at two of the sampling points a strong but transitory shift towards Proteobacteria was observed (Fig. 9a). In the second and third week an inoculum from the previous stages was used; however, this hardly influenced the taxonomic profile, which was constantly dominated by Bacteroidetes.

Upon termination of each acidification cycle, the high-strength liquors produced were transferred into bottles filled with nitrogen and stored at room temperature thereafter (Fig. 9b). The microbial composition in the stored liquor was analysed (Fig. 9, right) and yielded no significant changes at mesophilic temperature. However, a strong shift in the stored liquor originating from the thermophilic reaction was observed after incubation at room temperature (RT). After four days at RT, numbers of Bacteroidetes dramatically increased, yielding a stable taxonomic profile very similar to the

one of the mesophilic acidification in the concentration of chemical oxygen demand (COD) or VFA (Data not shown). The microbial profile of the thermophilic samples upon RT storage was not accompanied by any changes

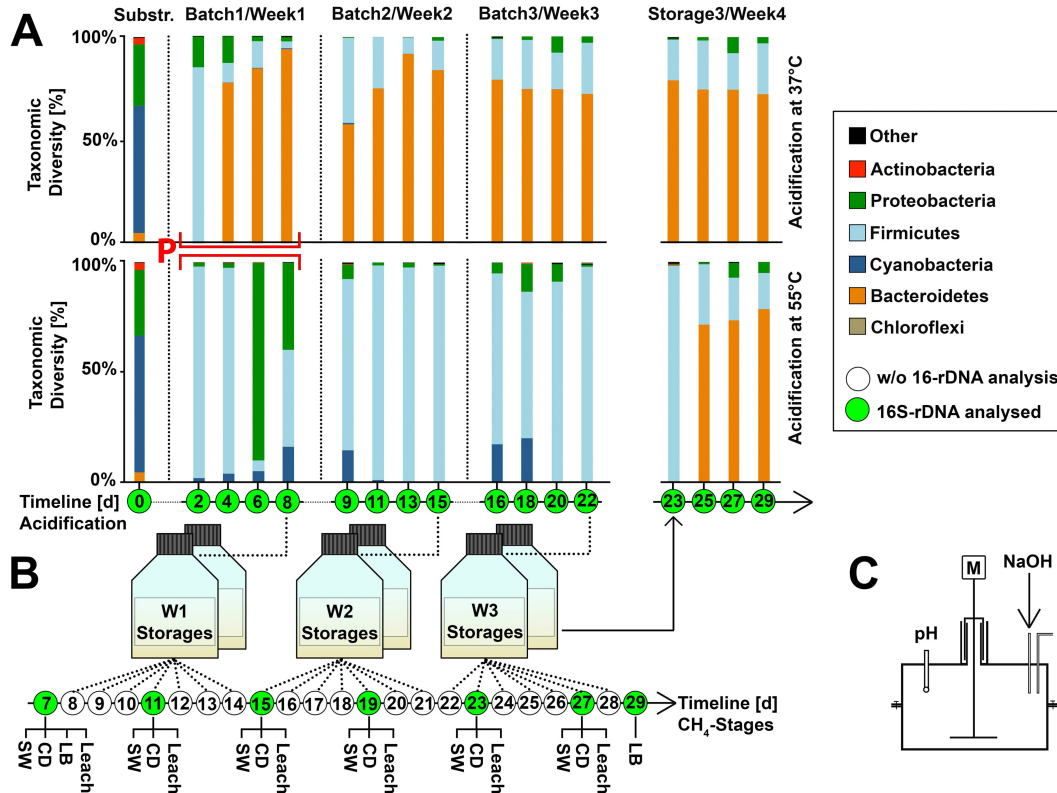


FIGURE 9: 16S-rDNA-based taxonomic profiles from untreated grass substrate, samples during acidification and stored hydrolysate, at 37 °C (upper panel) and 55 °C (lower panel) (a). Hydrolysate was filled in anaerobic storage bottles and from there it was transferred semicontinuously into various methane stages (b). For both, mesophilic and thermophilic acidogenesis continuous stirred tank reactors (CSTR) were used. Those were equipped with a pH sensor, which automatically regulated the inflow of NaOH for pH adjustment to 5.5 (c). Proteomic analysis was performed with samples from the first week of acidification (Highlighted with a red letter P). Green circles in the timeline correspond to days of taxonomic analysis (white circles were subjected to chemical analysis). The first column (Substr.) shows the taxonomic composition of the untreated grass biomass.

The results are in concordance with a previous work describing high titres of Bacteroidetes and Firmicutes during acidification of alginate under mesophilic conditions [24]. A microbiome dominated by Bacteroidetes and Firmicutes has also been reported for one-stage processes at mesophilic temperatures [9, 31, 32], but not for sewage sludge [7, 8]. There are no previous reports on the microbiome of acidification at thermophilic temperatures; however, a shift to Clostridia (Firmicutes) has been described for one-stage digesters [33, 34], similar to the increased titre of Firmicutes described in the present results.

Environmental parameters

Production of total volatile fatty acids (TVFAs) was more effective

at mesophilic temperatures than at thermophilic ones (Fig. 10). With 200 mg TVFA per gram of input COD, the mesophilic stage yielded twice as many TVFAs as at thermophilic temperatures (Fig. 10a). At 37 °C, the relative amount of acetic acid and propionic acid were much higher than at 55 °C (Fig. 10b). By contrast, an accumulation of butyric acid was observed at thermophilic temperatures.

To the best of our knowledge, there are no previous reports comparing taxonomic profiles of mesophilic and thermophilic biogas acidification stages.

There are reports, however, that thermophilic processes in onestage digesters result in higher degradation efficiency compared to mesophilic ones [34–37]. Previous works have reported long incubation times for adaption of the biocoenosis to thermophile temperatures, ranging from several months [35] to up to one year [37]. Therefore, successful adaption to high temperatures and well-chosen seed sludge might be crucial for a separated acidification step.

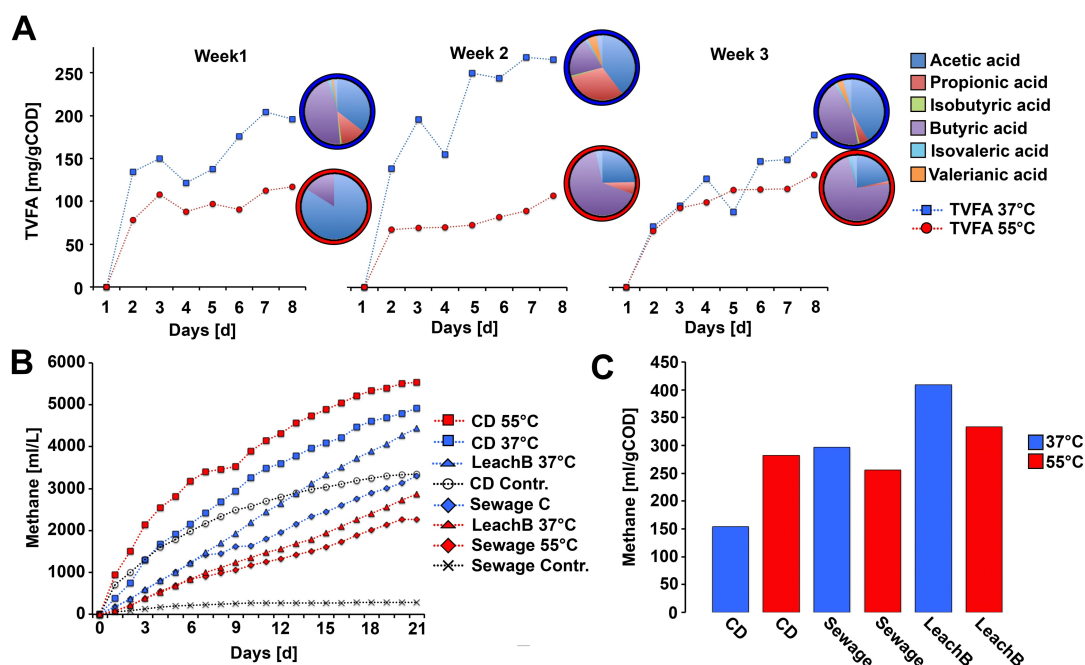


FIGURE 10: Chemical parameters during acidification and methane production: total amount of TVFA was monitored daily and samples obtained at the end of each acidification cycle were subjected to the determination of VFA spectra (a). Produced methane is shown as volume of methane per volume of sludge (b) and as volume of methane per mg of input COD (c).

In concordance with the reduced acid production in the thermophilic acidification, two of the corresponding methane stages (leach bed and semicontinuous batch with sewage) yielded more methane per gram of input COD with thermophilic liquor than with mesophilic. (Fig. 10c). However, in

the system containing seed sludge from a co-digester (CD), the yield from the thermophilic treated liquor was higher than in the one receiving mesophilic liquor. This might be related to the higher total solids (TS) content, high heterogeneity and high gasification activity also causing very high gas yields

in the negative control from the CD sludge (Fig. 10b). In concordance with a previous work [38], the liquefied COD from the produced high-strength liquor was efficiently transformed into methane, indicating no inhibitory effects.

Usage of the high-strength liquor produced High-strength liquor was stored in bottles at RT upon production, which were always flushed with nitrogen after opening to keep anoxic conditions. The liquor was semicontinuously fed into various methane stages (Figs. 9b, 10, 11).

The used seed sludge from the co-digester was very rich in Firmicutes, Synergistetes and Bacteroidetes, while the seed sludge from the sewage plant (SW) consisted mainly of Proteobacteria, Bacteroidetes, Spirochaeta and Chloroflexi (Matrix at day 7, Fig. 11). Both findings are in concordance with our previous report on several co-digester microbiomes [8]. The starting samples for the leach-bed systems (Matrix at day 7, Fig. 11) were taken 24 h after refilling the leach bed with sewage seed sludge. Compared to the original sewage, there was a dramatic decrease in Actinobacteria. This may be due to the high sensitivity of Actinobacteria to environmental changes, as sensitivity to environmental changes has been described for Actinobacteria in soil [39]. The two leach-bed systems were both rich in Chloroflexi, especially in the leach-bed biofilm (Fig. 11, Leach Bed). This is in concordance with other works describing high abundance of Chloroflexi in deep biofilm layers on building walls [40] and in the sediments of Winogradsky columns [41]. The input of the high-strength liquor, rich in Firmicutes and Bacteroidetes, did not result in an increase in those phyla in the sewage sludge batches or in the leach-bed systems (SW and Leach samples from Day 11 to Day 27, Fig. 11). Samples from both

systems remained rich in Chloroflexi and Spirochaeta, even though they received a daily microbial input rich in Firmicutes and Bacteroidetes. This highlights the stability of the underlying biocoenosis and suggests the potential of separated acidification as an important step in preventing the occurrence of major microbial disturbances in the biocoenosis of the respective sewage digesters. For example, an additional thermophilic acidification stage could be included in co-digestion in sewage digesters in order to improve the robustness of the active microbiome. The positive effect of codigesting organic matter with sewage sludge (e.g. food waste or energy grass) on the reactor performance has recently been reported [42, 43]. Moreover, the application of leachate in sewage digestion has been proposed too [44]. Our results indicate that using liquefied grass biomass (after separation from solids) might be a promising method for co-digestion with sewage. Large amounts of unused grass biomass, could still be valorised [29]. Although there have been attempts to add grass biomass into sewage sludge for co-digestion [45], co-digestion of liquefied grass biomass with sewage has not been demonstrated until now.

During the experiment, the lowered temperature in the storage bottle of the high-strength liquor at room temperature (Storage 3/Week 4, Fig. 9) resulted in a dramatically modified community composition of the thermophilic liquor after two days at RT. Thus, the transference of thermophilic high-strength liquor into a mesophilic sewage digester might destabilize the microbial community in the liquor and provide an advantage to the existing biocoenosis from the sewage digester. Using the high-strength liquor for co-digestion prevented the entry of solids into the water treatment circle.

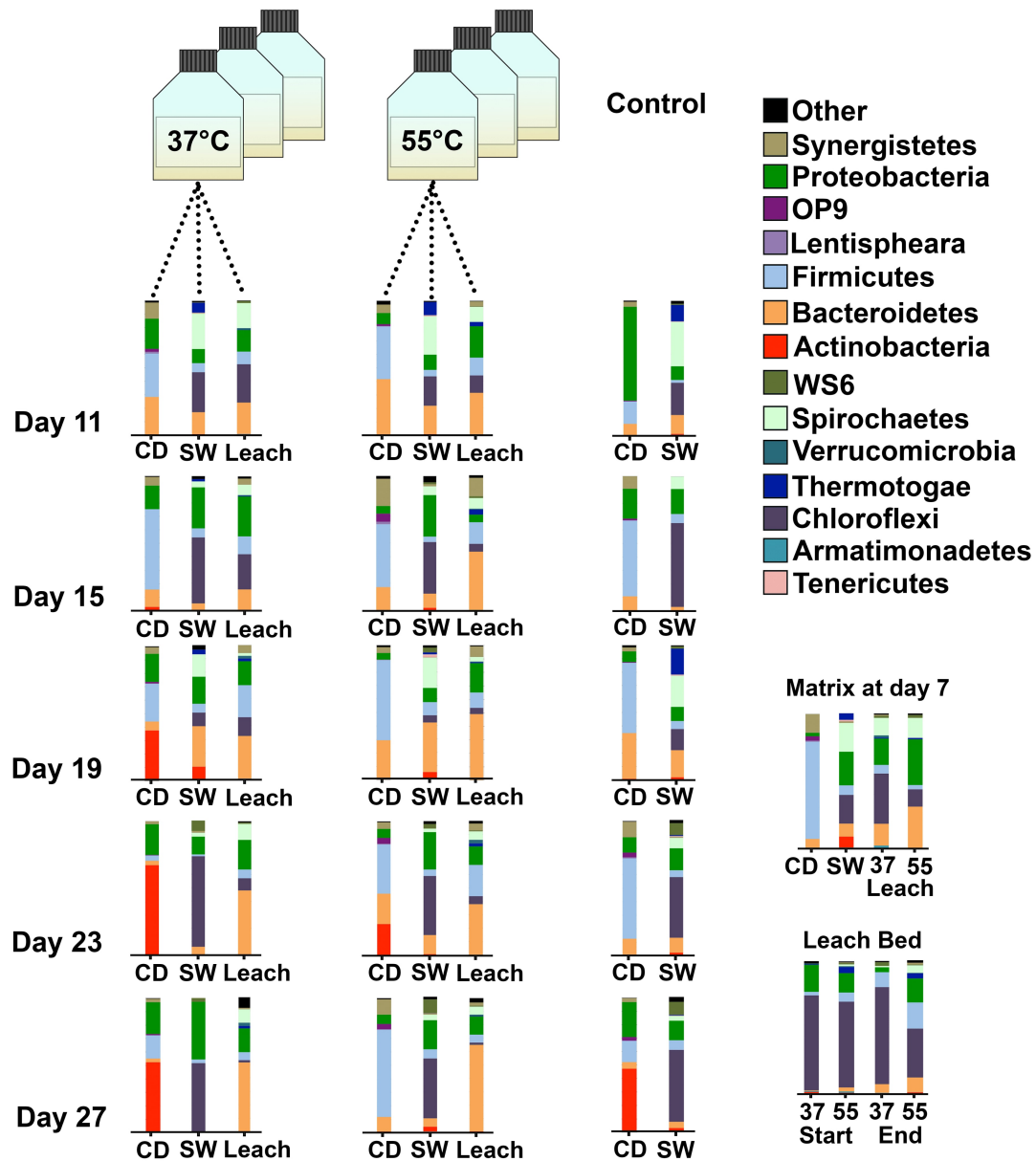


FIGURE 11: Bacterial community in the CH_4 -stages: Time-dependent taxonomic profiles at the phylum level over 20 days for various CH_4 -stages digesting hydrolysate from mesophilic and thermophilic acidification. All CH_4 -stages were performed at mesophilic temperatures. Control reactions were not fed. Taxonomic profiles of the sludges prior to the experimental setup were determined as controls, as well as the taxonomic profiles of the biofilms from the leach-bed systems. CD co-digester, SW sewage, Leach Leachate.

In the last days of the experiment, the sludge samples from the co-digester exhibited low levels of Firmicutes and Bacteroidetes, and high rates of Actinobacteria. This coincided with a reduction in the production of biogas [8]. Actinobacteria were described in previous works as important key players in the degradation of plant

material in compost [48] with effective enzymes that can allow large-scale application for breakdown of cellulosic plant material [49]. This is not necessarily contradictory with our results, since Actinobacteria survival and its efficiency for degradation of plant material could vary greatly at different nutrient concentrations due to their sensitivity to environmental changes as mentioned before. Although further work is needed to confirm this link, it is tempting to propose the identification and quantification of microbial key players as a marker of process efficiency. In the case of the leach-bed system, the last part of the experiment was characterized by higher amounts of Bacteroidetes in the liquid phase (Leach samples from Day 11 to Day 27, Fig. 11). It has to be stressed that the biofilm became denser during the experiment and thus a biofilm filtering effect could be responsible for the very clear supernatant observed at the end of the process, which might, in turn, have affected the microbial composition of the leachate.

Archaea were also detected through 16S-rDNA amplicon sequencing and identification (Fig. 12). The genus *Methanoculleus* was the most abundant one in most of the samples. The co-digester sludge contained small amounts of *Methanobacterium* and *Methanosarcina*, as previously reported for the same plant [8] (Matrix at day 7, Fig. 12). However, upon transferring the sludge into the batch systems, a rapid shift was observed, in terms of an overwhelming abundance of *Methanoculleus* (CD, SW and Leach-Bed Samples at day 11, Fig. 12). This might be related to stress factors caused by the sludge transference (e.g. changing reactor conditions or short-time exposure to oxygen), and it could be hypothesized that *Methanoculleus* is more resistant to these changes. This is consistent with previous reports on the robustness of *Methanoculleus*, which is particularly

resistant to inhibitors such as ammonia [50], phenol [51] or paraffin [52].

After eight days of incubation under constant conditions *Methanosaeta* and *Methanobacterium* started to recover in the batch reactions with the sewage seed sludge (Fig. 12), although no significant increases were observed for the leach-bed system. However, *Methanosaeta* proved frequent in the biofilm from the leach bed, (Fig. 12, Leach Bed). The occurrence of *Methanosaeta* in biofilms has been reported previously [53, 54]. This result highlights the need for a separate analysis of leach-bed samples and associated biofilms. In the co-digesters, *Methanosarcina* were also recovered as of day 23 (CD samples at day 23–27, Fig. 12).

Proteomic analysis on the high-strength liquor produced

Proteins were extracted from the samples d2, d4, d6 and d8 from the first cycle of acidification. The proteome at mesophilic and thermophilic temperatures proved strikingly different in the previous SDS-PAGE analysis (Additional file 1: Figure S3). This observation was approved by a principal component aggregation (PCA) from mass spectroscopy raw data (peptide) analysis, where samples not only separated into two groups by temperature (X-axis, Fig. 13b), but also showed dynamic changes in time (Y-axis, Fig. 13b).

At the first stages, plant proteins were detected in the greatest amounts, as expected from the mixed grass biomass used in all assays. However, in line with increasing incubation time, the ratio between plants and bacteria shifted due to massive microbial growth and/or degradation of plant material at 37 °C (Fig. 13a). However at 55 °C, there was a constant plant:bacteria ratio in the protein abundance, indicating a decrease in the total microbial population.

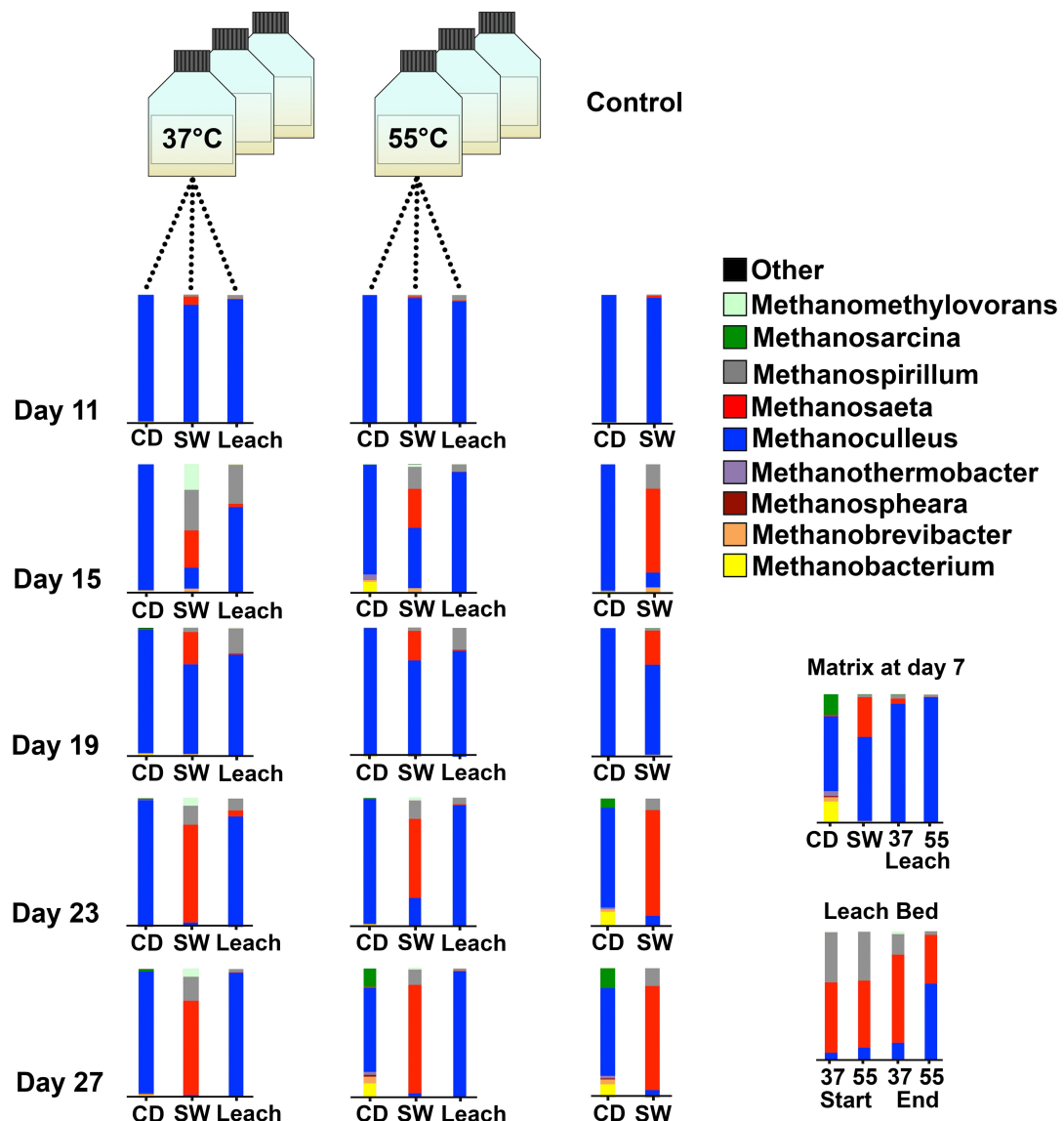


FIGURE 12: Archaeal community in the CH₄-stages: Time-dependent community behaviour at the genus level over 20 days for various CH₄-stages digesting hydrolysate from mesophile and thermophile acidification. All CH₄-stage measurements were performed at mesophilic temperatures. CD co-digester, SW?sewage, Leach Leachate.

An abundance of enzymes involved in carbohydrate metabolism and degradation in metaproteomes from both series of samples were identified using a protein database search for Bacteria and Archaea domains, although additionally diverse chaperones and heatshock proteins (e.g. 10 and 60 kDa chaperonins, and GroEL) were overrepresented in the thermophilic samples (Additional file 2: Table S4). Among the most abundant

proteins detected in all analysed samples, there was an almost complete set of glycolytic enzymes (glucose-6-phosphate isomerase, fructose-bisphosphate aldolase, triosephosphate isomerase, glyceraldehyde-3-phosphate dehydrogenase, phosphoglycerate kinase, enolase), as well as components of sugar transport systems (like the phosphotransferase system, PTS). These results indicate that the microbial

population is basically engaged in the degradation and catabolism of sugars in the fermentative phase of short-chain acid production, an observation that is coherent with

previous reports on the metaproteome [28] and metametabolome [55] of this kind of microbial communities.

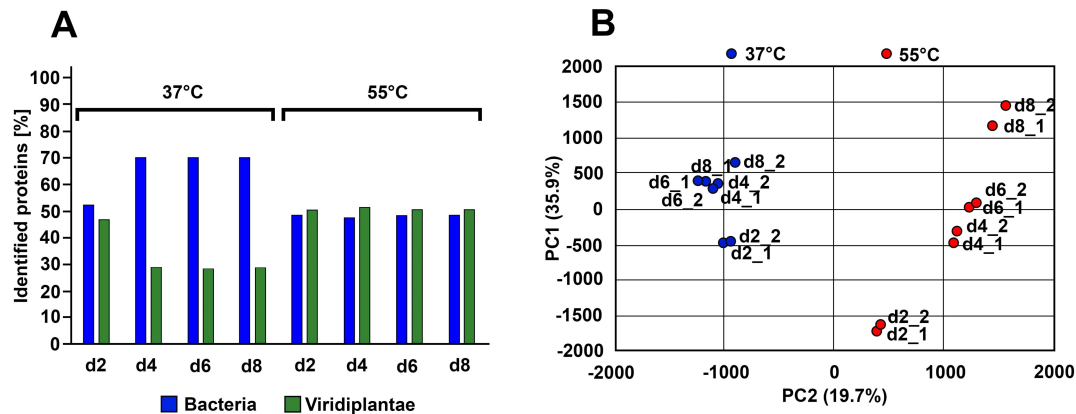


FIGURE 13: Bacteria and Viridiplantae proteomic profile evolution in the first cycle of acidification (a); PCA aggrupation of quantified peptides at mass spectroscopy analysis (b).

Label-free quantitative proteome analysis was performed to determine differentially expressed proteins between mesophilic and thermophilic temperatures (Additional file 3: Table S5). A total of 1731 proteins were quantified from samples d2, d4, d6 and d8 collected from the first cycle of acidification: 556 proteins increased and 176 decreased between mesophilic and thermophilic conditions (37 vs. 55 °C). Samples were compared using the Limma statistics software package. Differences in protein abundances clearly separated samples into two clusters corresponding to culture temperature, with the subset of proteins showing an increased expression that was richer at 37 than 55 °C (Fig. 14a). On comparing protein abundances during sampling time, 120 (out of 1731) proteins showed differential expression at 37 °C, whereas at 55 °C, the differentially expressed proteins were only 5 (out of 1731) (Fig. 14b). Remarkably, most differences were observed when comparing d2 and d4 samples, and d2

and d8 at mesophilic conditions, whereas at thermophilic conditions a small set of differential proteins was only detected when comparing samples d2 and d8 (Fig. 14b). Among the differentially expressed proteins at mesophilic conditions there is a notable representation of ribosomal proteins indicating a dynamic state of these microbial communities. The taxonomic profiles of metaproteome samples were in agreement with the presented metagenomic data.

Among the differentially expressed proteins in d2 samples at 37 °C, noteworthy was the presence of several membrane transport systems from Firmicutes species involved in sugar uptake. These were the PTS HPr-related protein and the cellobiose-specific PTS IIB component, and the PTS phosphocarrier protein HP. There was also an increase in haemolysin-type calcium-binding protein, with a predicted hydrolytic activity on O-glycosyl compounds and a carbohydrate-binding domain (CBM)

type 2 from an Alphaproteobacterium in d2 samples. Previous studies on mesophilic biogas-producing, cellulolytic communities have indicated

the abundance of sugar transporters and enzymes involved in polysaccharide degradation [9, 28, 56].

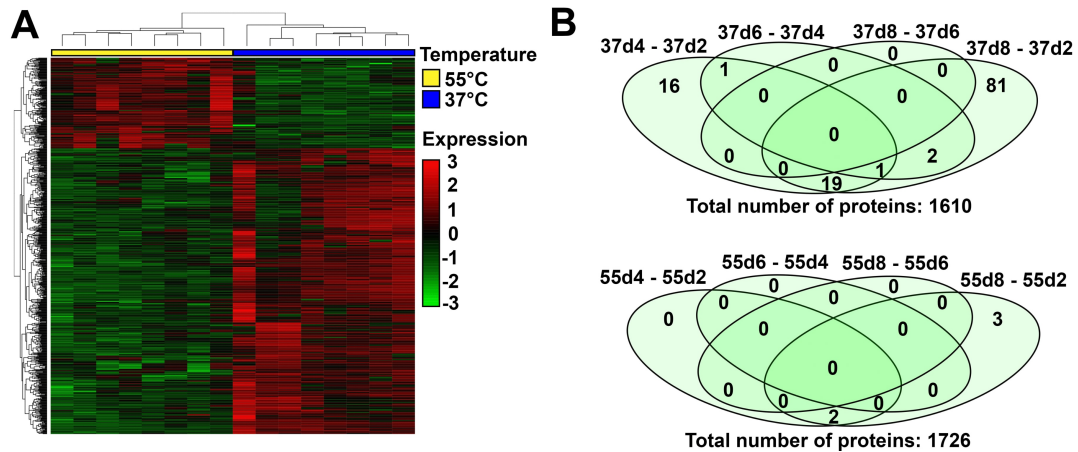


FIGURE 14: Proteomic differences between 37 and 55 °C: HCT for differentially expressed proteins between mesophilic and thermophilic conditions (a). Number of differentially expressed proteins (p value < 0.05) over time at two different culture temperatures: 37 °C (upper Venn diagram) and 55 °C (lower Venn diagram) (b).

Conclusions

Plant biomass (a mix of grass) was acidified at mesophilic and thermophilic temperatures. The taxonomic communities in both cases proved very different, and consisted of Bacteroidetes and Firmicutes at °C and Firmicutes and Proteobacteria at 55 °C. At the methane stage, *Methanosaeta*, *Methanomicrobium* and *Methanosarcina* proved highly sensitive to environmental changes whereas *Methanoculleus* proved to be very robust with all the seed sludges. At the end of the experiment, there was an increase in Actinobacteria in the semicontinuous batches containing co-digester seed sludge, which coincided with reduced biogas formation. Thus, Actinobacteria determination could be a useful prediction tool for biogas production.

Metaproteome analyses only detected significant expression differences in mesophilic samples, and collectively implied a dynamic microbial community

engaged in polysaccharide demolition and sugar fermentation as remarkable metabolic activities during the acidification phase. Thermophilic samples showed more stable protein composition with an abundance of chaperones suggesting a role in protein stability under thermal stress.

Materials and methods

Reactor performance

Acidification of grass was carried out in three sequential reactions, which were operated in parallel at 37 and 55 °C with a COD input concentration of 30 gO₂/L. Acidification occurred in tap water as a result of microbial activity. For the second and third cycle of acidification 5 % inoculum was applied from the previous reactions. After separating the liquid phase from the solids manually using a sieve, the resulting high-strength liquor was stored

under anaerobic conditions (nitrogen atmosphere) until further fermentation occurred in several methane stages (Fig. 9). Acidification was carried out in continuous stirred tank reactors with a total working volume of 5 L and equipped with a pH regulation system (BL 7916, Hanna Instruments, Germany) that stabilized the pH at 5.5 (Fig. 9). The high-strength liquor was stored until usage in glass bottles at RT. To ensure anaerobic atmosphere, the bottles were nitrogen-purged and a gasbag (TECOBAG, TESSERAUX Spezialverpackungen GmbH, Germany) was connected to verify that no further gas production occurred. High-strength liquor was digested in semicontinuous batch reactions, as well as two leach-bed systems. The setup of batch systems was carried out according to VDI 4630 [57]. Feeding was applied not only at the beginning of the experiment but semicontinuously by adding daily 33 mL/L day to the batch bottles, which corresponds to a solubilized COD of 0.51 gO₂/L for the mesophilic stage and 0.39 gO₂/L for the thermophilic stage.

The leach-bed systems consisted of packed columns with 3 L working volumes. They were filled with 2 L of seed sludge and 485 g of bed packing (Hel-X-Füllkörper, Christian Stöhr GmbH&Co.KG, Germany) and were fed equally to the batch bottles with 33 mL/L-d. Gas production was quantified with a MilliGascounter (Ritter Apparatebau GmbH, Germany) and collected in a gasbag for further analysis (TECOBAG, TESSERAUX Spezialverpackungen GmbH, Germany). In total, eight methane stages were set in place. Two leach-bed systems, three batch systems filled with low TS seed sludge (sewage) and three batch systems filled high TS seed sludge (CSTR, co-digester) (Additional file 4: Table S1 and Additional file 5: Table S2). The leach-bed systems were filled with sewage sludge and the leach bed contained a thick

biofilm from previous experiments also performed with sewage. All methane stages were set as duplets in order to compare methanisation of liquor from acidification, at 37 and 55 °C. Control reactions without feeding were performed (Fig. 9).

Sampling and environmental chemical analysis

A mixture of grass species was collected from a backyard in Jena (Germany) and mechanically ground. Mechanical treatment was performed using a conventional juicer (Angel Juicer 8500 s, Angel Co.LTD., Corea). After the mechanical treatment, grass juice and squashed solids were remixed and stored at -20 °C until use.

Sewage was collected from a water treatment plant in Jena (Jena). Sludge from a co-digester was collected from the continuous stirred tank reactor near the water treatment plant. Sludge samples and substrates were characterized by analysing TS and VS (Additional file 4: Table S1) and during the acid-producing step, the concentration of VFA and COD was monitored daily using conventional photometer-based assays (Nanocolor CSB15000 and Nanocolor organische Säuren 3000, Macherey-Nagel, Germany) (Fig. 10). At the end of each experiment, the VFA spectrum was determined at Eurofins Umwelt Ost GmbH, using a gas chromatograph (Shimadzu, Japan). A flame ionization detector was equipped with a DB.1701 column (Macherey-Nagel, Germany).

During methanisation of the high-strength liquor produced, the volume of biogas obtained was monitored daily, using a "COMBIMASS GA-m" gas measurement device (Binder, Germany), to determine the ratio of CO₂ and CH₄ (Fig. 10). Samples for DNA analysis were taken every two days for the acidification step and every four days for the methane stages. One milliliter of sample was mixed with 1

mL of pure ethanol and kept at -20°C until required. Additional samples from the acidification stages were taken for proteomic approaches (20 mL per sample). Samples for proteomic analysis were stored at -70°C until further analysis.

DNA extraction and amplification

To reduce the amount of humic acids and other inhibitors, samples were intensively washed: they were centrifuged at 20,000·g and resuspended in PBS buffer repeatedly until a clear supernatant was observed. DNA Extraction was performed using the PowerSoil DNA isolation KIT (Mo Bio Laboratories, USA). After a quality control on a 0.8 % (w/v) agarose gel and quantification with the Nanodrop-1000 Spectrophotometer (Thermo Scientific, Wilmington, DE, USA), variable regions V1–V3 from the 16S-rDNA gene were amplified. For amplification of bacterial 16S-rDNA sequences the universal primers 28F (5'-GAG TTT GAT CNT GGC TCA G-3') and 519R (5'-GTN TTA CNG CGG CKG CTG-3') were used (Additional file 6: Table S6 and Additional file 7: Table S7). Archaea target sequences were amplified using the primers Arch349F (5'-GYG CAS CAG KCG MGA AW-3') and Ar9r (5'- CCC GCC AAT TCC TTT AAG TTTC-3') (Additional file 8: Table S8). Resulting amplicons had a length of 500 bp for bacteria and 578 bp for archaea [58]. For amplification, after initial denaturation at 95°C for 5 min, 35 cycles of amplification (95°C for 30 s, 54°C for 30 s, and extension at 72°C for 1 min) were carried out. The reaction was completed with a 10-min elongation step at 72°C .

DNA-sequencing and analysis

All DNA-sampled were quantified using the Qubit[®] 2.0 Fluorometer (Invitrogen, Carlsbad, CA, USA). For bacteria and archaea, separate libraries were built. Approximately 100 ng of each sample

was added applying the amplicon fusion method (Ion Plus Fragment Library Kit, MAN0006846, Life Technologies). For quantification, the Agilent 2100 Bioanalyzer (Agilent Technologies Inc, Palo Alto, CA, USA) was used. PCRs were carried out applying the Ion PGM Template OT2 400 kit as stated by the manufacturer (MAN0007218, Revision 3.0 Life Technologies). For the final sequencing step, an Ion 318 Chip v2 on a Personal Genome Machine (PGM) (IonTorrent[™], Life Technologies) at Life Sequencing S.L. (Life Sequencing, Valencia, Spain) was used. Here the Ion PGM Sequencing 400 kit was applied, following the manufacturer's instructions (publication number MAN0007242, revision 2.0, Life Technologies).

After removing short (<100 bp) and low-quality (<q15) reads, resulting sequences were split and barcode sequences were trimmed. Final sequences were then analysed using Mothur [59]. Based on the k-mer algorithm, sequences were aligned to the 16S reference from the Greengenes database. In the case of eubacteria, assignments were performed at the phylum level. Assignments with a similarity percentage lower than 70 % were not considered for further analysis. In case of archaea, amplicons were analysed at the genus level and the cut-off was set to 93 %.

Protein extraction, identification and data analysis

Protein extraction was performed using the NoviPure Soil Protein Extraction Kit (MO BIOS Laboratories Inc). Total protein extracts were precipitated with TCA (Trichloroacetic Acid) to clean total extracts, and pellets were dissolved with 100 μL of 8 M Urea, 0.5 M TEAB (Triethylammonium bicarbonate buffer). The protein concentration in the samples was determined using Qubit[®] 2.0 Fluorometer (Invitrogen, Carlsbad, CA, USA). Then, 20 μg of

each sample was digested as described in the following protocol. Cysteine residues were reduced by 2 mM DTT (DL-Dithiothreitol) in 50 mM ABC (Ammoniumbicarbonate) at 60 °C for 20 min. Sulphydryl groups were alkylated with 5 mM IAM (iodoacetamide) in 50 mM ABC in the dark at room temperature for 30 min. IAM excess was neutralized with 10 mM DTT in 50 mM ABC, 30 min at room temperature. Each sample was subjected to trypsin digestion with 500 ng (100 ng/ μ L) of sequencing grade-modified trypsin (Promega) in 50 mM ABC at 37 °C overnight. The reaction was stopped with TFA (trifluoroacetic acid) at a final concentration of 0.1 %. Final peptide mixture was concentrated in a speed vacuum and suspended in 65 μ L of 2 % CAN, 0.1 %TFA. Finally, 1.5 μ g of each sample was used for protein identification by LC_MS/MS analysis and label-free differential expression analysis. For that 5 μ L of each sample was loaded onto a trap column (NanoLC Column, 3 μ m C18-CL, 75 μ m · 15 cm; Eksigent) and desalted with 0.1 % TFA at 3 μ L/min during 10 min. The peptides were then loaded onto an analytical column (LC Column, 3 μ C18-CL, 75 μ m · 12 cm, Nikkyo) equilibrated in 5 % acetonitrile 0.1 % FA (formic acid). Elution was carried out with a linear gradient from 5a35 % B in A for 120 min. (A: 0.1 % FA; B: ACN, 0.1 % FA) at a flow rate of 300 nL/min. Peptides were analysed in a mass spectrometer nanoESIqQTOF (5600 TripleTOF, ABSCIEX).

Eluted peptides were ionized applying 2.8 kV to the spray emitter. Analysis was carried out in a data-dependent mode. Survey MS1 scans were acquired from 350–1250 m/z for 250 ms. The quadrupole resolution was set to 'UNIT' for MS2 experiments, which were acquired 100–1500 m/z for 50 ms in 'high sensitivity' mode. Following which switch criteria were used: charge: 2+ to 5+; minimum intensity; 70 counts per

second (cps). Up to 25 ions were selected for fragmentation after each survey scan. Dynamic exclusion was set to 25 s.

ProteinPilot default parameters were used to generate peak list directly from 5600 TripleTof wiff files. The Paragon algorithm of ProteinPilot v 4.5 was used to search Uniprot bacteria and Archaea protein database with the following parameters: trypsin specificity, cys-alkylation and the search effort set to through with FDR to multiple test correction.

To avoid using the same spectral evidence in more than one protein, the identified proteins were grouped based on MS/MS spectra by the ProteinPilot Pro group algorithm. The Peak View v1.1 (SCIEX) software was used to generate peptide and protein areas from ProteinPilot result files and to perform a multivariant data analysis.

Differential expression analysis was performed using the Limma package (<http://bioconductor.org/packages/limma/>), fitting a linear model using an appropriate design matrix. A contrast matrix was set to make comparisons of interest, in our case 37 versus 55 °C. For the contrast of interest the package computed fold changes and t-statistics. After fitting a linear model, the standard errors were moderated using an empirical Bayes method to obtain moderated t-statistics. The function top Table was used to present a list of the proteins most likely to be differentially expressed for a given contrast. FDR was used to adjust the p value for multiple testing.

Acknowledgements

We thank our students and traineeships Robert Förster, Justus Hardegen, Sonia Casani and Sandra Jörg for technical assistance. Further we thank Dr. Peter Miethe from the research centre for medical technology and biotechnology (FZMB) in Bad Langensalza for his suggestions regarding the title. We

are grateful for funding of the work by the Federal Ministry of Economic Affairs and Energy in Germany (Funding Numbers FKZ03KB110A; 16KN041331, KF2112205SA4 and KF3400701SA4). Servei Central de Suport a la Investigació Experimental (SCSIE) from University of València belongs to ProteoRed, PRB2-ISCI, supported by grant PT13/0001, of the PE I+D+i 2013–2016, funded by ISCI and FEDERPT13/0001.

References

1. McCarty PL. The development of anaerobic treatment and its future. *Water Sci Technol.* 2001;44:149–56.
2. Wirth R, Kovács E, Maróti G, Bagi Z, Rákhely G, Kovács KL. Characterization of a biogas-producing microbial community by short-read next generation DNA sequencing. *Biotechnol Biofuels.* 2012;5:41.
3. Haarstrick A, Hempel DC, Ostermann L, Ahrens H, Dinkler D. Modelling of the biodegradation of organic matter in municipal landfills. *Waste Manag Res.* 2001;19:320–31.
4. Ng A, Melvin WT, Hobson PN. Identification of anaerobic digester bacteria using a polymerase chain reaction method. *Bioresour Technol.* 1994;47:73–80.
5. Godon JJ, Zumstein E, Dabert P, Habouzit F, Moletta R. Molecular microbial diversity of an anaerobic digester as determined by small-subunit rDNA sequence analysis. *Appl Environ Microbiol.* 1997;63:2802–13.
6. Ritari J, Koskinen K, Hultman J, Kurola JM, Kymäläinen M, Romantschuk M, Paulin L, Auvinen P. Molecular analysis of meso- and thermophilic microbiota associated with anaerobic biowaste degradation. *BMC Microbiol.* 2012;12:121.
7. Sundberg C, Al-Soud WA, Larsson M, Alm E, Yekta SS, Svensson BH, et al. 454 pyrosequencing analyses of bacterial and archaeal richness in 21 full-scale biogas digesters. *FEMS Microbiol Ecol.* 2013;85:612–26.
8. Abendroth C, Vilanova C, Günther T, Luschign O, Porcar M. Eubacteria and Archaea communities in seven mesophile anaerobic digester plants. *Biotechnol Biofuels.* 2015;8:87. doi:10.1186/s13068-015-0271-6.
9. Hanreich A, Schimpf U, Zakrzewski M, Schlüter A, Benndorf D, Heyer R, Rapp E, Pühler A, Reichl U, Klocke M. Metagenome and metaproteome analyses of microbial communities in mesophilic biogas-producing anaerobic batch fermentations indicate concerted plant carbohydrate degradation. *Syst Appl Microbiol.* 2013;36:330–8.
10. Heyer R, Kohrs F, Benndorf D, Rapp E, Kausmann R, Heiermann M, Klocke M, Reichl U. Metaproteome analysis of the microbial communities in agricultural biogas plants. *N Biotechnol.* 2013;30:614–22.
11. Baccay RA, Hashimoto AG. Acidogenic and methanogenic fermentation of causticized straw. *Biotechnol Bioeng.* 1984;26:885–91.
12. Dinopoulou G, Rudd T, Lester JN. Anaerobic acidogenesis of a complex wastewater: I. The influence of operational parameters on reactor performance. *Biotechnol Bioeng.* 1988;5:958–68.
13. Abendroth C, Wünsche E, Luschign O, Bürger C, Günther T. Producing high-strength liquor from mesophilic batch acidification of chicken manure. *Waste Manag Res.* 2015;33:291–4.
14. Gijzen HJ, Zwart KB, Verhagen FJ, Vogels GP. High-Rate two-phase process for the anaerobic degradation of cellulose, employing rumen microorganisms for an efficient acidogenesis. *Biotechnol Bioeng.* 1988;31:418–25.
15. Voolapalli RK, Stuckey DC. Hydrogen production in anaerobic reactors during shock loads—influence of formate production and H₂ kinetics. *Water Res.* 2001;35:1831–41.
16. Hwang S, Lee Y, Yang K. Maximization of acetic acid production in partial acidogenesis of swine wastewater. *Biotechnol Bioeng.* 2001;75:521–9.
17. Yu HQ, Fang HHP. Acidogenesis of dairy wastewater at various pH levels. *Water Sci Technol.* 2002;45:201–6.
18. Yu HQ, Fang HHP. Acidogenesis of gelatin-rich wastewater in an upflow anaerobic reactor: influence of pH and temperature. *Water Res.* 2003;37:55–66.
19. Demeyer D, Henderickx H, Van Nevel C. Influence of pH on fatty acid inhibition of

- methane production by mixed rumen bacteria. *Arch Int Physiol Biochim.* 1967;75:555–6.
20. Dareioti MA, Kornaros M. Anaerobic mesophilic co-digestion of ensiled sorghum, cheese whey and liquid cow manure in a two-stage CSTR system: effect of hydraulic retention time. *Bioresour Technol.* 2014;175:553–62.
21. Trzcinski AP, Stuckey DC. Contribution of acetic acid to the hydrolysis of lignocellulosic biomass under abiotic conditions. *Bioresour Technol.* 2015;185:441–4.
22. Kumar G, Park JH, Sivagurunathan P, Lee SH, Park DH, Kim SH. Microbial responses to various process disturbances in a continuous hydrogen reactor fed with galactose. *J Biosci Bioeng.* 2017;123:216–22.
23. Kumar G, Sivagurunathan P, Pugazhendhi A, Thi NBD, Zhen G, Kuppam C, Kadier A. A comprehensive overview on light independent fermentative hydrogen production from wastewater feedstock and possible integrative options. *Energy Convers Manag.* 2016;141:390–402.
24. Kumar G, Sivagurunathan P, Sen B, Kim SH, Lin CY. Mesophilic continuous fermentative hydrogen production from acid pretreated de-oiled jatropa waste hydrolysate using immobilized microorganisms. *Bioresour Technol.* 2017;240:137–43. doi:10.1016/j.biortech.2017. 03.059.
25. Koutinas A, Kanellaki M, Bekatorou A, Kandylis A, Pissaridi K, Dima A, Boura K, Lappa K, Tsafrakidou P, Stergiou PY, Foukis A, Gkini OA, Papamichael EM. Economic evaluation of technology for a new generation biofuel production using wastes. *Bioresour Technol.* 2016;200:178–85.
26. Park GW, Seo C, Jung K, Chang HN, Kim YC. A comprehensive study on volatile fatty acids production from rice straw coupled with microbial community analysis. *Bioprocess Biosyst Eng.* 2015;38:1157–66.
27. Seon J, Lee T, Lee SC, Pham HD, Woo HC, Song M. Bacterial community structure in maximum volatile fatty acids production from alginate in acidogenesis. *Bioresour Technol.* 2014;157:22–7.
28. Kohrs F, Heyer R, Magnussen A, Benndorf D, Muth T, Behne A, Rapp E, Kausmann R, Heiermann M, Klocke M, Reichl U. Sample prefractionation with liquid isoelectric focusing enables in depth microbial metaproteome analysis of mesophilic and thermophilic biogas plants. *Anaerobe.* 2014;29:59–67.
29. Jungers JM, Fargione JE, Sheaffer CC, Wyse DL, Lehman C. Energy potential of biomass from conservation grasslands in Minnesota, USA. *PLoS ONE.* 2013. doi:10.1371/journal.pone.0061209.
30. Sivagurunathan P, Kumar G, Mudhoo A, Rene ER, Saratale GD, Kobayashi T, Xu K, Kim SH, Kim DH. Fermentative hydrogen production using lignocellulose biomass: an overview of pre-treatment methods, inhibitor effects and detoxification experiences. *Renew Sust Energy Rev.* 2017;77:28–42.
31. Klocke M, Mähnert P, Mundt K, Souidi K, Linke B. Microbial community analysis of a biogas producing completely stirred tank reactor fed continuously with fodder beet silage as mono-substrate. *Syst Appl Microbiol.* 2007;30:139–51.
32. Ziganshin AM, Liebetreu J, Pröter J, Kleinsteuber S. Microbial community structure and dynamics during anaerobic digestion of various agricultural waste materials. *Appl Microbiol Biotechnol.* 2013;97:5161–74.
33. Moset V, Poulsen M, Wahid R, Højberg O, Møller HB. Mesophilic versus thermophilic anaerobic digestion of cattle manure: methane productivity and microbial ecology. *Microb Biotechnol.* 2015;8:787–800.
34. Ghasimi DSM, Tao Y, Kreuk M, Zandvoort MH, van Lier JB. Microbial population dynamics during long-term sludge adaptation of thermophilic and mesophilic sequencing batch digesters treating sewage fine sieved fraction at varying organic loading rates. *Biotechnol Biofuels.* 2015;8:171.
35. Kim M, Ahn YH, Speece RE. Comparative process stability and efficiency of anaerobic digestion; mesophilic vs. thermophilic. *Water Res.* 2002;36:4369–85.
36. Vindis P, Mursec B, Janzekovic M, Cus F. The impact of mesophilic and thermophilic anaerobic digestion on biogas production. *J Achiev Manuf Eng.* 2009;36:192–8.
37. Moset V, Poulsen M, Wahid R, Højberg O, Møller HB. Mesophilic versus

- thermophilic anaerobic digestion of cattle manure: methane productivity and microbial ecology. *Microb Biotechnol.* 2014;8:787–800.
38. McEniry J, Allen E, Murphy JD, O’Kiely P. Grass for biogas production: the impact of silage fermentation characteristics on methane yield in two contrasting biomethane potential test systems. *Renew Energy.* 2014;63:524–30.
39. Tang H, Shi X, Wang X, Hao H, Zhang XM, Zhang LP. Environmental controls over actinobacteria communities in ecological sensitive Yanshan mountains zone. *Front Microbiol.* 2016;7:343.
40. Kusumi A, Li X, Osuga Y, Kawashima A, Gu JD, Nasu M, Katayama Y. Bacterial communities in pigmented biofilms formed on the sandstone bas-relief walls of the Bayon Temple, Angkor Thom, Cambodia. *Microbes Environ.* 2013;28:422–31.
41. Esteban DJ, Hysa B, Bartow-McKenney C. Temporal and spatial distribution of the microbial community of Winogradsky columns. *PLoS ONE.* 2015. doi:10.1371/journal.pone.0134588.
42. Prabhu MS, Mutnuri S. Anaerobic co-digestion of sewage sludge and food waste. *Waste Manag Res.* 2016;34:307–15.
43. Maragkaki AE, Fountoulakis M, Kyriakou A, Lasaridi K, Manios T. Boosting biogas production from sewage sludge by adding small amount of agro-industrial by-products and food waste residues. *Waste Manag.* 2017. doi:10.1016/j.wasman.2017.04.024.
44. Guven H, Akca MS, Iren E, Keles F, Ozturk I, Altinbas M. Co-digestion performance of organic fraction of municipal solid waste with leachate: preliminary studies. *Waste Manag.* 2017. doi:10.1016/j.wasman.2017.04.039.
45. Zhang M, Yang C, Jing Y, Li J. Effect of energy grass on methane production and heavy metal fractionation during anaerobic digestion of sewage sludge. *Waste Manag.* 2016;58:316–23.
46. Gannoun H, Omri I, Chouari R, Khelifi E, Keskes S, Godon JJ, Hamdi M, Sghir A, Bouallagui H. Microbial community structure associated with the high loading anaerobic codigestion of olive mill and abattoir wastewaters. *Bioresour Technol.* 2016;201:337–46.
47. Rui J, Li J, Zhang S, Yan X, Wang Y, Li X. The core populations and cooccurrence patterns of prokaryotic communities in household biogas digesters. *Biotechnol Biofuels.* 2015;8:158.
48. Wang C, Dong D, Wang H, Müller K, Qin Y, Wang H, Wu W. Metagenomic analysis of microbial consortia enriched from compost: new insights into the role of Actinobacteria in lignocellulose decomposition. *Biotechnol Biofuels.* 2016;9:22.
49. Lewin GR, Carlos C, Chevrette MG, Horn HA, McDonald BR, Stankey RJ, Fox BG, Currie CR. Evolution and ecology of actinobacteria and their bioenergy applications. *Annu Rev Microbiol.* 2016;70:235–54.
50. Poirier S, Desmond-Le Quémener E, Madigou C, Bouchez T, Chapleur O. Anaerobic digestion of biowaste under extreme ammonia concentration: identification of key microbial phylotypes. *Bioresour Technol.* 2016;207:92–101.
51. Poirier S, Bize A, Bureau C, Bouchez T, Chapleur O. Community shifts within anaerobic digestion microbiota facing phenol inhibition: towards early warning microbial indicators? *Water Res.* 2016;100:296–305.
52. Wawrik B, Marks CR, Davidova IA, McInerney MJ, Pruitt S, Duncan K, Suflita JM, Callaghan AV. Methanogenic paraffin degradation proceeds via alkane addition to fumerate by “Smithella” spp. mediated by a syntrophic coupling with hydrogenotrophic methanogens. *Environ Microbiol.* 2016;8:2604–19.
53. Auguet O, Pijuan M, Batista J, Borrego CM, Gutierrez O. Changes in microbial biofilm communities during colonization of sewer systems. *Appl Environ Microbiol.* 2015;81:7271–80.
54. Jo Y, Kim J, Hwang S, Lee C. Anaerobic treatment of rice winery wastewater in an upflow filter packed with steel slag under different hydraulic loading conditions. *Bioresour Technol.* 2015;193:53–61.
55. Yang D, Fan X, Shi X, Lian S, Qiao J, Guo R. Metabolomics reveals stagespecific metabolic pathways of microbial communities in two-stage anaerobic fermentation of corn-stalk. *Biotechnol Lett.* 2014;36:1461–8.
56. Lü F, Bize A, Guillot A, Monnet V,

- Madigou C, Chapleur O, Mazéas L, He P, Bouchez T. Metaproteomics of cellulose methanisation under thermophilic conditions reveals a surprisingly high proteolytic activity. *ISME J.* 2014;8:88–102.
57. VDI 4630 (2006) Fermentation of organic materials, characterisation of the substrate, sampling, collection of material data, fermentation tests. Düsseldorf: *The Association of German Engineers (VDI)*.
58. Klindworth A, Pruesse E, Schweer T, Peplies J, Quast C, Horn M, et al. Evaluation of general 16S ribosomal RNA gene PCR primers for classical and next-generation sequencing-based diversity studies. *Nucleic Acids Res.* 2013;41:e1.
59. Schloss PD, Westcott SL, Ryabin T, Hall JR, Hartmann M, Hollister EB, et al. Introducing MOTHUR: open-source, platform-independent, community supported software for describing and comparing microbial communities. *Appl Environ Microbiol.* 2009;75:7537–41.

Chapter 3: Using robust microorganisms for new industrial approaches

Summary: To highlight the industrial connectivity of biomass pretreatment stages for anaerobic digesters, new technological approaches were designed and investigated. Firstly, a “Microbial Thermoelectric Cell” was developed, which allowed transformation of microbial heat into electricity. Above this, it was shown that anaerobic acidification is a well suited method for liquefaction of substrates with high

content of nitrogen or fibers, which in turn might facilitate nitrogen-stripping processes or digestion of substrates, which are rich in lignocellulose. And finally, it was found that separated acidification stages show a high resilience to heat-shocks, which allows the combination biological degradation processes with thermal treatments in anaerobic acidification stages.

Publication 3

Rodríguez-Barreiro, R., Abendroth, C., Vilanova, C., Moya, A., Porcar, M. *Towards a Microbial Thermoelectric Cell*. PlosOne. 2013; doi: 10.1371/journal.pone.0056358.



Publication 4

Abendroth, C., Wünsche, E., Luschnig, O., Bürger, C., Günther, T. Producing high-Strength liquor from mesophilic batch acidification of chicken manure. *Waste Manag Res*. 2015;33:291–294, doi: 10.1177/0734242X14568536.



Publication 5

Abendroth, C., Hahnke S., Simeonov, C., Klocke, M., Casani Miravalls, S., Ramm, P., Bürger, C., Luschnig, O., Porcar, M. Microbial communities involved in biogas production exhibit high resilience to heat shocks. *Bioresour Technol*. 2017; in press.



Publication 3**Towards a Microbial Thermoelectric Cell**

Raúl Rodríguez-Barreiro¹, Christian Abendroth¹, Cristina Vilanova¹, Andre's Moya^{1,2}, Manuel Porcar^{1,3*}

¹Cavanilles Institute of Biodiversity and Evolutive Biology, Universitat de València, València, Spain

²Unidad Mixta de Investigación en Genómica y Salud, Centro Superior de Investigación en Salud Pública (CSISP), València, Spain

³Fundació General de la Universitat de València, València, Spain

Abstract

Microbial growth is an exothermic process. Biotechnological industries produce large amounts of heat, usually considered an undesirable by-product. In this work, we report the construction and characterization of the first microbial thermoelectric cell (MTC), in which the metabolic heat produced by a thermally insulated microbial culture is partially converted into electricity through a thermoelectric device optimized for low Δ values. A temperature of 41°C and net electric voltage of around 250–600 mV was achieved with 1.7 L baker's yeast culture. This is the first time microbial metabolic energy has been converted into electricity with an ad hoc thermoelectric device. These results might contribute towards developing a novel strategy to harvest excess heat in the biotechnology industry, in processes such as ethanol fermentation, auto thermal aerobic digestion (ATAD) or bioremediation, which could be coupled with MTCs in a single unit to produce electricity as a valuable by-product of the primary biotechnological product. Additionally, we propose that small portable MTCs could be conceived and inoculated with suitable thermophilic or hyperthermophilic starter cultures and used for powering small electric devices.

Introduction

Both developed and fast growing developing countries exhibit steadily growing energy demands. Taking into account the limited nature of oil, coal and gas reservoirs, this could obviously lead to a shortage of standard (fossil) fuels in the relatively near future. The lack of sustainability of current fossil-centered energy strategies, as well as the recent extremely serious accident at Fukushima Daiichi power facility [1] have increased the concerns about the economic and environmental consequences of relying on these energy sources, leading to some dramatic shifts in energy policies, like in Germany [2]. It is widely accepted that massive fossil fuel consumption, which results in the production of nine billion metric tons of atmospheric carbon per year [3], is at least partially responsible for current global warming. Therefore, alternative non-fossil non-nuclear technologies are seen as promising, albeit not fully competitive. Among these, biomass-based energy has been suggested as one of the most promising technologies for renewable energy production [4, 5]. Biomass from crops; urban, industrial or agricultural wastes; green algae, cyanobacteria or other microbial cultures, are renewable organic resources that are suitable for energy production in the form of biofuels (mainly, but not limited to, bioethanol

and biodiesel), and electricity. Besides lignocellulosic combustion-based power production, a biological system allowing direct conversion of biomass into electricity already exists: a broad range of organic substances can be oxidized by electrogenic bacteria, which transfer electrons to an anode in a simple device known as a Microbial Fuel Cell (MFC). At the cathode, other useful products can be generated, including hydrogen, methane, and hydrogen peroxide [6, 7, 8]. The electric yield of MFCs has increased dramatically in recent years, mainly by increasing the ratio of the area of the electrodes/volume in the reactor, with best yields reaching up to 2–7 W/m². A moderate MFC unit, of about 1 L, can produce enough electricity to power a small propeller for more than one year [9]. However, MFCs seem to work better at small scales, as scaling-up faces important challenges [9].

Many bacterial species have been reported to display electroactive properties, including members of common genera such as *Clostridium*, *Pseudomonas*, *Geobacter* or *Shewanella*. A few eukaryotic microorganisms have been assayed for power production in MFCs. Baker's yeast *Saccharomyces cerevisiae* has proven able to transfer electrons to an anode in two independent studies [10, 11] with moderate efficiency. In both reports, researchers found net voltage values of about 0.33 V for 1 L reactors.

To date MFCs are still the only direct method to microbiologically convert biomass into electricity. Nonetheless, there is possibly another non-fuel alternative. Since microbial growth is an exothermic process, it produces heat, which is a by-product that usually goes unnoticed in lab-scale cultures but which has a strong impact on the design and performance of industrial-scale microbial fermentations. Almost 90 % of the heat produced in a microbial fermentation is reported to be metabolic

heat; and almost all this heat is removed through forced heat exchange [12].

The thermoelectric or Peltier-Seebeck effect is the direct conversion of electric voltage to temperature differences (Peltier effect) and vice-versa (Seebeck effect). Theoretically, an electric current would be produced by coupling an exothermic microbial culture with an endothermic reaction –or, alternatively, a heat sink– through a thermoelectric cell. If the thermal energy from exothermic microbial cultures could be turned into electricity efficiently, power-producing devices could be designed and coupled to existing microbial reactors within a range of applications (alcoholic fermentations, bioremediation, waste treatment, autotrophic thermal aerobic digestion ATAD, etc.). Here, we report the characterization of the first Microbial Thermoelectric Cell, a bioreactor specifically designed for power production through a completely different mechanism than that operating in MFCs: the thermoelectric effect. Our results might contribute to providing a new scenario for the future development of microbial-based cellular electricity facilities, which might be useful for local electric production and heat recycling in a wide range of biological processes.

Materials and Methods

Construction of the MTC

In order to implement a thermoelectric-based power generator, a reactor was designed able to i) sustain microbial growth; ii) remain thermally isolated on most of its surface; and iii) efficiently transfer heat through a relatively small area to a thermoelectric device. One of us (M. Porcar) had previously designed an LCC (Liquid Culture Calorimeter) for microbial growth, suitable for fine recordings of internal temperature changes through a thermocouple [13]. Based on the LCC, we conceived a Microbial Thermoelectric Cell (MTC hereon) to produce power from a

microbial culture by the Peltier-Seebeck effect. Figure 15 shows the structure of the MTC. The core of the reactor is a 1.9 L glass container from a commercial vacuum flask. The flask was placed inside an expanded polystyrene (EPS) box and the gap filled with a polyurethane foam spray (Silicex Fischer, Fisher Ibérica, Tarragona, Spain). The box was then inserted into a second EPS isolation box. The upper part of the MTC was drilled and a copper bar (20 mm in diameter) inserted through the hole. The upper part of the copper bar was adapted in order to allow a TE-Power Probe thermal harvester (MicroPelt, Germany) to be screwed through a 1/40 Whitworth thread (DIN 2999, JIS B0203, ISO 7/1). TE-Power Probe is a prototype of an integrated proximity thermoharvester designed to replace primary batteries in wireless systems operating in duty cycle mode. The key element of the TE-Power Probe is the MPG-D751 thermogenerator, which produces electricity from a rather low gradient of temperature. The TE-Power Probe is originally designed to attach to a heat source in the shape of piping that carries a hot fluid, and heat is dissipated through an aluminum heat sink, with the resulting temperature gradient allowing power production by the MPGD751 thermogenerator. In our experiments, temperature changes in different parts of the Probe were measured by PT-100 sensors. Since the TE-Power Probe is specifically designed to operate using natural convection to ambient air, we mounted it horizontally, as suggested by the manufacturer.

The two EPS isolation layers of the MTC were shaped so the round bottom of the vacuum flask would fit. The flask bottom was placed conveniently close (20 mm) to the bottom of the MTC in order to allow stirring by a magnetic stirrer. When recordings were to be taken, the MTC was first filled with 1.8 L of medium; a small magnet was added; the MTC was placed inside a

standard laboratory magnetic stirrer set at low speed (600 rpm); the inoculum was then added, and the copper bar with the screwed TE-Power Probe finally set in place.

Yeast Strains, Media and Culture Conditions

The following six diploid *S. cerevisiae* strains, from the wine industry or genetic modifications thereof, were used: EC118, L2056, 3aS2D, T73, D170, and TTRX2. All the strains were kindly provided by Prof. Emilia Matallana (IATA, Valencia, Spain). In order to assess their exothermic abilities, independent cultures were set in filter-sterilized YPD (20 g/L peptone, 10 g/L yeast extract, with 18% sugar), and the internal temperature of the cultures (grown overnight in non-isolated Erlenmeyer flasks) was continuously measured. Thermotolerance was assessed by growing the strains at 30, 37 and 41 °C. After an overnight incubation under low stirring, the OD₆₀₀ of the six overnight cultures was measured. For standard experiments after strain selection, the filtersterilized 18% sucrose YPD was inoculated with 1:50 of an overnight yeast pre-culture grown at 30 °C, and subjected to low stirring for 120 h.

Data Acquisition, Monitoring and Recording

The MTC was connected to a PC in order to record internal and external temperatures and the output current provided by the heat harvester TE-Power Probe (Fig. S1). The internal temperature of the MTC was measured by a thin T-type thermocouple inserted into the microbial culture and connected to a PC through a data logger, as previously described [13]. Another thermocouple recording room temperature was also set in place. The thermocouples were connected to an acquisition card inserted on the data logger, which was connected via a GPIB cable to a PC with an acquisition software that one

of us (R. Rodríguez-Barreiro) conceived specifically for this work (Fig. S1). The TE-Power Probe output was also connected to the PC, which yielded two additional temperature recordings by using two Pt-100 sensors (that of the cold and hot sides of the thermogenerator device) and the output voltage. The connections between the thermocouples and the data logger were performed on an icewater mixture to take into account the unwanted background electric voltage, due to the junction of dissimilar metals in the thermocouple-data logger connection. Finally, a thermocouple was inserted inside the box containing the ice-water mixture in order to verify that the temperature of the datalogger-thermocouple connections was kept at 0 °C.

Temperature records (and, when TE-Power Probe was connected, electric power) were taken every 6 minutes throughout the experiment.

Identification Assay to Estimate Broth Heat Capacity and Global Thermal Resistance of MTC

In order to estimate the heat capacity of the broth ($m \cdot C_p$) and the global thermal resistance (R_g), the MTC (without TE-Power Probe) was set up under the following conditions: first, an electrical resistance was placed inside the MTC to generate a controlled heat flow, as consequence of the Joule effect induced by an external voltage input through the resistance. Second, the MTC was loaded with room-temperature sterile broth with 1 g/L nipagine supplementation to avoid contamination by yeasts. Broth was subjected to continuous stirring and room temperature was kept constant. Throughout the experiment, broth and room temperatures and the power generated in the resistance were continuously measured. To ensure the

initial steady-state conditions (broth temperature equal to room temperature), the system was kept in the off mode for approximately 20 h before applying the input voltage.

Theory

The equation for the heat flow balance corresponding to the MTC we describe in this work can be stated as follows:

$$\sum \text{Heat accumulated} = \sum \text{Heat generated} - \sum \text{Heat lost} \quad (1)$$

Heat accumulated is a consequence of the variation in broth temperature. Since there is no forced cooling of the system, heat flow losses are due only to heat transfer from the culture to the environment through both the MTC surface and the TE-Power Probe thermogenerator. For calibration purposes, we first set the MTC to generate a heat flow from an electric resistance placed inside the vacuum flask through the Joule effect. In standard experiments, heat flow was obtained from the metabolic heat as a consequence of microbial growth.

Therefore, the heat flow balance equation can be written for the MTC as follows (a definition of all the symbols used throughout the MTC modelling is available in Table 2):

$$\dot{Q}_{acc} = P_J + \dot{Q}_p - \dot{Q}_{env} - \dot{Q}_{Th} \quad (2)$$

Where Q_{acc} is the heat flow accumulated in the broth; P_J is the heat flow due to the Joule effect; Q_p is the heat flow due to microbial metabolism; Q_{env} is the heat flow loss through the MTC surface to the environment; and Q_{Th} is the heat flow loss through the copper bar connected to the TE-Power Probe.

TABLE 2: Nomenclature used in MTC modelling.

Symbol	Description (units)
α	Seebeck coefficient (V/K)
I	Electrical current (A)
$m \cdot C_p$	Whole system heat capacity (J/K)
$m_b \cdot C_{pb}$	Broth heat capacity (J/K)
$m_v \cdot C_{pv}$	Vacuum flask heat capacity (J/K)
$m_w \cdot C_{pw}$	Insulation walls heat capacity (J/K)
P_J	Electrical input power due to the Joule effect (W)
P_e	Electrical power generated (W)
Q_{acc}	Accumulated heat flow (W)
Q_C	Net heat flow released through the cold side of the thermogenerator (W)
Q_{env}	Heat flow released to the environment (W)
Q_H	Net heat flow absorbed through the hot side of the thermogenerator (W)
Q_j	Heat flow due to the Joule effect inside of the thermogenerator (W)
Q_p	Heat produced by microbial metabolism (W)
Q_{sC}	Heat flow produced in the cold side of the thermogenerator due to the Seebeck effect (W)
Q_{sH}	Heat flow produced in the hot side of the thermogenerator due to the Seebeck effect (W)
Q_t	Heat flow loss due to the natural thermal conduction established between both sides of the thermogenerator (W)
Q_{Th}	Heat flow absorbed from the broth through the copper bar (W)
R	Electrical resistance (V)
R_{Cu}	Thermal resistance of the copper bar (K/W)
R_g	Global thermal resistance of the MTC (K/W)
R_i	Internal electrical resistance of the thermogenerator (V)
R_{Load}	Electrical resistance connected between the terminals of the thermogenerator (V)
R_{sk}	Thermal resistance of the heat sink (K/W)
R_{th}	Thermal resistance of the thermogenerator (K/W)
T_b	Broth temperature (K)
T_C	Temperature of the cold side of the thermogenerator (K)
T_{env}	Room temperature (K)
T_H	Temperature of the hot side of the thermogenerator (K)
ΔT_{th}	Difference of temperature between the hot and the cold sides of the thermogenerator (K)
T_v	Vacuum flask temperature (K)
T_w	Insulation walls temperature (K)
V_{ext}	Input voltage (V)
V_o	Voltage output in the terminals of the thermogenerator (V)

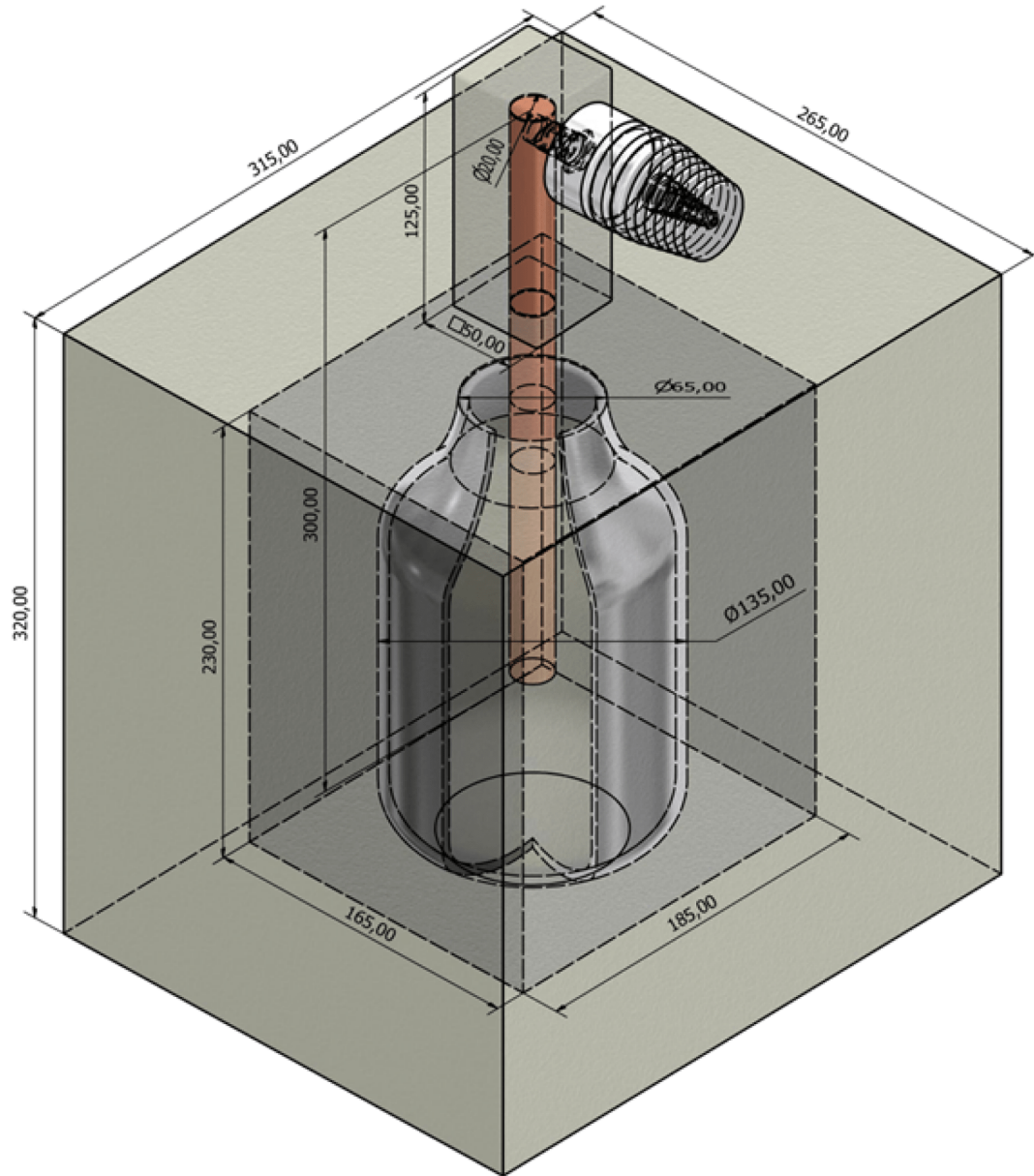


FIGURE 15: Schematic drawing of the Microbial Thermoelectric Cell (Auto-CAD). All dimensions are given in mm.

Accumulation Terms

Heat accumulation (Q_{acc}) in a particular body is determined by the variation in its temperature (dT_i/dt) and by its heat capacity ($m_i \cdot C_{pi}$). In the MTC, heat can be accumulated in the broth (subscript "b"), the vacuum flask ("v") and the insulation walls ("w"), as follows:

$$\dot{Q}_{acc} = m_b \cdot C_{pb} \cdot \frac{dT_b}{dt} + m_v \cdot C_{pv} \cdot \frac{dT_v}{dt} + m_w \cdot C_{pw} \cdot \frac{dT_w}{dt} \quad (3)$$

The MTC is a very simple system with a single sensor to measure the temperature of the broth. Therefore, the equation can be simplified:

$$\dot{Q}_{acc} \approx m \cdot C_p \cdot \frac{dT_b}{dt} \quad (4)$$

Where $m \cdot C_p$ represents the whole system heat capacity, deduced from the variation in culture temperature. This parameter can easily be determined

under a simplified experimental configuration using the model equations described below.

Loss Terms (I): Heat Flow Loss to the Environment

Energy losses through the MTC walls can be due to the natural heat flow (Q_{env}) from the warm internal broth to the relatively cool environment. Since insulation materials in the MTC display low emissivity values, radiation losses can be neglected and Q_{env} can be expressed as follows:

$$\dot{Q}_{env} = \frac{1}{R_g} \cdot (T_b - T_{env}) \quad (5)$$

Where R_g represents the global thermal resistance of the MTC and T_b and T_{env} are the temperatures of the broth and the environment, respectively. This thermal resistance can be experimentally determined under the same conditions described for $m \cdot C_p$.

Loss Terms (II): Heat Flow Loss Through the TE-Power Probe

The global heat flow through the copper bar (Q_{Th}) is the same than the heat flow absorbed by the hot side of the thermogenerator cell (Q_H) and is composed of: (i) a spontaneous flow due to the difference in temperature between the hot and cold sides of the thermogenerator cell, expressed as $(T_H - T_C)/R_{th}$; (ii) an induced heat flow as a consequence of the conversion of heat to electric power through the Seebeck effect. Then, the heat flow loss through the thermogenerator can be stated as follows [14]:

$$\dot{Q}_{Th} = \dot{Q}_H = \left(\frac{T_H - T_C}{R_{th}} \right) + (\alpha \cdot T_H \cdot I - \frac{1}{2} \cdot I^2 \cdot R_i) \quad (6)$$

Where $\alpha \cdot T_H \cdot I$ corresponds to heat absorbed by the thermogenerator due to the Seebeck effect, while the term $\frac{1}{2} \cdot I^2 \cdot R_i$ corresponds to the heat produced as a consequence of

the Joule effect, associated to the circulation of the electric current produced through the internal resistance of the thermogenerator. T_H and T_C represent the temperature of the hot and cold sides of the cell, whereas R_{th} and R_i correspond to its internal thermal and electrical resistance, respectively. α is the Seebeck coefficient of the thermogenerator and I is the electrical current obtained from the TE-Power Probe.

Generation Terms (I): Heat Flow Due to the Joule Effect

When an electrical resistance was placed inside the vacuum flask, a heat flow (P_J) was obtained as a consequence of applying an external voltage according to the Joule effect:

$$P_J = \frac{V_{ext}^2}{R} \quad (7)$$

Where V_{ext} is the input voltage and R is the electrical resistance.

Generation Terms (II): Heat Flow Due to Yeast Growth

When the electrical resistance was replaced by a yeast culture, the heat flow was generated as a consequence of the exothermic properties of yeast metabolism. This heat flow, represented as Q_p , was estimated for the different experimental configurations as described below. Taking all the equations described above together, the general energy balance (Eq. 2) can be written as:

$$m \cdot C_p \cdot \frac{dT_b}{dt} = P_J + \dot{Q}_p - \frac{(T_b - T_{env})}{R_g} - \dot{Q}_{Th} \quad (8)$$

Model Equations for the Estimation of $m \cdot C_p$ and R_g In order to calculate the global heat capacity and the global thermal resistance of the MTC ($m \cdot C_p$ and R_g , respectively), a simplified experimental set up was used. Briefly, heat flow was induced in the sterile broth by applying a constant input power

through a resistance according to the Joule effect. In this experiment, room temperature was kept constant and the TE-Power Probe was not mounted on the MTC. Therefore, Q_{Th} and Q_p terms (corresponding to the TE-Power Probe and the yeast, respectively) from Eq. 8 are null, so it can be written as the following first-order ODE:

$$m \cdot C_p \cdot \frac{dT_b(t)}{dt} = P_J - \frac{T_b(t) - T_{env}}{R_g} \quad (9)$$

A first-order EDO is mathematically characterized by its gain and its time constant, which can be estimated manually or with a standard mathematical software from experimental data. In Eq. 9, the gain (R_g) and the time constant ($m \cdot C_p \cdot R_g$) were estimated from the experimental values of T_b and P_J .

Estimation of Heat Yield Due to Yeast Metabolism and Calculation of the Electrical Power Generated

Heat yield due to yeast metabolism (Q_p) was estimated from Eq. 8, where the term P_J is null since no electrical resistance was set up inside the flask:

$$\dot{Q}_p = m \cdot C_p \cdot \frac{dT_b(t)}{dt} + \frac{T_b(t) - T_{env}(t)}{R_g} + \dot{Q}_{Th}(t) \quad (10)$$

In the assays where the TE-Power Probe was not included, the term Q_{Th} (the broth heat lost through the copper bar) is null, so Q_p was calculated from the experimental data of T_b and T_{env} using the estimations of $m \cdot C_p$ and R_g previously obtained.

When the TE-Power Probe was included, the metabolic heat yield was calculated from Eq. 10, along with the model equations for TE-Power Probe in order to estimate Q_{Th} (a detailed

description of these equations and a schematic representation of associated heat flows is available in Appendix S2 and Fig. S2, respectively). These model equations are dependent on the electrical configuration used in the thermogenerator during the assays. When no load resistance was connected to the terminals of the thermogenerator (no electrical power was taken out), the following equation for TE-Probe was used (for a detailed version of this open-circuit model, see Appendix S1):

$$\dot{Q}_{Th}(t) = \frac{\Delta T_{th}(t)}{R_{Th}} \quad (11)$$

ΔT_{th} represents the difference of temperature between the hot and the cold side of the thermogenerator, whereas R_{th} is the thermal resistance of the thermogenerator. Voltage output (V_o) of the terminals of the TE-Power Probe, which under this configuration is equal to the voltage generated in the Peltier cell, can be expressed as:

$$V_o(t) = \alpha \cdot \Delta T_{Th}(t) \quad (12)$$

Being α the Seebeck coefficient.

Otherwise, when a load resistance was fitted to achieve the maximum power from the thermogenerator, Eq.11 was replaced by Eq.13 (deduced in the maximum-power model of Appendix S2):

$$\dot{Q}_{Th}(t) = \frac{\alpha^2 \cdot \Delta T_{th}(t)}{R_i} \cdot \left(\frac{T_H(t)}{2} - \frac{\Delta T_{th}(t)}{8} + \frac{R_i}{\alpha^2 \cdot R_{th}} \right) \quad (13)$$

Where R_i and R_{th} are the internal electrical and thermal resistance, respectively.

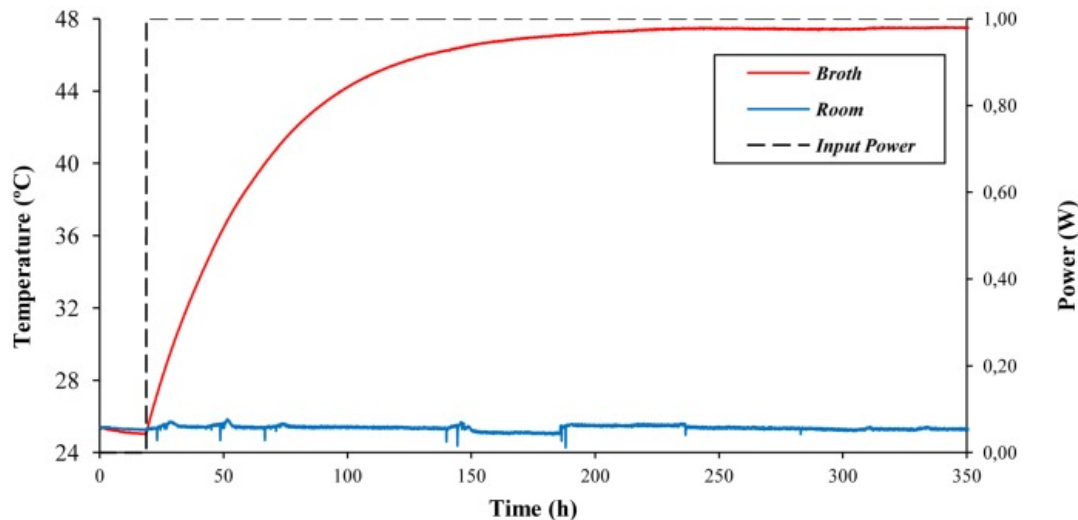


FIGURE 16: Time course of broth and room temperatures during the identification assay of broth heat capacity and global thermal resistance of the MTC. Recordings of room temperature (blue), broth temperature (red) and input power (dashed line) were taken every 6 min.

Under this configuration, voltage output (V_o) of the terminals of TE-Power Probe can be expressed as:

$$V_o(t) = \frac{\alpha \cdot \Delta T_{th}(t)}{2} \quad (14)$$

and the maximal power generated can be calculated as follows:

$$P_e(t) = \frac{V_o^2(t)}{R_i} \quad (15)$$

Results

Estimation of Broth Heat Capacity and Global Thermal Resistance of MTC

In order to characterize the thermal evolution of the MTC prior to the experiments with yeast cultures, an identification assay for $m \cdot C_p$ and R_g was set up. The time course of broth and room temperature during the experiment is shown in Figure 16. From a steady-state, in which room and broth temperature were the same (25.5 °C), a constant input power of 1 W was supplied, and the broth reached a

final temperature of 47.5 °C. The system gain (meaning the temperature increase divided by the input power) was 22 K/W, and the time constant (the time by which 63 % of the temperature increase is reached) was 43.5 h. According to the model equations, the gain represents the global thermal resistance of the MTC, and the broth heat capacity can be obtained by dividing the time constant by the gain. Thus, our estimated values for R_g and $m \cdot C_p$ are 22 K/W and 7118 J/K, respectively.

When the mathematical software was used to estimate R_g and $m \cdot C_p$ from the same experimental data, similar values were obtained ($R_g = 22$ K/W and $m \cdot C_p = 7100$ J/K) with a confidence level of 98.7 %.

Strain Selection and MTC Performance

All yeast strains exhibited similar performance in terms of exothermic potential and resistance to high temperatures, with strain D170 displaying slightly higher thermo-resistance (data not shown).

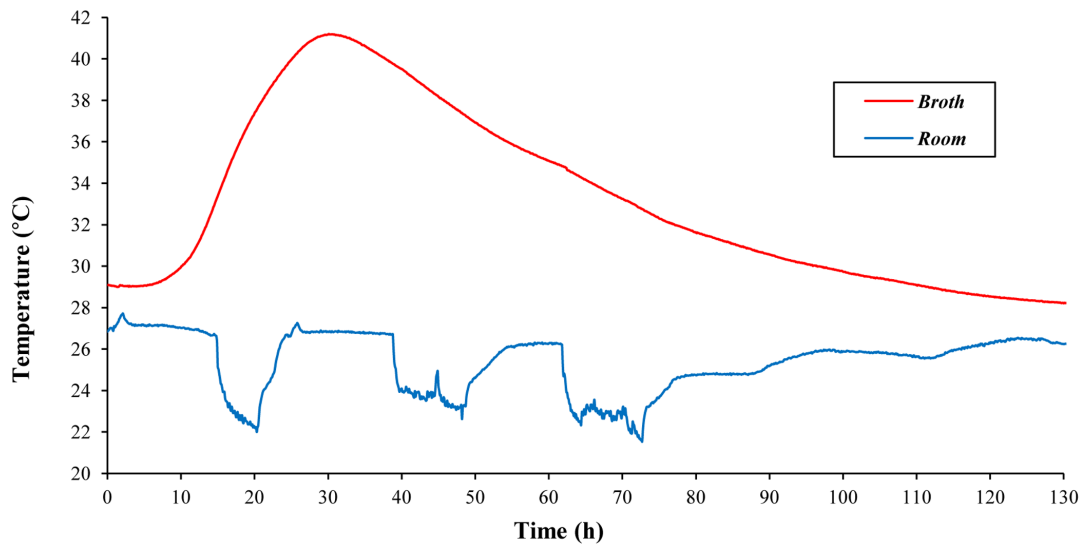


FIGURE 17: Typical performance of the MTC without TE-Power Probe. Experimental values of broth and room temperature (red and blue lines, respectively) are shown.

This strain was thus selected for further studies. When yeast strain D170 was inoculated into a pre-warmed 18% sucrose YPD medium and grown in the MTC without the copper bar and the TE-Power Probe set in place, the internal temperature dropped slowly (about 1 °C), stabilized and finally started to rise after 6 – 7 h. The temperature peaked after approximately 24 h and reached up to 41 °C. Figure 17 shows a typical experiment in which the maximum temperature is around twelve degrees higher than the initial temperature of the culture. After the peak, the yeast culture temperatures started dropping and reached the initial temperature after about 70 – 90 h. Despite the abrupt changes (22 °C – 27 °C) in room temperature as a consequence of switching the air conditioning on and off, the change in the internal temperature of the yeast culture was only mildly affected.

Estimation of Heat Yield Due to Yeast Growth

The heat yield due to yeast growth (Q_p) was estimated for each experimental set up (Fig. 18). In all the experiments, the estimated evolution of Q_p peaked

before broth temperature reached its maximum due to the high inertia of the broth ($m \cdot C_p$). In the assay carried out without TE-Power Probe (Fig. 18A), Q_p reached its maximum (1.96 W) after 20 h and remained above 0.2 W for 40 h. In an open-circuit configuration, maximum Q_p (almost 1.4 W) peaked after 10 h, reaching values above 0.2 W over 50 h (Fig. 18B). Maximum Q_p was obtained earlier in this case because a more concentrated inoculum was used, indicating that, as expected, there is a dependence between initial yeast concentration and time until Q_p maximum. Finally, under a load-resistance configuration, Q_p peaked (with a value of almost 1.5 W) after 20 h (as in the experiment without TE-Power Probe, in which the same initial yeast concentration was used), producing more than 0.2 W for 50 h (Fig. 18C). Our data show that when the TE-Power Probe was inserted, lower Q_p values were estimated from experimental data. In accordance, total energy generated by yeast metabolism, calculated as the area below the curve of Q_p , was higher in the experiment carried out without the TE-Power Probe (194,7 kJ) in comparison with those configurations in which it

was included (144,4 and 145,4 kJ for the open-circuit and the load-resistance set up, respectively). This might be due to the effect of the copper bar on effective broth stirring, which might be lower and therefore affect yeast growth.

Electricity Production with the MTC

Under the MTC insulation conditions assayed, the metabolic heat produced by strain D170 was partially transformed into electricity through the TE-Power Probe thermal harvester. When the TE-Power Probe was mounted in the yeast-culturing MTC under open circuit conditions, the internal temperature of the culture increased up to about 35 °C and remained higher than 32 °C for about 54 h (Fig. 19A). Under these conditions, electric voltage yielded around 250 mV (net value) for a two-day period, with significant, lower room temperature-associated peaks of about 350–600 net mV (Fig. 19A). The same experiment was performed under load resistance conditions (330 V, the same as that for the MPG-D751 thermogenerator) and produced an internal temperature peak of about 32 °C, with the culture being hotter than room temperature (which was constant in this experiment) for a period of 110 h (Fig. 19B). Under these conditions, a maximum of 290 mV were obtained on the electrical load resistance, corresponding to around 580 mV generated in the Peltier cell (Eq. 15). The maximum power obtained, corresponding to the maximum DT values, reached around 255 mW (net value).

The energy conversion yield was calculated for this latter experiment as the total electrical power generated (33.1 J) divided by the total heat energy produced by the yeasts (147.44 kJ, as calculated from the estimated heat yield represented in Fig. 19C). The

resulting value, 0.022%, was low, as expected from the poor efficiency of heat-harvesting devices such as the TE-Power Probe. Notwithstanding, it allowed the production of significant amounts of electrical power from relatively moderate values of DT.

Discussion

The results presented here clearly indicate that the exothermic nature of microbial growth can be exploited when transformed into significant electric voltage. We have designed and constructed the first Microbial Thermoelectric Cell, which consists of a simple, thermally insulated reactor, with a small heat exchange surface on which a thermoelectric prototype thermal harvester, equipped with a MPG-D751 thermogenerator device (TE-Power Probe) is mounted. The chosen thermogenerator is optimal for relatively high efficiencies in electric production at low ΔT values, such as those existing between an insulated yeast culture (41 °C, under our conditions) and room temperatures.

With a medium size MTC (smaller than two liters), we typically obtained 150–600 mV. These values are similar to those obtained with yeast-based MFCs for which net voltage values of about 0.33 V for 1 L reactors have been reported [10, 11].

It is noteworthy that MFCs and MTCs work on a totally different basis –albeit theoretically compatible– as MFCs produce electricity from direct microbial-mediated electron transfer from organic matter oxidation to an anode; whereas the MTC partially transforms metabolic thermal energy into electricity by the Seebeck effect. As it is also the case for MFCs, MTCs could be combined with other microbial processes.

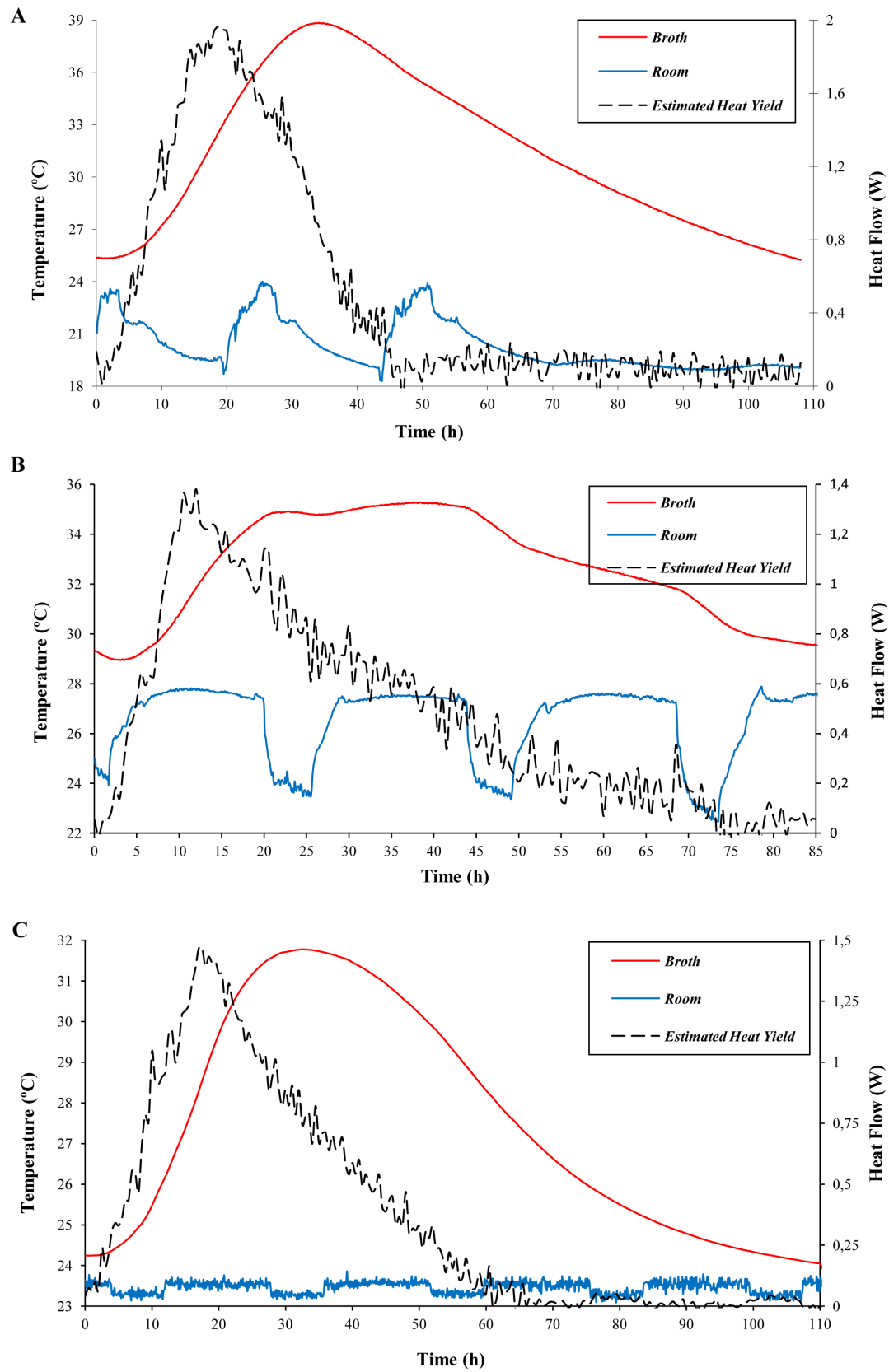


FIGURE 18: Time course of broth and room temperatures and heat yield due to yeast growth for different MTC configurations: without TE-Power Probe (A), open-circuit (B) and load-resistance (C). Experimental values of broth and room temperature (red and blue lines, respectively) were recorded every 6 min. Heat yield (dashed line) was estimated for each configuration.

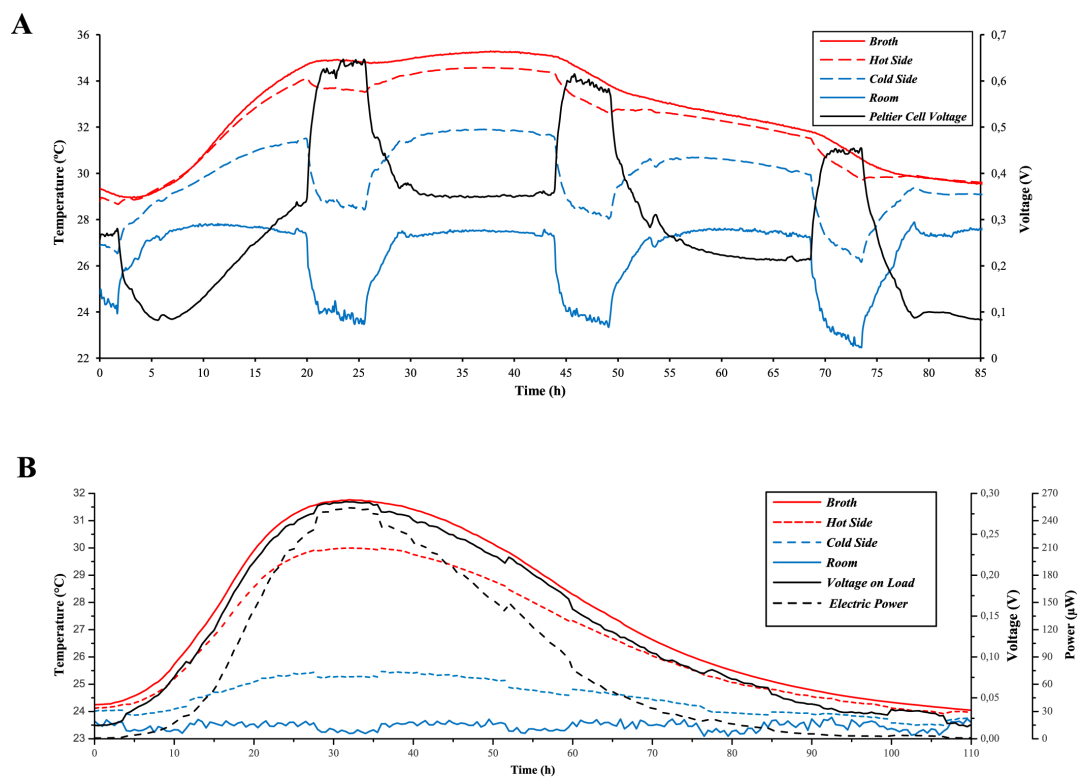


FIGURE 19: Electricity production by MTC under open-circuit (A) and load-resistance (B) configurations. The experimental temperature values of broth (red), room (blue), and thermogenerator hot and cold sides (red and blue dashed lines, respectively) are shown along with the evolution of voltage and power output (black continuous and dashed lines, respectively).

Baker's yeast *S. cerevisiae* was used for our MTC due to its wellknown exothermic growth under a range of different conditions. Indeed, any other microbial culture resulting in important heat production, such as ethanolic fermentation (beer, bread, wine, biofuels), auto thermal aerobic digestion (ATAD) or hydrocarbonpolluted soil bioremediation and bioaugmentation, could be coupled with MTCs into a single unit, with electricity production as a valuable sub-product of the main biotechnological purpose. In fact, metabolic heat is often seen in industry as an undesirable subproduct of large-scale microbial fermentations, and cooling facilities are often needed in order to maintain an optimum broth temperature [12, 15]. The conversion, albeit partial, of this heat into electricity would both help to control internal temperatures in biotechnological processes and contribute to energy savings by cogeneration. Interestingly, our results suggest that heat production through metabolic growth and heat flow through a thermogenerator can be tuned in such a way that no energy is needed to heat the broth up for microbial growth nor to cool it down in order to avoid excessive temperatures, known to abruptly stop the fermentation process.

It seems reasonable to predict that, in addition to yeast, other cultures might be suitable as heat producers in an MTC. For example, naturally-occurring thermophilic and hyperthermophilic bacteria, such as *Bacillus coagulans*, *Bacillus licheniformis* or many *Geobacillus* spp. strains, many of which can be isolated from extreme environments such as deep oil wells and the optimal growth of which is 50–60 °C. Additionally, these bacteria are reported as able to heat their own culture up to 50–55 °C [16]. The perfect candidate for MTC should meet the following criteria: (i) thermoresistant; (ii) strong exothermic ability; (iii) rapid and easy growth; and

(iv) an ability to grow and degrade high concentrations of carbon sources.

In the MTC we designed, the “cold side” of the system was an aluminum heatsink. In order to optimize electricity yield by increasing ΔT , a biological cooling system could theoretically be implemented, rather than simple convection-driven heat loss. In fact, methanogenic archaea have been reported to exhibit endothermic growth [7]. Although it is uncertain whether endothermia is a result of particular growth or of heat loss due to gas evaporation from the culture, the fact is that these microorganisms could be combined with those producing heat through a thermoelectric element in order to increase electricity production. These archaea have optimal growth at temperatures of around 37 °C, and this implies that the whole system should be finely tuned in order to regulate heat transfer across the thermoelectric element, allowing optimal microbial growth while maintaining as high a ΔT as possible.

The surface:volume ratio of microbial fermentors is a critical factor affecting heat loss to the environment and thus internal temperature of the culture. Although standard lab-scale microbial cultures produce heat, most of it is lost to environment due to high surface to volume ratio, resulting in the absence of any noticeable increase in internal temperature. However, large, production-scale bioreactors have been characterized thermodynamically and proved to work nearly adiabatically due to much lower surface to volume ratio compared to laboratory-scale non-insulated bioreactors [12]. The results presented here, together with previous reports on medium-scale liquid culture calorimeters [13], demonstrate that relatively small liquid cultures can also work almost adiabatically, provided proper insulation is provided and significant autothermal growth can be achieved. This implies that small

portable MTCs for electricity production could be envisaged, since most of the metabolic heat from microbial growth can be stored inside the MTC. These small thermoelectric cells could theoretically be used to power small electric devices. However, in order for MTCs to display higher electric yields, optimization of the thermoelectric elements should take place. Indeed, only 0.5–8% of the total heat flow is usually transformed into electricity through the thermoelectric plates. Interestingly, only 12% of the maximum theoretical efficiency is achieved in the best thermoelectric devices today [17], so there is still room for significant improvement in the optimization of this technology. There has been a dramatic increase in research into high efficiency thermoelectric devices in recent decades, with reports of significant improvements in ZT values, design optimization, and development of alternative materials. As proposed by [17], “TE solid-state heat engines could well play a crucial role in addressing some of the sustainability issues we face today”.

Other heat harvesting methods, such as absorption heat transformers or organic Rankine cycle, have been reported previously [18, 19]. However, these systems are space-consuming and involve mobile parts that require continuous maintenance. In contrast with these, solid-state thermoelectric systems are small, require almost no maintenance, and display high adaptability to a range of industrial designs [17].

In conclusion, this is the first report of microbial metabolic energy being converted into electricity with an ad hoc thermoelectric device, i.e., the Microbial Thermoelectric Cell. Our results show that even small volumes of broth are able to exhibit significant autothermal performance and produce electricity when properly insulated and set in such a way that heat exchange is minimized over the whole

surface, except the small area on which a (prototype) thermal harvester is mounted. Although the electric power we obtained was rather low, this work may contribute towards a novel strategy to harvest excess heat produced by the biotechnology industry, particularly if ongoing research into thermoelectric materials and design finally yields high efficiency thermoelectric devices.

Acknowledgments

We are very grateful to Emilia Matallana, for kindly supplying yeast strains, Julián Heredero, for his fine work manufacturing the copper bar, to Ruslan Klymenko for assistance with Figure 15 and to Fabiola Barraclough for correction of the English text. The technology described in this work has been found by us to hold not only for scientific publication, but also for patenting (Application number P201200977 at Spanish Office of Patents and Trademarks, OEPM).

References

1. Dauer LT, Zanzonico P, Tuttle RM, Quinn DM, Strauss HW. The Japanese tsunami and resulting nuclear emergency at the Fukushima Daiichi power facility: technical, radiologic, and response perspectives. *J Nucl Med.* 2011;52:1423–1432.
2. Gross M. Energy U-turn in Germany. *Curr Biol.* 2011; 21:379–381.
3. Lehmann J. A handful of carbon. *Nature.* 2007;447:143–144.
4. Kim D, Chang IS. Electricity generation from synthesis gas by microbial processes: CO fermentation to microbial fuel cell technology. *Bioresour Technol.* 2009;100:4527–4530.
5. Song C. Fuel processing for low-temperature and high-temperature fuel cells: Challenges, and opportunities for sustainable development in the 21st century. *Catal Today.* 2002;77:17–49.
6. Cheng S, Xing D, Call DF, Logan BE. Direct biological conversion of electrons into

- methane by electromethanogenesis. *Environ Sci Technol.* 2009;43: 3953–3958.
7. Liu H, Grot S, Logan BE. Electrochemically assisted microbial production of hydrogen from acetate. *Environ Sci Technol.* 2005;39:4317–4320.
8. Rozendal RA, Hamelers HVM, Euverink GJW, Metz SJ, Buisman CJN. Principle and perspectives of hydrogen production through biocatalyzed electrolysis. *Int J Hydrogen Energy.* 2006;31:1632–1640.
9. Logan BE. Scaling up microbial fuel cells and other bioelectrochemical systems. *Appl Microbiol Biotechnol.* 2010;85:1665–71.
10. Gunawardena A, Fernando S, To F. Performance of a yeast-mediated biological fuel cell. *Int J Mol Sci.* 2008;9:1893–1907.
11. Ducommon R, Favre MF, Carrard D, Fischer F. Outward electron transfer by *Saccharomyces cerevisiae* monitored with a bi-cathodic microbial fuel cell-type activity sensor. *Yeast.* 2010;27:139–148.
12. Türker M. Development of biocalorimetry as a technique for process monitoring and control in technical scale fermentations. *Thermochim Acta.* 2004;419:73–81.
13. Delás J, Notari M, Fore?s J, Pechuan J, Porcar M, et al. Yeast cultures with UCP1 uncoupling activity as a heating device. *N Biotechnol.* 2009;26:300–306.
14. Lineykin S, Ben-Yaakov S. Modeling and analysis of thermoelectric modules. *IEEE Trans Ind Appl.* 2007;43:505–512.
15. von Stockar U, van der Wielen LAM. Thermodynamics in biochemical engineering. *J Biotechnol.* 1997;59:25–37.
16. Ungwuanyi JO, Harvey LM, McNeil B. Diversity of thermophilic populations during thermophilic aerobic digestion of potato peel slurry. *J Appl Microbiol.* 2008;104:79–90.
17. Bell LE. Cooling, heating, generating power, and recovering waste heat with thermoelectric systems. *Science.* 2008;321:1457–1461.
18. Larjola J. Electricity from industrial waste heat using high-speed organic Rankine cycle (ORC). *Int J Prod Econ.* 1995;41:227–235.
19. Saidur R, Rezaei M, Muzammil WK, Hassan MH, Paria S, et al. Technologies to recover exhaust heat from internal combustion engines. *Renew Sust Energ Rev.* 2012;16:5649–5659.

Publication 4

Producing High-Strength Liquor from Mesophilic Batch Acidification of Chicken Manure

Christian Abendroth^{*1,2}, Erik Wünsche¹, Olaf Luschnig^{1,3}, Christoph Bürger¹ and Thomas Günther⁴

¹Bio H2 Energy GmbH, Jena, Germany

²Cavanilles Institute of Biodiversity and Evolutionary Biology, Universitat de València, València, Spain

³BioEnergie Verbund e.V., Jena, Germany

⁴Eurofins Umwelt Ost GmbH, Jena, Germany

Abstract

This report describes the results from anaerobic batch acidification of chicken manure as a mono-substrate studied under mesophilic conditions. The manure was diluted with tap water to prevent methane formation during acidification and to improve mixing conditions by reducing fluid viscosity; no anaerobic digester sludge has been added as an inoculum. Highest acidification rates were measured at concentrations of 10 gVS/L and 20 gVS/L; the pH value remained high (pH 6.9–7.9) throughout the test duration and unexpected fast methane formation was observed in every single batch. At substrate concentrations of 10 gVS/L there was a remarkable methane formation representing a value of 82% of the respective biochemical methane potential of chicken manure. Increasing substrate concentrations did not suppress methane formation but impaired acid production. Consequently, the liquor cannot be stored over longer periods but should immediately be used in a digestion process.

Introduction

During our research we investigated the batch acidification of chicken manure

(CM) with the aim of producing a strong liquor containing high concentrations of volatile fatty acids (VFA) as a substrate for anaerobic digesters. CM is an interesting substrate for anaerobic digestion. With chicken farming being one of the most intensive operations in agriculture [1], large amounts of CM with a considerable biogas potential are locally available. The manure is known for its high nitrogen content and the fermentation of CM has been described as difficult [1]. Therefore, Abouelenien et al. (2010) [2] suggested ammonia removal to improve digestion conditions. Nonetheless, the toxicity of ammonia derived from CM, in reality, prevents the use of CM for digestion. Several recent publications, including Niu et al. (2013) [3] and Fotidis et al. (2014) [4], are dealing with this problem. Other authors have described in detail the digestion process of CM [5, 6, 7]. They reported that the anaerobic digestion of CM is difficult at higher loadings of total solids (TS) (higher than 10% TS) and that an optimal concentration range is between 4% and 10% influent TS feed concentration. Webb and Hawkes (1985) [6] suggested the optimisation based on a two-stage process. Current works from Fu and Holtzapfel (2011) [8], Liu et al. (2012) [9], Yan et al. (2014) [10] or Jie et al. (2014)

[11] give insight into the optimization of acidification conditions in anaerobic digestion (AD) and the advantage of separately controlled acidification processes.

Although our work includes research into the two-stage process, the main focus is on the acidification step with CM as a mono-substrate. The key objective of this research was to produce high-strength liquor, rich in VFA by maximising the solubilisation of nutrients and production of VFA in a separately operated batch acidification step.

Material and methods

Substrate

CM was collected from a local poultry farm near Jena/Thuringia (Germany). The fresh CM, as described in Table 3, was dried at 40 °C in an oven with forced ventilation, ground in a ball mill, sieved through a 1 mm screen and thoroughly mixed to provide a homogeneous substrate. The drying procedure led to a 6.8% reduction of total nitrogen as compared with the fresh manure owing to ammonia losses. Table 3 shows substrate characteristics of the CM.

The biochemical methane potential (BMP) of CM was measured in batch experiments at 37 °C and over 21 days in accordance with the German standard method of VDI 4630 (2006) [12]. The final methane yield was 200 L CH₄/kg VS (corresponding to 56% methanisation of initially added chemical oxygen demand (COD)).

Batch experiments

Initial tests included short-term acidification experiments, which have been performed in 0.5 L SIMAX-bottles (duration between 4 to 5 days). Substrate concentrations were set up at 10, 20, 30, 40, 50, 60 and 100 gVS/L. Corresponding amounts of CM were suspended in 0.5 L of tap water stirred by a magnetic stirrer and heated to 37 °C. The bottles were then flushed with nitrogen to ensure anaerobic conditions. Each bottle had been connected to an eudiometer (liquid displacement system) for measurement of biogas formation.

Investigations into the long-term conditions for acidification formed the second part of our research. The experimental procedure was similar to the short-term batch acidification, but with an extended incubation time of 41 days. The CM was again suspended in tap water with initial substrate concentrations of 10, 20 and 40 gVS/L. The first acidification batches were set up without the addition of inoculation sludge, but this was changed for later batches, where we added 100 ml of the suspension from the previous batch (total volume 500 ml). Sampling occurred every 3 or 4 days through the bottle sampling port.

To ensure constant and accurate sampling conditions, gas and liquid samples were taken from two identical sets of bottles, one set for gas sampling and the other set for liquid sampling. This approach of sampling was chosen to avoid withdrawal of nutrients that could affect gas production rates. Biogas samples were taken from the eudiometers with a gas tight syringe and transferred into headspace vials displacing the barrier solution (saturated saline solution; pH 2).

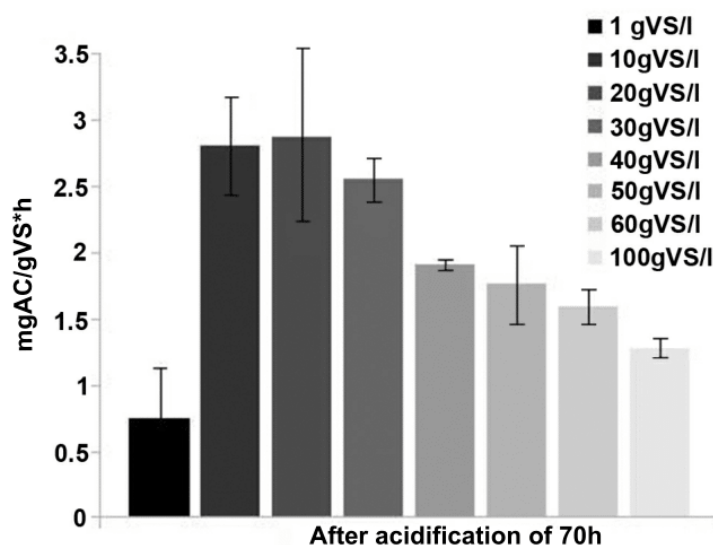


FIGURE 20: Characterisation of the acidogenesis: Acid-production (TVFA) per hour under conditions of different concentrations of VS. TVFA are given as acetic acid equivalent (AC).

TABLE 3: Chemical characteristics of dried CM (mean \pm standard deviation).

Parameter chicken manure	Unit	Dried
Total solids (TS)	% (W/W)	95.6 \pm 3.2
Volatile solids (VS)	% TS	69.4 \pm 0.9
Chemical oxygen demand (total COD)	mg g ⁻¹ TS	893 \pm 45
Total organic carbon (TOC)	% TS	36.3 \pm 4.7
Total nitrogen (TN)	% TS	5.5 \pm 1.5
Ammonia nitrogen (NH ₄ -N)	% TS	0.52 \pm 0.002
Total phosphorus	% TS	1.48 \pm 0.4
pH (CaCl ₂ -extract)	–	6.8 \pm 0.11

Analytical methods

The wet samples were dried overnight at 105 °C (TS). Volatile solids (VS) content was estimated as the loss of ignition by dry matter combustion at 525 °C. For all pH measurements, a pHmeter (WTW, Germany) with a glass electrode (Schott/Germany) was used. The concentration of individual volatile fatty acids (acetate, propionate, butyrate, isobutyrate, valerate, isovalerate and caproate) was determined by gas chromatography with a Shimadzu gas chromatograph/flame ionisation detector and equipped with a DB-1701 column (Macherey-Nagel, Germany).

For determination of soluble COD, the samples were passed through a 0.45- μ m-pore-size membrane filter. The COD of the filtrate was determined using a COD-Spectroquant test kit (Merck, Germany) and a digital photometer SQ 118 (Merck, Germany). Gas composition (CH₄, CO₂) was analysed with a Combimass GA-m (Bender, Germany) multi-gas monitor.

Results and discussion

Optimal CM concentration during acidification

The amount of total volatile fatty acids (TVFA) produced from dry CM was optimised in a first acidification step. Several initial substrate concentrations were investigated (Figure 20). Optimal acid production occurred at concentrations of between 10 gVS/L and 20 gVS/L. The rate of acid formation decreases substantially at low concentrations. CM-concentrations around 10 gVS/L show a four times higher acidification rate than the

initial CM-concentration of 1 gVS/L (a decrease from 2.8 mgTVFA/gVS h for the 10 gVS/L to 0.75 mgTVFA/gVS h for the 1 gVS/L). At higher concentrations than 20 gVS/L, the acidification rate decreases successively and drops to 1.28 mgTVFA/gVS h at a concentration of 100 gVS/L.

Although unexpected, we observed already during the first days methane formation. Therefore the methane formation during batch acidification was investigated in more detail in subsequent experiments.

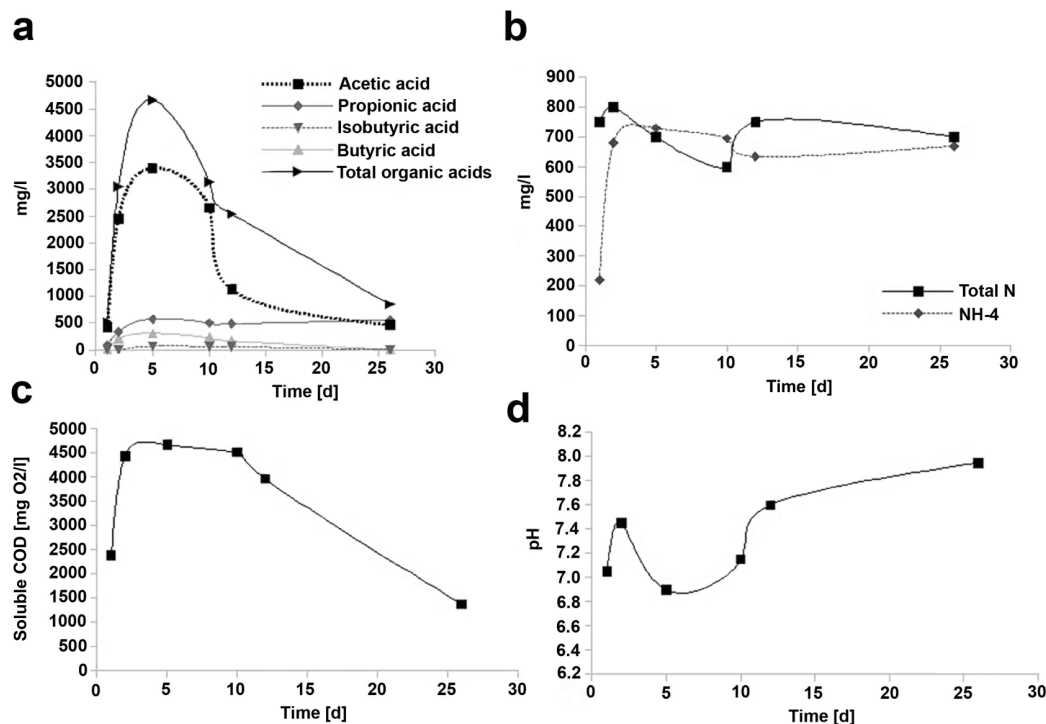


FIGURE 21: Long-term batch digestion of CM at an initial concentration of 10 g L⁻¹ VS. (a) Acid production, (b) total nitrogen and NH₄-N, (c) solubilised COD and (d) pH value.

Characterisation of the produced VFA-liquor

During long-term batch experiments, the hydrolysis and acidification of CM were investigated at a concentration of 10 gVS/L (equivalent to 12870 mg/L of COD). CM was rapidly degraded

to VFA under anaerobic conditions. Maximum TVFA concentration (4663 mg/L) was achieved at Day 4–5, indicating an acidification efficiency of 46% of COD (Figure 21(a)). Acetic acid was the predominant VFA species (3400 mg/L) followed by comparably

low concentrations of propionate and butyrate (<500 mg/L). The maximum TVFA concentration coincided with the peak of soluble COD (4680 mg/L) (Figure 21(c)). In total, 36.4% of the initially added COD was solubilised. Another parameter monitored was the reduction of organic nitrogen to ammonium (NH₄-N) (Figure 21(b)). The conversion took place within the first 3–5 days, with the final concentration close to total-N concentration in the feed. These data indicate a rapid and nearly complete degradation of organic nitrogen into soluble NH₄-N. This opens the possibility for a subsequent ammonia removal from the digestate prior to full methanisation.

In spite of intense VFA formation from CM, the pH of the batches did not drop below pH 6.9 (Figure 21(d)). The stabilisation of pH in a neutral range can give rise to methanogenic activity counteracting the accumulation of VFA.

Hence, after 5 days TVFA and soluble COD decreased slowly, reaching values as low as a third of the respective maximum value (Figure 21(a) and (c)) at Day 26. It has been concluded that methane formation was the cause for VFA reduction.

Methane formation during acidification

Gas production during batch CM acidification started at Day 2, followed by a short lag-phase until Day 5, indicating a diauxic growth curve (Figure 22). At a concentration of 10 gVS/L the continued anaerobic incubation of batches led to continuous production of methane starting on Day 2 and accelerating on Day 6. On Day 41, a cumulative methane production of 189 L CH₄/kg VS was measured. These values approximate the BMP of 200 L CH₄/kg VS.

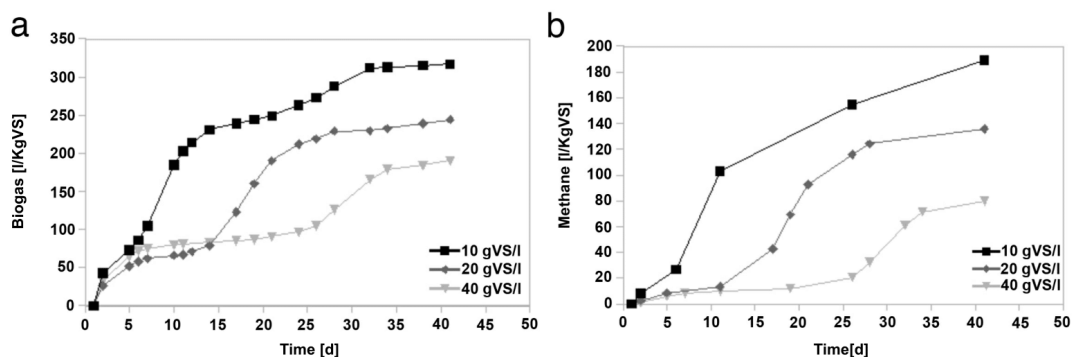


FIGURE 22: Analysis of the gas-production during batch-acidogenesis: (a) biogas formed per kgVS; (b) methane formed per kgVS.

The results indicate that under the chosen conditions of CM batch acidification, a significant methane production will occur. The early appearance of methane during the acidification process interferes with VFA accumulation and is expected to prevent a temporary storage of the liquor rich in VFA at ambient temperatures. Additional attempts to

stabilise TVFA-accumulation and to suppress methane formation failed. Using tap water instead of anaerobic digester sludge (ADS) for inoculation of batches was not sufficient to inhibit methane formation. Higher CM-concentrations led to impaired acidification and a delayed gas production, but did neither prevent methane formation. This is consistent with the observation of

Bujoczek et al. (2000) [7], who described 40 days of lag phase for digestion of undiluted CM. We concluded that elevated buffer capacity (ammonium and carbonate buffer systems) led to pH stabilisation of the liquid phase with values above pH 7, and these conditions were sufficient to maintain methanogenic activity in the VFA-liquor.

Conclusions

The results from our trials show optimal substrate concentration for CM batch acidification between 10 and 20 gVS/L with an maximum acidification rate of 2.8 mgTVFA/gVS h (acidification yields of 47%). The highest TVFA accumulation in the liquid phase corresponds to 450 mgVFA/gVS. A rapid hydrolysis of CM into soluble products is indicated by peaks in soluble COD, TVFA and the complete conversion of organic nitrogen into ammonia-N at Day 5. However, after Day 5, soluble COD and TVFA decrease significantly, accompanied by increasing methane formation, leading to consumption of VFA by methanogens. After 41 days, most of the CM is consumed for biogas formation. The approach to produce VFA-liquor from CM in an anaerobic batch process was successful with respect to rapid hydrolysis and acidification, and the use of an ADS-free process. However, the system failed in stabilising the accumulated VFA in the liquid phase and preventing methanogenic conditions. Therefore, the liquor should immediately be used in a digestion process.

Acknowledgements

We thank Manfred Schmid and Ursula Kepp for proofreading of the article and William Than SP (SP Multitech Malaysia) for the collaboration and regular access to his CM fed two-stage plant.

Funding

This work was supported by a grant of the German Federal Ministry of

Economics and Technology [ProInno II, grant VP2531901ST9 / ZIM, grant 16KN017626].

References

1. Abouelenien F, Nakashimada Y and Nishio. Dry mesophilic fermentation of chicken manure for production of methane by repeated batch culture. *J Biosci Bioeng.* 2009;107: 293–295.
2. Abouelenien F, Fujiwara W, Namba Y, et al. Improved methane fermentation of chicken manure via ammonia removal by biogas recycle. *Bioresour Technol.* 2010;101: 6368–6373.
3. Niu Q, Qiao W, Qiang H, et al. Mesophilic methane fermentation of chicken manure at a wide range of ammonia concentration: Stability, inhibition and recovery. *Bioresour Technol.* 2013;137:358–367.
4. Fotidis IA, Kougias PG, Zaganas ID, et al. Inoculum and zeolite synergistic effect on anaerobic digestion of poultry manure. *Environ Technol.* 2014;35:1219–1225.
5. Safley LM, Vetter RL, Smith D. Managing a poultry manure anaerobic digester. In: *Proceedings of the Fifth International Symposium on Agricultural Wastes, Agricultural Waste Utilization and Management.* 1985; Chicago, IL, 16-17 December, pp 491–499. St. Joseph, MI: ASAE Publication.
6. Webb AR and Hawkes FR. The anaerobic digestion of poultry manure: Variation of gas yield with influent concentration and ammonium-nitrogen levels. *Agr Wastes.* 1985;14:135–156.
7. Bujoczek G, Oleszkiewicz J, Sparling R, et al. High solid anaerobic digestion of chicken manure. *J Agr Eng Res.* 200;76:51–60.
8. Fu Z and Holtzaple MT. Anaerobic thermophilic fermentation for carboxylic acid production from in-storage air-lime-treated sugarcane bagasse. *Appl Microbiol Biot.* 2011;90:1669–1679.
9. Liu H, Wang J, Liu X, et al. Acidogenic fermentation of proteinaceous sewage sludge: Effect of pH. *Water Res.* 2012;46:799–807.
10. Yan BH, Selvam A and Wong JW. Application of rumen microbes to enhance

food waste hydrolysis in acidogenic leach-bed reactors. *Bioresour Technol.* 2014;168:64–71.

11. Jie W, Peng Y, Ren N, et al. Volatile fatty acids (VFAs) accumulation and microbial community structure of excess sludge (ES) at different pHs. *Bioresour Technol.*

2014;152:124–129.

12. VDI 4630. Fermentation of organic materials, characterisation of the substrate, sampling, collection of material data, fermentation tests. Düsseldorf, Germany: *The Association of German Engineers (VDI)*. (2006).

Publication 5

Microbial communities involved in biogas production exhibit high resilience to heat shocks

Christian Abendroth^{*1,2}, Sarah Hahnke³, Claudia Simeonov², Michael Klocke³,
Sonia Casani Miravalls⁴, Patrice Ramm³, Christoph Bürger⁴, Olaf Luschnig⁴,
Manuel Porcar^{*1,5}

¹Institute for Integrative Systems Biology (I2SysBio), Paterna, Valencia, Spain

²Robert Boyle Institut e.V., Jena, Germany

³Leibniz Institute for Agricultural Engineering and Bioeconomy (ATB),
Bioengineering, Potsdam, Germany

⁴Bio H2 Umwelt GmbH, Jena, Germany

⁵Darwin Bioprospecting Excellence, S.L. Parc Científic Universitat de Valencia,
Paterna, Valencia, Spain

Abstract

We report here the impact of heat-shock treatments (55 and 70 °C) on the biogas production within the acidification stage of a two-stage reactor system for anaerobic digestion and biomethanation of grass. The microbiome proved both taxonomically and functionally very robust, since heat shocks caused minor community shifts compared to the controls and biogas yield was not decreased. The strongest impact on the microbial profile was observed with a combination of heat shock and low pH. Since no transient reduction of microbial diversity occurred after the shock, biogas keyplayers, but also potential pathogens, survived the treatment. All along the experiment, the heat-resistant bacterial profile consisted mainly of Firmicutes, Bacteroidetes and Proteobacteria. Bacteroides and Acholeplasma were reduced after heat shocks. An increase was observed for Aminobacterium. Our results prove the stability to thermal stresses of the microbial communities involved in acidification, and the resilience in biogas production irrespectively of the thermal treatment.

Introduction

Anaerobic digestion is a highly sophisticated process that consists of four phases: hydrolysis, acidogenesis, acetogenesis, and methanogenesis [1]. In practice, all four stages are usually combined in a single reaction vessel, denominated as Completely or Continuously Stirred Tank Reactor (CSTR). However, several reports demonstrated the advantages of separating the degradation process into two stages optimized each either for acidification or methane-production [2, 3, 4, 5]. In the first stage, biopolymers are degraded into monomers such as different volatile short-chain fatty acids (VFAs). In the second stage, produced acids are converted into methane and carbon dioxide. A separated acidification stage is especially interesting, as it allows the production of valuable intermediates or by-products, such as VFAs [6] and molecular hydrogen [7]. In addition, having the acidification stage as a separate sub-system allows using substrates such as silages with high content of solids and high organic loading rates.

Besides biological pre-treatments, physical, chemical and physico-chemical methods are also used. All of them can make the biomass accessible to microbial enzymes and, hence, yield higher amounts of fermentable sugars [8]. Thermal pre-treatments, which require high amounts of energy, can successfully increase the accessibility of lignocellulose, but temperatures as high as 200 – 300 °C have been reported to be required [9]. However, recent studies suggest that lower temperatures such as 120 °C [10] or even 70 °C [11] can already significantly improve biomass degradability. In fact, a recent study reports improved hydrogen production from digesters with granular sludge after a mild heat-shock treatment [12]. Stable reactor performance has been reported even for hyperthermophilic digestion conditions up to at least 65 °C [13, 14]. At those temperatures, microorganisms require very long adaptation times [15]. Besides thermal tolerance, anaerobic microbiomes tend to be robust and adaptable to extreme conditions, including high ammonia levels [15, 16] or high salinity [17]. To reduce energetic demand and costs, and to avoid long adaptation times compared to long thermophilic processes, we aimed at exploring a new method for biogas production based on the application of mild thermal shocks throughout the process. The question we raised was whether acidifying microbiomes that are adjusted to mesophilic conditions, might tolerate short, hyperthermophilic heat shocks, and which would be the effect on the efficiency of the process. With the aim of combining thermal and biological pre-treatments, we constructed a two-stage two-phase system, heated the first stage cyclically up to 55 °C and 70 °C and investigated the impact of this treatment on the microbial community dynamics applying culture-dependent and cultivation-independent approaches. As

substrate of choice, grass biomass was chosen because of its high potential as renewable energy source [18], and because of its suitability for two-stage digestion [19].

Materials and methods

Fermentation conditions

Digestion experiments were performed in a two two-stage two-phase biogas reactor systems designed *ad hoc* for this work (Fig. 23). One two-stage system was used to investigate the impact of heat-shocks and a second one was used as a control system. The first stage of each system was used for acidification, and the second stage was used for subsequent methane formation. Additionally, each of the methane stages was filled with 1.58 Kg of bed packing (Christian Stöhr, Germany).

At the beginning of the experiment, each methane stage received 11.75 L of sewage seed sludge, and each acidification stage received 8 L of sewage sludge as inoculum. During acidification, fresh untreated grass biomass (Graminidae) consisting of 30.4% total solids (TS), 84.2% volatile solids (VS) of TS and a chemical oxygen demand (COD) of 260 mgO₂/g was used as solid phase. For every batch cycle, 96.2 g/L of grass VS were filled into a cylindrical sieve, which was located in the first stage for acidification to retain the solid phase during the percolation process. Leachate was percolated on the fixed grass bed to produce high-strength liquor, which was collected after every batch cycle of acidification. To keep the pH constantly at 6.0 or 6.8, a pH-regulation system was used for each acidification stage (BL 7916, Hanna Instruments, Germany). Collected liquor was stored under anoxic conditions at 4 °C and fed semi-continuously and manually into the methane stages. Each methane stage received daily

approximately 100 gCOD (8.5 gCOD/L). Digestate from the methane stages was stored under anoxic conditions at 4 °C and was used as leachate for the set-up of new acidification cycles (Fig. 24). Produced gas from all stages was collected in gasbags (Tecobag, Tesseraux, Germany) and analysed with

the Combimass Measurement device (Binder, Germany). Two multistage systems were performed in parallel and at mesophilic temperature (37 °C). The produced high strength liquor from the acidification stage from the first system was regularly exposed to heat shocks.

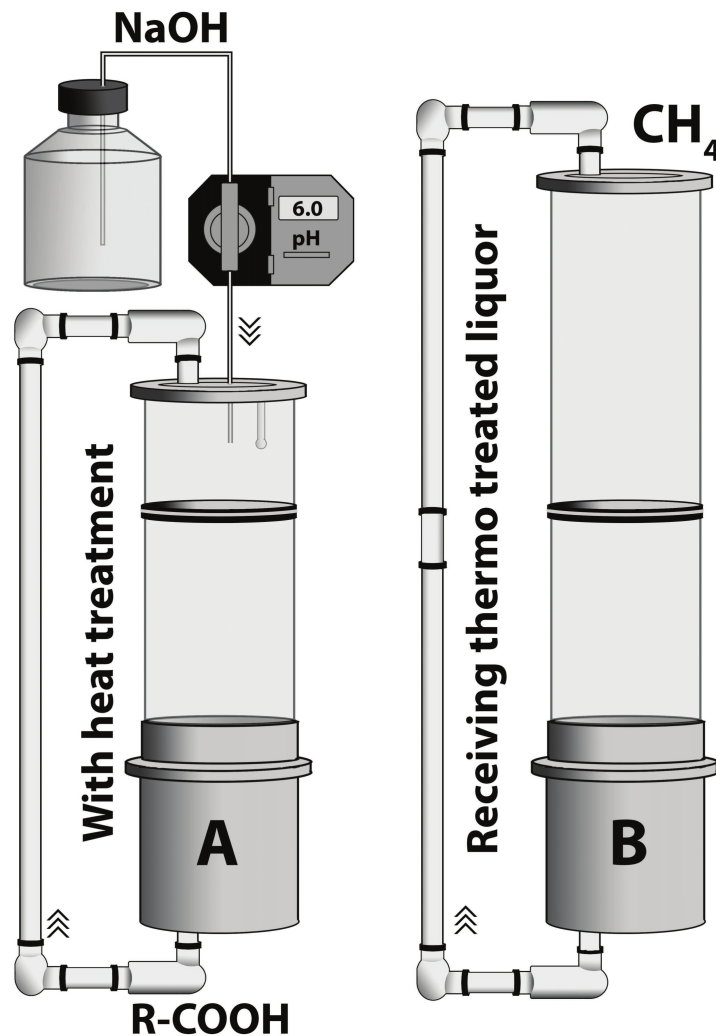


FIGURE 23: Experimental set-up: Reactor set-up consisting of a hydrolytic/acidogenic stage (A) and a methanogenic stage (B). Feeding of the methanogenic stage with the liquid phase from the hydrolytic/acidogenic stage and heat-treatment was performed manually on a daily basis. Two reactor systems were built, further referred as heat-shock system and control system.

Heat shocks and sampling

An overview about heat shock regimes is given in Figure 24. Heat shocks were applied manually transferring the

leachate into an incubator, where the leachate was heated up to 55 °C. After the core of the biomass reached that temperature, the liquor was further

incubated for 30 min and then refilled into the two-phase acidification stage. During the first 21 days, only one heat shock with 55 °C was carried out per week. From day 22 until day 42, the heat-shock temperature was increased to 70 °C, performed similarly, and three heat shocks were applied for each acidification cycle (Fig. 24 and 26). Between experimental day 21 and 2, there was a technical break in operation for two weeks.

A second, identical multistage system was used as control without heat shocks (further referred as control system). Samples for 16S-rRNA gene-amplicon high-throughput analysis were taken every second and seventh day of each acidification cycle. Additionally, at day 36, directly after a 70 °C heat shock, a sample for 16S-rRNA gene full length sequencing was taken, as well as a sample for microbial culturing at day 37.

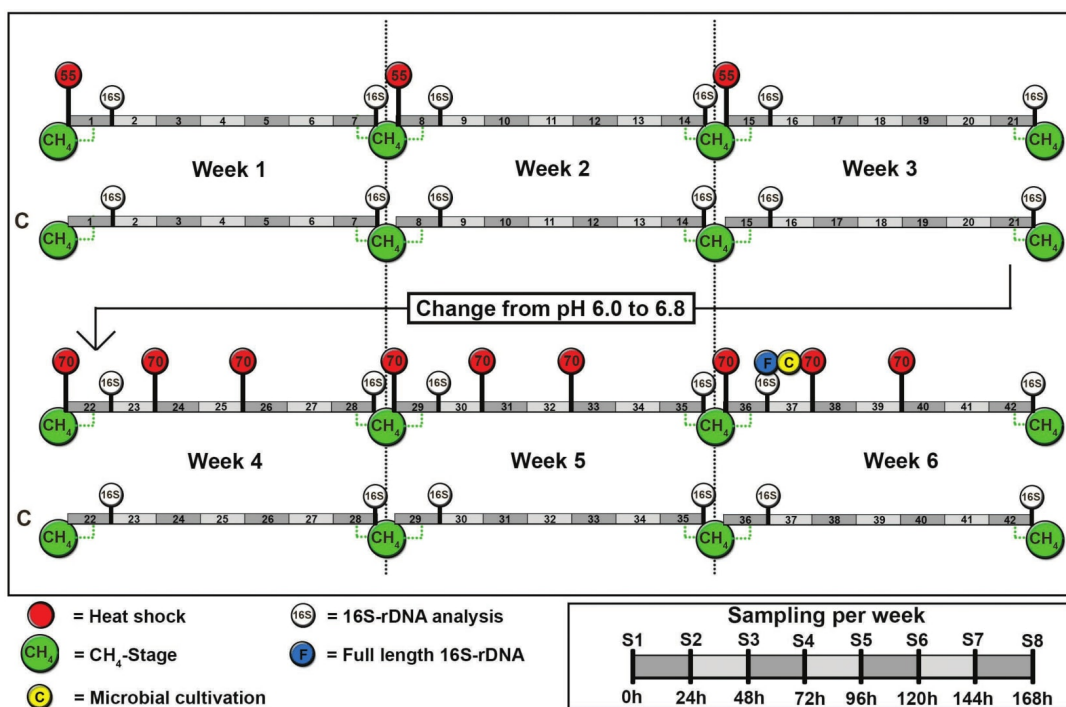


FIGURE 24: Experimental timeline: Acidification occurred in six cycles of one week each. Experimental week 3 and experimental week 4 were separated by a two-weeks interval. Green circles indicate the collection of liquor and the subsequent feeding into the methane stages. Collected digestates from the methane stages were used for setting up new acidification cycles.

Chemical and microbial process analysis

Analysis of chemical parameters was performed as previously described in Abendroth et al. (2017) [19]. Extraction of DNA, primer nucleotide sequences for bacteria, 16S-rRNA gene amplification, high-throughput amplicon sequencing with IonTorrent and sequence analysis was performed

as described by Abendroth et al. (2015) [20]. At day 36 of the experiment, the acidification stage from the heat-shock system was analysed through full length sequencing of the 16S-rRNA gene and anaerobic culturing approaches. Cloning and library construction was performed as described by Rademacher et al. (2012) [13].

Isolation of microbial strains

To isolate different bacteria, cultivation was performed under anoxic conditions on Reinforced Clostridial Agar (Oxoid Ltd.) and on modified DSMZ medium no. 350 (*Cellulomonas fermentans* medium). In contrast to the DSMZ medium 350 (DSMZ 2007), the modified medium contained (per liter) 2.0 g yeast extract, 0.5 g cellobiose, 2.0 g soluble starch, 1.0 g methyl cellulose and 15.0 g agar; the pH of the medium was 6.9. After autoclaving 10 mL/L vitamin solution was added according to DSMZ medium 141 (DSMZ 2017). The reactor sample was diluted 10^1 , 10^4 and 10^6 fold in anoxic Ringer's solution and aliquots of the dilutions were streaked on pre-reduced agar plates. After incubation at 37 °C in an anaerobic chamber single colonies were re-streaked until purification was achieved. A loop full of colonies of the isolates were suspended in 50 μ L molecular biological grade water and cells were lysed by consecutive freezing and thawing. Amplification and subsequent sequencing of the nearly full-length 16S rRNA gene of the strains was carried out using the primers 27F and 1492R as described by Hahnke et al. (2014) [21].

Results and discussion

Impact of heat-shocks on process performance

After applying heat shocks on the acidification stage, almost no differences of chemical parameters were observed between the heat-shock system and the control system (Fig 25). Solubilisation of chemical oxygen demand and production of total volatile fatty acids (TVFA) were monitored daily and found to reach similar values in both the heat-shock system and the control system (Fig. 25A). Additionally, similar

volumes of methane from the produced high-strength liquor were produced (Fig. 25B). During the first three weeks, when 55°C heat shocks were applied, 29.1 ± 11.4 gCOD/L and 15.9 ± 5.6 gTVFA/L were produced. The respective control showed 35.6 ± 6.8 gCOD/L and 20.5 ± 3.7 gTVFA/L. In the following three weeks, where heat shocks were more frequently applied and at a higher temperature (70 °C), concentrations of 26.9 ± 2.7 gCOD/L and 18.9 ± 0.8 gTVFA/L were measured. The corresponding control samples yielded 28.4 ± 5.7 gCOD/L and 19.6 ± 0.2 gTVFA/L. Even though the degradation efficiency was not detectably improved, no process inhibition was found either. At week 2 the heat-shock system and the control system showed both a higher COD compared to the other weeks. Very likely this is due to heterogeneity of the used substrate.

The high conversion of solubilized COD indicates that methanation was not inhibited in both methane stages (heat shock system and control system) (Fig. 25B). The produced amount of methane per g of solubilized COD was in both methane stages slightly above the theoretical maximum of 350 ml/gCOD due to small particles that remained in the collected high strength liquor from the acidification. In addition and in comparison to the control system, we observed in the heat-shock system a reduced methane formation in the acidification stage subjected to heat shocks. Compared to the methane stage, only low levels of methane were formed in the acidification stage of both reactor systems. In the acidification stage with 55 °C heat shocks, 67% less methane was formed than in the un-heated control. In the experiment with 70 °C, it was 40% less methane compared to the control (Fig. 25C).

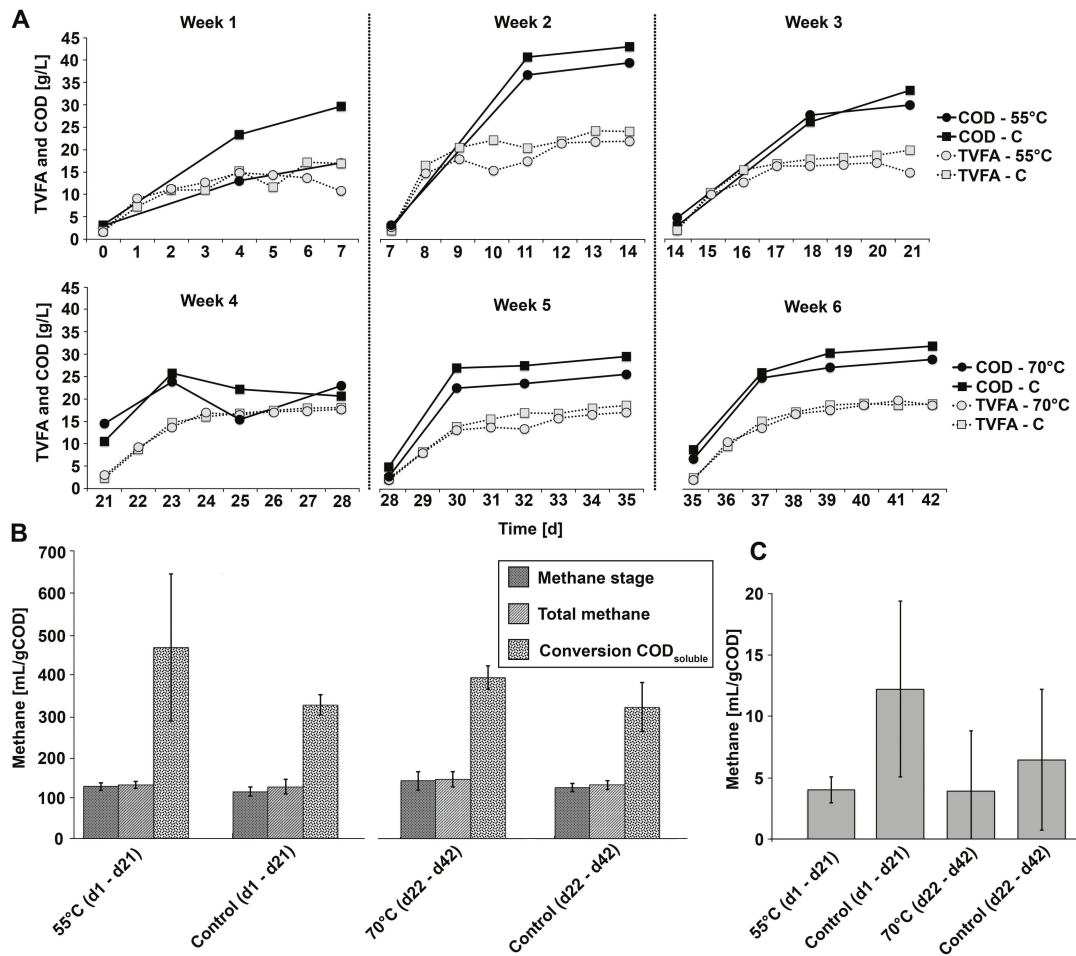


FIGURE 25: Chemical analysis: Produced total volatile fatty acids (TVFA) and solubilized chemical oxygen demand (COD) are given for both the heat-shock system and the control system (A). Produced methane as well as conversion efficiency of solubilized COD for acidification and methane stages is summarized for different time intervals: day 1 to 21; day 22 to 42 (B). The methane production from the acidification stage is shown in (C). Gas volume is given as a mean value for the total gas formation per week (for each batch cycle). Standard deviations were calculated with the mean value from experimental week 1 – 3 and experimental week 4 – 6.

Therefore, the reduction of methanogenic contaminations from the seed sludge in the acidification stage associated to heat treatments could help to separate acidification from methanation more efficiently in order to prevent loss of methane.

Post heat-shock transient microbial community

For each acidification cycle, samples for 16S-rRNA high throughput sequencing were taken at the second and last day (Fig. 24, 26). On the phylum level,

all sequences showed a profile mainly consisting of Firmicutes, Bacteroidetes and Proteobacteria (Fig. 26). This is in concordance with our previous studies on microbiomes from seven anaerobic digester plants in Germany, and acidification of grass biomass [19, 18]. During experimental weeks 1 – 3 Proteobacteria were especially enriched, whereas Bacteroidetes tended to decrease in the control non-shocked reactor. The high abundance of Proteobacteria is in concordance with a study published by Weerasekara et

al. (2016)[22], where Proteobacteria increased in frequency in wastewater due to acidic conditions. In our experiment, by changing the pH to 6.8 (experimental week 4 – 6), the amount of Proteobacteria was dramatically reduced and, in the heat shocked system the phylum Bacteroidetes recovered. This indicates a high microbial redundancy, as the change of dominating microbial groups showed no negative effects on the degradability of the used grass biomass. On genus level, *Bacteroides*, *Prevotella*, *Enterococcus*, *Clostridium* and *Pseudomonas* were abundant during experimental weeks 1 – 3. Raising the pH to 6.8 at day 21 was associated with a dramatic shift in the microbial composition, consisting mainly of *Bacteroides*, *Streptococcus*, *Aminobacterium*, *Clostridium* and *Tissierella* (Fig. 26). The fact that even three shocks per cycle at 70 °C did not cause permanent shifts in the microbial composition, but only transient modifications indicates that the mesophilic microbiomes from anaerobic digesters exhibit high resilience against

heat shocks, while being more sensitive to pH changes.

Interestingly, many sequences remained unclassified on the genus level (Fig. 26). This is in accordance with other studies on biogas facilities, e.g., based on previous study on NGS [23], where also many unclassified species were detected.

Heat shocks and pathogens

Microbial culturing as well as culture-independent 16S-rDNA full-length sequencing was used to assess microbiota on species level (Fig. 24). Surprisingly, many opportunistic pathogenic species listed with risk level 2 in the TRBA (technical rules for biological working materials from the German committee for biological working materials, 2004) were detected, namely *Bacteroides ovatus*, *Bacteroides thetaiotaomicron*, *Bacteroides uniformis*, *Citrobacter werkmanii*, *Enterococcus gallinarum*, *Globicatella sulfidifaciens*, *Streptococcus lutetiensis*, *Corynebacterium freneyi*, *Escherichia hermannii*, *Lactococcus garvieae*, or *Proteus mirabilis*.

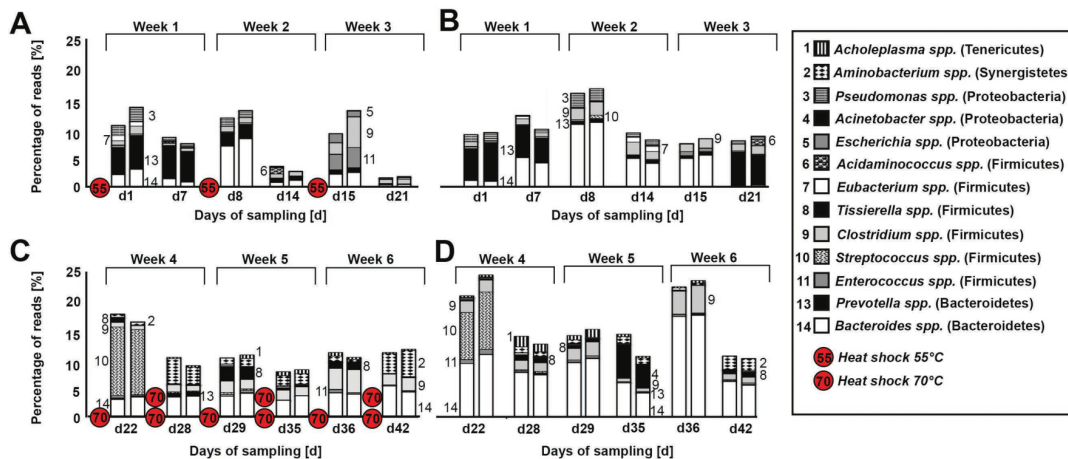


FIGURE 26: Microbiome composition of heat-shocked samples. Microbial composition is given as a percentage of all analysed bacterial sequences. Sequences were classified on the genus level. Values for samples from the experiment with 55 °C heat shocks are shown in A; and C corresponds to the 70 °C heat shocks. Values for samples from the control system without heat shocks are shown in B and D. All samples were analysed as duplicates.

The application of sewage sludge as seed sludge might explain the occurrence of detected pathogens mentioned before, as sewage is well known for its content of pathogenic bacteria [24]. The fact that corresponding genera were observed in high abundance (Fig. 26) also implies a high abundance of these pathogens. In conclusion, abundant heat treatments at 70 °C were not sufficient to suppress potential pathogenic genera.

Conclusions

The response of microbial populations present in mesophilic acidification stages to short heat cycles was investigated. The studied microbiomes proved very robust, since the same amount of methane was produced in heat-shocked samples compared to the control ones. Heat-shocks caused only minor, transient community shifts and the strongest impact on the microbiome was observed with a combination of heat shock and low pH. Potential pathogenic genera remained abundant; and several pathogens were still found after the heat treatment. Our results can be the first step towards future approaches combining microbial-driven acidification and thermal treatments as a new pre-treatment methodology.

Acknowledgements

We thank our student Justus Hardegen for technical assistance. Further, we are grateful for funding of the work by the German Federal Ministry of Economic Affairs and Energy (grant no. KF 2050830SA4, KF 3400701SA4, KF 2112205SA4 and 03KB110A). SH and MK thank Kerstin Mundt for the excellent technical assistance.

References

1. Haarstrick A, Hempel DC, Ostermann L, Ahrens H, Dinkler D. Modelling of the biodegradation of organic matter in

municipal landfills. *Waste Manage. Res.* 2001; 19: 320–331.

2. Baccay RA, Hashimoto AG. Acidogenic and methanogenic fermentation of causticized straw. *Biotechnol. Bioeng.* 1984; 26: 885–891.

3. Dinopoulou G, Rudd T, Lester JN. Anaerobic acidogenesis of a complex wastewater: I. The influence of operational parameters on reactor performance. *Biotechnol. Bioeng.* 1988; 5: 958–68.

4. Gijzen HJ, Zwart KB, Verhagen FJ, Vogels GP. High-Rate two-phase process for the anaerobic degradation of cellulose, employing rumen microorganisms for an efficient acidogenesis. *Biotechnol. Bioeng.* 1988; 31: 418–425.

5. Abendroth C, Wünsche E, Luschnig O, Bürger, C., Günther, T. Producing high-strength liquor from mesophilic batch acidification of chicken manure. *Waste Manage. Res.* 2015a.; 33: 291–294.

6. Koutinas A, Kanellaki M, Bekatorou A, Kandylis A, Pissaridi K, Dima A, Boura K, Lappa K, Tsafrakidou P, Stergiou PY, Foukis A, Gkini OA, Papamichael EM. Economic evaluation of technology for a new generation biofuel production using wastes. *Bioresour. Technol.* 2016; 200: 178–185.

7. Voolapalli RK, Stuckey DC. Hydrogen production in anaerobic reactors during shock loads – influence of formate production and H₂ kinetics, *Water Res.* 2001; 35: 1831–1841.

8. Mood SH, Golfeshan AH, Tabatabaei M, Jouzani GS, Najafi GH, Gholami M, Ardjmand M. Lignocellulosic biomass to bioethanol, a comprehensive review with a focus on pretreatment. *Renew Sust. Energ. Rev.* 2013; 27: 77–93.

9. Yan W, Acharjee TC, Coronella CJ, Vasquez VR. Thermal pretreatment of lignocellulosic biomass. *Environ Prog. Sustain.* 2009; 28: 435–440.

10. Ennouri H, Miladia B, Diaz SZ, Güelfoc LAF, Solera R, Hamdi M, Bouallagui H. Effect of thermal pretreatment on the biogas production and microbial communities balance during anaerobic digestion of urban and industrial waste activated sludge. *Bioresour. Technol.* 2016; 214: 184–191.

11. Gonzales-Fernandez C, Sialve B, Bernet N, Steyer JP. Thermal pretreatment to improve methane production of

- Scenedesmus biomass. *Biomass Bioenerg.* 2012; 40: 105–11.
12. Alibardi L, Favaro L, Lavagnolo MC, Basaglia M, Casella S. Effects of heat treatment on microbial communities of granular sludge for biological hydrogen production. *Water Sci. Technol.* 2012; 66: 1483–1490.
13. Rademacher A, Nolte C, Schönberg M, Klocke M. Temperature increases from 55 to 75°C in a two-phase biogas reactor result in fundamental alterations within the bacterial and archaeal community structure. *Appl. Microbiol. Biotechnol.* 2012; 96: 565–576.
14. Algapani DE, Qiao W, Su M, di Pumpo F, Wandera SM, Adani F, Dong R. Bio-hydrolysis and bio-hydrogen production from food waste by thermophilic and hyperthermophilic anaerobic process. *Bioresour. Technol.* 2016; 216: 768–777.
15. Moset V, Poulsen M, Wahid R, Højberg O, Møller HB. Mesophilic versus thermophilic anaerobic digestion of cattle manure: methane productivity and microbial ecology. *Microb. Biotechnol.* 2014; 8: 787–800.
16. Tian H, Fotidis IA, Mancini E, Angelidaki I. Different cultivation methods to acclimatise ammonia-tolerant methanogenic consortia. *Bioresour. Technol.* 2017; 232: 1–9.
17. Vrieze JD, Christiaens MER, Walraedt D, Devooght A, Ijaz UZ, Boona N. Microbial community redundancy in anaerobic digestion drives process recovery after salinity exposure. *Water Research.* 2016; 111: 109–117.
18. Jungers JM, Fargione JE, Sheaffer CC, Wyse DL, Lehman C. Energy potential of biomass from conservation grasslands in Minnesota, USA. *PLoS ONE.* 2013; 8(4):e61209.
19. Abendroth C, Vilanova C, Günther T, Luschnig O, Porcar M. Eubacteria and Archaea communities in seven mesophile anaerobic digester plants. *Biotechnol. Biofuels.* 2015; 8:87, doi 10.1186/s13068-015-0271-6.
20. Abendroth C, Simeonov C, Peretó J, Antúnez O, Gavidia R, Luschnig O, Porcar M. From grass to gas: microbiome dynamics of grass biomass acidification under mesophilic and thermophilic temperatures. *Biotechnol. Biofuels.* 2017; 10:171, doi 10.1186/s13068-017-0859-0.
21. Hahnke S, Striesow J, Elvert M, Mollar X, Klocke M. *Clostridium bornimense* sp. nov., isolated from a mesophilic, two-phase, laboratory-scale biogas reactor. *Int J Syst Evol Microbiol.* 2014;64, 2792–2797.
22. Weerasekara AW, Jenkins S, Abbott LK, Waite I, McGrath JW, Larma I, Eroglu E, O'Donnell A, Whiteley AS. Microbial phylogenetic and functional responses within acidified wastewater communities exhibiting enhanced phosphate uptake. *Bioresour. Technol.* 2016;220, 55–61.
23. Maus I, Koeck DE, Cibis KG, Hahnke S, Kim YS, Langer T, Kreubel J, Erhard M, Bremges A, Off S, Stolze Y, Jaenicke S, Goesmann A, Sczyrba A, Scherer P, König H, Schwarz WH, Zverlov VV, Liebl W, Pühler A, Schlüter A, Klocke M. Unraveling the microbiome of a thermophilic biogas plant by metagenome and metatranscriptome analysis complemented by characterization of bacterial and archaeal isolates. *Biotechnol. Biofuels.* 2016; 9:171, doi 10.1186/s13068-016-0581-3.
24. Arthurson V. Proper Sanitization of Sewage Sludge: a Critical Issue for a Sustainable Society. *Appl Environ Microbiol.* 2008; 74: 5267–5275.

Chapter 4: New taxa with foreseeable roles in biorefinery

Summary: Multiple bacterial strains with foreseeable roles in biorefinery were isolated and investigated. Two new Firmicutes isolates (strain HV4-6-A5C and strain HV4-5-B5C), were obtained from the hydrolysis stage of a mesophilic and anaerobic two-stage lab-scale leach-bed system for biomethanation of fresh grass. It is assumed that the bacterial isolates contribute to plant biomass degradation. Above this and with the aim of isolating robust lipolytic microbial strains, we have analyzed the bacterial communities inhabiting two domestic extreme environments: a thermophilic sauna and a dishwasher filter.

Publication 6

Abendroth C, Hahnke S, Codoñer FM, Klocke M, Luschnig O, Porcar M. Complete genome sequence of a new Firmicutes species isolated from anaerobic biomass hydrolysis, *Genome Announc.* 2017; 5:40, e00686-17, doi: 10.1128/genomeA.00686-17.



Publication 7

Hahnke S, Abendroth C, Codoñer FM, Porcar M, Luschnig O, Klocke M. Complete genome sequence of a new Ruminococcaceae bacterium isolated from anaerobic biomass hydrolysis.

Under preparation

Publication 8

Tanner K, Abendroth C, Porcar M. Warm and wet: robust lipase-producing bacteria from the indoor environment, *bioRxiv.* 2017, doi: 10.1101/148148.



Publication 6

Complete genome sequence of a new Firmicutes species isolated from anaerobic biomass hydrolysis

Christian Abendroth^{1,2,3}, Sarah Hahnke⁴, Francisco M. Codoñer⁵, Michael Klocke⁴,
Olaf Luschnig⁶, Manuel Porcar^{*1,2,7}

¹Cavanilles Institute of Biodiversity and Evolutionary Biology, Universitat de València, Paterna, València, Spain. ²Institute for Integrative Systems Biology (I2SysBio, Universitat de València-CSIC), 46020 València, Spain. ³Robert Boyle Institute e.V., Im Steinfeld 10, 07751 Jena, Germany ⁴Leibniz Institute for Agricultural Engineering and Bioeconomy (ATB), Bioengineering, Potsdam, Germany ⁵Lifesequencing SL, Paterna, Valencia, Spain ⁶Bio H2 Umwelt GmbH, Jena, Germany ⁷Darwin Bioprospecting Excellence, S.L. Parc Científic Universitat de València C/ Catedrático Agustín Escardino Benlloch, 9

Abstract

A new Firmicutes isolate, strain HV4-6-A5C, was obtained from the hydrolysis stage of a mesophilic and anaerobic two-stage lab-scale leach-bed system for biomethanation of fresh grass. It is assumed that the bacterial isolate contributes to plant biomass degradation. Here, we report a draft annotated genome sequence of this organism.

Degrading bacteria, most of them isolated from soil, play relevant roles in the turnover of different types of material, such as petrol [1], pollutants [2], metal [3], and cellulose [4, 5]. In the case of plant biomass degradation in biogas reactors, such microorganisms play an important role in making hardly accessible polymeric carbon sources available for other organisms for the production of biogas.

In this study, we present the genome sequence of a new Firmicutes isolate, strain HV4-6-A5C, which has a putative role in the microbial metabolic network for plant biomass degradation. This strain was isolated from a lab-scale leach-bed biogas reactor system, which

operated at 37°C with fresh grass as the sole substrate. Isolation was performed on Reinforced Rlostridial Agar (Oxoid Ltd.) after the diluted hydrolysate was reincubated with microcrystalline cellulose as the sole carbon source.

We applied a massive genome sequencing approach using the Illumina NextSeq 500 platform. A Nextera XT library with a mean insert size of 350 nucleotides (nt) was constructed and sequenced with a combination of 150-bp paired-end (PE) reads. A total of 29.2 million PE sequences, with a mean length of 149.85 nt, were obtained. Sequences were filtered by quality, and a total of 29.15 million PE sequences with a Q value higher than 20 (mean Q = 33.17) were included in the assembly. The sequences were assembled with SPAdes version 3.10.1 [6], using default parameters and a k-mer value that provided us with the lowest number of contigs, the longest contig, the largest N50 value, and the highest percentage of clean sequences. With a k-mer of 77, a total of 106 contigs were obtained. The total size of the genome was approximately 3.3 Mb, with an estimated GC content of 33.43 %, a

longest contig size of 276,895 bp, and an N50 of 113,179 bp.

The assembled genome sequences were annotated using the Prokka version 1.11 annotation pipeline [7], which involved predicting tRNAs, rRNAs, mRNAs, and signal peptides in the sequences using Aragorn, RNAmmer, Prodigal, and SignalP, respectively [8–11].

The genome contains 5,376 elements, of which 5,311 are open reading frames (ORFs; 2,723 canonical and 2,588 noncanonical) and 65 are encoded structural RNAs (sRNAs)—i.e., 5 ORFs for rRNAs and 60 ORFs for tRNAs.

Using BLAST we compared the contigs with all genome sequences available in the database. According to the PCOP [12] and the AAI [13], the genome can be classified as a species belonging to the genus *Clostridium*. Based on the average nucleotide sequence identity (ANI) (14), the closest related species was *Sporanaerobacter acetigenes*, showing an identity of only 71.13 %, which indicates that the novel strain represents a new species within the phylum Firmicutes.

Accession number(s). The genome described in the present article corresponds to the strain HV4-6-A5C deposited in the database for microbial strains (DSMZ) with the deposit number DSM 104144. The results of the whole-genome project have been deposited at DDBJ/EMBL/GenBank under the accession no. FXVB02000001 to FXVB02000106 with the name HV4-6-A5C1.

Acknowledgements

We are grateful for the funding provided by the German Federal Ministry of Economic Affairs and Energy (grant no. KF 2050830SA4, KF 3400701SA4, and KF 2112205SA4).

References

1. Pérez-Hernández I, Ochoa-Gaona S, Adams RH, Rivera-Cruz MC, Pérez-Hernández V, Jarquín-Sánchez A, Geissen V, Martínez-Zurimendi P. Growth of four tropical tree species in petroleum-contaminated soil and effects of crude oil contamination. *Environ Sci Pollut Res Int.* 2017;24:1769–1783.
2. McCormick ML, Adriaens P. Carbon tetrachloride transformation on the surface of nanoscale biogenic magnetite particles. *Environ Sci Technol.* 2004;38:1045–1053.
3. Kip N, van Veen JA. The dual role of microbes in corrosion. *ISME J.* 2015;9:542–551.
4. Singh N, Mathur AS, Tuli DK, Gupta RP, Barrow CJ, Puri M. Cellulosic ethanol production via consolidated bioprocessing by a novel thermophilic anaerobic bacterium isolated from a Himalayan hot spring. *Biotechnol Biofuels.* 2017;10:73.
5. Poszytek K, Ciekowska M, Sklodowska A, Drewniak L. Microbial consortium with high cellulolytic activity (MCHCA) for enhanced biogas production. *Front Microbiol.* 2016;7:324.
6. Bankevich A, Nurk S, Antipov D, Gurevich AA, Dvorkin M, Kulikov AS, Lesin VM, Nikolenko SI, Pham S, Prjibelski AD, Pyshkin AV, Sirotkin AV, Vyahhi N, Tesler G, Alekseyev MA, Pevzner PA. SPAdes: a new genome assembly algorithm and its applications to single-cell sequencing. *J Comput Biol.* 2012;19:455–477.
7. Seemann T. Prokka: rapid prokaryotic genome annotation. *Bioinformatics.* 2014;30:2068–2069.
8. Laslett D, Canback B. ARAGORN, a program to detect tRNA genes and tmRNA genes in nucleotide sequences. *Nucleic Acids Res.* 2004;32:11–16.
9. Lagesen K, Hallin P, Rødland EA, Staerfeldt HH, Rognes T, Ussery DW. RNAmmer: consistent and rapid annotation of ribosomal RNA genes. *Nucleic Acids Res.* 2007;35:3100–3108.
10. Hyatt D, Chen GL, Locascio PF, Land ML, Larimer FW, Hauser LJ. Prodigal: prokaryotic gene recognition and translation

initiation site identification. *BMC Bioinformatics*. 2010;11:119.

11. Petersen TN, Brunak S, von Heijne G, Nielsen H. SignalP 4.0: discriminating signal peptides from transmembrane regions. *Nat Methods*. 2011;8:785–786.

12. Qin QL, Xie BB, Zhang XY, Chen XL, Zhou BC, Zhou J, Oren A, Zhang YZ. A proposed genus boundary for the

prokaryotes based on genomic insights. *J Bacteriol*. 2014;196:2210–2215.

13. Rodriguez-R LM, Konstantinidis KT. Bypassing cultivation to identify bacterial species. *Microbe Magazine*. 2014;9:111–118.

14. Richter M, Rosselló-Móra R. Shifting the genomic gold standard for the prokaryotic species definition. *Proc Natl Acad Sci U S A*. 2009;106:19126–19131.

Publication 7

Complete genome sequence of a new Ruminococcaceae bacterium isolated from anaerobic biomass hydrolysis

Sarah Hahnke¹, Christian Abendroth^{2,3}, Francisco M. Codoñer⁴, Manuel Porcar^{2,3,6}, Olaf Luschnig⁵, Michael Klocke*¹

¹Leibniz Institute for Agricultural Engineering and Bioeconomy (ATB), Bioengineering, Potsdam, Germany ²Institute for Integrative Systems Biology (I2SysBio, Universitat de València-CSIC), 46020 València, Spain. ³Robert Boyle Institute e.V., Im Steinfeld 10, 07751 Jena, Germany ⁴Lifesequencing SL, Paterna, Valencia, Spain ⁵Bio H2 Umwelt GmbH, Jena, Germany ⁶Darwin Bioprospecting Excellence, S.L. Parc Científic Universitat de València C/ Catedrático Agustín Escardino Benlloch, 9

Abstract

A new Ruminococcaceae isolate, strain HV4-5-B5C, was isolated from a mesophilic and anaerobic two-stage laboratory-scale leach-bed system for biomethanation of fresh grass. Genomic as well as 16S rRNA gene sequence analysis indicated that the new bacterial strain is affiliated with the family Ruminococcaceae but does not belong to any of the currently described genera. Here, we report a draft annotated genome sequence of this organism.

Anaerobic digestion is a promising technology to generate biofuels and multiple products [1]. However, lignocellulolytic biomass can only be degraded incompletely and biomass pretreatment is necessary to facilitate the microbial degradation process [2]. Besides biomass pretreatment, it is further possible to improve the degradation of plant biomass by inoculating hydrolytic bacterial strains [3]. In order to enrich a community of hydrolytic bacteria, a mesophilic and anaerobic two-stage laboratory-scale leach-bed system for biomethanation of fresh grass was set up, from which bacterial strains were isolated.

In this context, we present the genome of the new Ruminococcaceae bacterium strain HV4-5-B5C, which has a putative role in the microbial metabolic network for plant biomass degradation, as it was isolated from a reactor with fresh grass as the sole substrate. The strain originates from a leach-bed biogas reactor system, which operated at 37°C. Isolation was performed under anoxic conditions on Anaerobic agar acc. to Brewer (Merck) after the diluted hydrolysate has been re-incubated with microcrystalline cellulose as sole carbon source.

We used a massive genome sequencing approach as implemented in the Illumina NextSeq 500 platform and a Nextera XT library with a mean insert size of around 300 nt was constructed and sequenced in a combination of 150 PE. Over 20 million (21,629,863) PE sequences with a mean of 150,32 nt were obtained. After quality filtering we obtained a total of 21.61 million PE sequences with a Q value higher than 20 (mean Q = 32.71) that were used in the assembly step. Spades (4) version 3.10.1 was used for the assembly with the parameters by default using the k-mer that provided us with the lowest number of contigs, the longest contig, the largest N50 and the highest percentage of clean sequences

(k-mer =127). A total of 5019 contigs were obtained from them, 76 contigs had over 500 nt, these 76 contigs resulted in a total genome size of around 3.01 Mb with an estimated GC content of 52.50 %, the longest contig was 581,597 nt and the N50 of the assembly is 360,256 nt. The assembled genome sequences were annotated using the Prokka annotation pipeline, version 1.11 (5), which involves predicting tRNA, rRNA, and mRNA genes and signal peptides in the sequences using Aragorn (6), RNAmmer (7), Prodigal (8), and SignalP (9), respectively.

The genome contains 2,945 elements, where 2,878 are ORF (2,325 canonical and 553 non-canonical) and 67 encoded structural RNAs (sRNAs), i.e., 6 for rRNA and 61 for tRNA.

Using BLAST we compared the contigs with all genome sequences available at the database. According to the percentage of conserved proteins (POCP) (10) and the average amino acid identities (AAI) (11) the organism could not be classified as species of a currently described genus. Based on the POCP, the closest related genus was *Clostridium* showing 38.31 % identity. Based on the average nucleotide sequence identity (ANI) (12), the closest related species was *Clostridium sporosphaeroides*, showing an identity of only 68.83 % with ANIBlast and *Clostridium leptum* with a 88.36 % with ANI-MUMmer. Using the EzBioCloud identification tool 16S rRNA gene sequence comparisons revealed *Caproiciproducens galactitolivorans* as the closest affiliated species sharing 93.3 % sequence identity with the type strain. These results indicate that the novel bacterial strain represents a new species and possibly a new genus within the family Ruminococcaceae.

Accession number(s). The microbial strain has been deposited at the German collection of microorganisms and cell cultures (DSMZ) with the deposit number DSM 104463.

The results of the whole genome project have been deposited at DDBJ/EMBL/GenBank under the accession no. FXYJ02000001-FXYJ02000076. The version described here is the first draft version.

Acknowledgements

We are grateful for funding of the work by the German Federal Ministry of Economic Affairs and Energy (grant numbers KF 2050830SA4, KF 3400701SA4 and KF 2112205SA4).

References

1. Strong PJ, Kalyuzhnaya M, Silverman J, Clarke WP. A methanotroph-based biorefinery: Potential scenarios for generating multiple products from a single fermentation. *Bioresour Technol.* 2016;215:314–323.
2. Paudel SR, Banjara SP, Choi OK, Park KY, Kim YM, Lee JW. Pretreatment of agricultural biomass for anaerobic digestion: Current state and challenges. *Bioresour Technol.* 2017;245:1194–1205.
3. Poszytek K, Ciezkowska M, Sklodowska A, Drewniak L. Microbial Consortium with High Cellulolytic Activity (MCHCA) for Enhanced Biogas Production. *Front Microbiol.* 2016;7–324.
4. Bankevich A, Nurk S, Antipov D, Gurevich AA, Dvorkin M, Kulikov AS, Lesin VM, Nikolenko SI, Pham S, Prjibelski AD, Pyshkin AV, Sirotkin AV, Vyahhi N, Tesler G, Alekseyev MA, Pevzner PA. SPAdes: a new genome assembly algorithm and its applications to single-cell sequencing. *J Comput Biol.* 2012;19:455–477.
5. Seemann T. Prokka: rapid prokaryotic genome annotation. *Bioinformatics.* 2014;30:2068–2069.
6. Laslett D, Canback B. ARAGORN, a program to detect tRNA genes and tmRNA genes in nucleotide sequences. *Nucleic Acids Res.* 2004;32:11–16.
7. Lagesen K, Hallin P, Rødland EA, Staerfeldt HH, Rognes T, Ussery DW. RNAmmer: consistent and rapid annotation of ribosomal RNA genes. *Nucleic Acids Res.* 2007;35:3100–3108.

8. Hyatt D, Chen GL, Locascio PF, Land ML, Larimer FW, Hauser LJ. Prodigal: prokaryotic gene recognition and translation initiation site identification. *BMC Bioinformatics*. 2010;11:119.
9. Petersen TN, Brunak S, von Heijne G, Nielsen H. SignalP 4.0: discriminating signal peptides from transmembrane regions. *Nat Methods*. 2011;8:785–786.
10. Qin QL, Xie BB, Zhang XY, Chen XL, Zhou BC, Zhou J, Oren A, Zhang YZ. A proposed genus boundary for the prokaryotes based on genomic insights. *J Bacteriol*. 2014;196:2210–2215.
11. Rodriguez-R LM, Konstantinidis KT. Bypassing cultivation to identify bacterial species. *Microbe Magazine*. 2014;9:111–118.
12. Richter M, Rosselló-Móra R. Shifting the genomic gold standard for the prokaryotic species definition. *Proc Natl Acad Sci U S A*. 2009;106:19126–19131.

Publication 8

Warm and wet: robust lipase-producing bacteria from the indoor environment

Kristie Tanner^{†1}, Christian Abendroth^{†1,2}, Manuel Porcar^{*1,5}

¹Institute for Integrative Systems Biology (I2SysBio, Universitat de València-CSIC), 46020 València, Spain. ²Robert Boyle Institute e.V., Im Steinfeld 10, 07751 Jena, Germany ³Darwin Bioprospecting Excellence, S.L. Parc Científic Universitat de València C/ Catedrático Agustín Escardino Benlloch, 9

Abstract

Lipases are key biocatalysts with important biotechnological applications. With the aim of isolating robust lipolytic microbial strains, we have analyzed the bacterial communities inhabiting two domestic extreme environments: a thermophilic sauna and a dishwasher filter. Scanning electron microscopy revealed biofilm-forming and scattered microorganisms in the sauna and dishwasher sample, respectively. A culture-in-dependent approach based on 16S rRNA analysis indicated a high abundance of Proteobacteria in the sauna sample; and, a large amount of Proteobacteria, Firmicutes, Cyanobacteria and Actinobacteria in the dishwasher filter. With a culture-dependent approach, we isolated 48 bacterial strains, screened their lipolytic activities on media with tributyrin as the main carbon source, and finally selected five isolates for further characterization. These strains, all of them identified as members of the genus *Bacillus*, displayed optimum lipolytic peaks at pH 6.5 and with 1-2 % NaCl, and the activity proved very robust at a wide range of pH (up to 11.5) and added NaCl concentrations (up to 4 %). The thermal, pH and salt robustness of the selected isolates is a valuable attribute for these strains, which are promising as highly tolerant bio-detergents. To our knowledge, this is the first report regarding the isolation from an indoor

environment of *Bacillus* strains with a high potential for industry.

Introduction

In the past decade, research programs on indoor environments have resulted in an increasing data matrix of taxonomic and ecological interest [1, 2]. Attention has especially been paid to frequently used domestic places that are, on many occasions, overgrown with potential pathogenic bacteria, like in the recently described coffee-machine or refrigerator bacteriomes [3, 4]. It is important to stress that indoor environments mimic natural, often extreme, environments. For example, refrigerators are almost as cold as tundra and thus rich in cold-adapted bacteria, whereas sun-exposed artificial flat surfaces, such as solar panels, are home of a rich desert-like biocenosis [5]. Therefore, bioprospecting nearby indoor extreme environments is a poorly explored but yet promising screening strategy that might yield bacterial strains with new or improved biotechnological applications. Indeed, and besides the obvious medical implications, another reason to further investigate indoor microbiomes is the search of enzymes with high industrial significance, especially as novel biocatalysts [6]. A very well known (natural) precedent is the discovery of the extremophile bacterium *Thermus aquaticus* [7], whose thermoresistant Taq

polymerase allowed the revolutionary development of Polymerase Chain Reaction in the last decades of the 20th century.

Within the current repertoire of available enzymes, esterases are particularly suitable for industrial processes, since they are stable in organic solvents and can freely reverse the enzymatic reaction from hydrolysis to synthesis [8]. Lipases have also been highlighted as key biocatalysts for biotechnological applications, such as the production of new biopolymeric materials and biodiesel, or the synthesis of fine chemicals like therapeutics, agrochemicals, cosmetics and flavors [9]. Their stereoselective properties make them able to recognize enantiomers and enantiotopic groups, while many other enzymes for hydrolysis are just capable of metabolizing one antipode of the specific substrate [10].

Environments with extreme and/or oscillating temperatures are of special interest, due to the opportunity of finding esterases that are active at wide intervals of temperature and that can thus be used under a range of industrial conditions, such as those present in dishwashers or washing machines. A new and promising esterase has recently been discovered in the thermophilic bacterium *Thermogutta terrifontis*. This enzyme retains up to 95 % of its activity after incubation for 1h at 80 °C [11]. A cold-active and solvent-tolerant lipase from *Stenotrophomonas maltophilia* has also been reported, with retention of 57 % of its activity at 5 °C and more than 50 % of its activity in pure organic solvents [12]. More examples of extremophilic enzymes with industrial potential include thermoalkalophilic esterases from *Geobacillus* sp., which have all proven active at high temperature (65 °C) and at pH of up to 10 [13]; or a cold-adapted esterase from *Pseudoalteromonas arctica*, which still retained 50 % of its activity at the freezing point of water [14].

Upon discovery, extremophile enzymes can often be further optimized to improve their industrial use, as it was the case for the thermal stability and activity in the cold-adapted lipase B from *Candida antarctica* through chemical linking of amino groups of the lipase to oxidized polysaccharides using reducing agents [15].

Bioprospecting indoor extreme environments could yield new lipolytic microbial strains harbouring previously uncharacterized esterases and other enzymes. In the present work, we have focused on the microbial communities inhabiting two high-temperature, domestic environments: a thermophilic sauna and a dishwasher. We have isolated 48 bacterial strains, many of them lipase-producing bacteria. Furthermore, we have characterized five of them, displaying robust lipase activities with promising biotechnological applications.

Material and methods

Sampling

Environmental samples were taken from a sauna and from a dishwasher. The sauna, set at a temperature of approximately 45 °C and with 100 % relative humidity, is a publicly-owned facility located in a communal swimming pool in Valencia (Spain) and therefore did not require specific permission for the sampling. A biofilm-like mass below the aluminium bench of the sauna was collected in a sterile 50 mL Falcon tube and was stored at -20 °C until required. The dishwasher sample was collected from the filter of a domestic Siemens dishwasher (property of one of the co-authors of this work, MP), Model sm6p1s. The sample was obtained by scratching the inner surface of the filter with a sterile bladder and the resulting biomass was kept at -20 °C until required.

Scanning electron microscopy

Biomass samples were fixed on a 0.2 μm membrane filter (Merck Millipore Ltd, Tullagreen, Cork, Ireland) using para-formaldehyde 2% - glutaraldehyde 2.5 %. A volume of 5 ml was pressed two times through the filter. The filter was washed with Milli-Q water (Merck Millipore Ltd, Tullagreen, Cork, Ireland) and then dehydrated in ethanol (gradually increasing concentration). Dehydrated samples were placed in microporous capsules of 30 μm in pore size (Ted Pella Inc.) and immersed in absolute ethanol. Critical point drying was performed in an Autosamdri 814 (Tousimis). Once dried, samples were placed on SEM stubs by means of silver conducting paint TAAB S269. Stubs were examined under a scanning electron microscope Hi-tachi S-4100.

16S-rDNA analyses with Ion Torrent

DNA was retrieved from sauna and dishwasher samples using the PowerSoil DNA Isolation Kit (MO BIO Laboratories, USA). DNA quality was analyzed using a Nanodrop-1000 Spectro-photometer (Thermo Scientific, Wilmington, DE, USA). A 500 bp long fragment from the hypervariable 16S-rDNA regions V1–V3 was amplified using the universal primers 28F (5'-GAG TTT GAT CNT GGC TCA G-3') and 519R (5'-GTN TTA CNG CGG CKG CTG-3'). The quality of the resulting amplicons was checked on a 0.8 % (w/v) agarose gel. Amplicons were precipitated with 3M potassium acetate and isopropanol. Sequencing libraries were constructed using 100 ng of the DNA pool and performing the amplicon fusion method (Ion Plus Fragment Library Kit, MAN0006846, Life Technologies). Both libraries (Sauna and Dishwasher) were quantified with the Agilent2100 Bioanalyzer (Agilent Technologies Inc, Palo Alto, CA, USA) prior to clonal amplification. Emulsion PCRs were carried out with the Ion

PGM Template OT2 400 kit as described following the user guide provided by the manufacturer (MAN0007218, Revision 3.0 Life Technologies). Libraries were sequenced in an Ion 318 Chip v2 on a Personal Genome Machine (PGM) (Ion-Torrent™, Life Technologies) at Life Sequencing S.L. (Life Sequencing, Valencia, Spain), using the Ion PGM Sequencing 400 kit and following the manufacturer's protocol (publication number MAN0007242, revision 2.0, Life Technologies). Short reads (<100bp) and low quality reads (<q15) were removed upon sequencing at the sequencing center. Resulting sequences were analyzed by phylotyping with the MOTHRU software [16]. Amplicons were aligned to the 16S-reference from the Greengenes database. Classification was performed using the k-mer algorithm. Assignments with a similarity percentage lower than 80 % were discarded.

Isolation of microbial strains

Lysogenic broth (LB) and Reasoner's 2A (R2A) agar [17] media were used for bacterial culturing. Samples were suspended in PBS-buffer, vortexed, spread on LB and R2A plates and incubated at 37 °C and 55 °C for one day. Thermophilic and thermo-resistant strains were picked, grown in liquid culture and stored in 20 % Glycerol at -70 °C.

Lipolytic Activity and microbial identification

Tributylin-containing medium is frequently used when screening for lipase-producing microorganisms [18,19], as the degradation of this compound generates clear halos around the lipolytic colonies in the otherwise turbid medium. Samples (1 μL) from the cryo-preserved strains were directly spotted on minimal medium [20], which contained tributyrin (10 mL/L) as main carbon source. Incubations were performed at 4 °C, 20 °C, 37

°C, 46 °C and 55 °C. After 5 days of incubation, the diameter of the halos around lipase-producing strains was measured.

16S rRNA sequencing of selected strains

Hypervariable 16S-rDNA regions V1–V3 of the selected strains were amplified by colony PCR using 28F and 519R primers and sequenced with the Sanger method by the Sequencing Service of the University of Valencia (Spain). This allowed the identification of the five selected isolates at a genus level. In order to identify the isolates at a species level, further *Bacillus* spp. primers were used to amplify: the TU elongation factor (*tufGPF* and *tufGPR*) [21], a group-specific 16S rRNA region (B-K1/F and B-K1/R1) [22], an endoglucanase gene (*ENIF* and *EN1R*) [23] and a glycosyltransferase (*Ba-G206F* and *Ba-G1013R*) [24]. The resulting sequences were manually edited using Pregap4 (Staden Package, 2002) to eliminate low-quality base calls. The final sequence for each isolate was compared to sequence databases using the NCBI BLAST tool.

Lipolytic assays varying pH and salt conditions

Lipase production of the five selected strains was tested on solid minimal medium supplemented with tributyrin (10 mL/L), adjusted to a range of pH (6.5, 8, 9.5 and 11.5), and with or without additional 4 % NaCl. Two microliters of each strain were spotted on each combination of pH and salt media and incubated at 4, 20, 37, 46 or 55 °C for 5 days. After incubation, the diameters of the halos were measured.

In order to determine the optimal conditions for the lipase production of the five selected strains, two microliters of each strain were spotted on additional combinations of pH and salt (pH 6.5, 8, 9.5 and 11.5; NaCl 0, 1, 2, 3 and 4 %). The plates were incubated for five days

at 37 °C. The assay was performed in triplicate.

Results and Discussion

Scanning Electron Microscopy

The samples obtained from a wet sauna and a dishwasher filter proved rich in microorganisms, as deduced by observation under SEM (Fig 27). In the sauna sample, microorganisms were mostly present in the form of a very dense biofilm almost totally embedded in a smooth matrix, very likely made of EPS (Fig 27A); whereas the dishwasher filter sample consisted mainly of food debris with scattered microorganisms (Fig 27B).

16S-rDNA analyses with Ion Torrent

The taxonomic diversity of the two samples was determined by high throughput-sequencing, performed as described in Materials and Methods, and resulted in very different taxonomic profiles of both samples (Fig 27C and 27D). Proteobacteria were overwhelmingly abundant in the sauna sample, accounting for more than 90 % of the reads (Fig 27C). Of those, alpha-, beta- and gamma-proteobacteria were present at similar frequencies, each accounting for more than 20 % of the assigned sequences. Minor taxa with frequencies of 1–5 % included Bacteroidetes, Actinobacteria and Acidobacteria. The dishwasher filter was characterized by large amounts of Proteobacteria, Firmicutes (Bacilli, most of them), Cyanobacteria and Actinobacteria; and very low amounts of other taxa (Fig 27D).

These results are consistent with previous reports on these two extreme environments. Lee et al. [25] characterized the bacterial community contaminating the floor of a hot and dry sauna, which proved rich in Firmicutes, Gamma-proteobacteria and Beta-proteobacteria. Another

report by Kim et al. [26] of a 64 °C dry sauna revealed a population with Firmicutes, Gamma-proteobacteria, Beta-proteobacteria and Deinococci as the most frequent taxa. As mentioned above, our samples were rich Beta- and Gammaproteobacteria, although we also detected Alpha-proteobacteria, which were absent in the works by Kim et al. [25] and Lee et al. [26]. Reciprocally, we did not detect Firmicutes or Deinococci with our 16S rRNA analysis, while both taxa were found by those two previous reports. Concerning the dishwasher samples, a previous report by Savage

et al. [27] characterized, among other household surfaces, the bacteria present in the dishwasher rinse reservoir. According to that previous report, bacterial population in the dishwasher consists of Proteobacteria, Firmicutes, Cyanobacteria and Actinobacteria, which corresponds to the taxonomic profile we found in the dishwasher filter. Nevertheless, Euryarcheota and Bacteroidetes that were found in the rinse reservoir [27] were not detected in the filter in the present work.

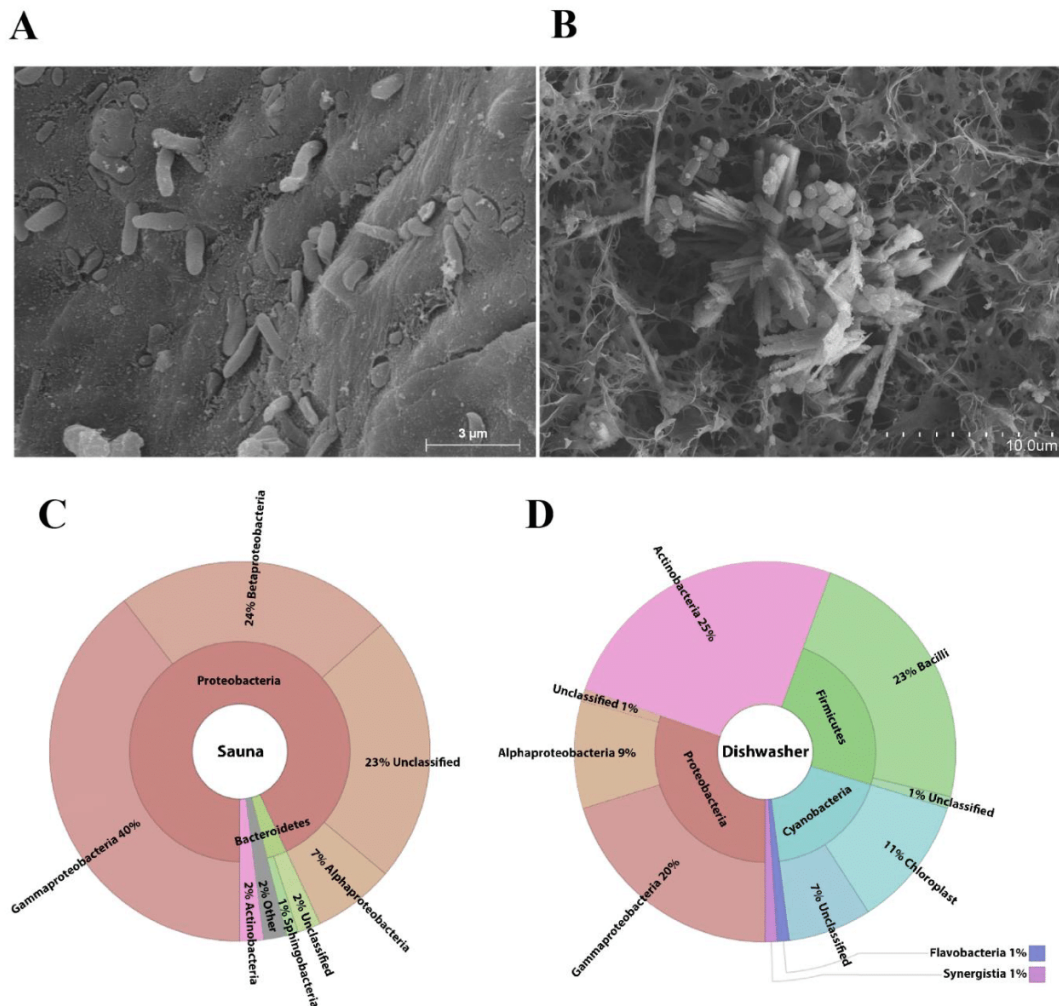


FIGURE 27: Scanning electron micrographs from the sauna (A) and the dishwasher (B) samples; taxonomic diversity estimated by 16S amplicon sequencing of sauna (C) and dishwasher (D). The sauna (C) sample was especially rich in Proteobacteria; whereas the dishwasher filter (D) also contained high amounts of Firmicutes, Cyanobacteria and Actinobacteria.

Culturing strains and lipolytic activity screening

Bacterial colonies randomly selected among those with a strong growth on LB and R2A plates were restreaked to yield a collection of strains, and lipase production was screened after growth for five days in tributyrin-containing media, as described in materials and methods. Lipase production of all the strains is shown in Fig 28A. Most of the strains (72 and 79 % of the sauna and dishwasher strains, respectively) displayed some level of lipolytic activity. In general, sauna strains were able to produce lipases within a broader range of temperature, including, in two cases, values as high as 46 °C and as low as 4 °C. At least in these cases, though, lipases are not only produced, but are fully functional at extreme temperatures as deduced by this assay. In contrast, strains from the dishwasher displayed lipolytic activity within a smaller range of temperatures, in most cases only around 37 °C within the tested range. Interestingly, lipolytic activity, as deduced by halo diameter, was maximum at 46 °C in several sauna strains, although no strains produced detectable lipolysis at 55 °C.

On the basis of this first screening for lipolytic activities, five strains were selected for further assays. Those included the strains with the broadest temperature activity range: S22 and S23, both active in all temperatures tested except at 55 °C; and D3, D11 and D18, the three dishwasher samples active at both 20 °C and 37 °C. In order to assess the potential of these five strains for biotechnological purposes (in terms of lipase production under extreme environmental conditions), they were taxonomically identified and subjected to a stress test under a range of temperatures and pH conditions, performed in minimum media with and without 4 % added salt. Lipase activity was tested under different temperatures, NaCl and pH conditions, and results are shown in Fig 28B. Again,

sauna samples exhibited a broad range of thermal stability, with medium to large halos at pH values mildly acid to moderately alkaline (6.5–9.5) and even in the presence of 4 % NaCl (pH 8 and 9.5). Interestingly, very alkaline (11.5) conditions, combined with high salt contents correlated with an increased thermal range of lipase production and activity for both S22 and S23, which increased from 20 °C up to 46 °C. In general, though, salt addition yielded smaller haloes at any temperature compared to standard media.

Regarding the strains we isolated from the dishwasher filter, assays performed with minimum media (without salt) adjusted to a wide range of pH values and incubated at different temperatures revealed the alkaliphility of their lipolytic abilities, both in terms of thermal broad range at alkaline pH values, and intensity of the activity as deduced by halo sizes (Fig 28B). Addition of NaCl to the media resulted in smaller haloes and, at least for pH values of 8–9.5, in a narrower thermal activity range. In the three dishwasher strains, the combination of 4 % added NaCl and high (11.5) pH resulted in an altered thermal range of activity. At least in one case (D11) addition of 4 % NaCl partially restored the lack of activity observed with no added salt and at a pH of 11.5.

Sequencing of a 16S rRNA gene fragment allowed identification of all five isolates as *Bacillus* sp. Further sequencing of the TU elongation factor (*tufGP* primers) and the group-specific 16S rRNA region (BK-1 primers) revealed D11 strain as *Bacillus megaterium* (with 99 and 100 % identity, respectively); and S22/S23 strains as *Bacillus pumilus* (with 100 and 99 % identity in the case of *tufGP* and BK-1 primers, respectively). D3 was not completely identified, and remains as *Bacillus* sp., possibly *B. subtilis*, *B. amyloliquefaciens*, *B. methylotrophicus* or *B. velentznesis*. D18 was identified as *B. cereus*/*B. thuringiensis*.

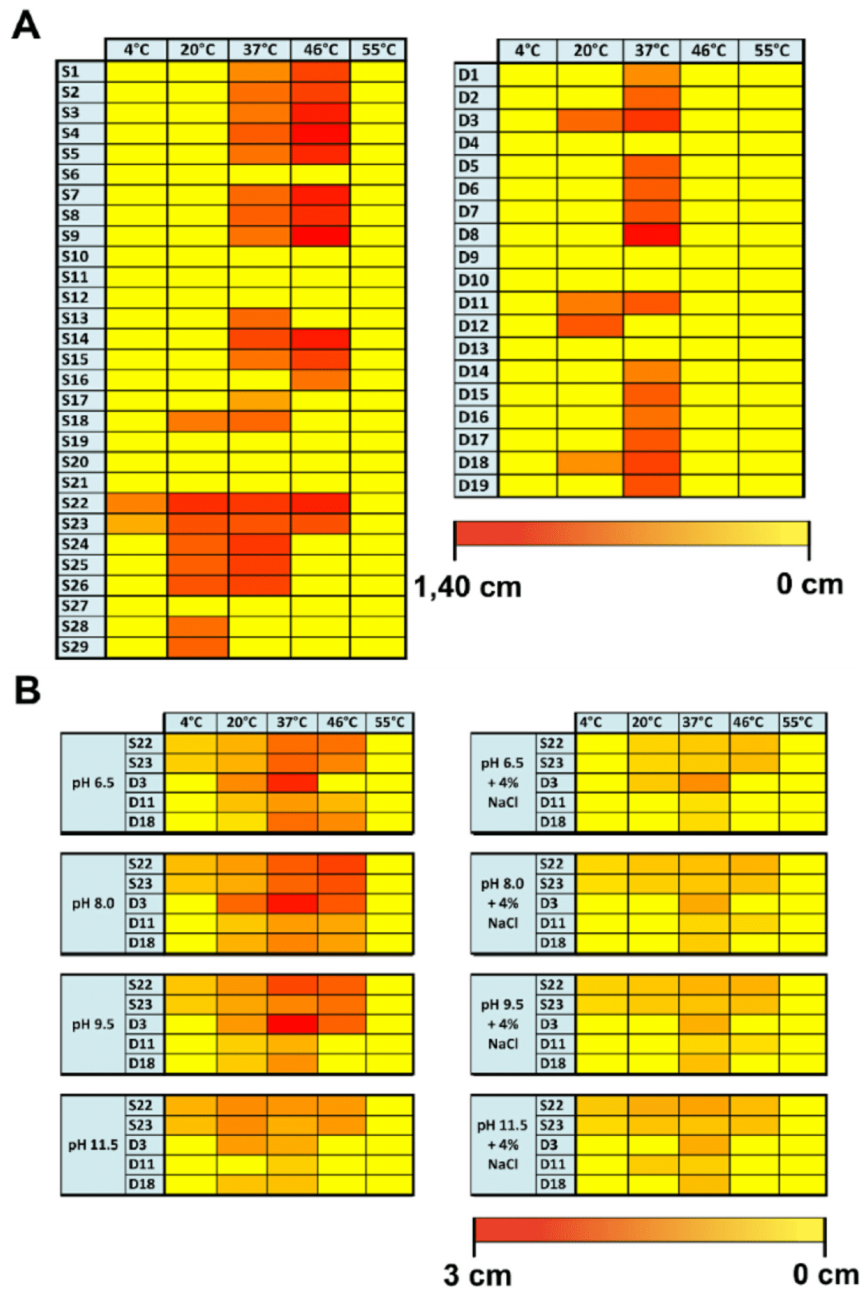


FIGURE 28: Heatmaps of lipolytic activity. (A) Isolates from the sauna and from the dishwasher contained mainly strains with lipolytic activity. Strains from the sauna exposed lipolytic activity within a broader range of temperature. Sauna samples with the widest range of temperature were S22 and S23. In the dishwasher most samples showed lipolytic activity at 37 °C and only sample D3, D11 and D18 had lipolytic activity at two tested temperatures. (B) Heatmap of lipolytic activity of selected strains from sauna (S22, S23) and dishwasher (D3, D11, D18) under different pH (6.5, 8, 9.5, 11.5) and temperature conditions (4, 20, 37, 46 and 55 °C) in minimal medium or minimal medium with 4 % NaCl.

Robustness of the selected isolates in varying pH and salt conditions

In order to characterize the robustness of lipolytic activity of the five selected strains under alkaline and/or high salinity conditions, the strains were tested on combined pH and salt contents conditions, at 37 °C. Lipolytic activity results are shown in Fig 29.

In general, all strains displayed a very robust lipase activity under different salt and pH conditions when grown at 37 °C, as deduced by the relatively flat 3D profile (Fig 29), although halo diameters generally decreased towards extreme salt values (0 % and 4 % NaCl). Specifically, D11 and D18 (Fig 29D and 29E, respectively) were the most robust lipase producers, followed by S22 and S23 (Fig 29A and 29B, respectively). In contrast, D3 (Fig 29C) was the least robust strain, with variations in activity depending on pH conditions and an even higher salt-dependent variation: lipolytic activity ranged from undetectable in very alkaline conditions to very large (2.45 cm) haloes at pH 6.5 with 1 % NaCl.

Aside from the robustness observed, the five selected strains displayed clear optimum peaks at pH 6.5 with 2 % NaCl for S22 and S23; and with 1 % NaCl for D3, D11 and D18. D3 displayed the highest lipolytic activity under optimum conditions, with halo diameters of up to 2.45 cm, followed by S22 and S23, both with diameters of up to 1.35 and 1.40 cm, respectively. Strains D11 and D18 displayed the lowest lipolytic activity, with maximum halos of 0.76 and 1.17, respectively.

Bacillus sp. have been previously reported to produce thermostable lipases [28, 29, 30, 31]. Regarding the *Bacillus* species that we have isolated and identified in the present work, they are known to produce thermoresistant lipases, some of them stable at very low or very high pH values. For example, thermostable lipases can be found in

B. megaterium (a monoacyl-glycerol lipase and a carboxylesterase, Uniprot accession number: A0A0H4RCB5 and G2RXU5). Furthermore, a thermostable extracellular lipase has been described for this species, which is capable of retaining 100 % of its activity at 50 °C, and becomes stimulated in the presence of acetone, DMSO, isopropanol and several reducing agents [32]. On the other hand, there are several thermostable lipases known for the *B. cereus* group (Uniprot accession number: A0A0B5NXJ9; A0A090YL00; A0A0A0WM49) and for the *B. subtilis* group [33, 34]. *Bacillus pumilus* is well-known for its thermostable lipases, as many reports describe lipase fully or partially functional at high temperatures [35, 36, 37, 38, 39], including a lipase that is able to resist temperatures up to 100 °C [36]. Even lipases that are functional at both high temperatures and high or low pH values have been described [37, 38]. Finally, *B. pumilus*, has been identified as the most efficient lipolytic enzymes producer out of 65 strains analysed in a previous report [39]. In fact, in our experiments, isolates S22 and S23 were among the three strains with the highest lipolytic activity, and both of these were identified as *B. pumilus*.

In summary, we have identified from domestic environments several *Bacillus* spp. which are strong producers of robust lipolytic enzymes, and this is in concordance with the literature on strains of this genus isolated from other environments. It has to be highlighted that, in our assays, the lipases corresponding to the isolated strains showed high activity at wide ranges of pH (6.5–11.5), temperature (4 °C–46 °C) and salt (up to 4 % NaCl), and that all measurements were performed in-situ within their host organisms. Therefore, not only the bacteria are able to produce lipases under these conditions, but also these lipases are perfectly functional. Further tests of the lipase extracts will shed light on the

robustness of the lipolytic activity itself, bacterial production.
without the limitations caused by the

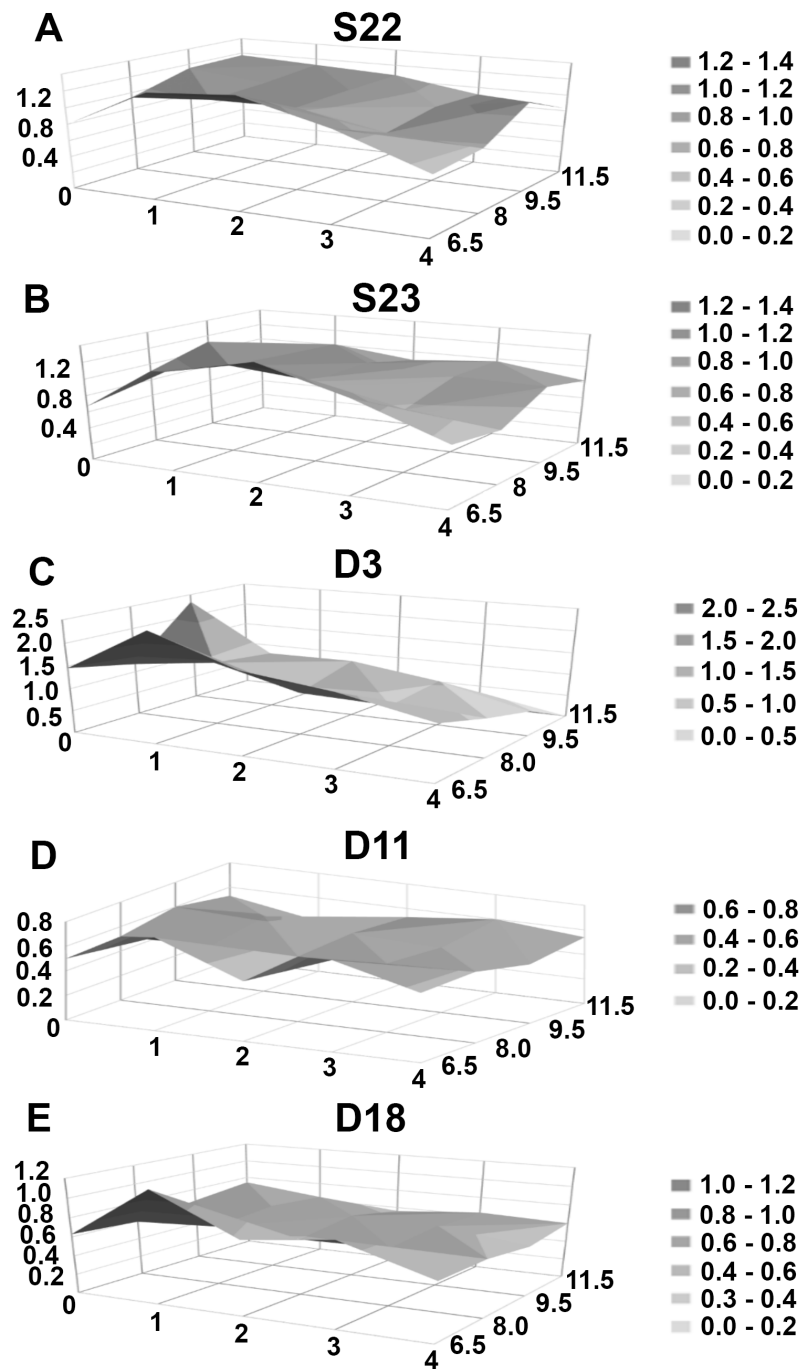


FIGURE 29: Surface graphs of lipolytic activities of the five selected strains (S22, S23, D3, D11 and D18) under different pH (6.5, 8, 9.5 and 11.5) and NaCl (0, 1, 2, 3 and 4 %) conditions. Diameter of the lipolysis haloes (cm) is represented in the Y axis, whereas salt and pH conditions are represented in the X and Z axis, respectively. Halo sizes are in grey to dark grey as indicated at the right side of each graph.

Our results suggest that the isolated strains may be used as robust chassis for lipase production, and these lipases may be used in the industry as robust bio-detergents. As described in the works mentioned above, especially *B. pumilus* seems to be of interest, since it shows a very strong lipolytic activity and since it adapts, according to our data, most efficiently to different conditions of pH, salt and temperature. This is especially interesting, since we found no previous description of *Bacillus* lipases, which work efficient in wide range of pH, salt and temperature at the same time. The present work shows for the first time the potential of domestic environments as a source of *Bacillus* strains with potential biotechnological applications.

Conclusions

The present work is the first screening of extreme indoor environments specifically aiming at the identification of biotechnological relevant bacterial strains able to produce robust enzymes, in our case, robust lipases. Our results reveal that such domestic environments are promising sources for the identification of robust enzymatic activities, as we have managed to isolate five strains with stable lipolytic activity under a wide range of temperature, salt and pH conditions. These metabolic capabilities can be especially useful as components of robust bio-detergents. Furthermore, this work might be the first step of a new view on the human-associated indoor microbiome, focused on ecological aspects and on biotechnological applications.

Acknowledgements

We thank C. Vilanova and X. Baixeras for assistance with electron microscopy. Further the authors are indebted to E. L. James for inspiring us to choose the title for the present work.

Supplementary

S1 Data. Sequences obtained from high-throughput 16S rRNA sequencing of the DNA isolated from the sauna sample.

S2 Data. Sequences obtained from high-throughput 16S rRNA sequencing of the DNA isolated from the dishwasher sample.

References

1. Kelley ST, Gilbert JA. Studying the microbiology of the indoor environment. *Genome Biol.* 2013;14:202.
2. Adams RI, Bateman AC, Bik HM, Meadow JF. Micro-biota of the indoor environment: a meta-analysis. *Microbiome.* 2015;3:49.
3. Vilanova C, Iglesias A, Porcar M. The coffee-machine bacteriome: biodiversity and colonisation of the wasted coffee tray leach. *Sci Rep.* 2015;5: doi: 101038/srep17163.
4. Jackson V, Blair IS, McDowell DA, Kennedy J, Bolton DJ. The incidence of significant foodborne pathogens in domestic refrigerators. *Food Control.* 2007;18:346–351.
5. Dorado-Morales P, Vilanova C, Peretó J, Codoñer FM, Ramón D, Porcar M. A highly diverse, desert-like microbial biocenosis on solar panels in a Mediterranean city. *Sci Rep.* 2016;6:29235.
6. Antranikian G, Vorgias CE, Bertoldo C. Extreme environments as a resource for microorganisms and novel biocatalysts. *Adv Biochem Eng Biot.* 2005;96:219–262.
7. Brock TD, Freeze H. *Thermos aquaticus* gen. n. and sp. N., a nonsporulating extreme thermophile. *J Bacteriol.* 1969;98:289–297.
8. Littlechild JA. Enzymes from extreme environments and their industrial applications. *Front Bioeng and Biotechnol.* 2015;3:161.
9. Jaeger KE, Eggert T. Lipases for biotechnology. *Curr Opin Biotech.* 2002;13:390–397.
10. Rogalska E, Nury S, Douchet I, Verger R. Microbial lipases: structures, function and industrial applications. *Biochem Soc T.* 1997;25:161–164.

11. Sayer C, Isupov MN, Bonch-Osmolovskaya E, Little-child JA. Structural studies of a thermophilic esterase from a new Planctomycetes species, *Thermogutta terrifontis*. *FEBS J*. 2015;282:2846–2857.
12. Li M, Yang L, Xu G, Wu J. Screening, purification and characterization of a novel cold-active and organic sol-vent-tolerant lipase from *Stenotrophomonas maltophilia* CGMCC 4254. *Bioresource Technol*. 2013;148:114–120.
13. Tekedar HC, Sanli-Mohamed G. Molecular cloning, over expression and characterization of thermoalkalophilic esterases isolated from *Geobacillus* sp. *Extremophiles*. 2011;2:203–211.
14. Al Khudary R, Venkatachalam R, Katzer M, Elleuche S, Antranikian G. A cold-adapted esterase of a novel marine isolate, *Pseudoalteromonas arctica*: gene cloning, enzyme purification and characterization. *Extremophiles*. 2010;3:273–285.
15. Siddiqui KS, Cavicchioli R. Improved thermal stability and activity in the cold-adapted lipase B from *Candida antarctica* following chemical modification with oxidized polysaccharides. *Extremophiles*. 2005;6:471–476.
16. Schloss PD, Westcott SL, Ryabin T, Hall JR, Hartmann M, Hollister EB, et al. Introducing MOTHUR: open-source, platform-independent, community-supported software for describing and comparing microbial communities. *Appl Environ Microbiol*. 2009;75:7537–7541.
17. Reasoner DJ, Geldereich EE. A new medium for the enumeration and subculture of bacteria from potable water. *Appl Environ Microbiol*. 1985;49(1):1–7.
18. Mobarak-Qamsari E, Kasra-Kermanshahi R, Moosavinejad Z. Isolation and identification of a novel, lipase-producing bacterium, *Pseudomonas aeruginosa* KM110. *Iran J Microbiol*. 2011;3:92–98.
19. Kumar D, Kumar L, Nagar S, Raina C, Parshad R, Gupta VK. Screening, isolation and production of li-pase/esterase producing *Bacillus* sp. Strain DVL2 and its potential evaluation in esterification and resolution reactions. *Arch Appl Sci Res*. 2012;4(4):1763–1770.
20. Vilanova C, Marín M, Baixeras J, Latorre A, Porcar M. Selecting microbial strains from pine tree resin: biotechnological applications from a terpene world. *PLoS One*. 2014;9(6): e100740.
21. Caamaño-Antelo S, Fernández-No IC, Böhme K, Ezzat-Alnakip M, Quintela-Baluja M, Barros-Velázquez J, et al. Genetic discrimination of foodborn pathogenic and spoilage *Bacillus* spp. Based on three housekeeping genes. *Food Microbiol*. 2015;46:288–298.
22. Wu XY, Walker MJ, Homitzky M, Chin J. Development of a group-specific PCR combined with ARDRA for the identification of *Bacillus* species of environmental significance. *J Microbiol Methods*. 2006;64: 107-119.
23. Ashe S, Maji UJ, Sen R, Mohanty S, Maiti NK. Specific oligonucleotide primers for detection of endoglucanase positive *Bacillus subtilis* by PCR. *Biotech*. 2014;4:461–465.
24. Kim W, Kim JY, Cho SL, Nam SW, Shin JW, Kim YS, et al. Glycosyltransferase – a specific marker for the discrimination of *Bacillus anthracis* from the *Bacillus cereus* group. *J Med Microbiol*. 2008;57:279–286.
25. Lee JY, Park DH. Characterization of bacterial community contaminating floor of a hot and dry sauna. *J Bacteriol Virol*. 2012;42(4):313–320.
26. Kim BS, Seo JR, Park DH. Variation and characterization of bacterial communities contaminating two saunas operated at 64 °C and 72 °C. *J Bacterio Virol*. 2013;43:195–203.
27. Savage AM, Hills J, Driscoll K, Fergus DJ, Grunden AM, Dunn RR. Microbial diversity of extreme habitats in human homes. *PeerJ*. 4:e2376; DOI 10.7717/peerj.2376
28. Shariff FM, Rahman RN, Basri M, Salleh AB. A newly isolated thermostable lipase from *Bacillus* sp. *Int J Mol Sci*. 2011;12:2917–2934.
29. Sivaramakrishnan R1, Muthukumar K. Isolation of thermostable and solvent-tolerant *Bacillus* sp. lipase for the production of biodiesel. *Appl Biochem Biotechnol*. 2012;166: 1095–1111.
30. Bora L, Bora M. Optimization of extracellular thermophilic highly alkaline lipase from thermophilic *Bacillus* sp isolated from hot spring of Arunachal Pradesh, India. *Braz J Microbiol*. 2012;43: 30–42.

31. Surendhiran D, Sirajunnisa AR, Vijay M. An alternative method for production of microalgal biodiesel using novel *Bacillus* lipase. 3. *Biotech.* 2015;5:715–725.
32. Sekhon A, Dahiya N, Tiwari RP, Hoondal GS. Properties of a thermostable extracellular lipase from *Bacillus megaterium* AKG-1. *J Basic Microbiol.* 2005;45:147–54.
33. Iqbal SA, Rehman A. Characterization of Lipase from *Bacillus subtilis* I-4 and Its Potential Use in Oil Contaminated Wastewater. *Braz. arch. biol. technol.* 2015;58:789–797.
34. Senthilkumar B, Meshachpaul D, Sethumadhavan R, Rajasekaran R. Selection of effective and highly thermostable *Bacillus subtilis* lipase A template as an industrial biocatalyst-A modern computational approach. *Front. Biol.* 2015;10:508–519.
35. Akbulut N, Tuzlakoğlu Öztürk M, Pijning T, İşsever Öztürk S, Gümüsel F. Improved activity and thermostability of *Bacillus pumilus* lipase by directed evolution. *J Biotechnol.* 2012;164:123–129.
36. Laachari F, Bergadi F, Sayari A, Elabed S, Mohammed I, Harchali H, Ibnsouda SK. Biochemical characterization of a new thermostable lipase from *Bacillus pumilus* strain. *Turk J Biochem.* 2015;40(1):8–14.
37. Ma J, Ma Y, Wei W, Wei DZ. In vivo functional expression of an extracellular Ca²⁺-independent *Bacillus pumilus* lipase in *Bacillus subtilis* WB800N. *Annals of Microbiology.* 2015;65: 1973–1983.
38. Kumar R, Sharma A, Kumar A, Singh D. Lipase from *Bacillus pumilus* RK31: Production, Purification and Some Properties. *World Appl Sci J.* 2012;16:940–948.
39. Kalapatapu VP, Battina R, Iska BR. Isolation and identification of lipase producing *Bacillus pumilus* GN9. *GJRA.* 2016;doi 10.15373/22778160.

General Results and Discussion

Microbial markers to evaluate anaerobic process performance

Methanogenic archaea are key players in anaerobic methane production [1], and they have been taxonomically well characterized before [2]. However, they represent only a fraction of the microbial species that appear in anaerobic digestion processes. Usually, between 1–20 % of the species involved are methanogenic archaea and the remaining organisms are mainly bacteria, especially from the phyla Bacteroidetes, Firmicutes, Proteobacteria, Chloroflexi and Spirochaeta [3]. Dynamic relations

between those phyla are still obscure and it remains unclear under which specific conditions certain phyla are dominating digestion processes. To gain a deeper understanding of the dynamic microbial behaviour in digester plants, one of the most comprehensive characterizations of microbial communities of mesophilic biogas-producing facilities was performed during this thesis.

Three kinds of industrial sludges with very different chemical parameters were compared based on 16S-rRNA amplicon high-throughput sequencing, namely sewage sludge, leachate and highly viscous sludge from continuous stirred tanks reactors (CSTRs).

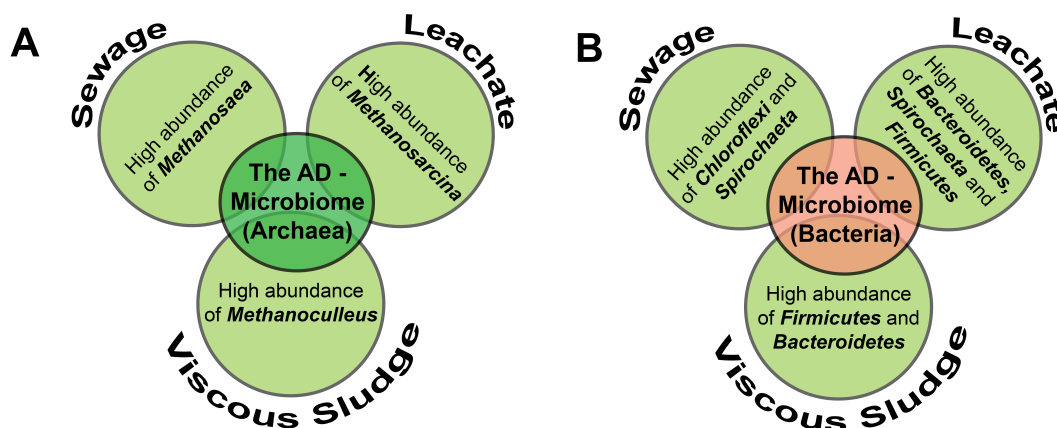


FIGURE 30: Comparison of methanogenic microbiomes at mesophilic temperatures: Typical microbial groups of sewage sludge, leachate from leach-bed processes and highly viscid codigester sludge are shown for archaea (A) and bacteria (B). The shown scheme was concluded from figure 7 and 8 (Publication 1).

As described in publication 1, each of the three sludge types exhibited a characteristic microbial profile. A high amount of *Methanosarcina*, *Methanoculleus* and *Spirochaeta* was characteristic for leachate, sewage

was particularly rich in *Methanosaea*, *Spirochaeta* and *Chloroflexi*. In comparison to sewage sludge and leachate, the viscous CSTR-sludge was especially rich in *Firmicutes* and *Methanoculleus*. The observed three

key-microbiomes are shown in figure 30. In the future, the performed profiling could help to develop effective screening assays for different kinds of digesters.

Archaeal markers: The microbial profiling of industrial digesters and digestion experiments from publication 1 and 2 yielded much information about microbial groups that might serve as hypothetic markers of anaerobic process performance (Fig. 31 and Fig. 32). It was observed that *Methanosarcina*

and *Methanoculleus* are methanogenic species that can especially be found in co-fermenters with high loading rates. *Methanosarcina* was particularly enriched in the leachate from leach-bed systems. By contrast, the high amount of *Methanoculleus* in highly viscous co-digester sludge might indicate that *Methanoculleus* growths preferred in biofilms, which is in concordance with previous studies [4, 5].

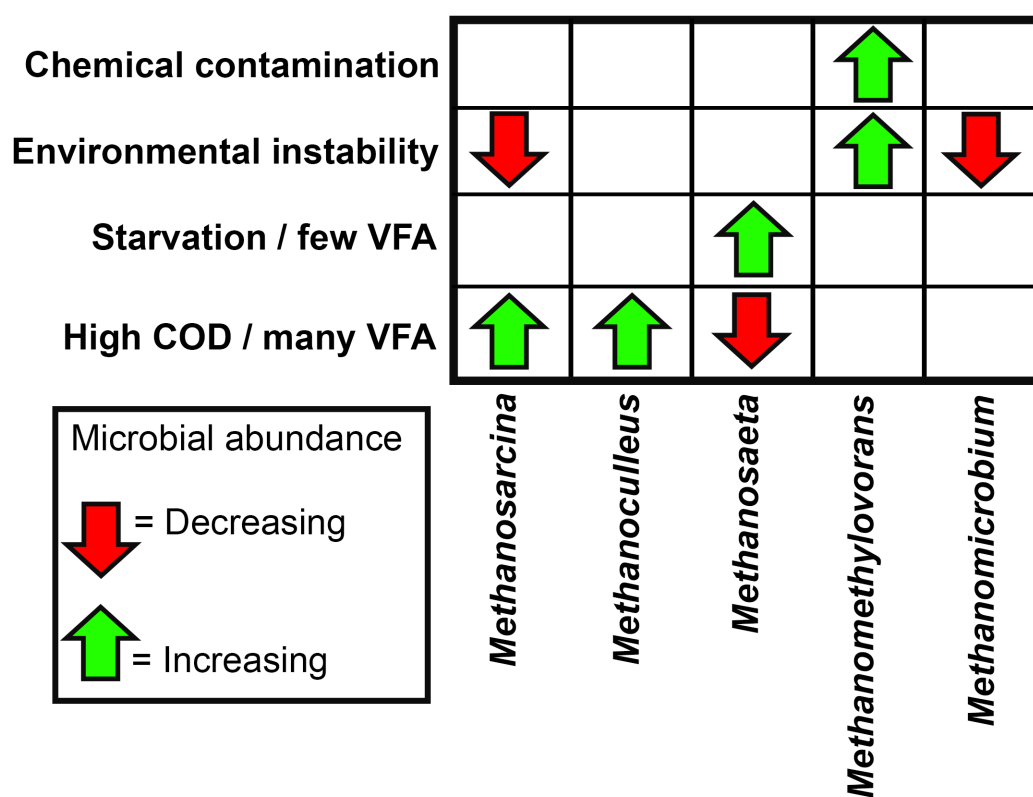


FIGURE 31: Hypothetic methanogenic markers of anaerobic digestion conditions: The abundance of methanogenic key groups might indicate several process conditions, such as chemical contamination, environmental instability, starvation and high concentrations of chemical oxygen demand (COD) or volatile fatty acids (VFAs). The shown scheme was concluded comparing chemical parameters and 16S-rRNA gene amplicon profiles from publication 1 and 2.

Unlike the co-digester sludge from industrial biogas plants, sewage sludge from water treatment plants was particularly rich in the genus *Methanosaeta*. Similar results were

described in a previous study [3]. This indicates that the growth of *Methanosaeta* is accelerated by low concentrations of chemical oxygen demand (COD) and volatile fatty acids (VFAs).

Moreover, it was observed in publication 2 that *Methanosaeta*, *Methanomicrobium* and *Methanosarcina* were highly sensitive to environmental changes, unlike *Methanoculleus*. Therefore, reduced levels of the first three genera might indicate microbial process instabilities due to, for example, oxidative stress, environmental changes or changes in temperature. It was further observed that the only sampled codigester that received coferments from Biodiesel production (Publication 1) contained high levels of *Methanomethylovorans*, which might therefore function as an indicator of chemical contaminations, which might in turn indicate process instability in industrial digesters. Therefore, using taxonomic profiling to analyze different reactor conditions might allow a more effective regulation of anaerobic digestion processes and to optimize many digester plants. For example, the finding of *Methanosarcina* in co-digester plants might indicate starvation and the potential for a higher loading rate. On the other hand, an increased abundance of the species *Methanoculleus* and/or *Methanosarcina* might indicate a successful adaption to a higher loading rate. A sudden decrease of *Methansarcina* and/or *Methanomicrobium* might indicate that the change of environmental conditions was too sharp and that the loading rate should not be further increased. Moreover, a sudden drop of the abundance of *Methanosarcina* and/or *Methanomicrobium* might indicate the occurrence of a toxic compound, e.g. due to the application of a new substrate or a change of environmental conditions (such as a lowered temperature caused by seasonal changes). In summary, the screening of dynamic changes of *Methanosarcina*, *Methanoculleus*, *Methanosaeta*, *Methanomicrobium* and *Methanomethylovorans* might help to optimize their growth conditions, which in turn might maximize the organic load limit.

Bacterial markers: Besides archaeal taxa, bacterial key-groups were compared (Publications 1, 2 and 5). Leachate from codigesters contained high amounts of Bacteroidetes, Firmicutes and Spirochaetes. The fact that Spirochaetes are present in sewage sludge, but not in highly viscous codigesters, indicates that they might be a marker of low viscosity, which improves the mobility of involved microorganisms. In contrast to the leachate and the highly viscid codigester sludge, the sewage sludge was especially rich in the phylum Chloroflexi. Therefore, the presence of Chloroflexi might be regarded as an indicator of low concentrations of VFAs and COD. Similar observations were made for Actinobacteria. It was observed that the amount of Actinobacteria increases in the digestate from highly viscid co-digester sludge (Publication 1, figure 7). In a second experiment, in which viscid codigester sludge was incubated for several weeks with a reduced biomass input compared to the original biogas plant, an increase in Actinobacteria was observed (Publication 2, figure 11). Therefore, as discussed for *Methanosaeta* before, the presence of Actinobacteria and/or Chloroflexi might be a good proxy for starvation, which in turn might indicate the potential for higher loading rates. It can be further hypothesized that increasing amounts of Firmicutes and Bacteroidetes (as well as the taxa *Methanoculleus* and *Methanosarcina* that were described in the previous section) might indicate an overload in biomass in water treatment plants. As shown in figure 30, sewage plants are adapted to acetoclastic methanogens. The occurrence of hydrogenotrophic archaea, or eubacterial groups, which are adapted to high concentrations of COD and VFAs, might indicate that the acetoclastic methanogens are not able to process the loading rate. Therefore, the loading rate should be lowered.

Harsh conditions							↑
Increasing viscosity			↓				
Uncomplete degradation						↑	
Starvation / few VFA				↑	↑		
High COD / many VFA	↑	↑					
	Firmicutes	Bacteroidetes	Spirochaetes	Chloroflexi	Actinobacteria	Cyanobacteria	Proteobacteria

Microbial abundance

↓ = Decreasing

↑ = Increasing

FIGURE 32: Hypothetic bacterial markers of anaerobic digestion conditions: The abundance of bacterial key groups might indicate several process conditions, such as chemical contamination, environmental instability, starvation and high concentration of COD or VFAs. The shown scheme was concluded comparing chemical parameters and 16S-rRNA gene amplicon profiles from publication 1 and 2.

Paving the crossroad of bio-refinery

Besides new microbial surveillance strategies, there are other ways to optimize anaerobic digester plants. As described in the introduction, anaerobic digestion is linked to many other industrial fields of biorefinery. Therefore, anaerobic digestion might also be understood as “crossroad of biorefinery”. And for paving the crossroad of biorefinery, acidifying pretreatment stages could have a key-role. Microbe-driven acidification as a pre-treatment stage for biogas plants is a promising technology, as it allows the production of several organic acids [7], hydrogen [8] and carbon dioxide (e.g. for the growth of algae) [9]. Furthermore, it facilitates energy production on demand, as acidified (pre-degraded) biomass can be retained in the acidification stage and rapidly transformed into

methane when energy is needed. One of the key aims of this thesis was to highlight acidification stages as a future crossroad for integrated biorefinery. To this end, acidification experiments were performed, providing insights into the multi-functionality and connectivity of multiple waste streams, and into microbiome stability. Finally, new microbial strains that can potentially play a role in the optimization of biorefinery processes were isolated from acidification and other artificial environments.

To highlight multi-functionality of acidification stages, a microbial thermoelectric cell (MTC) was developed and patented (WO002014049181A1). Although the results are merely preliminary, the MTC could theoretically be combined with a biological pre-treatment step for anaerobic digestion. The MTC allows

for substrate degradation and for the production of electricity from exothermic microorganisms. During the experiments with the MTC, yeast was used as an exothermic microorganism, which also allows the production of ethanol.

Another new technological approach tested during this thesis was the combination of heat-shock treatments and microbe-driven acidification. Heat-shocks had very little influence on the microbiomes tested, which allowed the combined use of heat-shock treatments and biological acidification for reducing methanogenic contaminations and improving substrate degradation. We observed no improved degradation efficiency after heat-shock treatments compared to the control; however, positive effects in terms of biogas productivity were reported for a mild thermal treatment of algae by another research group [10]. Therefore, further experiments should be carried out, to investigate the full potential of combining heat-shock and acidification processes. Different substrates should be compared to determine substrates that show improved degradability due to this new treatment. Moreover, higher temperatures could be tested to investigate to which temperatures acidifying microbiomes show a high thermoresistance. The application of heat-shocks with other stressors, such as for example ultrasound could be investigated. This has previously been reported on anaerobic digester sludge, showing increased biogas production rates up to 42 % [11].

Besides the presented technological approaches, there are several other scientific works that demonstrate the possibility for technological upgrades of biological pre-treatment stages. For example, it has recently been shown that the application of electrical current can stimulate the hydrolytic phase of anaerobic digestion [12]. In another work, it was demonstrated

that magnetite nanoparticles improve the anaerobic degradation of the toxic compound p-chloronitrobenzenes (p-ClNB), presumably by promoting the intracellular electron transfer by acting as electron conduits [13]. Searching for similar technologies as the presented MTC, it was further found that researchers have been able to combine microbial fuel cells (MFCs) with two-stage wastewater treatment [14], which might increase the energy efficiency during the treatment.

Altogether, the possibility for combining anaerobic pre-treatment stages with MTCs, MFCs, heat-shocks, electron conduits and electrodes for microbial stimulation demonstrates a high potential for the technological improvement of anaerobic digestion systems.

To demonstrate the potential to treat multiple waste streams within the acidification stage, the anaerobic treatment of grass biomass was analyzed and is shown in publication 2 and 3. Additionally, the acidification of chicken dung (CM) was investigated in publication 4. Chicken dung and grass biomass are challenging substrates, as grass biomass has a high content of lignocellulolytic fibres and CM results in toxic concentrations of ammonia. But yet, both substrates are economically attractive, as they are available in large quantities, as discussed in publication two and four.

In seeking alternative treatment methods to facilitate the digestion of grass biomass, we applied (publication 5) a pre-treatment of grass biomass in an acidifying leach-bed process, producing up to 250 mg of volatile fatty acids per g of chemical oxygen demand. As grass biomass contains large amounts of fibres, it is difficult to successfully pump and mix the resulting fibre-rich digester sludge. Additionally, it is energetically not attractive to circulate large amounts of fibres in a digester plant, since

they are partly not degradable (Olaf Luschnig, Personal communication, Bio H2 Umwelt GmbH, Germany). Therefore, liquefying the grass biomass before transferring it into the methane stage can make the digestion process more energy-efficient. A very interesting approach was recently published by the university of Kassel (Germany) [15]. A screw press was used to treat grass biomass. Separated solids can be used as solid fuels and liquids can be used for subsequent anaerobic digestion. Like this, even non degradable solids can be used to produce energy, and fibres are not disturbing the digestion process. Besides our presented results with grass biomass, we have shown that with optimal input concentrations (between 10 and 20 g of volatile solids per litre) successful liquefaction of chicken dung can be achieved too. Producing high-strength liquor from chicken manure might improve conditions for the removal of nitrogen and particles, especially sand. However, at optimal CM-input concentrations, the high ammonia stabilizes the pH at a value (6.8 - 7.8), where methanation becomes possible. As demonstrated in publication 5, heat-shock experiments with grass biomass yielded a reduction in methanogenic contaminations. Therefore, application of heat-shocks on CM-acidification might be a promising means of overcoming the methanogenic contaminations in chicken dung. Because of that, microbe-driven acidification and application of heat-shocks might, in combination, allow successful liquefaction of chicken dung with no or very little loss of COD due to methanogenic contamination.

The importance of engineered microbiomes for industrial applications has been acknowledged in previous reports, as for example in the work from Sheth et al. (2016), where the

Another possibility to overcome methanogenic contaminations might be an increased CM-concentration. Higher CM concentrations cause higher concentrations of ammonia, which in turn inhibits methanogenesis. However, higher levels of ammonia affect acidifying microorganisms negatively too (Publication 4). Therefore, the concentration of solubilised COD and VFAs would decrease as well. However, after collecting the produced high-strength liquor, the amount of nitrogen in the remaining solids is strongly reduced. Remaining solids with lowered nitrogen concentrations could be returned and mixed with new substrate fractions in subsequent batch cycles in order to increase the efficiency of COD solubilisation. The proposed digestion strategy is illustrated in figure 33.

Robustness of methanogenic and acidifying microbiomes

The manipulation of acidifying microbiomes is an important challenge for the production of high-value metabolites. As described in the introduction, it is known that many economically attractive metabolites are produced during acidification, such as multiple organic acids, alcohols or hydrogen. However, except for bioaugmentation with selected microbial species, no designs of complex and anaerobic microbiomes producing a certain spectrum of metabolites within anaerobic digestion systems have been reported to date.

authors proposed the development of a toolbox allowing the in-situ engineering of complex microbiomes [16]. Moreover, the use of drugs, antibiotics, probiotics, signal molecules, genetic engineering or

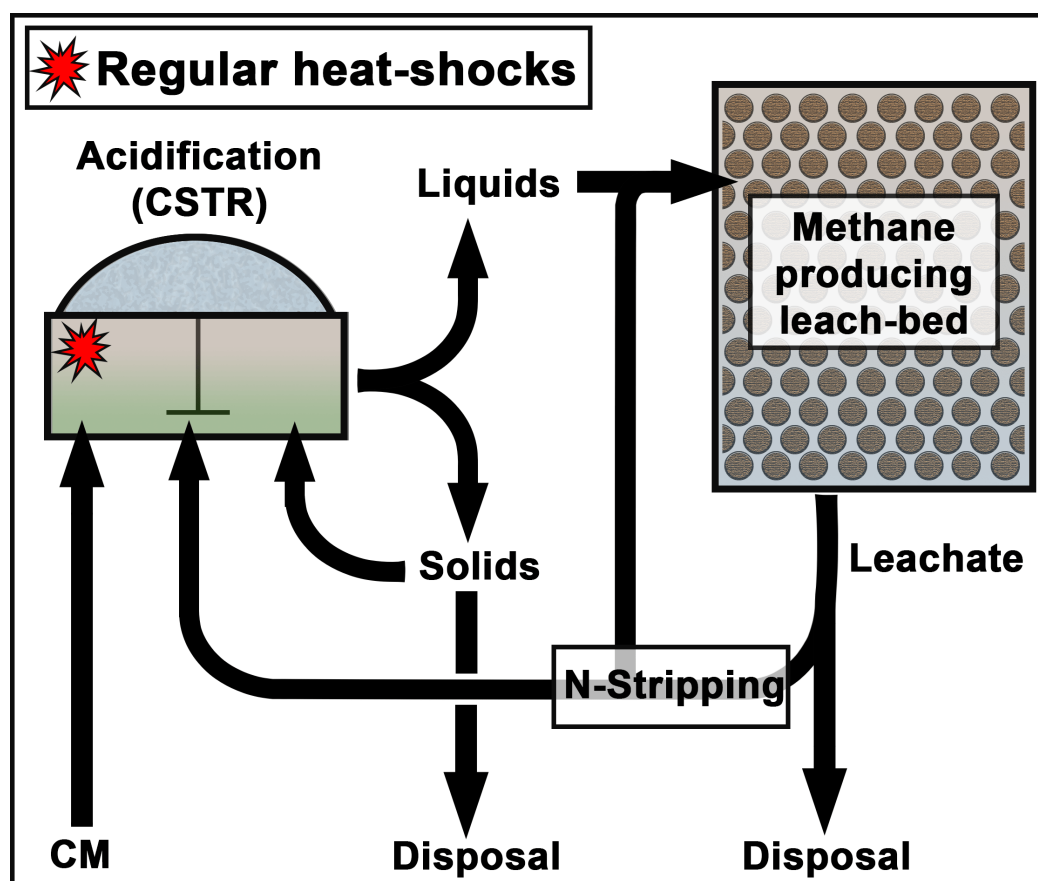


FIGURE 33: Hypothetical industrial flowchart for anaerobic digestion of high concentrated chicken manure: Very high concentrations of chicken manure (higher than 40 gVS/L) might prevent methanogenesis but would also impair acidification. Therefore, it is suggested to recirculate the solids after ammonia has been removed in the liquid phase (Interpretation based on publication 4). Additionally, regular heat-shocks might be applied to suppress methanogenesis more efficiently (As described in publication 5).

controlling environmental conditions for fine-tuning microbiomes has extensively been discussed, especially from the point of medical applications [17, 18]. Even though the previously discussed methods allow to change microbiome compositions, we are still not able to design artificial microbiomes from scratch that are as complex as anaerobic microbiomes or soil microbiomes. The complexity of actively shaping acidifying microbiomes was demonstrated by the heat-shock experiments in publication 5. Even with regular heat-shocks at 70°C, the underlying microbiome was only minimally affected. On the other hand, constant high temperatures of

55°C caused a permanent microbial shift towards Firmicutes (Publication 2). Interestingly, after changing the thermophilic conditions to mesophilic ones, the biocenosis quickly changed to a Bacteroidetes rich profile that is typically observed under mesophilic conditions. Much further research remains to be done in order to fully understand the complexity of anaerobic interaction within complex microbiomes and to be able to engineer a microbiome in a predictable way.

Bioprospecting: Even though the engineering of complex anaerobic microbiomes is a still far away scientific goal, the inoculation of certain strains

of interest might be already in reach. Much prior research has explored bioaugmentation approaches, and its prospective application in the industry (e.g. for improved degradation efficiency [19, 20], recovery from toxicant exposure [21], or reduction of odour [22]). To broaden the variety of potential strains that can be used for bioaugmentation while also helping to understand the complex underlying microbiomes of anaerobic digesters, researchers are searching for new strains with potential biotechnological applications in relation to anaerobic digestion and biorefinery [23, 24, 25]. Searching for new biotechnologically applicable strains, we isolated multiple *Bacillus* strains with high lipolytic activity (publication 8). Bioaugmentation experiments with lipolytic bacteria would be especially informative, as so far there is only one publication that is focussed on bioaugmentation with lipolytic bacteria [20]. In this context, it has to be highlighted that the before mentioned *Bacillus* strains were isolated under harsh conditions from a dishwasher and a thermophilic Sauna (publication 8) and showed high thermoresistance. Therefore, they might be applied under harsh conditions in the industry, for example as microbial bio-detergents. These strains could also be used in anaerobic digesters. Even though those strains are not originating from anaerobic digesters, it is worth trying to perform bioaugmentation with strains from other habitats. In fact, in a recently published work, microorganisms from compost were successfully inoculated into an anaerobic digester, where they improved cellulolytic activity [26.] Up to date, many thermophilic or thermoresistant lipases have been isolated and characterized already. However, the presented *Bacillus* strains

in this thesis are the first ones from an indoor environment, which indicates that also indoor environments should be screened in the future for potential industrially applicable strains.

Besides the mentioned lipolytic strains, we isolated and sequenced two new Firmicutes species with a potential role in the degradation of plant biomass (publication 6 and 7). The need of new species, which are involved in degradation of plant biomass has been stressed in a recent work, where more than 100 new cellulolytic strains were isolated [27]. Coming back to leach-bed acidification of grass biomass (publication 5), where 25 % of the input COD was liquefied, cellulolytic strains might help to increase the percentage of solubilized COD. In this context the newly isolated strains might be promising, as they were already isolated from fermentation of grass biomass. However, a field test, or a biochemical characterization of the strains still remains to be done.

Robustness of methanogenic microbiomes: The key for economically attractive bioaugmentation procedures is a stable integration of a microorganism of choice into microbiomes of anaerobic digesters. As anaerobic digestion systems contain highly dynamic microbiomes with high microbial redundancy [28, 29], this raises the question of how effectively outsider strains of interest can be integrated in microbiomes of such complexity. To analyze the manipulability of the three key microbiomes described in publication 1, acidic high-strength liquor was produced from grass biomass and fed in multiple methane stages, containing sewage sludge and highly viscous co-digester sludge (publication 2).

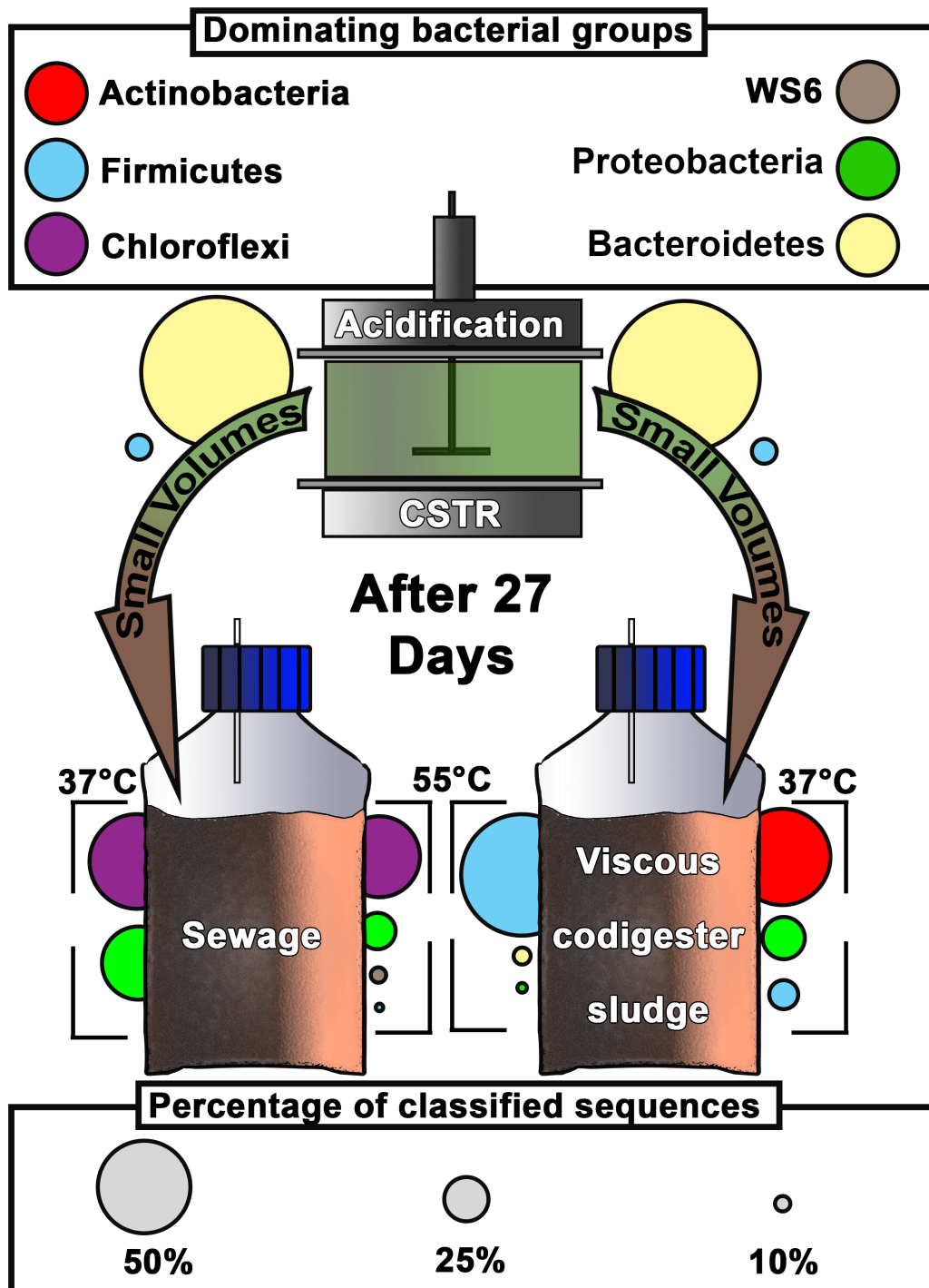


FIGURE 34: Stability of microbiomes from methane-producing digesters against bioaugmentation with inoculum from acidification stages (According to taxonomic profiles from 16S-rRNA gene amplicon sequencing shown in figure 9, 11,12 publication 2): High-strength liquor from the separated acidification stage causes no obvious changes in the anaerobic digester microbiome. This indicates high microbial stability. Dominating phyla with abundance higher than 5 % of classified sequences are shown.

The dynamic behaviour of the sequencing. All methane stages were microbiomes was analysed based on equally fed with high-strength liquor in 16S-rRNA high-throughput amplicon order to test whether the biocenosis from

the high-strength liquor had any effect on the composition of microbiomes from methanogenic digesters.

Interestingly, the microbial composition of each sludge type remained similar to the original samples before feeding. The inoculum from the acidification stage contained mainly Bacteroidetes, but no increase of this phylum was observed in the used sewage sludge, or in the highly viscous co-digester sludge (Fig. 2). This means that both methane producing microbiomes were very robust against external contaminations. This resistance against microbiota from biological input-material is a useful fact, as it reduces the chance that methanogenic microbiomes can be affected negatively by microbiota from any substrate of choice. However, this highlights potential difficulties with bioaugmentation approaches. Therefore, the successful manipulation of anaerobic microbiomes in the near future will require new inoculation strategies.

One way to overcome this robustness might be to inoculate strains belonging to a phylum, which is already dominant under the given conditions. To give here an example: As described in publication 5, a low pH seems to give a growth advantage to Proteobacteria. Combining a low pH in the acidification with the inoculation of promising strains from the phylum Proteobacteria, might improve the chance for a successful bioaugmentation.

Robustness of acidifying microbiomes:

It is known that in anaerobic methane stages the biocenosis at mesophilic conditions is different from that at thermophilic conditions [30, 31, 32]. In fact, several articles describe methanogenic archaea, which are specialized on thermophilic temperatures [33, 34, 35]. It has also been demonstrated that Firmicutes grow particularly well under thermophilic conditions, while under mesophilic conditions Bacteroidetes can

be found in high numbers too [36]. However, the mentioned studies are restricted to one-stage digestion; this thesis, by contrast, sought to analyse the differences between mesophilic and thermophilic microbiomes from separated acidification stages. To this end, grass biomass was acidified in parallel under mesophilic and thermophilic conditions and compared based on both, 16S-rRNA gene amplicon sequencing and proteomics. As reported for methane stages from co-fermenters, the acidifying microbiome was dominated by Firmicutes and Bacteroidetes. Under thermophilic conditions, high numbers of heat-shock proteins were found, the proteome's behaviour was considerably less dynamic than it was under mesophilic conditions, and Cyanobacteria were detected, which is likely explained by the presence of chloroplasts from incomplete degradation of plant biomass. However, as described in other publications, usually very long adaptation phases are required for thermophilic one-stage digesters [37, 38], from which one can conclude that the acidifying microbiomes need long adaptation phases too. Additionally, the application of an inoculum from other thermophilic digesters might facilitate the adaptation. However, although acidifying microbiomes struggled to adapt to thermophilic conditions, in subsequent experiments in which repeated heat-shocks of 55°C and 70°C were applied, a high level of thermoresistance was observed (Fig. 3). Only methanogenic archaea were shown to be highly sensitive to heat-shocks during these experiments. Therefore, the application of heat-shocks can be an effective method for separating acidifying microbiomes from methanogenic ones. As mentioned before, acidification stages with high concentrations of ammonia tend to produce small amounts of methane due to methanogenic contaminations.

Therefore, the application of heat-shocks could help to prevent COD losses due to methanogenic contamination. In this context, it is very interesting that a strong community shift from Proteobacteria to Bacteroidetes/Firmicutes was observed when the pH was changed from 6.0 to 6.8 (publication 5). When using an inoculum

and applying long incubation periods, a sudden pH-drop might destabilize the evolved community tremendously. Therefore, it is recommended to keep the pH even during acidification well balanced at a constant pH-value.

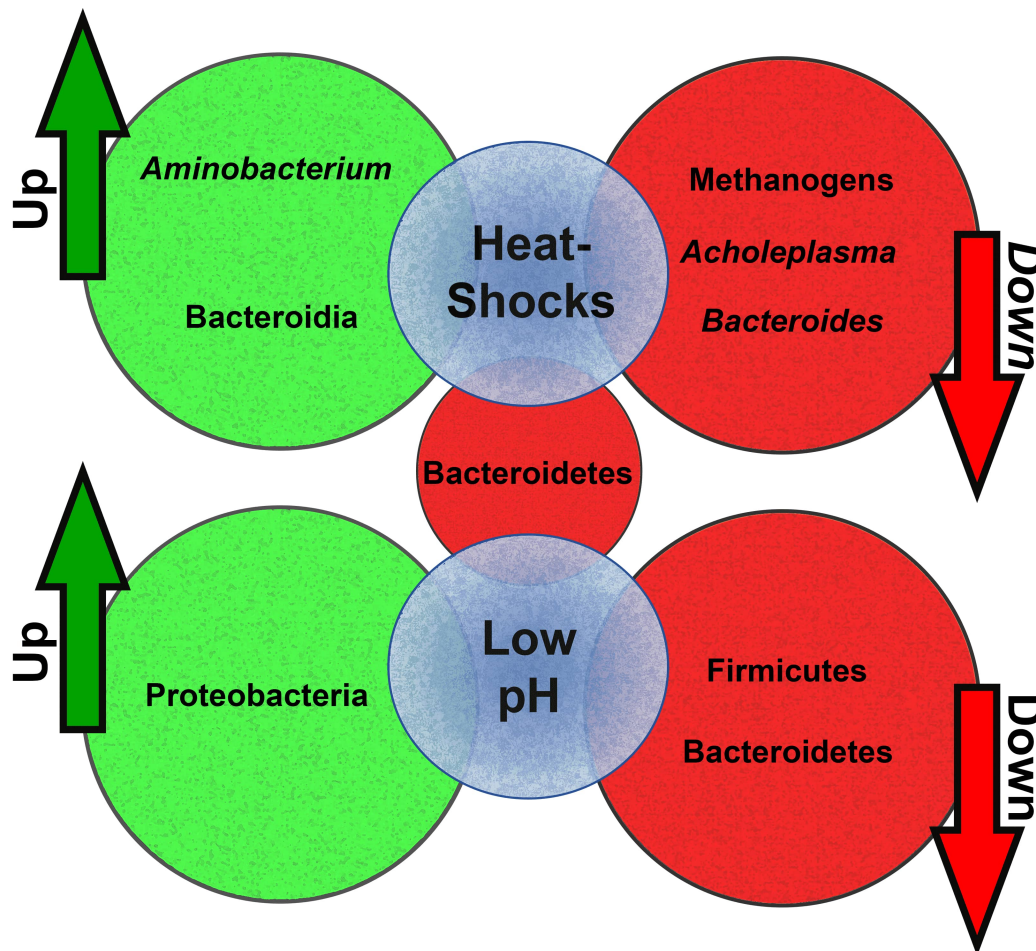


FIGURE 35: Microbial robustness of high-strength liquor against mild heat-shocks: Regular heat-shocks of 55°C or 70°C had minimal effect on the microbial composition, except for methanogenic archaea, which could be effectively suppressed. Transient shifts were only observed for few microbial groups, which are indicated in the shown scheme.

References

1. Jo De Vrieze, Tom Hennebel, Nico Boon, Willy Verstraete. Methanosarcina: The rediscovered methanogen for heavy duty biomethanation. *Biores Technol.* 2012;112:1–9.
2. Liu Y. Taxonomy of Methanogens, in: Timmis KN, McGenity, TJ, van der Meer JR, de Lorenzo V (Eds.), *Handbook of Hydrocarbon and Lipid Microbiology*, Springer, 2010, Heidelberg, pp. 547–558.
3. Sundberg C, Al-Soud WA, Larsson M, Alm E, Yekta SS, Svensson BH, et al. 454 pyrosequencing analyses of bacterial and

- archaeal richness in 21 full-scale biogas digesters. *FEMS Microbiol Ecol.* 2013;85:612–26.
4. Bengelsdorf FR, Gabris C, Michel L, Zak, Kazda M. Syntrophic microbial communities on straw as biofilm carrier increase the methane yield of a biowaste-digesting biogas reactor. *AIMS Bioeng.* 2015;2:264–276.
5. Weiß S, Lebuhn M, Andrade D, Zankel A, Cardinale M, Birner-Gruenberger R, Somitsch W, Ueberbacher BJ, Guebitz GM. Activated zeolite-suitable carriers for microorganisms in anaerobic digestion processes?. *Appl Microbiol Biotechnol.* 2013;97: 3225–3238.
6. Dareioti MA, Kornaros M. Anaerobic mesophilic co-digestion of ensiled sorghum, cheese whey and liquid cow manure in a two-stage CSTR system: Effect of hydraulic retention time, *Bioresour Technol.* 2014;175:553–562.
7. Zhou M, Yan B, Wong JWC, Zhang Y. Enhanced volatile fatty acids production from anaerobic fermentation of food waste: A mini-review focusing on acidogenic metabolic pathways. *Bioresour Technol.* 2017; doi: 10.1016/j.biortech.2017.06.121.
8. Gijzen HJ, Zwart KB, Verhagen FJ, Vogels GP. High-Rate two-phase process for the anaerobic degradation of cellulose, employing rumen microorganisms for an efficient acidogenesis. *Biotechnol Bioeng.* 1988;31:418–425.
9. Cheng J, Ye Q, Xu J, Yang Z, Zhou J, Cen K. Improving pollutants removal by microalgae *Chlorella* PY-ZU1 with 15 % CO₂ from undiluted anaerobic digestion effluent of food wastes with ozonation pretreatment. *Bioresour Technol.* 2016;216:273–279.
10. Gonzales-Fernandez, C., Sialve, B., Bernet, N., Steyer, J.P. Thermal pretreatment to improve methane production of *Scenedesmus* biomass. *Biomass Bioenergy.* 2016;40:105–111.
11. Pérez-Elvira S, Fdz-Polanco M, Plaza FI, Garralón G, Fdz-Polanco F. Ultrasound pre-treatment for anaerobic digestion improvement. *Water Sci Technol.* 2009;60:1525–32.
12. Samani S, Abdoli MA, Karbassi A, Amin MM. Stimulation of the hydrolytic stage for biogas production from cattle manure in an electrochemical bioreactor. *Water Sci Technol.* 2016;74:606–15.
13. Xu X, Gao X, Jin J, Vidonish J, Zhu L. A novel bioelectrode and anaerobic sludge coupled system for p-CINB degradation by magnetite nanoparticles addition. *Environ Sci Pollut Res.* 2017;24:16220–16227.
14. Ren L, Ahn, Y, Logan BE. A Two-Stage Microbial Fuel Cell and Anaerobic Fluidized Bed Membrane Bioreactor (MFC-AFMBR) System for Effective Domestic Wastewater Treatment. *Environ Sci Technol.* 2014; 48:4199–4206.
15. Wachendorf M, Richter F, Fricke T, Graß R, Neff R. Utilization of semi-natural grassland through integrated generation of solid fuel and biogas from biomass. I. Effects of hydrothermal conditioning and mechanical dehydration on mass flows of organic and mineral plant compounds, and nutrient balances. *Grass Forage Sci.* 2009;64:132–143.
16. Sheth RU, Cabral V, Chen SP, Wang HH. Manipulating Bacterial Communities in situ Microbiome Engineering. *Trends Genet.* 2016;32:189–200.
17. Foo JL, Ling H, Lee YS, Chang MW. Microbiome engineering: Current applications and its future. *Biotechnol J.* 2017;12:1600099.
18. Kali A. Human Microbiome Engineering: The Future and Beyond. *J Clin Diagn Res.* 2015;9:01–04.
19. Duran M, Tepe N, Yurtsever D, Punzi VL, Bruno C, Mehta RJ. Bioaugmenting anaerobic digestion of biosolids with selected strains of *Bacillus*, *Pseudomonas*, and *Actinomyces* species for increased methanogenesis and odor control, *Appl Microbiol Biotechnol.* 2006;73:960–966.
20. Cirne DG, Björnsson L, Alves M, Mattiasson B. Effects of bioaugmentation by an anaerobic lipolytic bacterium on anaerobic digestion of lipid-rich waste. *J Chem Technol Biotechnol.* 2006;81:1745–1752.
21. Schauer-Gimenez AE, Zitomer DH, Maki JS, Struble CA. Bioaugmentation for improved recovery of anaerobic digesters after toxicant exposure. *Water Res.* 2010;44:3555–3564.
22. Tepe N, Yurtsever D, Mehta RJ, Bruno C, Punzi VL, Duran M. Odor control during post-digestion processing of biosolids through bioaugmentation of anaerobic digestion. *Water Sci Technol.* 2008;57:589–94.

23. Hahnke S, Striesow J, Elvert M, Mollar X, Klocke M., 2014. *Clostridium bornimense* sp. nov., isolated from a mesophilic, two-phase, laboratory-scale biogas reactor. *Int J Syst Evol Microbiol.* 64, 2792–2797.
24. Boltianskaya Y, Detkova E, Pimenov N, Kevbrin V. *Proteinivorax hydrogeniformans* sp. nov., an anaerobic, haloalkaliphilic bacterium fermenting proteinaceous compounds with high hydrogen production. *Antonie Van Leeuwenhoek.* 2017; doi: 10.1007/s10482-017-0949-9.
25. Koeck DE, Mechelke M, Zverlov VV, Liebl W, Schwarz WH. *Herbivorax saccincola* gen. nov., sp. nov., a cellulolytic, anaerobic, thermophilic bacterium isolated via in sacco enrichments from a lab-scale biogas reactor. *Int J Syst Evol Microbiol.* 2016;66:4458–4463.
26. Kinet R, Destain J, Hilgsmann S, Thonart P, Delhalle L, Taminau B, Daube G, Delvigne F. Thermophilic and cellulolytic consortium isolated from composting plants improves anaerobic digestion of cellulosic biomass: Toward a microbial resource management approach. *Bioresour Technol.* 2015;189:138–44.
27. Poszytek K, Ciekowska M, Sklodowska A, Drewniak L.; Microbial Consortium with High Cellulolytic Activity (MCHCA) for Enhanced Biogas Production. *Front Microbiol.* 2016;7:324.
28. De Vrieze J, Christiaens MER, Walraedt D, Devooght A, Ijaz UZ, Boon N. Microbial community redundancy in anaerobic digestion drives process recovery after salinity exposure. *Water Res.* 2017;111:109–117.
29. Ju F, Fang HHP, Zhang T. Application of Metagenomics, in: Environmental Anaerobic Technology—Environmental protection and Resource Recovery, Ju F, Fang HHP, Zhang T (Eds.), *Imperial College Press*, 2015, London pp. 73–108.
30. Zhu X, Kougiaris PG, Treu L, Campanaro S, Angelidaki I. Microbial community changes in methanogenic granules during the transition from mesophilic to thermophilic conditions. *Appl Microbiol Biotechnol.* 2017;101:1313–1322.
31. Sassi HP, Ikner LA, Abd-Elmaksoud S, Gerba CP, Pepper IL. Comparative survival of viruses during thermophilic and mesophilic anaerobic digestion. *Sci Total Environ.* 2017;615:15–19.
32. Stiborova H, Wolfram J, Demnerova K, Macek T, Uhlík O. Bacterial community structure in treated sewage sludge with mesophilic and thermophilic anaerobic digestion. *Folia Microbiol (Praha).* 2015;60:531–539.
33. Zinder SH, Cardwell SC, Anguish T, Lee M, Koch M. Methanogenesis in a Thermophilic (58°C) Anaerobic Digester: Methanotrix sp. as an Important Aceticlastic Methanogen. *Appl Environ Microbiol.* 1984;47:796–807.
34. Ferguson TJ, Mah RA. Isolation and Characterization of an H₂-Oxidizing Thermophilic Methanogen. *Appl Environ Microbiol.* 1983;45:265–274.
35. Jones WJ, Leigh JA, Mayer F, Woese CR, Wolfe RS. *Methanococcus jannaschii* sp. nov., an extremely thermophilic methanogen from a submarine hydrothermal vent. *Arch Microbiol.* 1983;136:254–261.
36. Moset V, Poulsen M, Wahid R, Højberg O, Møller HB. Mesophilic versus thermophilic anaerobic digestion of cattle manure: methane productivity and microbial ecology. *Microb Biotechnol.* 2015;8:787–800.
37. Kima K, Ahn YH, Speece RE. Comparative process stability and efficiency of anaerobic digestion; mesophilic vs. thermophilic. *Water Research-* 2002;36:4369–4385.
38. Bousková A, Dohányos M, Schmidt JE, Angelidaki I. Strategies for changing temperature from mesophilic to thermophilic conditions in anaerobic CSTR reactors treating sewage sludge. *Water Res.* 2005;39:1481–1488.

Conclusions

Anaerobic digestion is attracting particular attention because of its potential to produce electrical energy, heat, fertilizer and many industrially relevant metabolites at the same time. Due to this multifunctionality and the wide variety of possible input substrates, anaerobic digestion could be regarded as a crossroad for biorefinery and waste management. However, to pave this crossroad, some work remains to be done. Due to the complexity of microbiomes from anaerobic digesters, it is extremely difficult to manipulate and design anaerobic microbiomes performing specified functions, such as butyric acid production or hydrogen production. In order to shed light on this important area of research, this thesis has elucidated the robustness and dynamic behaviour of anaerobic digester plants and highlighted the importance of separated acidification stages for future developments in biorefinery. The main findings and conclusions can be summarized as follows:

- Three key- microbiomes can be defined, which are specific for sewage sludge, highly viscous co-digester sludge and leachate from leach-bed systems. All three microbiomes are strongly related to their underlying environmental parameters (COD, TOC, total nitrogen contents, conductivity, TVFA, TS, VS, pH, and volume of biogas).
- The methanogens *Methanosarcina*, *Methanoculleus*, *Methanomethylovorans*, *Methanosaeta* and *Methanomicrobium* might be promising proxies for digestion conditions in respect to the content of COD/VFAs, crucial environmental changes and content of toxic substances.
- The dynamic behaviour of the phyla Chloroflexi, Actinobacteria, Firmicutes, Bacteroidetes, Proteobacteria, Spirochaeta and Cyanobacteria (Chloroplasts) might be indicators in respect to the content of COD/VFAs or crucial environmental changes too.
- Acidification stages seem to be dominated by Bacteroidetes, Proteobacteria and Firmicutes and Firmicutes are especially enriched under thermophilic conditions.
- Separated acidification allows treatment of multiple wastes, which are difficult to digest in one-stage digesters, as for example grass biomass or chicken dung.
- We developed the first Microbial Thermoelectric Cell (MTC), which is compatible with anaerobic digestion and suitable for use in the pre-treatment stage. The MTC allows for the simultaneous production of ethanol and electric energy. Remnants might be used in a subsequent methane-producing stage.
- In seeking further new pre-treatment methods, we investigated the possibility of combining thermal pre-treatment with microbe-driven acidification. Surprisingly, we observed only minimal impacts of heat-shocks in the microbial composition. Therefore, it might be

possible in the future to combine heat-shocks with acidification processes to improve biomass pre-treatment.

- We identified a number of strains with the potential to improve biorefinery processes. We isolated several *Bacillus* strains from a sauna and a dishwasher, which are notable for their lipolytic activity.

This also shows for the first time that the indoor environment might yield industrial applicable microorganisms. In addition, we isolated two new Firmicutes strains from the acidification of grass biomass, which indicates that anaerobic environments have the potential to yield new strains with potential roles in the biorefinery industry.

Resumen en castellano

Resumen global de la temática

Microbiomas industriales

Desde los inicios de la industrialización en el siglo dieciocho, el ser humano ha ido abriéndose paso a paso una ventana a la microbiología industrial. Las nuevas industrias emergentes han dado lugar a nuevos nichos microbiológicos, muchos de ellos caracterizados por presentar altas temperaturas o estreses químicos. Se han descubierto microorganismos capaces de degradar contaminantes industriales, incluyendo bifenilo, organoclorina, pesticidas, dioxinas/furanos [1], petróleo [2], organohaluro [3], y muchos más. La capacidad de los microorganismos para crecer en ambientes extremos es de especial interés para la microbiología aplicada, ya que estos ambientes son una fuente prometedora de enzimas y microorganismos con potenciales aplicaciones industriales [4]. Algunos ejemplos de estas aplicaciones incluyen la obtención de una esterasa termoestable a partir de la bacteria *Thermus thermophiles* [6], el aislamiento de una lipasa activa a bajas temperaturas y tolerante a distintos solventes a partir de *Stenotrophomonas maltophilia* [6] o la obtención de una esterasa termoalcalofílica a partir de *Geobacillus* sp. [7]. Otro hábitat extremo que, debido a la reciente crisis energética mundial ha adquirido un gran interés, es el lodo anaeróbico procedente de tratamientos de agua o de procesos de co-digestión anaerobia. La digestión anaerobia (DA) es un proceso que lleva a la formación de metano, el cual puede ser quemado para

producir energía. Los procesos de DA son muy completos y permiten realizar tratamientos muy variados, aprovechar innumerables fuentes de desecho y generar solapamientos y sinergias complejos con diferentes campos de la industria y de la biorrefinería (Fig. 36A). La digestión anaeróbica (DA) ocurre en cuatro fases: hidrólisis, acidogénesis, acetogénesis y metanogénesis. Durante la hidrólisis se produce la degradación de proteínas, lípidos, hidratos de carbono y celulosa. Los ácidos grasos, aminoácidos y azúcares resultantes son transformados, durante la fase de acidogénesis, en ácidos grasos volátiles (AGV) y alcoholes, los cuales finalmente son degradados a acetato, H₂ y CO₂ en un proceso llamado acetogénesis. Por último, los microorganismos metanógenos hidrogenotróficos y acetotróficos utilizan el acetato, el H₂ y el CO₂ para la formación de metano (Fig. 36C).

Se han llevado a cabo investigaciones sobre procesos de DA durante más de un centenar de años, desde los trabajos iniciales de Söhngen (1906) [10] o Coolhas (1928) [11]; sin embargo, es necesario seguir investigando en este tema para poder comprender mejor los microbiomas anaerobios. En general, la diversidad microbiana en los procesos de DA es especialmente alta a temperaturas mesofílicas [12] y, de hecho, se descubren regularmente nuevas especies en lodos anaeróbicos [13, 14, 15]. Se han descrito una gran cantidad de especies no identificadas a través de la secuenciación de alto rendimiento del gen que codifica para el ARN ribosómico (ARNr) 16S [16]. La falta de conocimientos sobre muchas de las especies bacterianas presentes en

los digestores anaeróbicos complica el análisis de los microbiomas a niveles taxonómicos más bajos. Por ello, los estudios sobre las bacterias implicadas en procesos de DA se restringen frecuentemente al análisis a niveles taxonómicos más altos, como es el caso de los estudios realizados por Goux et al. [17] y Lebhuhn et al. [18], en los cuales

se describió una gran abundancia de Firmicutes y Bacteroidetes. En cambio, las comunidades de arqueas implicadas en procesos de DA parecen estar mejor caracterizadas, ya que las secuencias pueden ser clasificadas normalmente a nivel de género o, incluso, de especie [19].

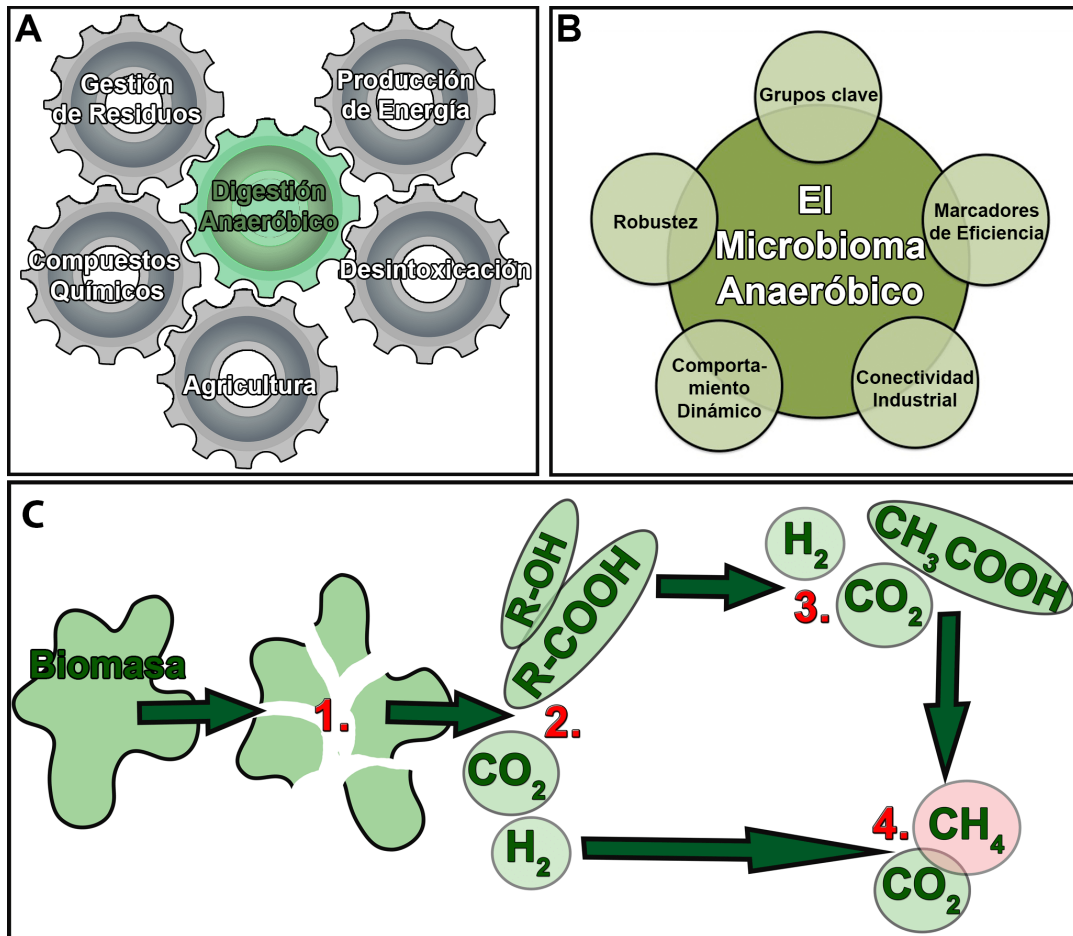


FIGURE 36: El papel central de la digestión anaerobia en la biorrefinería. La digestión anaerobia es una tecnología multifuncional que permite el entrecruzamiento de múltiples campos de la industria (A). La clave de esta multifuncionalidad reside en la presencia de microbiomas muy diversos y robustos y, por tanto, uno de los objetivos principales de la presente tesis es obtener una mejor comprensión de los microbiomas anaeróbicos (B). La digestión anaerobia se divide en cuatro fases (C): (1) La biomasa se hidroliza y se transforma en moléculas más pequeñas (hidrólisis); (2) Durante la acidogénesis, la biomasa hidrolizada se convierte en ácidos orgánicos, alcoholes, hidrógeno y dióxido de carbono; (3) Tiene lugar la acetogénesis, fase en la cual se forman principalmente ácido acético, hidrógeno y dióxido de carbono; (4) Finalmente, estas sustancias son usadas para la formación de metano (metanogénesis).

El conocimiento incompleto sobre las comunidades bacterianas en procesos de DA sugiere que existe un gran potencial para el futuro de la biorrefinería. En un trabajo reciente, se aislaron más de 100 cepas de bacterias degradadoras de celulosa de una planta de biogás [20]. En otro trabajo se aisló, a partir de digestato, una nueva especie metanotrófica perteneciente al género *Methylocaldum* y con gran potencial en la producción eficiente de metanol [21]. El lodo procedente de los procesos de DA también es una fuente prometedora de bacterias productoras de lipasas y proteasas. Recientemente, se ha aislado una nueva esterasa de la familia VII adaptada al frío a partir de purines [22], y una nueva cepa de *Bacillus subtilis* (IND19) que permite la producción simultánea de carboximetilcelulosa y proteasa a partir de excrementos de vaca [23].

En su conjunto, estos trabajos sugieren que los lodos anaeróbicos procedentes de diferentes procesos de DA pueden contener microbiomas muy diversos y con un gran potencial industrial que merece la pena investigar. Esto concuerda con otros trabajos previos que han destacado la importancia de la DA en las aplicaciones biotecnológicas durante los años noventa [24, 25].

Allanando el camino de la encrucijada de la biorrefinería integrada

El metano, al ser uno de los principales productos derivados de procesos de DA, tiene un papel prometedor en la biorrefinería. Además de su papel como fuente de energía, también puede ser usado para el crecimiento de metanótrofos, que constituyen una fuente viable de proteínas que pueden ser usadas como suplementos alimenticios. Además, los metanótrofos son una fuente prometedora de otros productos, ya que acumulan osmolitos

(por ejemplo ectoína o sacarosa), fosfolípidos, biopolímeros y enzimas [26]. Sin embargo, la DA no se restringe sólo a la producción de metano.

Los efluentes líquidos resultantes de las plantas de producción de biogás, debido a su alto contenido en nitrógeno y fósforo, pueden ser usados como fertilizantes y facilitan la producción eficiente de algas [27, 28]. Además, las fibras obtenidas a partir de la degradación anaerobia de plantas pueden usarse para realizar procesos de sacarificación, llevando a la producción de azúcares y lignina, productos que a su vez pueden usarse para la producción de ácido propiónico, ácido succínico, dioles, butanol, etanol, fibras de carbono y biopolímeros. A través de procesos termoquímicos, la lignina también puede ser usada para la producción de calor, electricidad, gas de síntesis y fenólicos. Y, finalmente, las fibras sólidas pueden transformarse en bioaceite o biocarbón a través de procesos de pirólisis [28,29].

La producción de productos biológicos a través de procesos de DA es especialmente interesante ya que permite la valorización de múltiples fuentes de residuos, como por ejemplo las microalgas mixtas [30], los lodos procedentes de industrias de pulpa o de papel [31] o los residuos municipales [32]. La fermentación anaerobia de residuos múltiples también conlleva la degradación de múltiples agentes contaminantes, como fenoles [33] o parafina [34].

La fragmentación de los procesos de DA en procesos de dos etapas se convierte en una posibilidad interesante a la hora de usar la digestión anaerobia para generar una interconexión sinérgica entre múltiples procesos de biorrefinería. Desde los años ochenta, los científicos han descrito la posibilidad de separar las fases de hidrólisis y acidogénesis de las fases de acetogénesis y metanogénesis [35, 36, 37]. Los niveles bajos de pH y las altas concentraciones de AGV llevan a una inhibición de la metanogénesis

[38]. A su vez, la inhibición de la metanogénesis lleva a la acumulación de AGVs interesantes, como por ejemplo ácido acético, láctico, propiónico o butírico. Los AGVs son productos interesantes ya que pueden usarse como químicos de plataforma en múltiples reacciones químicas [39], aunque la extracción de estos ácidos sigue siendo un gran reto [40]. Y, finalmente, la inhibición de la metanogénesis permite además la producción de hidrógeno [41].

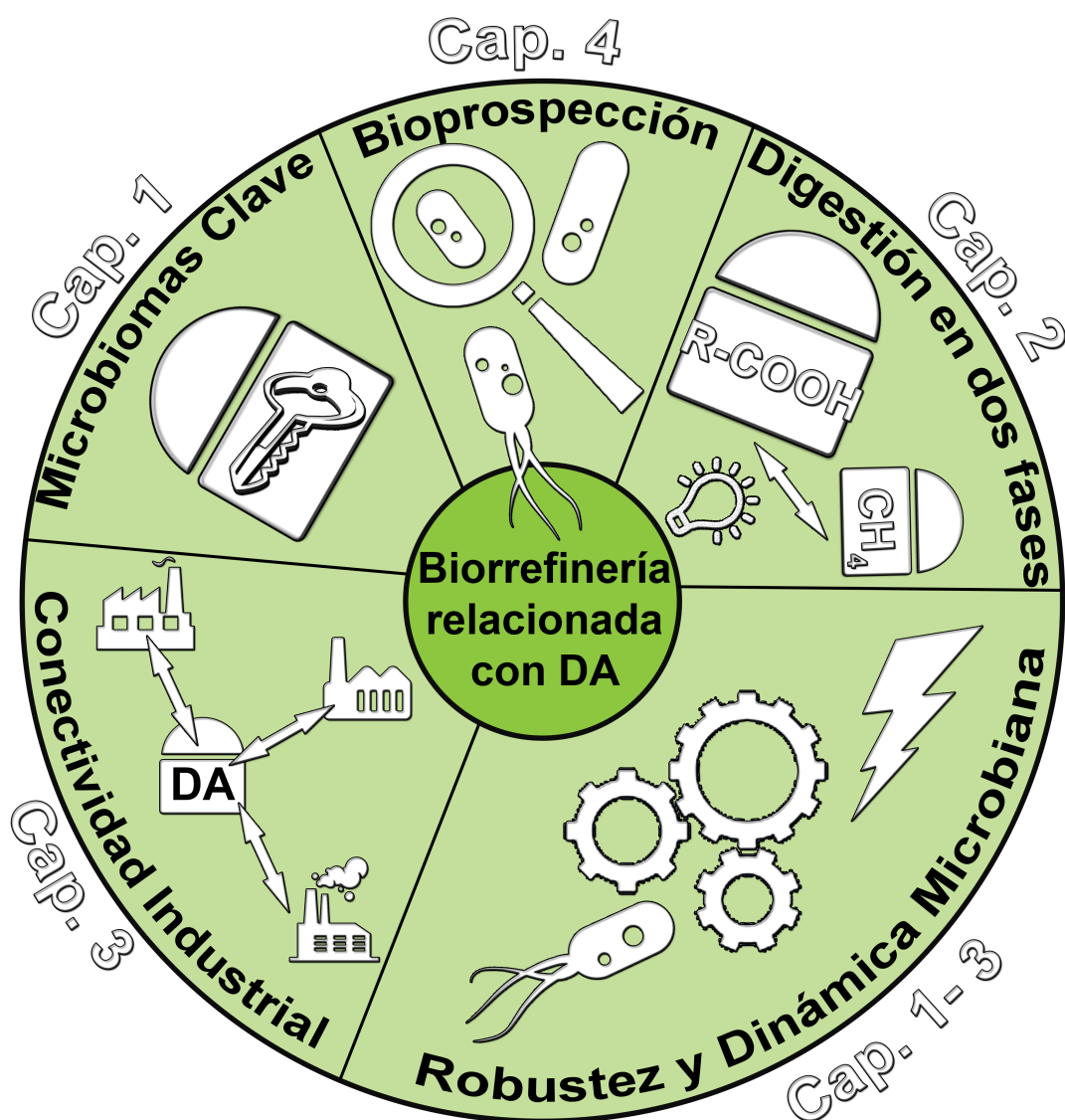


FIGURE 37: Estructura de la presente tesis doctoral: Es necesario obtener un conocimiento más profundo sobre el comportamiento del microbioma en procesos de digestión anaerobia para conseguir, en el futuro, una interconexión entre los distintos campos de la biorrefinería industrial donde la digestión anaerobia sea el punto de unión. A partir de esta idea, la presente tesis se centra en los temas representados en la imagen, y los capítulos correspondientes se indican en la parte externa del círculo.

La gran variedad de posibles aplicaciones resultantes de la separación de fases en procesos de DA puede favorecer la interconexión sinérgica entre los diferentes campos de la biorrefinería. Sin embargo, para llegar a ese objetivo, es necesario adquirir unos conocimientos más profundos sobre la diversidad microbiana y la robustez de los microbiomas anaerobios. Por tanto, se ha diseñado la presente tesis doctoral con el fin de arrojar luz sobre el comportamiento dinámico y robustez de los microbiomas propios de la digestión anaerobia. En la figura 37 se muestra la estructura global de la tesis.

Resultados principales

Marcadores microbianos para la evaluación del rendimiento de los procesos anaeróbicos:

Las arqueas metanógenas son los agentes clave en la producción anaerobia de

metano [42], y se han caracterizado taxonómicamente en estudios anteriores [43]. Sin embargo, estos representan tan solo una fracción de las especies microbianas que aparecen en los procesos de DA. Normalmente entre 1-20 % de las especies implicadas son arqueas metanógenas, y el resto de organismos son principalmente bacterias, pertenecientes sobretodo a los phyla Bacteroidetes, Firmicutes, Proteobacteria, Chloroflexi y Spirochaeta [44]. Las relaciones dinámicas entre estos phyla y las condiciones específicas bajo las cuales ciertos phyla dominan el proceso de digestión siguen siendo aún poco conocidas. En esta tesis se ha realizado una de las caracterizaciones más exhaustivas hasta la fecha de las comunidades microbianas características de plantas de producción mesofílica de biogás con el fin de adquirir un entendimiento más profundo sobre el comportamiento microbiano dinámico en las plantas de digestión.

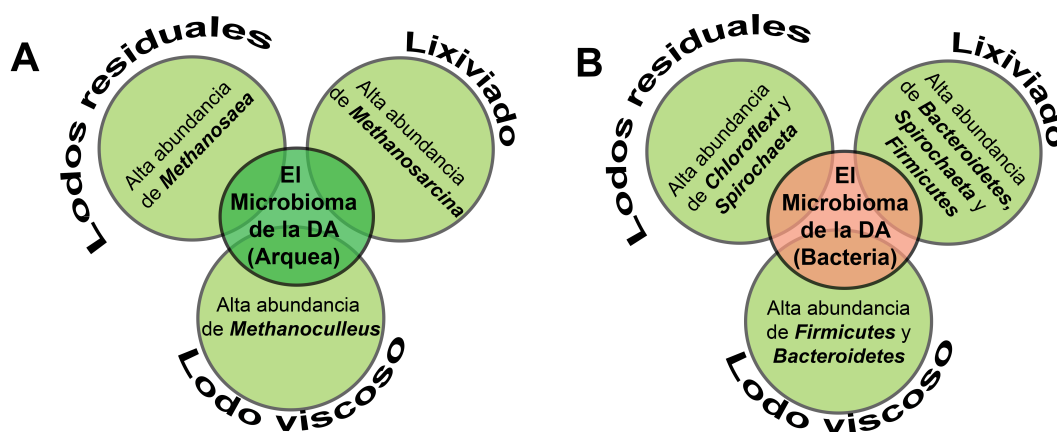


FIGURE 38: Comparación de microbiomas metanógenos a temperaturas mesofílicas: Se muestran los principales taxones microbianos - arqueas (A) y bacterias (B) - en lodos residuales, en lixiviado procedente de procesos de lixiviación en lecho fijo y en lodos de alta viscosidad procedentes de codigestores. El esquema mostrado se ha obtenido a partir de las figuras 7 y 8 (publicación 1).

Se compararon, a través de secuenciación de alto rendimiento del ARNr 16S, tres tipos diferentes de lodos

industriales caracterizados por poseer parámetros químicos muy distintos: lodo residual, lixiviado y lodo de alta

viscosidad procedente de reactores continuos de tanque agitado (CSTRs). Tal y como se describe en la publicación 1, cada tipo de lodo exhibió un perfil microbiano característico. El lixiviado se caracterizó por poseer altas cantidades de *Methanosarcina*, *Methanoculleus* y *Spirochaeta*, mientras que el lodo residual presentaba gran cantidad de *Methanosaeta*, *Spirochaeta* y *Chloroflexi*. En comparación con el lodo residual y el lixiviado, el lodo de alta viscosidad de CSTR era rico en Firmicutes y *Methanoculleus*. Los tres microbiomas clave detectados se detallan en la figura 38. En el futuro, estos perfiles pueden ayudar en el desarrollo de ensayos de escrutinio eficaces para diferentes tipos de digestores.

Arqueas marcadoras: La descripción en las publicaciones 1 y 2 de los perfiles microbianos de digestores industriales y de varios experimentos de digestión ha proporcionado mucha información sobre grupos microbianos que puede ser de utilidad a la hora de determinar marcadores hipotéticos del rendimiento de procesos anaeróbicos (Fig. 39 y Fig. 40). En primer lugar, se observó que *Methanosarcina* y *Methanoculleus* son especies metanógenas encontradas frecuentemente en fermentadores con altas velocidades de carga. *Methanosarcina* era particularmente abundante en el lixiviado de los sistemas de lecho fijo. En cambio, la gran cantidad de *Methanoculleus* presente en el lodo de alta viscosidad podría indicar que este microorganismo crece preferentemente en forma de biofilm, en concordancia con estudios previos [45, 46].

A diferencia del lodo del codigestor procedente de plantas industriales de biogás, en el lodo residual procedente de plantas de tratamiento de aguas era particularmente abundante el género *Methanosaeta*, tal y como se había descrito en un estudio anterior [44]. Esto sugiere que los valores bajos de DQO y de AGVs aceleran el crecimiento de *Methanosaeta*.

Además, se observó que *Methanosaeta*, *Methanomicrobium* y *Methanosarcina* eran muy sensibles a los cambios ambientales, a diferencia de *Methanoculleus*. Por tanto, unos niveles reducidos de los tres primeros géneros mencionados podría indicar inestabilidades en el proceso microbiano debido a, por ejemplo, estrés oxidativo, cambios ambientales o cambios en la temperatura. Se observó además que sólo el codigestor muestreado que había recibido cofermentos procedentes de producción de biodiesel (Publicación 1) contenía altas cantidades de *Methanometilovorans*, lo que podría indicar contaminación química y, por tanto, podría ser usando como una indicación de inestabilidades del proceso de digestión en biodigestores industriales.

Por tanto, el uso de la caracterización taxonómica para analizar las distintas condiciones de los reactores puede ser de gran utilidad para optimizar y regular de manera más eficaz los procesos de DA. Por ejemplo, la presencia de *Methanosarcina* en plantas de codigestión podría indicar inanición y la posibilidad de incrementar la tasa de carga. Por otro lado, una alta abundancia de *Methanoculleus* y/o *Methanosarcina* podría indicar una adaptación exitosa a un incremento en la tasa de carga. Una disminución repentina de *Methanosarcina* y/o *Methanomicrobium* podría indicar cambios demasiado bruscos en las condiciones ambientales y, por tanto, la necesidad de detener el incremento de la tasa de carga. Además, una caída repentina en la cantidad de *Methanosarcina* y/o *Methanomicrobium* podría ser indicativo de la presencia de un compuesto tóxico, por ejemplo debido al uso de un nuevo sustrato o a cambios en las condiciones ambientales (tal como una bajada en la temperatura causada por cambios estacionales). En resumen, el estudio de los cambios dinámicos en la cantidad de *Methanosarcina*, *Methanoculleus*, *Methanosaeta*, *Methanomicrobium* y

Methanometilovorans puede ayudar en la optimización de sus condiciones de crecimiento que, a su vez, puede servir para maximizar el límite de carga orgánica.

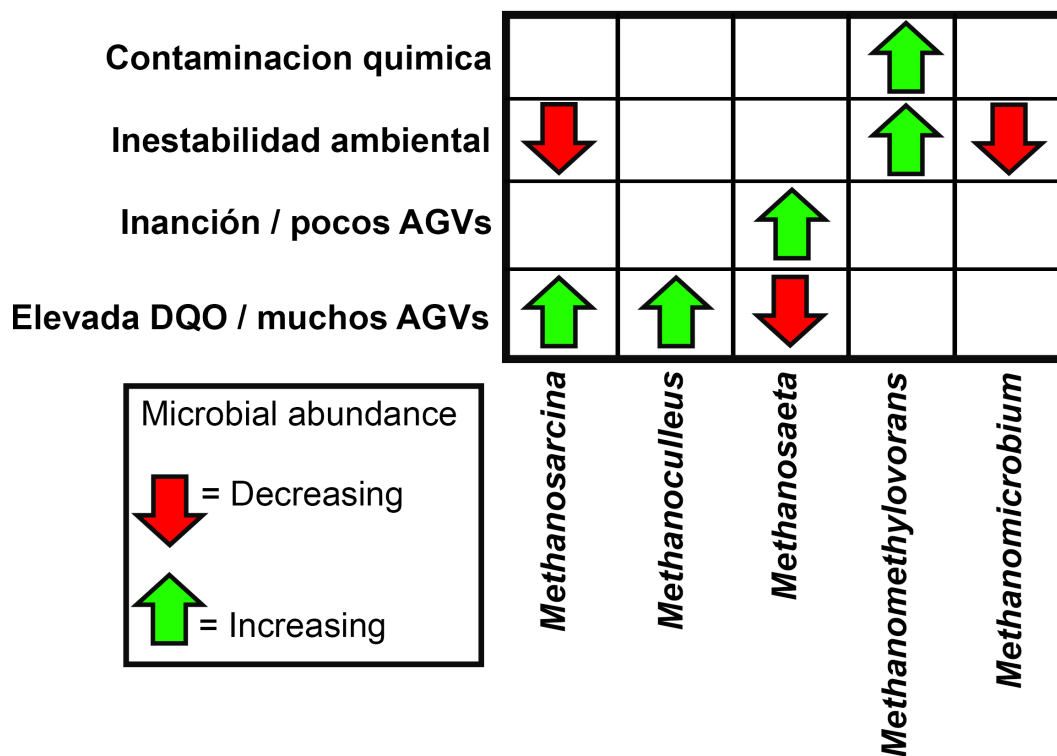


FIGURE 39: Marcadores metanógenos hipotéticos de condiciones de digestión anaeróbica: la abundancia de ciertos grupos metanógenos clave podría indicar diversas condiciones del proceso, tales como contaminación química, inestabilidad ambiental, inanición alta demanda química de oxígeno (DQO) o ácidos grasos volátiles (AGV). El esquema mostrado se ha obtenido al comparar los parámetros químicos y los perfiles taxonómicos del ARNr 16S de las publicaciones 1 y 2.

Marcadores bacterianos: Además de los taxones pertenecientes a arqueas, se compararon grupos bacterianos claves (Publicaciones 1, 2 y 5). El lixiviado procedente de codigestores presentaba una alta cantidad de Bacteroidetes, Firmicutes y Spirochaetas. El hecho de que las Spirochaetas estén presentes en lodos residuales pero no en lodos de alta viscosidad indica que podrían usarse como marcadores de baja viscosidad, una parámetro que mejora la movilidad de los microorganismos implicados en el proceso. A diferencia del lixiviado y del lodo de alta viscosidad, en el lodo residual era particularmente abundante

el phylum Chloroflexi. Por tanto, la presencia de Chloroflexi podría indicar bajas concentraciones de AGVs y DQO. Se realizaron observaciones similares en el caso de Actinobacterias: había una mayor cantidad de Actinobacteria en el digestato de lodo de alta viscosidad (Publicación 1, figura 7). En un segundo experimento, el lodo de alta viscosidad se incubó durante varias semanas con una aportación de biomasa reducida en comparación con la planta de biogás original, y se observó un aumento en la cantidad de Actinobacterias (Publicación 2, figura 11). Por tanto, tal y como se ha comentado en el caso

previo de *Methanosaeta*, la presencia de Actinobacteria y/o Chloroflexi podría ser un buen indicador en casos de inanición y esto, a su vez, podría ser una advertencia de la necesidad de incrementar la tasa de carga.

Se podría hipotetizar que un incremento en las cantidades de Firmicutes y Bacteroidetes (así como de los taxones *Methanoculleus* y *Methanosarcina* descritos en la sección anterior) podría indicar una sobrecarga en las plantas

de tratamiento de aguas. Tal y como se muestra en la figura 38, los metanógenos acetoclásticos están adaptados a las plantas depuradoras. La presencia de arqueas hidrogenotróficas o de grupos de eubacterias adaptadas a altas concentraciones de AGVs y DQP podría indicar que los metanógenos acetoclásticos no son capaces de procesar la tasa de carga y, por tanto, esta tasa debería reducirse.

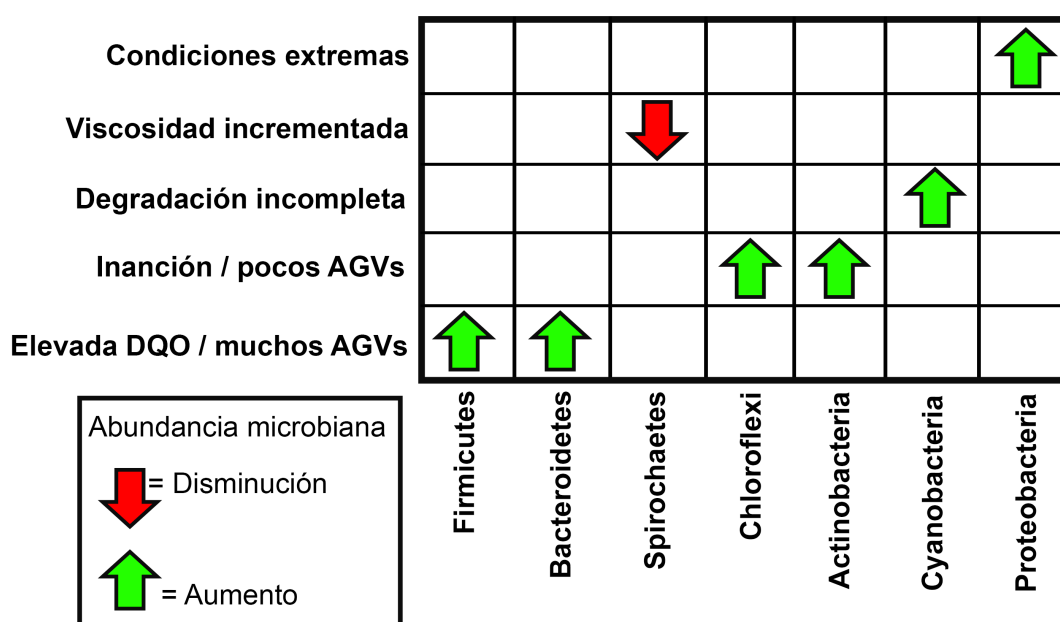


FIGURE 40: Marcadores hipotéticos de las condiciones de digestión anaerobia. La abundancia de grupos bacterianos claves podría indicar ciertas condiciones del proceso, tales como contaminación química, inestabilidad ambiental, inanición o altas concentraciones de DQP o AGVs. El esquema mostrado se ha obtenido a partir de la comparación de los parámetros químicos con los perfiles taxonómicos resultantes de la secuenciación del ARNr 16S descritos en las publicaciones 1 y 2.

Pavimentando la encrucijada de la biorrefinería integrada

Aparte de las nuevas estrategias microbianas de vigilancia hay otras formas de optimizar las plantas de DA. Tal y como se describe en la introducción, la digestión anaerobia esta asociada a muchos otros sectores de la industria de la biorrefinería. Por tanto, la digestión anaerobia podría entenderse

también como una “encrucijada de los procesos biorrefinería”. Y para allanar el camino de dicha encrucijada de la biorrefinería podría tener un papel muy importante la aplicación de una etapa de pretratamiento acidificante. La acidificación impulsada por microorganismos como una etapa previa al tratamiento en las plantas de biogás es una tecnología prometedora ya que permite la producción de varios

ácidos orgánicos [47], hidrógeno [48] y dióxido de carbono (por ejemplo para el crecimiento de algas) [49]. Además, facilita la producción de energía bajo demanda, ya que la biomasa acidificada (y pre-degradada) puede ser retenida en la fase de acidificación y rápidamente transformada a metano cuando haya necesidad de producir energía. Uno de los objetivos principales de esta tesis es subrayar la importancia de las fases de acidificación como punto de encrucijada en la biorrefinería integrada. Para ello, se han realizado experimentos de acidificación que han permitido conocer la multifuncionalidad y la conectividad de múltiples flujos de residuos, así como la estabilidad de los microbiomas. Finalmente, se han aislado a partir de fases de acidificación y de otros ambientes artificiales nuevas cepas microbianas que podrían desempeñar un papel en la optimización de los procesos de biorrefinería.

Para destacar la multifuncionalidad de las fases de acidificación se ha desarrollado y patentado (WO002014049181A1) una célula microbiana termoeléctrica (CMT). Aunque estos resultados son preliminares, la CMT podría ser combinada teóricamente con una fase biológica de pretratamiento en procesos de DA. La CMT permite la degradación de sustratos y la producción de electricidad mediante el uso microorganismos exotérmicos. En los experimentos con la CMT se usaron levaduras como microorganismos exotérmicos, llevando a la producción de etanol.

Otra aproximación tecnológica puesta a prueba durante la presente tesis ha sido la combinación de tratamientos de choque térmico y de acidificación generada por microorganismos. Los microbiomas analizados apenas mostraron cambios al ser tratados con choques térmicos, lo que permitió el uso de tratamientos combinados de choque térmico y acidificación biológica con el

fin de intentar reducir contaminaciones metanógenas y de mejorar la degradación de sustratos. La eficiencia de degradación no se vio mejorada tras la aplicación de los tratamientos de choque térmico en comparación con los controles; sin embargo, se han descrito previamente efectos positivos derivados de tratamientos térmicos suaves en algas [50]. Por tanto, se han de llevar a cabo más experimentos con el fin de investigar todas las posibles combinaciones de tratamientos de choque térmico con procesos de acidificación. Por ejemplo, se deberían probar diferentes sustratos para seleccionar aquellos con los cuales este tratamiento resulte en una mayor eficiencia de degradación. Además, se deberían realizar pruebas con temperaturas más elevadas para describir con detalle las características de termoresistencia de los microbiomas acidificantes. El uso de choques térmicos junto con otros factores estrés, como por ejemplo ultrasonidos, también debería estudiarse. Este último caso ha sido descrito previamente en lodos de digestores anaerobios, resultando en un incremento en la tasa de producción de biogás de hasta un 42 % [51].

Además de las aproximaciones tecnológicas aquí descritas, hay otros trabajos científicos que han estudiado la posibilidad de insertar mejoras tecnológicas en las fases de pretratamientos biológicos. Por ejemplo, se ha descrito recientemente que la aplicación de corrientes eléctricas puede llevar a la estimulación de la fase hidrolítica de los procesos de digestión anaerobia [52]. En otro estudio se demostró que las nanopartículas de magnetito pueden mejorar la digestión anaerobia del compuesto tóxico p-cloronitrobenzeno (p-CINB), supuestamente actuando como conductos eléctricos y fomentando la transferencia intracelular de electrones [53]. En el caso de tecnologías similares a la CMT, se han realizado trabajos previos en los cuales se han combinado

pilas de combustible microbianas con tratamientos de aguas residuales de dos fases, resultando en un incremento en el rendimiento energético durante el tratamiento [54].

En conjunto, la posibilidad de combinar las fases de pretratamiento anaerobio con CMTs, pilas de combustible microbianas, choques térmicos, conductos eléctricos y electrodos para la estimulación microbiana demuestra el gran potencial de las mejoras tecnológicas en los sistemas de digestión anaerobia.

Para demostrar el potencial de tratar múltiples cadenas de residuos con una fase de acidificación, se describe el tratamiento anaerobio de biomasa herbácea en las publicaciones 2 y 3. Además, en la publicación 4 se ha investigado el proceso de acidificación en estiércol de gallina (EG). El EG y la biomasa herbácea son sustratos complejos, ya que la biomasa herbácea presenta altas cantidades de fibras lignocelulolíticas y el EG genera concentraciones tóxicas de amoníaco. Aun así, ambos sustratos son económicamente atractivos debido a su disponibilidad en grandes cantidades, tal y como se comenta en las publicaciones 2 y 4.

Al buscar un método de tratamiento alternativo para facilitar la digestión de biomasa herbácea, se aplicó (publicación 5) un pretratamiento de biomasa herbácea en un proceso de lixiviación acidificante en lecho fijo, llevando a la producción de hasta 250 mg de AGVs por gramo de DQO. Debido a las grandes cantidades de fibras presentes en la biomasa herbácea, resulta difícil bombear y mezclar correctamente el lodo rico en fibras resultante. Además, la circulación de grandes cantidades de fibras en una planta de digestión no resulta atractivo desde un punto de vista económico ya que las fibras no son totalmente degradables (Olaf Luschnig, Comunicación personal, Bio H2 Umwelt GmbH, Alemania). Por tanto, la

licuefacción de la biomasa herbácea antes de su transferencia a la etapa de formación de metano podría resultar en una mayor eficiencia energética del proceso de digestión. Un grupo de investigadores de la Universidad de Kassel (Alemania) ha publicado recientemente una aproximación muy interesante basada en el uso de una prensa de tornillo para el tratamiento de biomasa herbácea [55]. Los sólidos separados pueden ser usados como combustibles sólidos, y los líquidos pueden ser usados para procesos de digestión anaerobia. Así, hasta los sólidos no degradables pueden ser usados para la producción de energía y las fibras no alteran el proceso digestivo. Además de los resultados obtenidos con biomasa herbácea, se ha demostrado que es posible conseguir una licuefacción exitosa de EG usando unas concentraciones óptimas de entrada de entre 10 y 20 gramos de sólidos volátiles por litro. La producción de hidrolizado a partir de EG puede mejorar las condiciones para la eliminación de nitrógeno y partículas, especialmente arena. Sin embargo, a concentraciones óptimas de EG, los valores elevados de amoníaco estabilizan el pH a valores de 6.8-7.8, a los cuales es posible la metanización. Tal y como se describe en la publicación 5, los experimentos de choque térmico con biomasa herbácea resultaron en una reducción en las contaminaciones metanógenas. Por tanto, la aplicación de choques térmicos en los procesos de acidificación de EG puede ser una forma prometedora de acabar con las contaminaciones metanógenas en EG, y la aplicación combinada de acidificación microbiana y de choques térmicos podría llevar a una licuefacción exitosa de EG con bajos niveles de pérdida de DQO debido a contaminación metanógena.

Otra posibilidad a la hora de evitar contaminaciones metanógenas puede ser el uso de concentraciones elevadas de EG, ya que esto lleva a la acumulación

de elevadas concentraciones de amoníaco que, a su vez, inhibe la metanogénesis. Sin embargo, los niveles altos de amoníaco también afectan negativamente a los microorganismos acidificantes (Publicación 4) y, con ello, podrían bajar las concentraciones de DQO soluble y VFAs. Sin embargo, después de recoger el hidrolizado producido, se observó una gran reducción en la cantidad de nitrógeno

presente los sólidos restantes. Estos sólidos restantes con concentraciones bajas de nitrógeno se pueden devolver y mezclar con nuevas fracciones de sustrato en ciclos posteriores con el fin de incrementar la eficiencia de solubilización de DQO. La estrategia de digestión propuesta se puede observar en la figura 41.

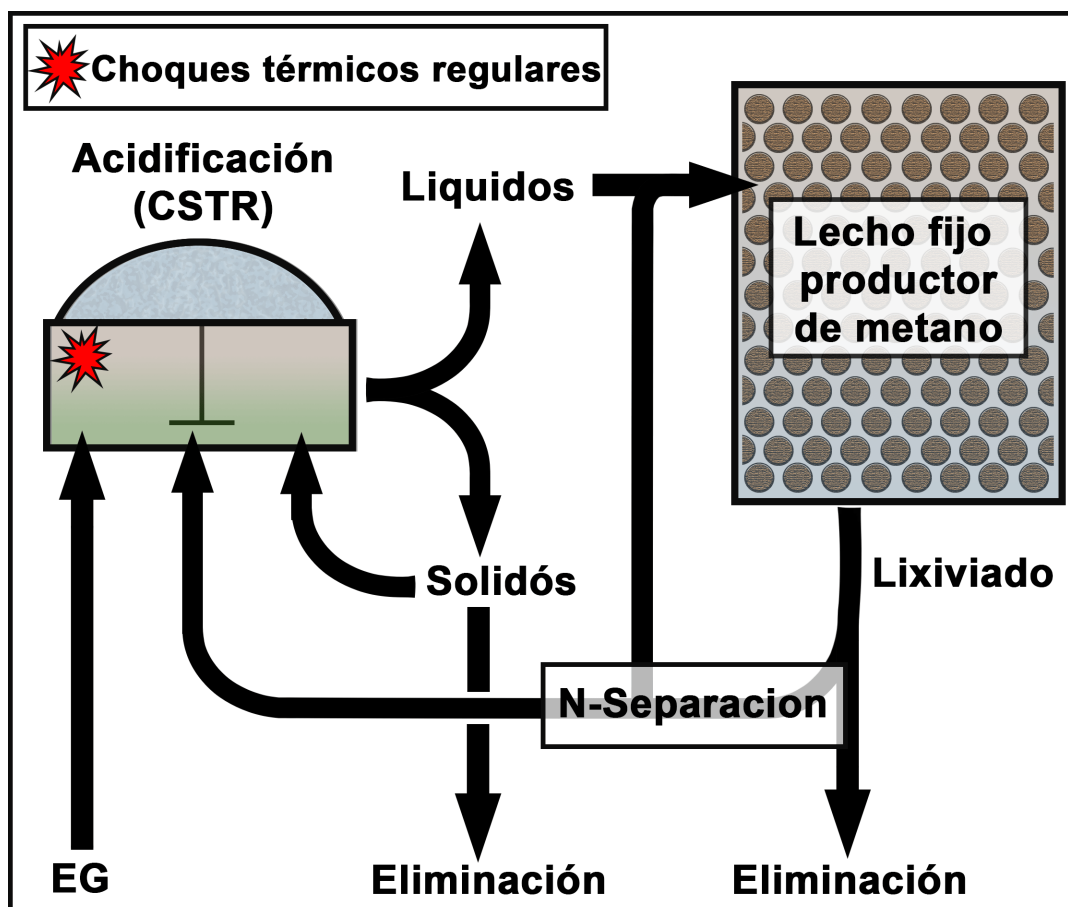


FIGURE 41: Diagrama de flujo de un proceso hipotético de digestión anaerobia de elevadas concentraciones de estiércol de gallina (EG): altas concentraciones de EG (mayores que 40 gVS/L) podrían prevenir metanogénesis pero también impedirían el proceso de acidificación. Por tanto, se sugiere usar una recirculación de los sólidos después de la eliminación de amoníaco en la fase líquida (interpretación basada en la publicación 4). Adicionalmente, se pueden aplicar choques térmicos de manera regular para inhibir la metanogénesis de manera más eficiente (descrito en la publicación 5).

Robustez de los microbiomas metanógenos y acidificantes

La manipulación de microbiomas acidificantes es un desafío importante a la hora de producir metabolitos de valor elevado. Tal y como se describe en la introducción, se sabe que durante la fase de acidificación se producen muchos metabolitos económicamente atractivos, tales como múltiples ácidos orgánicos, alcoholes o hidrógeno. Sin embargo, a excepción de procesos de bioaumentación con especies microbianas seleccionadas, hasta la fecha no se ha descrito ningún diseño de microbioma complejo y anaerobio que produzca un espectro concreto de metabolitos dentro del proceso de digestión anaerobia.

La importancia del diseño de microbiomas para aplicaciones industriales se ha descrito en estudios previos, como por ejemplo en el trabajo de Sheth et al. (2016), en el cual los autores proponen desarrollar una caja de herramientas que permita el diseño in situ de microbiomas complejos [56]. Además, el uso de fármacos, antibióticos, probióticos, moléculas señal, ingeniería genética o condiciones ambientales controladas para la mejora de los microbiomas se ha descrito de manera extensiva, sobretodo desde el punto de vista de las aplicaciones médicas [57, 58]. Aunque los métodos ya descritos permiten alterar la composición de los microbiomas, aún no somos capaces de diseñar desde cero microbiomas artificiales que sean tan complejos como los microbiomas anaerobios o los microbiomas de suelo. La complejidad asociada a la alteración de microbiomas anaeróbicos se ha demostrado con los experimentos de choque térmico descritos en la publicación 5: incluso con choques térmicos regulares a 70°C el microbioma basal apenas se vio afectado. En cambio, la aplicación de temperaturas altas y contantes de 55°C llevan a un cambio permanente en el microbioma,

que pasa a ser rico en Firmicutes (Publicación 2). Curiosamente, el cambio de condiciones termofílicas a mesofílicas generó rápidamente un cambio en la comunidad bacteriana hacia un perfil rico en Bacteroidetes, que es típico de condiciones mesofílicas. Es necesario seguir investigando con el fin de entender la complejidad de las interacciones entre los ambientes anaerobios y sus microbiomas, y para conseguir finalmente diseñar un microbioma que se pueda comportar de forma predecible.

Bioprospección: Aunque el diseño de microbiomas anaerobios complejos sigue siendo un objetivo lejano, en la actualidad es posible realizar una inoculación con ciertas cepas de interés. Varias investigaciones previas han explorado aproximaciones basadas en la bioaumentación y han estudiado su potencialidad en aplicaciones industriales (por ejemplo para mejorar la eficiencia de degradación [59, 60], para la recuperación después de una exposición tóxica [61], o para la reducción de olores [62]). En la actualidad se están realizando búsquedas de nuevas cepas con potenciales aplicaciones biotecnológicas en procesos de digestión anaerobia y biorrefinería. Con esto se pretende ampliar la variedad de cepas disponibles para procesos de bioaumentación a la vez que se amplía la comprensión de los microbiomas complejos propios de procesos de digestión anaerobia [63, 64, 65]. En la presente tesis se ha realizado una búsqueda de nuevas cepas con aplicación biotecnológica y se han aislado varias cepas de *Bacillus* sp. con actividad lipolítica (publicación 8). Sería de gran interés realizar experimentos de bioaumentación con bacterias lipolíticas ya que, hasta la fecha, solo hay una publicación centrada en el uso de este tipo de bacterias para procesos de bioaumentación [60]. En este contexto, cabe destacar que las cepas de *Bacillus* previamente mencionadas se han aislado

de ambientes expuestos a condiciones extremas (una sauna termofílica y un lavaplatos) y demostraron ser muy termoresistentes (publicación 8). Por tanto, podrían ser utilizados en aplicaciones industriales bajo condiciones extremas, por ejemplo como biodetergentes microbianos o en procesos de digestión anaerobia. Aunque las cepas no proceden originalmente de digestores anaeróbicos, podría ser útil realizar pruebas de bioaumentación con cepas de distintos ambientes. De hecho, en un trabajo reciente se inocularon con éxito microorganismos procedente de compost en un digestor anaeróbico, lo que resultó en un incremento en la actividad celulolítica [66].

Hasta la fecha se han aislado y caracterizado muchas lipasas termofílicas o termoresistentes. Sin embargo, las cepas de *Bacillus* descritas en la presente tesis son las primeras aisladas a partir de un ambiente de interior, lo que indica que estos ambientes interiores también pueden ser fuentes importantes de nuevas cepas microbianas con potenciales aplicaciones industriales.

Además de las cepas lipolíticas mencionadas, en la presente tesis se ha aislado y secuenciado dos nuevas especies de Firmicutes con un posible papel en la degradación de biomasa vegetal (publicación 6 y 7). En un trabajo reciente se destacó la necesidad de encontrar nuevas especies implicadas en la degradación de biomasa vegetal y se aislaron más de 100 cepas nuevas con actividad celulolítica [20]. Volviendo a la acidificación de lixiviado en lecho fijo de biomasa vegetal (publicación 5), donde el 25 % de la entrada de DQO estaba licuada, la inserción de cepas celulolíticas podría ayudar a incrementar el porcentaje de DQO solubilizado. En este contexto, las nuevas cepas aisladas podrían ser prometedora, ya que se aislaron a partir de una fermentación de biomasa vegetal. Sin embargo, para poder usarlo en aplicaciones industriales

futuras sería necesario realizar pruebas y caracterizaciones bioquímicas de las cepas.

Robustez de microbiomas metanógenos: la clave para realizar procesos de bioaumentación económicamente atractivos está en una integración estable de un microorganismo de interés en un microbioma propio de un digestor anaerobio. Debido a que los sistemas de digestión anaerobia contienen microbiomas muy dinámicos y con una gran redundancia microbiana [67, 68], esto plantea la cuestión de cómo de efectiva puede ser la integración de cepas de interés en microbiomas de tal complejidad. Para analizar la manipulabilidad de los tres microbiomas clave descritos en la publicación 1, se produjo hidrolizado a partir de biomasa herbácea y ésta se usó para alimentar múltiples fases de metanogénesis de digestores que contenían lodos residuales y lodos de alta viscosidad de codigestores (publicación 2). El comportamiento dinámico de los microbiomas se analizó a través de secuenciación de alto rendimiento de amplicones del gen ARNr 16S. Todas las fases de metanogénesis se alimentaron por igual con hidrolizado con el fin de observar si la comunidad microbiana del hidrolizado tenía algún efecto en la composición del microbioma propio de los digestores metanogénicos.

Resulta interesante que la composición microbiana de cada tipo de lodo permanecieron similar a la composición de las muestras originales antes de la alimentación con hidrolizado. El inoculo de la fase de acidificación contenía principalmente Bacteroidetes, pero no se observó un incremento en este taxón ni el lodo residual ni en el lodo de alta viscosidad (Fig. 42). Esto sugiere que ambos microbiomas productores de metano son muy robustos frente a contaminaciones externas.

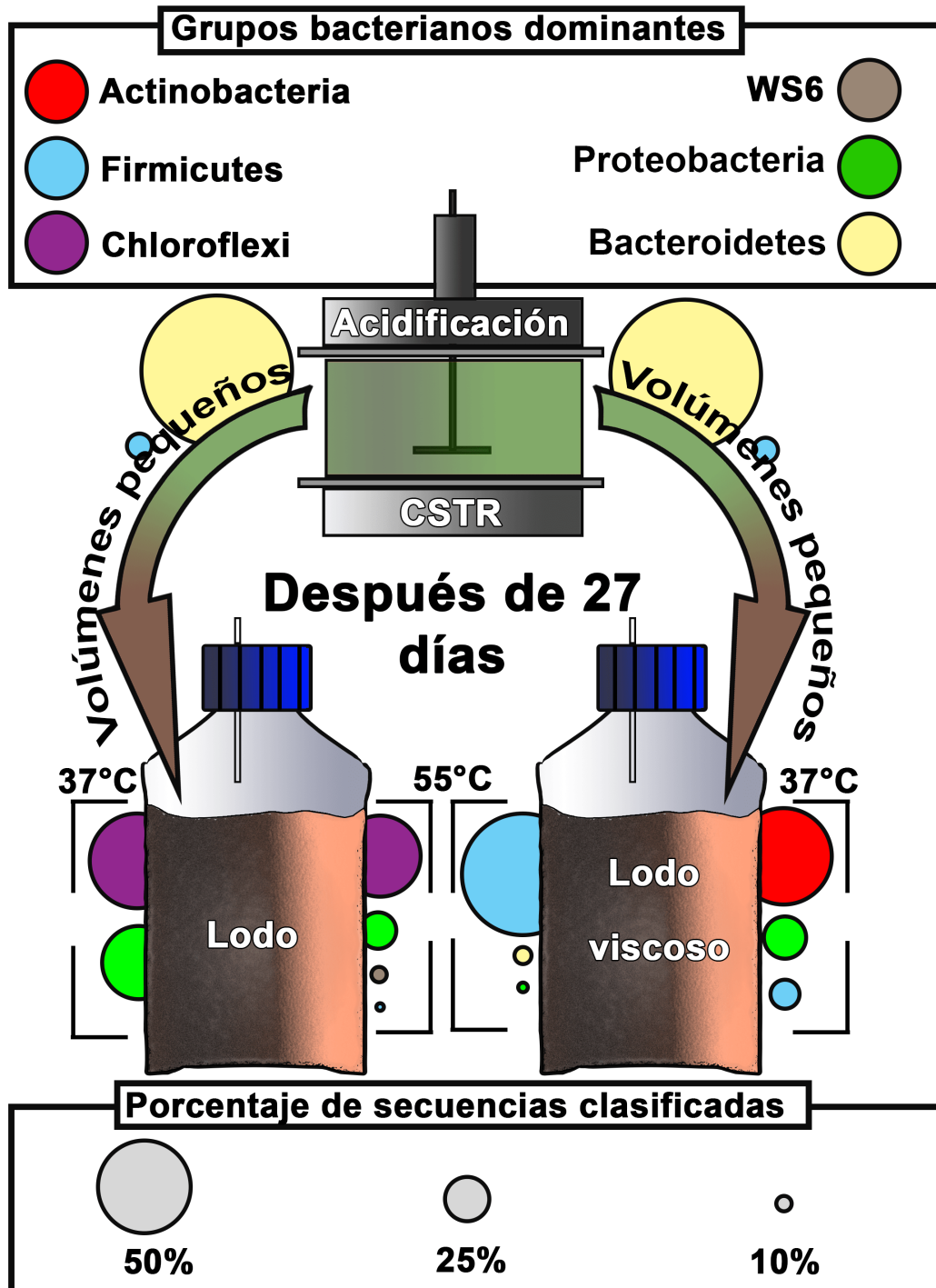


FIGURE 42: Estabilidad de los microbiomas de digestores productores de metano contra procesos de bioaumentación usando inóculos de fases de acidificación (según los perfiles taxonómicos del gen ARNr 16S mostrados en las figuras 9, 11 y 12; publicación 2). La inoculación de hidrolizado procedente de la fase de acidificación separada no causa ningún cambio visible en el microbioma del digestor anaeróbico, indicando una gran estabilidad microbiana. Se muestran los phyla dominantes con una abundancia mayor del 5 % de las secuencias clasificadas.

La resistencia frente a la microbiota del material biológico de entrada es una información de gran utilidad, ya que implica una reducción de la posibilidad de que los microbiomas metanogénicos puedan verse afectados negativamente por la microbiota de cualquier sustrato de interés. Sin embargo, esto resalta las dificultades asociadas a las aproximaciones de bioaumentación. Por tanto, la manipulación exitosa de microbiomas anaerobios en el futuro cercano requerirá nuevas estrategias de inoculación.

Un posible forma de superar esta excesiva robustez podría ser a través de la inoculación de cepas pertenecientes a algún phylum que ya sea dominante en ese ambiente concreto y en esas condiciones determinadas. Por ejemplo, en la publicación 5 se describe que valores bajos de pH aparentemente favorecen el crecimiento de Proteobacteria. Se podría realizar un proceso de bioaumentación, por tanto, combinando un valor bajo de pH en la fase de acidificación con la inoculación de cepas prometedoras de phylum Proteobacteria.

Robustez de microbiomas acidificantes: Se conoce que, en la fase de metanogénesis, el microbioma en condiciones mesofílicas es diferente a aquel presente en condiciones termofílicas [69, 70, 71]. De hecho, hay varios artículos en el que se describen arqueas metanógenas especializadas a temperaturas termofílicas [72, 73, 74]. También se ha demostrado que los miembros del pylum Firmicutes crecen particularmente bien en condiciones termofílicas, mientras que en condiciones mesofílicas también hay una gran abundancia de Bacteroidetes [75]. Sin embargo, los estudios mencionados se restringen a procesos digestivos de una sola fase; esta tesis, en cambio, pretende analizar las diferencias entre los microbiomas mesofílicos y termofílicos de fases separadas de

acidificación. Para ello, se acidificó biomasa herbácea paralelamente en condiciones mesofílicas y termofílicas, y se realizó una comparación mediante secuenciación del ARNr 16S y mediante análisis proteómico. Tal y como se describió para las fases de metanogénesis en cofermentadores, el microbioma acidificante era rico sobretodo en Firmicutes y Bacteroidetes. Bajo condiciones termofílicas se encontraron muchas proteínas de choque térmico, el comportamiento del proteoma era menos dinámico en comparación con las condiciones mesofílicas, y se detectaron Cyanobacterias, que puede ser debido a la presencia de cloroplastos a causa de una degradación incompleta de la biomasa vegetal. Sin embargo, se ha descrito en otras publicaciones que se necesitan fases de adaptación largos en digestores termofílicos de una fase [76, 77], sugiriendo que los microbiomas acidificantes también podrían necesitar largas fases de adaptación. Adicionalmente, la aplicación de un inóculo procedente de otro digestor termofílico podría facilitar la adaptación.

Sin embargo, aunque los microbiomas acidificantes tuvieron dificultades a la hora de adaptarse a las condiciones termofílicas, en experimentos posteriores en los cuales se aplicaron choques térmicos de 55 y 70 °C de manera repetida se observaron niveles elevados de termoresistencia (Fig. 43). Tan solo las arqueas metanógenas demostraron ser altamente sensibles a los choques térmicos durante estos experimentos. Por tanto, la aplicación de choques térmicos puede ser un método eficaz para separar los microbiomas acidificantes de los microbiomas metanógenos. Tal y como se ha mencionado antes, las fases de acidificación con elevadas concentraciones de amoníaco tienden a producir bajas cantidades de metano por contaminaciones metanógenas. Por

tanto, la aplicación de choques térmicos puede ayudar a prevenir pérdidas de DQO debido a contaminaciones metanógenas. En este contexto, es muy interesante destacar que se observó un desplazamiento en la comunidad bacteriana de Proteobacteria a Bacteroidetes/Firmicutes al producir un cambio en el pH de 6.0 a 6.8 (publicación 5). En caso de utilizar un inóculo y de aplicar tiempos de incubación largos, una caída repentina en el pH puede desestabilizar la

comunidad. Por tanto se recomienda mantener el pH a valores constantes, incluso durante la fase de acidificación. En conjunto, los resultados presentados demuestran que los microbiomas acidificantes son resistentes frente a contaminaciones microbianas / procesos de bioaumentación y frente a la aplicación de choques térmicos cortos, pero a la vez son sensibles a cambios duraderos en los parámetros ambientales.

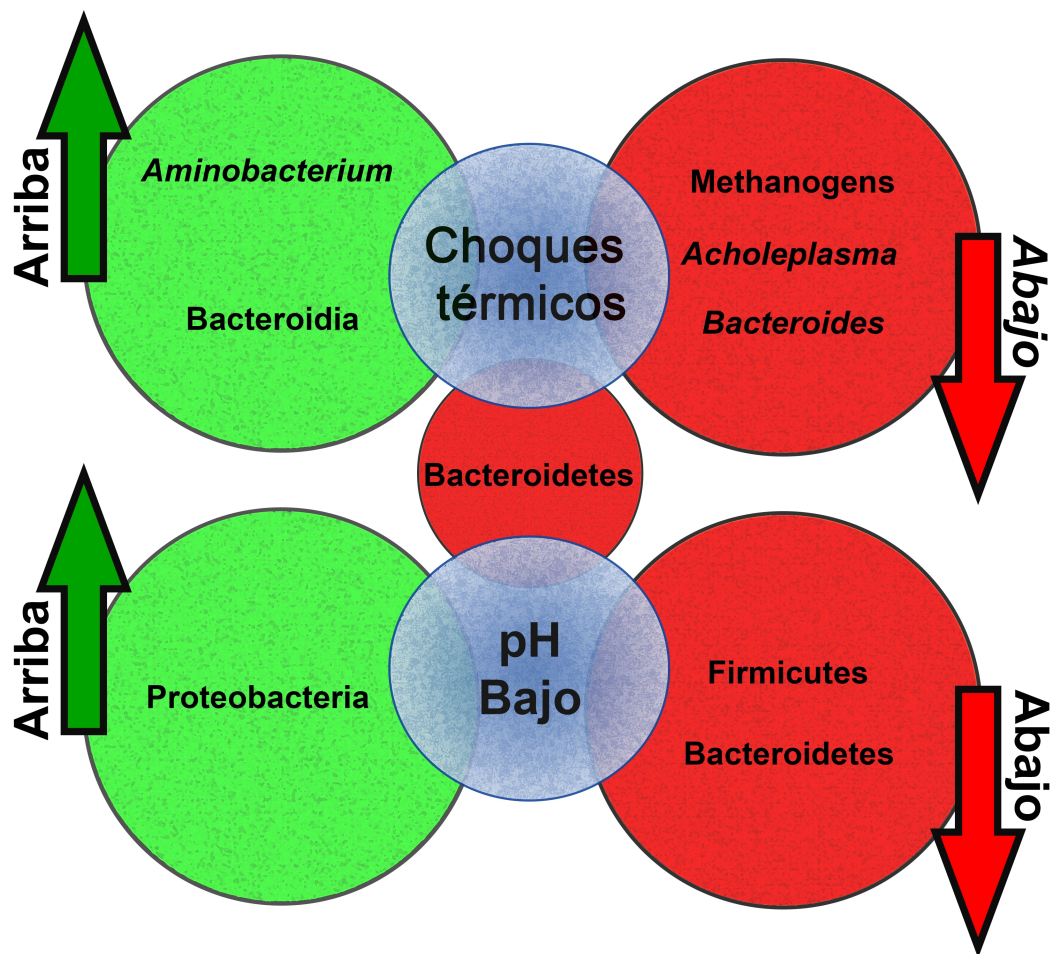


FIGURE 43: Robustez microbiana de hidrolizado ante choques térmicos suaves: el tratamiento con choques térmicos regulares de 55 o 70 °C apenas afectó a la composición microbiana a excepción de las arqueas metanogénicas, cuyo crecimiento fue inhibido con éxito. Se observaron cambios transitorios en algunos grupos microbianos que se indican en el esquema.

Además, en la figura 26 (publicación 2) se puede observar que, incluso en los reactores acidificantes sin choques térmicos y con valores constantes de pH, ocurren cambios en la comunidad microbiana. Sin embargo, es necesario seguir investigando para poder manipular de manera exitosa los microbiomas acidificantes con el fin de mejorar la interconectividad de la fase de acidificación con los diferentes campos de la industria. En el futuro, los mecanismos de interés en este contexto podrían ser mecanismos regulatorios para reducir la robustez de los microbiomas implicados antes de los procesos de bioaumentación, y mecanismos de estabilización que reduzcan los cambios microbianos después del proceso de bioaumentación. Además, se deberían desarrollar métodos que confieran una ventaja en términos de crecimiento a las cepas de interés inoculados frente a los otros microorganismos implicados. Una posibilidad de alcanzar este objetivo podría ser la co-inoculación de cepas microbianas que estabilicen a la cepa de interés inoculada.

Conclusiones

La digestión anaerobia está atrayendo la atención debido a su potencial para producir energía eléctrica, calor, fertilizantes, y a la vez muchos otros metabolitos con relevancia industrial. Debido a esta multifuncionalidad y a la gran variedad de posibles sustratos de entrada, la digestión anaerobia podría considerarse como una encrucijada para los procesos de biorrefinería y tratamiento de residuos. Sin embargo, es necesario realizar muchos más estudios para poder pavimentar esta encrucijada. Debido a la complejidad de los microbiomas de los digestores anaerobios, es extremadamente difícil manipular y

diseñar microbiomas anaerobios para realizar funciones específicas, como podría ser la producción de ácido butírico o hidrógeno. Para contribuir al conocimiento sobre esta área de investigación tan importante, esta tesis ha descrito la robustez y el dinamismo de las plantas de digestión anaerobia y ha remarcado la importancia de separar las fases de acidificación para el futuro desarrollo de la biorrefinería. Los resultados y las conclusiones principales se resumen a continuación:

- Se pueden definir tres microbiomas clave que son específicos para lodos residuales, lodos de alta viscosidad de codigestores y sistemas de lixiviado de lecho fijo. Los tres microbiomas están muy relacionados con sus parámetros ambientales (DQO, carbón orgánico total, contenido total en nitrógeno, conductividad, ácidos grasos volátiles totales, sólidos totales, sólidos volátiles, pH, y volumen de biogás).
- Los metanógenos *Methanosarcina*, *Methanoculleus*, *Methanometilovorans*, *Methanosaeta* y *Methanomicrobium* pueden ser potenciales marcadores para indicar las condiciones de digestión en cuanto a contenido de DQO/AGVs, cambios ambientales y presencia de sustancias tóxicas.
- El comportamiento dinámico de los phyla Cloroflexi, Actinobacteria, Firmicutes, Bacteroidetes, Proteobacteria, Spirochaeta y Cianobacteria (Cloroplastos) también podrían usarse como indicadores de las condiciones de digestión.
- Las fases de acidificación parecen estar dominadas por Bacteroidetes, Proteobacteria y Firmicutes, siendo estos últimos especialmente abundantes bajo condiciones termofílicas.

- La separación de la fase de acidificación permite el tratamiento de múltiples residuos que son difíciles de digerir en digestores de una fase, como es el caso de la biomasa herbácea o del estiércol de gallina.
- Se ha desarrollado la primera Célula Microbiana Termoeléctrica (CMT), que es compatible con la digestión anaerobia y adecuado para su uso en fases de pretratamiento. La CMT permite producir simultáneamente etanol y energía eléctrica, y los restos podrían usarse en una fase posterior de producción de metano.
- Para buscar nuevos métodos de pretratamiento se ha investigado la posibilidad de combinar pretratamientos térmicos con procesos de acidificación microbiana. Sorprendentemente, los choques térmicos demostraron tener un mínimo impacto en la composición microbiana. Por tanto, en un futuro se podrían combinar tratamientos con choque térmico con procesos de acidificación para mejorar el pretratamiento de biomasa.
- Se han identificado una serie de cepas con gran potencial para mejorar los procesos de biorrefinería. Se han aislado varias cepas de *Bacillus* de una sauna y de un lavaplatos, y estas cepas se caracterizan por tener una gran actividad lipolítica, lo que sugiere que los ambientes de interior también pueden ser fuentes importantes de microorganismos con aplicaciones industriales. Además, se ha aislado dos nuevas cepas a partir de la acidificación de biomasa herbácea, lo que indica que los ambientes anaerobios tienen la potencialidad

de proporcionar nuevas cepas con importantes papeles en la industria de la biorrefinería.

References

1. Chakraborty J, Das S. Molecular perspectives and recent advances in microbial remediation of persistent organic pollutants. *Environ Sci Pollut Res Int*. 2016;17:16883–16903.
2. Haghollahi A, Fazelipour MH, Schaffie M. The effect of soil type on the bioremediation of petroleum contaminated soils. *J Environ Manage*. 2016;180:197–201.
3. Jugder BE, Ertan H, Bohl S, Lee M, Marquis CP, Manefield M; 2016. Organohalide Respiring Bacteria and Reductive Dehalogenases: Key Tools in Organohalide Bioremediation. *Front Microbiol*. 2016;7:249. doi: 10.3389/fmicb.2016.00249.
4. Preiss L, Hicks DB, Suzuki S, Meier T, Krulwich TA. Alkaliphilic Bacteria with Impact on Industrial Applications, Concepts of Early Life Forms, and Bioenergetics of ATP Synthesis. *Front Bioeng Biotechnol*. 2015;3:75. doi: 10.3389/fbioe.2015.00075.
5. Leis B, Angelov A, Mientus M, Li H, Pham VT, Lauinger B, Bongen P, Pietruszka J, Gonçalves LG, Santos H, Liebl W. (2015). Identification of novel esterase-activity enzymes from hot environments by use of the host bacterium *Thermus thermophilus*. *Front Microbiol*. 2015 Apr 8;6:275. doi: 10.3389/fmicb.2015.00275.
6. Li M, Yang L, Xu G, Wu J. Screening, purification and characterization of a novel cold-active and organic solvent-tolerant lipase from *Stenotrophomonas maltophilia* CGMCC 4254. *Bioresour Technol*. 2013;148:114–120.
7. Tekedar HC, Sanli-Mohamed G. Molecular cloning, over expression and characterization of thermoalkalophilic esterases isolated from *Geobacillus* sp. *Extremophiles*. 2011;2:203–211.
8. Ferry JG. Methane from Acetate. *Jour. Bacteriol*. 1992;174:5489–5495.
9. Haarstrick A, Hempel DC, Ostermann L, Ahrens H, Dinkler D. Modelling of the biodegradation of organic matter in municipal landfills. *Waste Manag Res*. 2001;19:320–331.

10. Söhngen HL. Het Ontstaan en Verdwijnen van Waterstoff onder den invloed van het organische Leven. 1906; Dissertation, Delft.
11. Coolhas, C. Zur Kenntnis der Dissimilation Fettsaurer. *Centr. Bakt. II.* 1928;75:161–170.
12. Gagliano MC, Braguglia CM, Gallipoli A, Gianico A, Rossetti S. Microbial diversity in innovative mesophilic/thermophilic temperature-phased anaerobic digestion of sludge. *Environ Sci Pollut Res Int.* 2015;22:7339–7348.
13. Zhang YZ, Fang MX, Zhang WW, Li TT, Wu M, Zhu XF. *Salimesophilobacter vulgaris* gen. nov., sp. nov., an anaerobic bacterium isolated from paper-mill wastewater. *Int J Syst Evol Microbiol.* 2013;63:1317–1322.
14. Müller B, Sun L, Westerholm M, Schnürer A. Bacterial community composition and fhs profiles of low- and high-ammonia biogas digesters reveal novel syntrophic acetate-oxidising bacteria. *Biotechnol Biofuels.* 2016;9:48. doi: 10.1186/s13068-016-0454-9.
15. Hahnke S, Langer T, Koeck D, Klocke M. Description of *Proteiniphilum saccharofermentans* sp. nov., *Petrimonas mucosa* sp. nov. and *Fermentimonas caenicola* gen. nov., sp. nov. isolated from mesophilic lab-scale biogas reactors and emended description of the genus *Proteiniphilum*. *International Journal of Systematic and Evolutionary Microbiology.* 2016;66:1466–1475.
16. Maus I, Koeck DE, Cibis KG, Hahnke S, Kim YS, Langer T, Kreubel J, Erhard M, Bremges A, Off S, Stolze Y, Jaenicke S, Goesmann A, Sczyrba A, Scherer P, König H, Schwarz WH, Zverlov VV, Liebl W, Pühler A, Schlüter A, Klocke M. Unraveling the microbiome of a thermophilic biogas plant by metagenome and metatranscriptome analysis complemented by characterization of bacterial and archaeal isolates. *Biotechnol Biofuels.* 2016;9:171. doi: 10.1186/s13068-016-0581-3.
17. Goux X, Calusinska M, Lemaigre S, Marynowska M, Klocke M, Udelhoven T, Benizri E, Delfosse P. Microbial community dynamics in replicate anaerobic digesters exposed sequentially to increasing organic loading rate, acidosis, and process recovery. *Biotechnol Biofuels.* 2015;8:122. doi: 10.1186/s13068-015-0309-9.
18. Leubhn M, Hanreich A, Klocke M, Schlüter A, Bauer C, Pérez CM. Towards molecular biomarkers for biogas production from lignocellulose-rich substrates. *Anaerobe.* 2014;10–21.
19. Heeg K, Pohl M, Sontag M, Mumme J, Klocke M, Nettmann E. Microbial communities involved in biogas production from wheat straw as the sole substrate within a two-phase solid-state anaerobic digestion. *Syst Appl Microbiol.* 2014;37:590–600.
20. Poszytek K, Cieczkowska M, Skłodowska A, Drewniak L. Microbial Consortium with High Cellulolytic Activity (MCHCA) for Enhanced Biogas Production. *Front Microbiol.* 2016;7:324. doi: 10.3389/fmicb.2016.00324.
21. Sheets JP, Ge X, Li YF, Yu Z, Li Y. Biological conversion of biogas to methanol using methanotrophs isolated from solid-state anaerobic digestate. *Bioresour Technol.* 2016;201: 50–57.
22. Cheng X, Wang X, Qiu T, Yuan M, Sun J, Gao J. Molecular cloning and characterization of a novel cold-adapted family VIII esterase from a biogas slurry metagenomic library. *J Microbiol Biotechnol.* 2014;24:1484–1489.
23. Vijayaraghavan P, Arun A, Al-Dhabi NA, Vincent SG, Arasu MV, Choi KC. Novel *Bacillus subtilis* IND19 cell factory for the simultaneous production of carboxy methyl cellulase and protease using cow dung substrate in solid-substrate fermentation. *Biotechnol Biofuels.* 2016;9:73. doi: 10.1186/s13068-016-0481-6.
24. Morris JG. Obligately anaerobic bacteria in biotechnology. *Appl Biochem Biotechnol.* 1994;48:75–106.
25. Wallace RJ. Ruminant Microbiology, Biotechnology, and Ruminant Nutrition: Progress and Problems. *J Anim. Sci.* 1994;72:2992–3003.
26. Strong PJ, Kalyuzhnaya M, Silverman J, Clarke WP. A methanotroph-based biorefinery: Potential scenarios for generating multiple products from a single fermentation. *Bioresour Technol.* 2016;215:314–323.
27. Cheng J, Ye Q, Xu J, Yang Z, Zhou J, Cen K. Improving pollutants removal by microalgae *Chlorella* PY-ZU1 with 15% CO₂ from undiluted anaerobic digestion effluent of food wastes with ozonation pretreatment.

- Bioresour Technol.* 2016;216:273–279.
28. Sawatdeenarunat C, Nguyen D, Surendra KC, Shrestha S, Rajendran K, Oechsner H, Xie L, Khanal SK. Anaerobic biorefinery: Current status, challenges, and opportunities. *Bioresour Technol.* 2016;215:304–313.
29. Fabbri D, Torri C; 2016. Linking pyrolysis and anaerobic digestion (Py-AD) for the conversion of lignocellulosic biomass. *Curr Opin Biotechnol.* 2016;38:167–73.
30. Daelman MR, Sorokin D, Kruse O, van Loosdrecht MC, Strous M. Haloalkaline Bioconversions for Methane Production from Microalgae Grown on Sunlight. *Trends Biotechnol.* 2016;3:450–457.
31. Gottumukkala LD, Haigh K, Collard FX, van Rensburg E, Görgens J; 2016. Opportunities and prospects of biorefinery-based valorisation of pulp and paper sludge. *Bioresour Technol.* 2016;215:37–49.
32. Chen P, Xie Q, Addy M, Zhou W, Liu Y, Wang Y, Cheng Y, Li K, Ruan R. Utilization of municipal solid and liquid wastes for bioenergy and bioproducts production. *Bioresour Technol.* 2016;215:163–172.
33. Poirier S, Bize A, Bureau C, Bouchez T, Chapleur O. Community shifts within anaerobic digestion microbiota facing phenol inhibition: Towards early warning microbial indicators? *Water Res.* 2016;100:296–305.
34. Wawrik B, Marks CR, Davidova IA, McNerny MJ, Pruitt S, Duncan K, Suflita JM, Callaghan AV; 2016. Methanogenic paraffin degradation proceeds via alkane addition to fumerate by ?*Smithella?* spp. mediated by a syntrophic coupling with hydrogenotrophic methanogens, *Environ Microbiol.* doi: 10.1111/1462-2920.13374.
35. Baccay RA, Hashimoto AG. Acidogenic and methanogenic fermentation of causticized straw. *Biotechnol Bioeng.* 1984;8:885–891.
36. Dinopoulou G, Rudd T, Lester JN. Anaerobic acidogenesis of a complex wastewater: I. The influence of operational parameters on reactor performance. *Biotechnol Bioeng.* 1988;31, 958–968.
37. Gijzen HJ, Zwart KB, Verhagen FJ, Vogels GP. High-Rate two-phase process for the anaerobic degradation of cellulose, employing rumen microorganisms for an efficient acidogenesis. *Biotechnol Bioeng.* 1988;31:418–425.
38. Demeyer D, Henderickx H, Van Nevel C. Influence of pH on fatty acid inhibition of methane production by mixed rumen bacteria. *Arch Int Physiol Biochim.* 1967 75:555–556.
39. Zhou M, Yan B, Wong JWC, Zhang Y. Enhanced volatile fatty acids production from anaerobic fermentation of food waste: A mini-review focusing on acidogenic metabolic pathways. *Bioresour Technol.* 2017; doi: 10.1016/j.biortech.2017.06.121.
40. Koutinas A, Kanellaki M, Bekatorou A, Kandyli P, Pissaridi K, Dima A, Boura K, Lappa K, Tsafrakidou P, Stergiou PY, Foukis A, Gkini OA, Papamichael EM. Economic evaluation of technology for a new generation biofuel production using wastes. *Bioresour Technol.* 2016;200:178–185.
41. Dareioti MA, Kornaros M. Anaerobic mesophilic co-digestion of ensiled sorghum, cheese whey and liquid cow manure in a two-stage CSTR system: Effect of hydraulic retention time, *Bioresour Technol.* 2014;175:553–562.
42. Jo De Vrieze, Tom Hennebel, Nico Boon, Willy Verstraete. Methanosarcina: The rediscovered methanogen for heavy duty biomethanation. *Biores Technol.* 2012;112:1–9.
43. Liu Y. Taxonomy of Methanogens, in: Timmis KN, McGenity, TJ, van der Meer JR, de Lorenzo V (Eds.), *Handbook of Hydrocarbon and Lipid Microbiology, Springer*, 2010, Heidelberg, pp. 547–558.
44. Sundberg C, Al-Soud WA, Larsson M, Alm E, Yekta SS, Svensson BH, et al. 454 pyrosequencing analyses of bacterial and archaeal richness in 21 full-scale biogas digesters. *FEMS Microbiol Ecol.* 2013;85:612–26.
45. Bengelsdorf FR, Gabris C, Michel L, Zak, Kazda M. Syntrophic microbial communities on straw as biofilm carrier increase the methane yield of a biowaste-digesting biogas reactor. *AIMS Bioeng.* 2015;2:264–276.
46. Weiß S, Lebuhn M, Andrade D, Zankel A, Cardinale M, Birner-Gruenberger R, Somitsch W, Ueberbacher BJ, Guebitz GM. Activated zeolite-suitable carriers for microorganisms in anaerobic digestion processes?. *Appl Microbiol Biotechnol.*

- 2013;97: 3225–3238.
47. Zhou M, Yan B, Wong JWC, Zhang Y. Enhanced volatile fatty acids production from anaerobic fermentation of food waste: A mini-review focusing on acidogenic metabolic pathways. *Bioresour Technol.* 2017; doi: 10.1016/j.biortech.2017.06.121.
48. Gijzen HJ, Zwart KB, Verhagen FJ, Vogels GP. High-Rate two-phase process for the anaerobic degradation of cellulose, employing rumen microorganisms for an efficient acidogenesis. *Biotechnol Bioeng.* 1988;31:418–425.
49. Cheng J, Ye Q, Xu J, Yang Z, Zhou J, Cen K. Improving pollutants removal by microalgae *Chlorella* PY-ZU1 with 15 % CO₂ from undiluted anaerobic digestion effluent of food wastes with ozonation pretreatment. *Bioresour Technol.* 2016;216:273–279.
50. Gonzales-Fernandez, C., Sialve, B., Bernet, N., Steyer, J.P. Thermal pretreatment to improve methane production of *Scenedesmus* biomass. *Biomass Bioenergy.* 2016;40:1052111.
51. Pérez-Elvira S, Fdz-Polanco M, Plaza FI, Garralón G, Fdz-Polanco F. Ultrasound pre-treatment for anaerobic digestion improvement. *Water Sci Technol.* 2009;60:1525–32.
52. Samani S, Abdoli MA, Karbassi A, Amin MM. Stimulation of the hydrolytic stage for biogas production from cattle manure in an electrochemical bioreactor. *Water Sci Technol.* 2016;74:606–15.
53. Xu X, Gao X, Jin J, Vidonish J, Zhu L. A novel bioelectrode and anaerobic sludge coupled system for p-CINB degradation by magnetite nanoparticles addition. *Environ Sci Pollut Res.* 2017;24:16220–16227.
54. Ren L, Ahn, Y, Logan BE. A Two-Stage Microbial Fuel Cell and Anaerobic Fluidized Bed Membrane Bioreactor (MFC-AFMBR) System for Effective Domestic Wastewater Treatment. *Environ Sci Technol.* 2014; 48:4199–4206.
55. Wachendorf M, Richter F, Fricke T, Graß R, Neff R. Utilization of semi-natural grassland through integrated generation of solid fuel and biogas from biomass. I. Effects of hydrothermal conditioning and mechanical dehydration on mass flows of organic and mineral plant compounds, and nutrient balances. *Grass Forage Sci.* 2009;64:132–143.
56. Sheth RU, Cabral V, Chen SP, Wang HH. Manipulating Bacterial Communities by in situ Microbiome Engineering. *Trends Genet.* 2016;32:189–200.
57. Foo JL, Ling H, Lee YS, Chang MW. Microbiome engineering: Current applications and its future. *Biotechnol J.* 2017;12:1600099.
58. Kali A. Human Microbiome Engineering: The Future and Beyond. *J Clin Diagn Res.* 2015;9:01–04.
59. Duran M, Tepe N, Yurtsever D, Punzi VL, Bruno C, Mehta RJ. Bioaugmenting anaerobic digestion of biosolids with selected strains of *Bacillus*, *Pseudomonas*, and *Actinomyces* species for increased methanogenesis and odor control. *Appl Microbiol Biotechnol.* 2006;73:960–966.
60. Cirne DG, Björnsson L, Alves M, Mattiasson B. Effects of bioaugmentation by an anaerobic lipolytic bacterium on anaerobic digestion of lipid-rich waste. *J Chem Technol Biotechnol.* 2006;81:1745–1752.
61. Schauer-Gimenez AE, Zitomer DH, Maki JS, Struble CA. Bioaugmentation for improved recovery of anaerobic digesters after toxicant exposure. *Water Res.* 2010;44:3555–3564.
62. Tepe N, Yurtsever D, Mehta RJ, Bruno C, Punzi VL, Duran M. Odor control during post-digestion processing of biosolids through bioaugmentation of anaerobic digestion. *Water Sci Technol.* 2008;57:589–94.
63. Hahnke S, Striesow, J, Elvert, M., Mollar, X., Klocke, M., 2014. *Clostridium bornimense* sp. nov., isolated from a mesophilic, two-phase, laboratory-scale biogas reactor. *Int J Syst Evol Microbiol.* 64, 2792–2797.
64. Boltyanskaya Y, Detkova E, Pimenov N, Kevbrin V. *Proteinivorax hydrogeniformans* sp. nov., an anaerobic, haloalkaliphilic bacterium fermenting proteinaceous compounds with high hydrogen production. *Antonie Van Leeuwenhoek.* 2017; doi: 10.1007/s10482-017-0949-9.
65. Koeck DE, Mechelke M, Zverlov VV, Liebl W, Schwarz WH. *Herbivorax saccincola* gen. nov., sp. nov., a cellulolytic, anaerobic, thermophilic bacterium isolated via in sacco enrichments from a lab-scale biogas reactor. *Int J Syst Evol Microbiol.* 2016;66:4458–4463.
66. Kinet R, Destain J, Hilgsmann S,

- Thonart P, Delhalle L, Taminiau B, Daube G, Delvigne F. Thermophilic and cellulolytic consortium isolated from composting plants improves anaerobic digestion of cellulosic biomass: Toward a microbial resource management approach. *Bioresour Technol.* 2015;189:138–44.
67. De Vrieze J, Christiaens MER, Walraedt D, Devooght A, Ijaz UZ, Boon N. Microbial community redundancy in anaerobic digestion drives process recovery after salinity exposure. *Water Res.* 2017;111:109–117.
68. Ju F, Fang HHP, Zhang T. Application of Metagenomics, in: *Environmental Anaerobic Technology–Environmental protection and Resource Recovery*, Ju F, Fang HHP, Zhang T (Eds.), *Imperial College Press*, 2015, London pp. 73–108.
69. Zhu X, Kougias PG, Treu L, Campanaro S, Angelidaki I. Microbial community changes in methanogenic granules during the transition from mesophilic to thermophilic conditions. *Appl Microbiol Biotechnol.* 2017;101:1313–1322.
70. Sassi HP, Ikner LA, Abd-Elmaksoud S, Gerba CP, Pepper IL. Comparative survival of viruses during thermophilic and mesophilic anaerobic digestion. *Sci Total Environ.* 2017;615:15–19.
71. Stiborova H, Wolfram J, Demnerova K, Macek T, Uhlik O. Bacterial community structure in treated sewage sludge with mesophilic and thermophilic anaerobic digestion. *Folia Microbiol (Praha).* 2015;60:531–539.
72. Zinder SH, Cardwell SC, Anguish T, Lee M, Koch M. Methanogenesis in a Thermophilic (58°C) Anaerobic Digester: Methanotrix sp. as an Important Aceticlastic Methanogen. *Appl Environ Microbiol.* 1984;47:796–807.
73. Ferguson TJ, Mah RA. Isolation and Characterization of an H₂-Oxidizing Thermophilic Methanogen. *Appl Environ Microbiol.* 1983;45:265–274.
74. Jones WJ, Leigh JA, Mayer F, Woese CR, Wolfe RS. *Methanococcus jannaschii* sp. nov., an extremely thermophilic methanogen from a submarine hydrothermal vent. *Arch Microbiol.* 1983;136:254–261.
75. Moset V, Poulsen M, Wahid R, Højberg O, Møller HB. Mesophilic versus thermophilic anaerobic digestion of cattle manure: methane productivity and microbial ecology. *Microb Biotechnol.* 2015;8:787–800.
76. Kima K, Ahnb YH, Speecea RE. Comparative process stability and efficiency of anaerobic digestion; mesophilic vs. thermophilic. *Water Research-* 2002;36:4369–4385.
77. Bousková A, Dohányos M, Schmidt JE, Angelidaki I. Strategies for changing temperature from mesophilic to thermophilic conditions in anaerobic CSTR reactors treating sewage sludge. *Water Res.* 2005;39:1481–1488.

Appendix A

Original publication reprints



RESEARCH ARTICLE

Open Access



Eubacteria and archaea communities in seven mesophile anaerobic digester plants in Germany

Christian Abendroth^{1,2}, Cristina Vilanova¹, Thomas Günther³, Olaf Luschnig^{2,4} and Manuel Porcar^{1,5*}

Abstract

Background: Only a fraction of the microbial species used for anaerobic digestion in biogas production plants are methanogenic archaea. We have analyzed the taxonomic profiles of eubacteria and archaea, a set of chemical key parameters, and biogas production in samples from nine production plants in seven facilities in Thuringia, Germany, including co-digesters, leach-bed, and sewage sludge treatment plants. Reactors were sampled twice, at a 1-week interval, and three biological replicates were taken in each case.

Results: A complex taxonomic composition was found for both eubacteria and archaea, both of which strongly correlated with digester type. Plant-degrading *Firmicutes* as well as *Bacteroidetes* dominated eubacteria profiles in high biogas-producing co-digesters; whereas *Bacteroidetes* and *Spirochaetes* were the major phyla in leach-bed and sewage sludge digesters. *Methanoculleus* was the dominant archaea genus in co-digesters, whereas *Methanosarcina* and *Methanosaeta* were the most abundant methanogens in leachate from leach-bed and sewage sludge digesters, respectively.

Conclusions: This is one of the most comprehensive characterizations of the microbial communities of biogas-producing facilities. Bacterial profiles exhibited very low variation within replicates, including those of semi-solid samples; and, in general, low variation in time. However, facility type correlated closely with the bacterial profile: each of the three reactor types exhibited a characteristic eubacteria and archaea profile. Digesters operated with solid feedstock, and high biogas production correlated with abundance of plant degraders (*Firmicutes*) and biofilm-forming methanogens (*Methanoculleus* spp.). By contrast, low biogas-producing sewage sludge treatment digesters correlated with high titers of volatile fatty acid-adapted *Methanosaeta* spp.

Keywords: Biogas, Eubacteria, Archaea, Methanogens, Anaerobic digesters

Background

Knowledge of the effects of greenhouse gases on the climate dates back to the 1970s, with CO₂ representing a key greenhouse gas [1]. Today, there is general assent on the urgent need to reduce greenhouse gases in order to mitigate climate change [2, 3]. One of the main strategies to meet this goal requires shifting from fossil to renewable energy sources. In fact, it is expected that by 2020, 20 % of total energy consumption in Europe will be covered by renewable energies [4].

Biomass is a very promising alternative energy source, in particular as a source of biogas. Indeed, almost 70 % of all renewable energies in Europe came from biomass management in 2010 [5], with Germany being a leader in the biomass-based bioeconomy. During recent years, as supported by the EEG (German law for renewable energies) [6], the number of biogas plants and biogas production has increased dramatically in Germany. For example, in 2012, 7200 biogas plants in Germany provided enough energy to power 5.3 million households [7]. Despite this success, the underlying microbial biocenoses of biogas-producing facilities are not yet fully understood, and the whole methanogenesis process is often referred to as a “black box” even in some of the recent literature [7–9]. In the last decades, substantial

* Correspondence: manuel.porcar@uv.es

¹Cavanilles Institute of Biodiversity and Evolutionary Biology, Universitat de València, 46020 Valencia, Spain

⁵Fundació General de la Universitat de València, València, Spain
Full list of author information is available at the end of the article

efforts have been undertaken to shed light on the microbial communities involved in the anaerobic digestion process, as deduced by 16S-rDNA sequencing [10–13], *mcrA* gene-based analysis [14, 15], or metagenomic approaches [16, 17].

Different microbial profiles have been reported for biogas production plants fed with different types of biomass. For example, the microbial diversity in a completely stirred digester fed with fodder beet silage as a monosubstrate is reported to be particularly rich in *Clostridiales*, *Deltaproteobacteria*, *Bacilli*, and *Bacteroidetes* [18]. Other studies describe the effect of biowaste sludge maturation on the microbial profile within a thermophilic digester, which contained mainly *Clostridia* [19]; while the microbial communities in lab-scale reactors fed with casein, starch, and cream are particularly abundant in *Firmicutes* and *Bacteroidetes* [20]. Given these reports, we could say that microbial profiles of anaerobic digesters are, to some extent, specific for each biogas reactor/biomass type. This raises the question whether a common core of microbial key players does exist for anaerobic digesters in general. It is indeed possible to find common microbial actors when higher taxonomic levels are compared. For instance, it is known how methanogenic archaea (genus *Methanosaeta*) dominates environments with low acetate, while increasing amounts of inhibiting substances (like volatile fatty acids or hydrogen sulfide) foster *Methanosarcina* spp. growth [21]. Under thermophilic conditions, *Methanosarcina* spp. proves more frequent than *Methanosaeta* spp. Regarding eubacteria, the phyla *Firmicutes* and *Bacteroidetes* play an important role in anaerobic digestion [13, 22] and within *Firmicutes*, the class *Clostridia* is the most abundant group [18, 23]. Regarding bacteria, and similarly to methanogens stressed above, eubacterial profiles of anaerobic co-digesters and from the anaerobic stage of sewage plants are typically different [13].

In the present work, we have performed a holistic analysis of seven different digesters at two distinct time points (2 × 9 reactors, sampled within 1 week) from Thuringia, Germany (Fig. 1; Table 1). The digesters corresponded to three different configurations: completely mixed and continuously stirred single-stage tank reactors for sewage sludge digestion (SS); leach-bed digesters operating discontinuously in batches (LB); and a two-stage system consisting of a vertical plug flow reactor followed by an upright continuously stirred tank digester and a final digestate storage tank (hereafter referred to as CD, standing for co-digester). With the exception of the digestate storage tank, which was operated at room temperature (RT), all facilities were operated at mesophilic temperature. The analysis included chemical characterization and biogas measurement of the samples and the determination of the archaea and eubacteria taxonomic profiles by 16S amplicons sequencing on three

replicates of each reactor/time. Our results reveal that microbial profiles were strongly dependent on reactor type and moderately dependent on the facility/particular reactor sampled. We also found that profiles were stable in time and exhibited a low degree of variation within the three replicates analyzed. Globally, the 54 subsamples sequenced are the most comprehensive microbial characterization of biogas communities performed to date.

Results and discussion

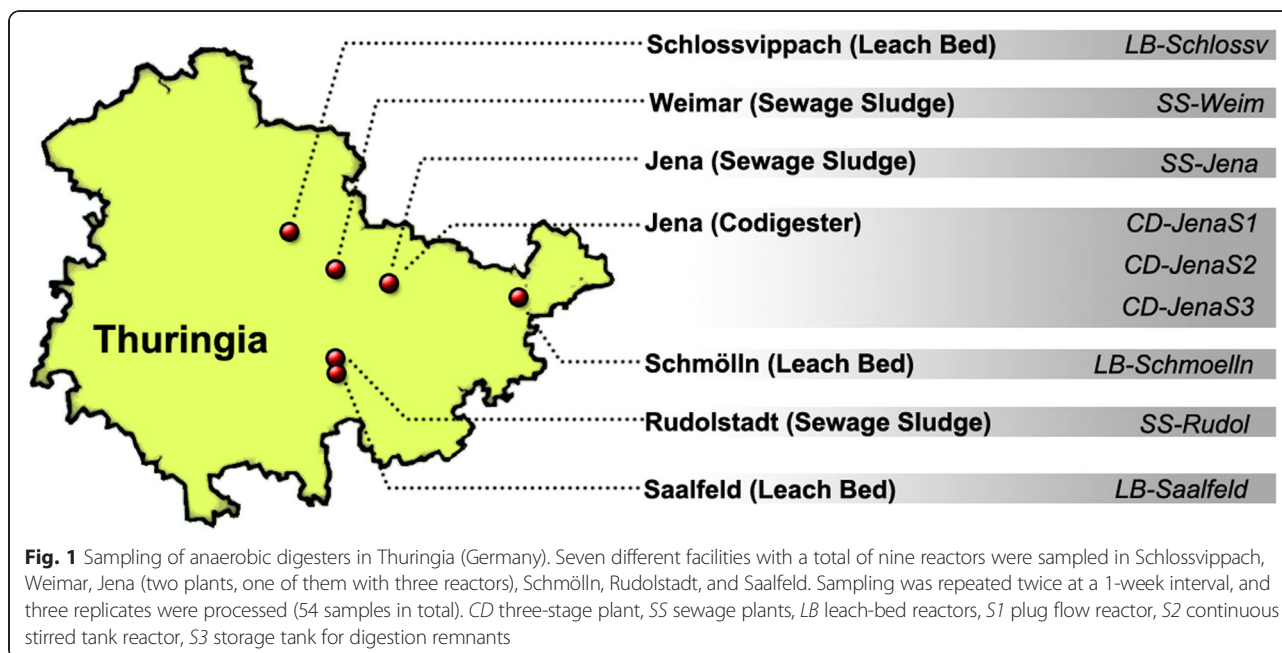
Chemical parameters

Eleven parameters were measured for each of the reactor samples: COD (chemical oxygen demand), TOC (total organic carbon), total nitrogen content (N), electrical conductivity, TVFA (total volatile fatty acids), TS (total solids), VS (volatile solids), pH, biogas yield, and concentrations of CH₄ and CO₂ (Additional file 1: Table S1). Biogas yields were obtained from lab-scale batch experiments, whereas all the other parameters originated from in situ measurements of digester samples. Batch experiments were performed without adding substrates and obtained biogas yields depended only on the organic fraction within the sludge samples.

After normalizing the data, successive combinations of three parameters (permutation) were plotted in a Gnuplot multiplot (Fig. 2). The resulting data matrix included biogas production but not methane and CO₂ concentration, in order to avoid redundancies. This resulted in three clearly defined clouds, each corresponding to one of the different digester facility types (Fig. 2a). SS and CD values were plotted in two opposed vertices of the plot, with LB located in an intermediate position. The yield of biogas produced is shown in Fig. 2b and the highest yields are plotted as a relatively small cloud (black dots) overlapping with the extremes of the CD cloud. As a general conclusion, parameter values were higher (corresponding in general with high nutrient contents) when biogas production was highest. In a second statistical approach, this observation was verified by a principal component analysis (Additional file 2: Figure S1), where samples coming from the same type or reactor clustered together and notably differed from those from other reactor types.

Taxonomic composition of eubacteria

Eubacteria from all samples were identified by high-throughput sequencing as described in “Material and methods” section, and phylum-level results are shown in Fig. 3. There was little variation between replicates, clearly indicating that differences in taxonomic composition accounted for the differences found between reactors and time. Similarly, different sampling times resulted in very small variations in the taxonomic profile, being the taxonomic composition of each sample very constant after 1 week. Only in one case (LB reactor



in Saalfeld) that a substantial shift was detected in the amount of *Bacteroidetes* and *Spirochaetes* after 1 week.

The taxonomic composition of the samples correlated closely with reactor type. Indeed, three different profiles were observed, each corresponding to a particular facility type. CD samples were dominated by the phylum *Firmicutes*, with nearly 46–60 % of classified sequences assigned to *Firmicutes* in the first two stages and less than 20–32 % in the third stage (remnant storage); followed by *Bacteroidetes*, which proved mainly in the third stage, when it accounted for up to 73 % of the total identified taxa. The three CD digesters contained low amounts of *Synergistetes*, and the remnant storage contained moderated amounts of *Actinobacteria*, *Proteobacteria*, *Spirochaetes*, and *Tenericutes* (Fig. 3a).

The second facility type (LB) displayed a totally different microbial composition (Fig. 3b) with comparatively fewer *Firmicutes* reads (between 3 and 19 % of total sequences). The microbial LB communities were dominated by *Spirochaetes* (30 and 72 % of the total reads), along with *Bacteroidetes* (11 and 47 %). The third phylum, *Thermotogae*, reached low to moderate frequencies in LB facilities in Schmölln and Saalfeld (between 2 and 19 %), and it was absent in the six replicates of Schlossvippach. Minor counts of *Actinobacteria* and *Proteobacteria* were also detected. The third profile was associated with the sewage sludge digesters (Fig. 3c). Although the SS facilities showed certain similarities compared to the LB facilities, the overall microbial composition differed from both CD and LB reactors. In common with the LB samples, SS reactors contained high amounts of *Bacteroidetes* and *Spirochaetes* (*Bacteroidetes* between 13 and 51 %, *Spirochaetes*

between 27 and 50 %). However, unlike the CD and LB facilities, SS reactors were particularly rich in *Chloroflexi* (9 and 39 %) and *Proteobacteria* (4–9 %). Besides the aforementioned taxa, small amounts of *Actinobacteria*, *Synergistetes*, and *Thermotogae* were also observed.

Minor variations or sub-profiles of the three main biomass-associated profiles were detected. For example, two of the three Jena CD reactors were very similar, while the third one displayed higher eubacteria diversity. This might be due to the fact that the last stage (remnants) was kept at RT instead of mesophile temperatures. Although LB and SS samples corresponded to two main profiles, one location of each type (LB-Schlossvippach and SS-Rudolstadt) exhibited a characteristic presence/absence of one particular taxon: the former typically lacked *Thermotogae*, which was well represented in the other two LB plants; while SS Rudolstadt was particularly rich in *Chloroflexi* (Fig. 3b, c). The absence of *Thermotogae* in the LB reactor from Schlossvippach may be due to the fact that the solid phase is mainly heated up by the leachate (without extra heating in the solids storage—“garage”), which can lead to irregularities in temperature. In the Schlossvippach sample, it took more than 1 week to heat up a newly filled garage (Christoph Bürger and Kevin Lindner personal communication).

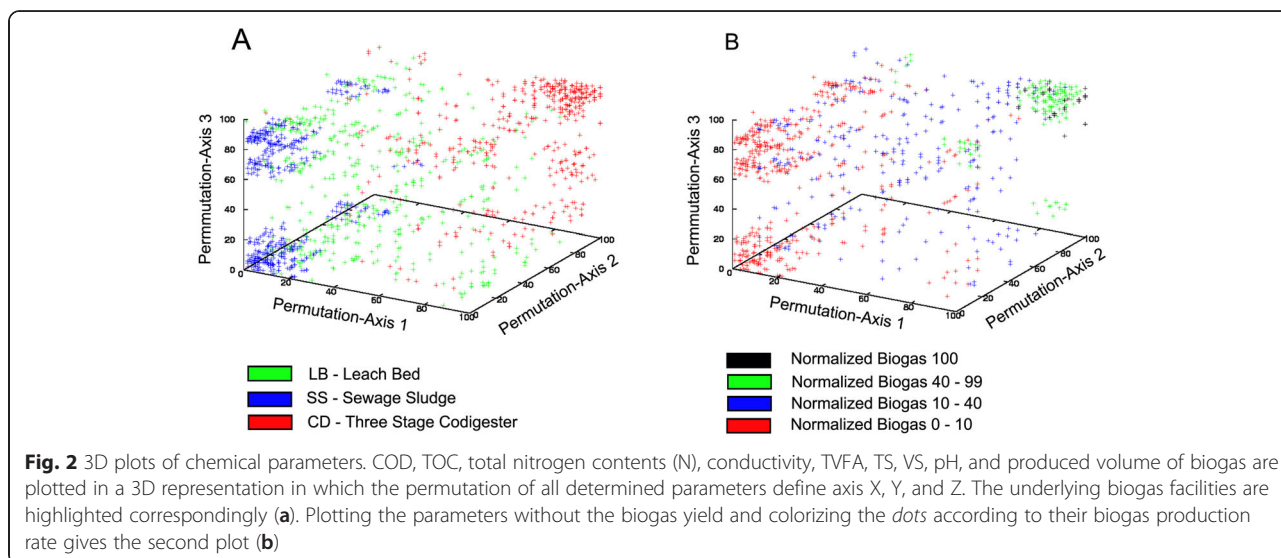
In general, taxonomic eubacteria profiles strongly correlated with the biomass type. The differences observed between CD and SS reactors are in accordance with previous studies [13] describing an overall difference between sewage sludge and co-fermentation regarding the microbial profile. The high amount of *Bacteroidetes* and *Firmicutes* in CD reactors is also consistent with

Table 1 Overview of sampled digester types and input feeding based on descriptive data

Sample	Digester type	Input materials	Plant configuration
LB-Schmölln	Leach-bed batch digester	Silage, straw, cow manure	Batch process (11 batches) Digester volume: $11 \times 800 \text{ m}^3$ Leachate tank: 1000 m^3 Batch process duration: 26–29 days Gas production: $0.7 \text{ m}^3/\text{m}^3 \times \text{day}$ OLR: $1.3 \text{ kg} \times \text{VS}/\text{m}^3 \times \text{day}$
CD-Jena	Two-stage digester (vertical plug flow reactor/stirred tank)	Silage, farm manure, Livestock farming waste	Two-stage process Stage 1 (plug flow): 790 m^3 Stage 2 (CSTR): 2000 m^3 Stage 3 (final storage tank): 3800 m^3 HRT: 87 days Gas production: $1.2 \text{ m}^3/\text{m}^3 \times \text{day}$ OLR: $3.0 \text{ kg} \times \text{VS}/\text{m}^3 \times \text{day}$
SS-Jena	Completely mixed tank digester	Mono-digestion of municipal sewage sludge	Single stage process (2 digesters) Digester volume: $2 \times 2000 \text{ m}^3$ HRT: 21 days Gas production: $0.6 \text{ m}^3/\text{m}^3 \times \text{day}$ OLR: $1.8 \text{ kg} \times \text{VS}/\text{m}^3 \times \text{day}$
SS-Weimar	Completely mixed tank digester	Mono-digestion of municipal sewage sludge	Single stage process Digester volume: 3200 m^3 HRT: 29 days Gas production: $0.6 \text{ m}^3/\text{m}^3 \times \text{day}$ OLR: $0.96 \text{ kg} \times \text{VS}/\text{m}^3 \times \text{day}$
LB-Schlossvippach	Leach-bed batch digester	Cow manure, straw, <i>feed residues</i>	Batch process (8 batches) Leachate tank: 1000 m^3 Digester volume: $8 \times 330 \text{ m}^3$ Batch process duration: 32–35 days Gas production: $0.5 \text{ m}^3/\text{m}^3 \times \text{day}$ OLR: $2.1 \text{ kg} \times \text{VS}/\text{m}^3 \times \text{day}$
SS-Rudolstadt	Completely mixed tank digester	Co-digestion of municipal and industrial sewage sludge with <i>seasonally available</i> co-substrates (biodiesel waste)	Single-stage process (2 digesters) Digester volume: $2 \times 2000 \text{ m}^3$ HRT: 25 days Gas production: $0.3 \text{ m}^3/\text{m}^3 \times \text{day}$ OLR: $0.54 \text{ kg} \times \text{VS}/\text{m}^3 \times \text{days}$
LB-Saalfeld	Leach-bed batch digester	Organic fraction of municipal solid waste	Batch process (9 batches) Digester volume: $9 \times 826 \text{ m}^3$ Leachate tank: 1060 m^3 Batch process duration: 33 days Gas production: $0.7 \text{ m}^3/\text{m}^3 \times \text{day}$ OLR: $0.9 \text{ kg} \times \text{VS}/\text{m}^3 \times \text{day}$

Gas production is given in cubic meter of produced gas per cubic meter of sludge per day

HRT hydraulic retention time, CSTR continuous stirred-tank reactor, OLR organic loading rate

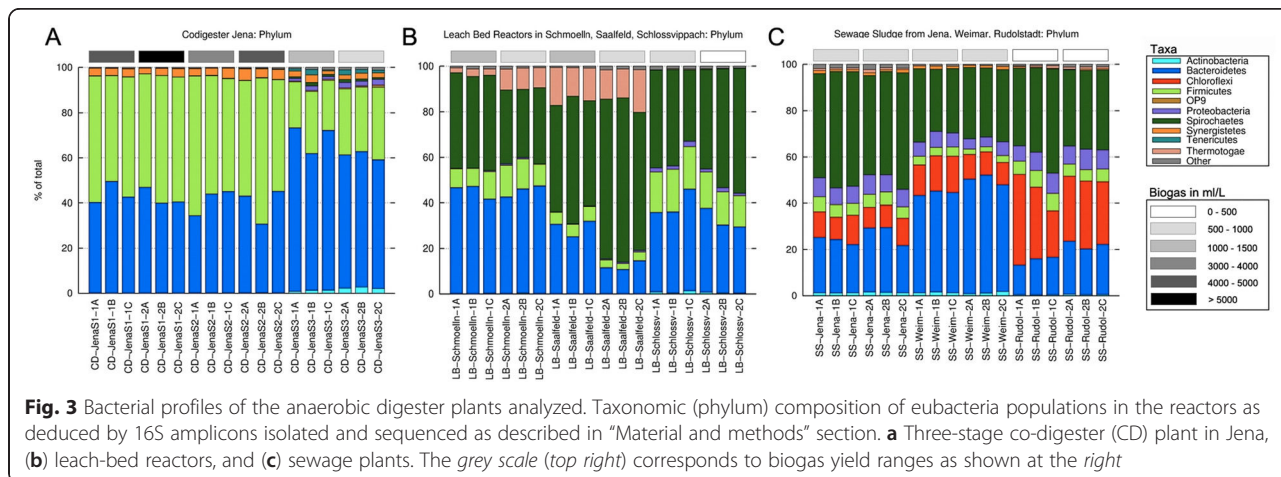


previous reports [13, 18, 22, 24]. One reason for the abundance of *Firmicutes* could be the high content in TS derived from plant material (Additional file 1: Table S1), which probably fosters biofilm formation. *Firmicutes* have been described as main degraders of cellulosytic material [24] and are abundant in biofilms of water supply systems [25, 26]. LB and SS reactors, both containing liquid substrates, had high titers of the very mobile and efficient swimmer *Spirochaete*, described as able to swim in high viscous gel-like liquids, such as those found in LB reactors [27]. It has to be highlighted that the observed microbial profiles for the LB samples were only those from leachate, and that the solid fraction of LB systems might be rich in *Firmicutes* due to the high percentage of solids. The abundance of *Chloroflexi* in SS reactors has previously been reported. In fact, different *Chloroflexi* species have been found in more than 60 sewage reactors in

different European countries based on FISH experiments [28] and also in other facilities around the world [29]. The prevalence of *Proteobacteria* and *Bacteroidetes* is in accordance with the work by Wang et al. [30] on the microbial profile of domestic sewage outfalls.

The different taxonomic profiles we found correlated to biogas yield. For instance, the phylum *Chloroflexi* was detected in sewage plants, where very low biogas yields were measured. Also, *Proteobacteria* were only found in the plants with low biogas yields (digestate storage of the three-stage plant, Schlossvippach, and all sewage samples), while *Firmicutes* were particularly abundant in reactors with high biogas yields (CD samples). However, differences in biogas yield might also be a consequence of the concentration of TS, which is especially high in CD reactors.

In summary, our results are strongly consistent with previous reports demonstrating patchiness of the



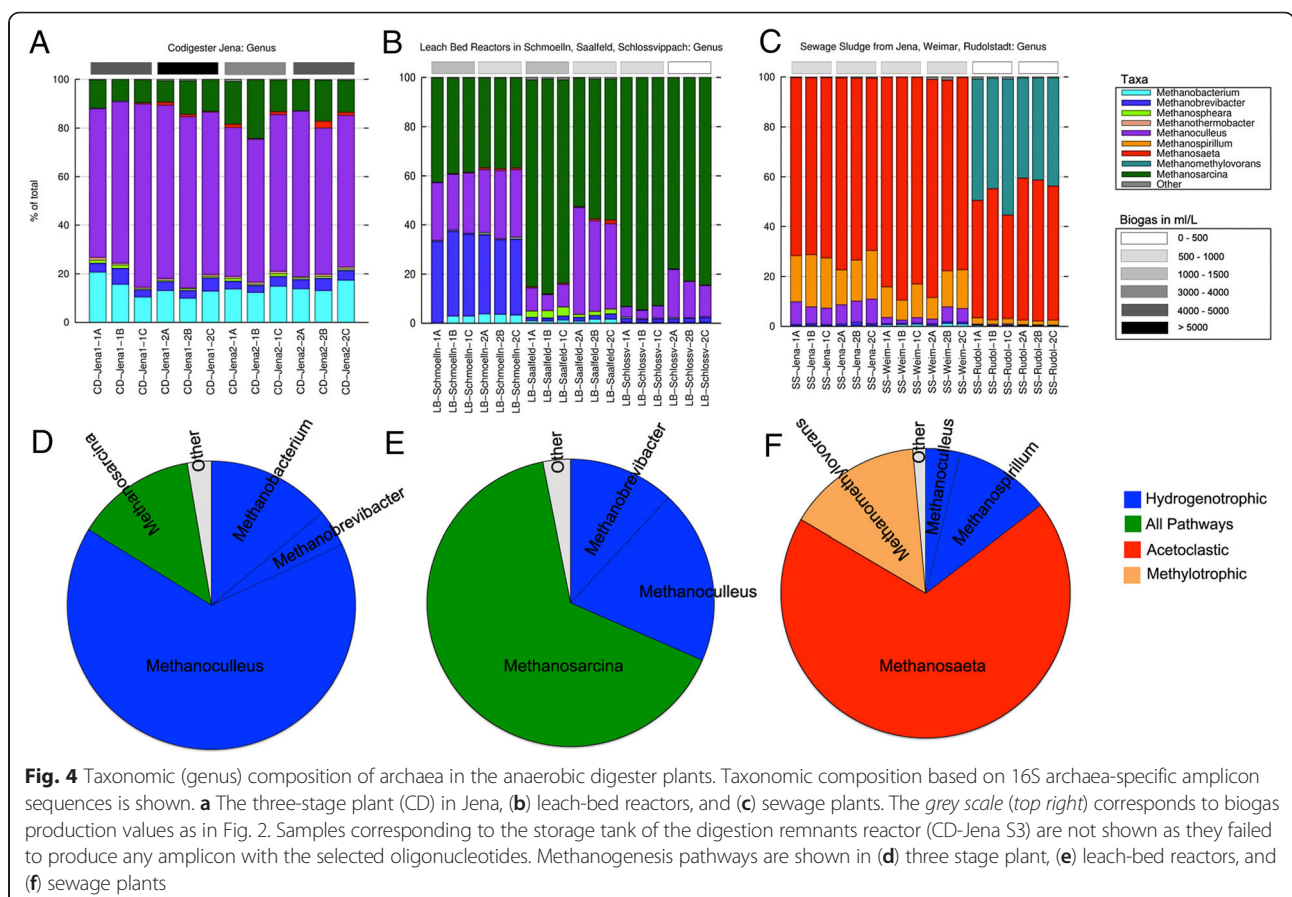
digesters in terms of the distribution of bacterial populations [31]. This strongly suggests ecological parameters (i.e. liquid/solid substrate or biomass type) are the key factors shaping microbial communities; but also reveal an important, albeit secondary, role of the facility/reactor on this mainly biomass-associated distribution of the taxonomic profiles.

Taxonomic composition of archaea

The taxonomic composition of the sampled reactors in terms of archaea contents is shown in Fig. 4. The data correspond to all but one reactor (three replicates and two time points), corresponding to the third stage of the Jena CD reactor, from which no archaeal DNA could be amplified. CD reactors were dominated by archaea belonging to the genus *Methanoculleus* (Fig. 4a), accounting for 59–76 % of all the sequences. A significant amount of *Methanosarcina* (9–24 %), *Methanobacterium* (10–21 %), and *Methanobrevibacter* (3–7 %) was detected, as well as infrequent genera such as *Methanosphaera*, *Methanothermobacter*, and *Methanosaeta*. In contrast, LB digesters were characterized by substantially smaller amounts of *Methanoculleus* (3–44 %); and by the abundance of *Methanosarcina* (37–95 %). One of

the three LB-digesters showed a very high amount of *Methanobrevibacter* (31–35 %), whereas the other two reactors had very low amounts (1–2 %). Minor genera were *Methanobacterium*, *Methanosphaera*, and *Methanosaeta*. In the SS samples, *Methanosaeta* proved the most prevalent genus with a total number of reads between 42 and 88 % (Fig. 4c). While *Methanosaeta* was detected in high amounts in all the SS reactors, the frequency of other genera differed among SS digesters. The biogas plant in Rudolstadt was very rich in *Methanomethylovorans* (40–55 %), while the other two SS reactors showed a relatively high amount of *Methanoculleus* (1–10 %) and *Methanospirillum* (8–21 %).

As in the eubacteria profiles, three main taxonomic combinations were found to correlate with the three reactor types. The CD samples showed a strikingly similar profile independently on the replicate, reactor, or time sampled. LB and SS reactors did exhibit sub-profiles with no variation within replicates and dependent on the sampling time (Schlossvippach and Saalfeld) or on the location sampled (Rudolstadt). The two LB facilities from Schlossvippach and Saalfeld showed an increased amount of *Methanoculleus* after 1 week, while the amount of *Methanosarcina* decreased during this period.



It is likely that genus *Methanoculleus* is more abundant in the solid fraction of these LB systems due to the high percentage of solids. Rudolstadt samples had the typical *Methanosaeta* abundance of SS reactors but were characterized by an exceptionally high frequency of *Methanomethylovorans*. The presence of *Methanosarcina* and *Methanoculleus* correlated to high yields of biogas, while low biogas yields correlated with higher amounts of *Methanosaeta*.

Since methane production is solely due to the archaeal community and the different methanogenesis pathways are well known and genus-linked, we studied the expected methanogenesis pathways in each facility type according to the average taxonomic distribution (Fig. 4d–f). Interestingly, each facility type displayed a different combination of methanogenesis pathways. The CD reactors were very rich in archaea using the hydrogenotrophic pathway (Fig. 4d); LB reactors were dominated by *Methanosarcina* and thus with the ability to use all known pathways for methane production (Fig. 4e); and SS reactors were characterized by containing high rates of archaea using the acetoclastic pathway for methane production (Fig. 4f).

The archaea composition we describe here for the different reactor types is generally in accordance with that reported in previous studies. The prevalence of *Methanoculleus* in CD reactors was also found in other works with classical anaerobic digesters [22, 32, 33]. Although other studies describe a prevalence of *Methanosarcina* in this reactor type [34], our data is in concordance with other works linking *Methanosarcina* to LB reactors [35, 36]. The differences in TS levels between CD and LB reactors might be the key factor explaining their differences in microbial composition. The TS content of LB reactors was much lower (Additional file 1: Table S1), so the surface available for the growth of biofilm-forming species, such as *Methanoculleus* [37], was limited compared to CD reactors. Indeed, previous reports have found a prevalence of *Methanoculleus* in the solid fraction of LB reactors [36, 38]. Additionally, a lower number of TS may hamper the formation of spatial syntrophic relationships between acetate-oxidizing bacteria and hydrogenotrophic methanogens such as *Methanoculleus*. This might lead to an increase in growth of acetoclastic methanogens such as *Methanosarcina*, able to directly metabolize acetate (Fig. 4d–f). These findings are in concordance with previous reports on the link between high content of TS and a high frequency of hydrogen-using methanogens compared to acetoclastic methanogens [39–42].

The finding that *Methanosaeta* is the dominating genus in all SS digesters is consistent with other screenings [21, 43, 44]. However, the abundance of *Methanomethylovorans* in the SS digester in Rudolstadt might be connected to the presence of particularly high amounts

of oil and alcohols such as methanol, since this particular digester was supplemented with remnants from biodiesel production, and the prevalence of this organism has been reported in sewage sludge reactors supplemented with molasses alcohol wastewater [45].

The genus *Methanospirillum* was more abundant in the SS reactors in Jena and Weimar but not in Rudolstadt. This genus proved, along with *Methanolinea*, particularly abundant in a previous SS characterization [46], suggesting that *Methanospirillum* and *Methanosaeta* are two competing genera within the anaerobic digestion process of SS sludge.

Conclusions

The present work describes a holistic characterization of, to the best of our knowledge, the widest screening of biogas production facilities performed to date. We studied nine reactors, three replicates, and two time points (1-week interval) yielding 54 subsamples, the taxonomic diversity of which was determined for both archaea and eubacteria contents. Despite the heterogenous nature of some of the samples (especially those from CD reactors), our data reveal a very small effect of inter-replicate variation. All our results suggest a strong link between reactor type and taxonomic profile (for both archaea and bacteria), as well as an additional, significant effect of the location/particular reactor on the microbial community. Additionally, the three reactor types yielded separate blocks when chemical parameters were plotted in 3D and a principal component analysis was performed. Taken together, our results confirm the tight link between digester type, chemical parameters, and microbial biocenoses and also support the existence of a very stable microbial core adapted to each reactor type. Furthermore, our study provides a strong dataset for future diagnostic strategies aiming to predict biogas production of mesophile reactors on the basis of their microbial composition.

Materials and methods

Sampling

Seven anaerobic reactors accounting for nine different reactors from Thuringia, Germany, were sampled twice at a 1-week interval. These biogas plants included co-digesters, leach bed, and sewage sludge treatment plants (Fig. 1). Triplet samples from the first sampling time point were labelled as 1A, 1B, and 1C; whereas triplet samples from the second time point were labelled as 2A, 2B, and 2C.

An overview of the sampled digester types and input feedings is shown in Table 1. Additional file 1: Table S1 and Additional file 3: Table S2 show specific environmental chemical parameters regarding biogas production, biogas composition, and VFA spectrum. All sampled digester

types were operated at mesophilic temperature (except the sampled storage chamber for digestion remnants, which was left at RT). For the chemical analysis, a total volume of 5 L was collected in buckets via a sampling port at each plant. The sampling procedure was similar for all plants and stages (SS plants, LB systems, and all the stages of the one-phase CD). In the case of the LB facilities, only leachate from the leach tank could be collected. Small amounts of sample were then transferred into Falcon tubes, which were directly frozen on dry ice to prevent further microbial growth or DNA degradation, and immediately sent on dry ice from Thuringia to Valencia (Spain) for DNA isolation and sequencing. The remaining sludge was transferred to the laboratory of Bio H2 Energy GmbH in Jena. From this sludge, 1.5 L was used for gas production analysis directly upon sampling. The remaining 3.5 L of sludge was aliquoted into smaller plastic boxes and stored at $-20\text{ }^{\circ}\text{C}$ for further analysis at Eurofins and Bio H2 companies.

Determination of biogas production

For each anaerobic digester sample, 1.5 L was incubated in batch-experiments for 1 week at $37\text{ }^{\circ}\text{C}$. Incubation bottles (0.5 L) were filled with 0.5 L of sample (three bottles per sample without additional feeding), connected to a liquid displacement device (eudiometer, custom-built model calibrated by the German Eichamt), and the whole setup was flushed with nitrogen to ensure an anaerobic atmosphere. Biogas yield was measured as produced volume of biogas per volume of sludge sample [mL/L]. The concentration of CO_2 and CH_4 in the produced biogas was determined with the "Binder COMBIMASS GA-m" gas-measurement device (Binder, Germany).

Measurement of chemical parameters

Totals solids (TS), volatile solids (VS), chemical oxygen demand (COD), electrical conductivity, and total organic carbon (TOC) were determined according to German standard measurement methods [47]. Total nitrogen was determined as previously described (VDLUFA-Methodenbuch II, 3.5.2.7). The VFA spectrum was determined with a gas chromatograph (Shimadzu, Japan). The flame ionization detector was equipped with a DB.1701 column (Machery-Nagel/Germany).

DNA extraction from reactor samples

Three DNA samples were prepared from each sludge sample. In order to reduce the amount of inhibiting substances (especially humic acids), biomass was sedimented by centrifugation (5–10 min at 20,000 g for SS and LB samples, and 15 min at 20,000 g for CD samples) and washed several times with sterile PBS buffer until a clear supernatant was observed. DNA was isolated with

the "PowerSoil DNA isolation KIT" (Mo Bio Laboratories, USA) following the manufacturer's instructions. Long centrifugations were performed (5–10 min at 20,000 g for SS and LB samples, and 15 min at 20,000 g for CD samples) to ensure an almost complete removal of particles and cell fragments after the mechanical bead treatment.

Finally, DNA quality was checked on a 0.8 % (w/v) agarose gel and quantified with Nanodrop-1000 Spectrophotometer (Thermo Scientific, Wilmington, DE, USA).

PCR amplification

In order to survey bacterial diversity, a 500-bp fragment of the V1-V3 hypervariable region of the 16S ribosomal RNA gene was PCR-amplified from all the samples with universal primers 28F (5'-GAG TTT GAT CNT GGC TCA G-3') and 519R (5'-GTN TTA CNG CGG CKG CTG-3'). In the case of archaea, primers Arch349F (5'-GYG CAS CAG KCG MGA AW-3') and Ar9r (5'-CCC GCC AAT TCC TTT AAG TTTC-3') were used to amplify a 578-bp fragment of the 16S region [48]. A short (10–12 nucleotides) barcode sequence was included at the 5' end of the oligonucleotides used as forward primers in order to assign sequences to samples after high-throughput sequencing. All the amplifications were performed under the following thermal cycling conditions: initial denaturing at $95\text{ }^{\circ}\text{C}$ for 5 min, followed by 35 cycles of denaturing at $95\text{ }^{\circ}\text{C}$ for 30 s, annealing at $54\text{ }^{\circ}\text{C}$ (for both, bacteria and archaea) for 30 s, and extension at $72\text{ }^{\circ}\text{C}$ for 1 min, finalized by a 10-min elongation at $72\text{ }^{\circ}\text{C}$. The resulting amplicons were checked on a 0.8 % (w/v) agarose gel and purified by precipitation with 3 M potassium acetate (pH = 5) and isopropanol. Pure amplicons were quantified with the Qubit[®] 2.0 Fluorometer (Invitrogen, Carlsbad, CA, USA), and two equimolar pools of bacteria and archaea amplicons, respectively, were prepared from all the samples.

Ion torrent sequencing

Two sequencing libraries were constructed with 100 ng of the eubacteria and archaea amplicon pool, respectively, by the amplicon fusion method (Ion Plus Fragment Library Kit, MAN0006846, Life Technologies). Each library was quantified with the Agilent2100 Bioanalyzer (Agilent Technologies Inc, Palo Alto, CA, USA) prior to clonal amplification. Emulsion PCRs were carried out applying the Ion PGM Template OT2 400 kit as described in the user guide (MAN0007218, Revision 3.0 Life Technologies) provided by the manufacturer. Finally, the libraries were sequenced in an Ion 318 Chip v2 on a Personal Genome Machine (PGM) (IonTorrent[™], Life Technologies) at Life Sequencing S.L. (Life Sequencing, Valencia, Spain), using the Ion PGM Sequencing 400 kit following the manufacturer's protocol (publication

number MAN0007242, revision 2.0, Life Technologies). Sequence statistics are shown in Additional file 4: Table S3.

Sequence analysis and taxonomic classification

Raw sequences obtained from the sequencing center were processed with the MOTHRU software [49]. Short (<100 bp) and low-quality (<q15) reads were removed in a first step. The degenerated forward primer sequence was searched among the resulting sequences, and reads were discarded if either the primer (three mismatches allowed) or the barcode sequence was missing. Sequences were then split into groups based on barcode matches, and both primer and barcode sequences were trimmed. Finally, each resulting sequence was aligned to the ribosomal 16S reference Greengenes database and taxonomy was assigned based on nucleotide similarity with the k-mer algorithm. Assignments based on a similarity percentage lower than 70 % were not considered for further analysis.

Statistics

A principal component analysis (PCA) was performed using the Statgraphics software. Data from COD, TOC, total nitrogen contents (N), conductivity, TVFA, TS, VS, pH, and biogas corresponding to all samples were normalized, and two components explaining almost 90 % of the total variance were used for plotting. Row-stacked histograms, representing taxonomic profiles (Figs. 3 and 4), were prepared using Gnuplot and modified with Photoshop to insert grey bars representing intervals of biogas production. Pie charts (Fig. 4) were plotted in Excel.

In order to plot all environmental chemical parameters in one diagram (Fig. 2), the *plot* and *multiplot* commands of Gnuplot were combined to plot the permutation of all normalized parameters (normalized to values between 0 and 100). Each combination with three chosen variables was plotted and overlaid with the other combinations using the Gnuplot *multiplot* command. Since nine parameters were measured (COD, TOC, total nitrogen contents, conductivity, TVFA, TS, VS, pH, and volume of biogas), 84 resulting combinations were overlaid in the plot (Fig. 2a).

Additional files

Additional file 1: Table S1. Chemical environmental parameters of analyzed sludge samples and volume and composition of produced biogas (w/o VFA, error \pm 10 %).

Additional file 2: Figure S1. Principal component analysis (PCA) performed on the chemical environmental parameters measured for all samples. Data were normalized, and two components explaining nearly 90 % of the total variance were used for plotting.

Additional file 3: Table S2. Content of VFA in the sampled reactors (error \pm 10 %).

Additional file 4: Table S3. Sequencing statistics.

Abbreviations

AD: Anaerobic digestion; ADS: Anaerobic digester sludge; CD: Co-digester; COD: Chemical oxygen demand; LB: Leach bed; TOC: Total organic carbon; TS: Total solids; TVFA: Total volatile fatty acids; VFA: Volatile fatty acids; VS: Volatile solids.

Competing interests

The authors declare that they have no competing interests.

Authors' contributions

CA, OL, TG, and MP designed the work. CA performed sampling and DNA extraction. CA and CV analyzed the bioinformatic data. CA and TG performed the chemical analyses. CA, CV, and MP wrote the manuscript. All authors have read and approved the final version of the manuscript.

Acknowledgements

We thank the German Federal Ministry of Economics and Technology (ZIM, grant 16KN017627) for supporting this work. We also thank the plant operators for providing samples and descriptive data (Table 1).

Author details

¹Cavanilles Institute of Biodiversity and Evolutionary Biology, Universitat de València, 46020 Valencia, Spain. ²Bio H2 Energy GmbH, Im Steinfeld 10, 07751 Jena, Germany. ³Eurofins Umwelt Ost GmbH, Löbstedter Straße 78, 07749 Jena, Germany. ⁴BioEnergie Verbund e.V., Im Steinfeld 10, 07751 Jena, Germany. ⁵Fundació General de la Universitat de València, València, Spain.

Received: 23 January 2015 Accepted: 9 June 2015

Published online: 18 June 2015

References

- Damon PE, Kunen SM. Global cooling? *Science*. 1976;193:447–53.
- Bagley JE, Miller J, Bernacchi CJ. Biophysical impacts of climate-smart agriculture in the midwest United States. *Plant Cell Environ*. 2014. doi:10.1111/pce.12485.
- Scoma A, Rebecchi S, Bertin L, Fava F. High impact biowastes from South European agro-industries as feedstock for second-generation biorefineries. *Crit Rev Biotechnol*. 2014;1–15.
- European Commission. Renewable energy road map renewable energies in the 21st century: building a more sustainable future. KOM (2006) 848 final. Brussels: European Commission; 2007.
- Eurostat—database, source code ten00081 and ten00082. Primary production of renewable energy, 2000 and 2010. [http://epp.eurostat.ec.europa.eu/statistics_explained/index.php/File:Primary_production_of_renewable_energy_2000_and_2010-fr.png]
- BGBI (Bundesgesetzblatt) Teil 1. Gesetz zur Neuregelung des Rechts der Erneuerbaren Energien im Strombereich und zur Änderung damit zusammenhängender Vorschriften vom 25.10.2008, 2074–2100; 2008.
- Rademacher A, Hanreich A, Bergmann I, Klocke M. Black-Box-Biogasreaktor—mikrobielle Gemeinschaften zur Biogasfermentation. *BIOspektrum*. 2012;18:727–9.
- Wiese J, König R. From a black-box to a glass-box system: the attempt towards a plant-wide automation concept for full-scale biogas plants. *Water Sci Technol*. 2009;60:321–7.
- Koch C, Müller S, Harms H, Harnisch F. Microbiomes in bioenergy production: from analysis to management. *Curr Opin Biotechnol*. 2014;27:65–72.
- Nettmann E, Bergmann I, Pramschüfer S, Mundt K, Plogsties V, Hermann C, et al. Polyphasic analyses of methanogenic archaeal communities in agricultural biogas plants. *Appl Environ Microbiol*. 2010;76:2540–8.
- Jaenicke S, Ander C, Bekel T, Bisdorf R, Dröge M, Gartemann KH, et al. Comparative and joint analysis of two metagenomic datasets from a biogas fermenter obtained by 454-pyrosequencing. *PLoS One*. 2011;6:e14519.
- Sträuber H, Schröder M, Kleinstüber S. Metabolic and microbial community dynamics during the hydrolytic and acidogenic fermentation in a leach-bed process. *Energy Sustain Soc*. 2012;2:13.

13. Sundberg C, Al-Soud WA, Larsson M, Alm E, Yekta SS, Svensson BH, et al. 454 pyrosequencing analyses of bacterial and archaeal richness in 21 full-scale biogas digesters. *FEMS Microbiol Ecol*. 2013;85:612–26.
14. Luton PE, Wayne JM, Sharp RJ, Riley PW. The *mcrA* gene as an alternative to 16S rDNA in the phylogenetic analysis of methanogen populations in landfill. 2002. p. 3521–30.
15. Nettmann E, Bergmann I, Mundt K, Linke B, Klocke M. Archaea diversity within a commercial biogas plant utilizing herbal biomass determined by 16S rDNA and *mcrA* analysis. *J Appl Microbiol*. 2008;105:1835–50.
16. Rademacher A, Zarzewski M, Schlüter A, Schönberg M, Szczepanowski R, Goemann A, et al. Characterization of microbial biofilms in a thermophilic biogas system by high-throughput metagenome sequencing. *FEMS Microbiol Ecol*. 2012;79:785–99.
17. Solli L, Håvelsrud OE, Horn SJ, Rike AG. A metagenomic study of the microbial communities in four parallel biogas reactors. *Biotechnol Biofuels*. 2014;7:146.
18. Klocke M, Mähner P, Mundt K, Souidi K, Linke B. Microbial community analysis of a biogas-producing completely stirred tank reactor fed continuously with fodder beet silage as mono-substrate. *Syst Appl Microbiol*. 2007;30:139–51.
19. Goberna M, Insam H, Franke-Whittle IH. Effect of biowaste sludge maturation on the diversity of thermophilic bacteria and archaea in an anaerobic reactor. *Appl Environ Microbiol*. 2009;75:2566–72.
20. Kampmann K, Raterin S, Kramer I, Schmidt M, Zerr W, Schnell S. Unexpected stability of Bacteroidetes and Firmicutes communities in laboratory biogas reactors fed with different defined substrates. *Appl Environ Microbiol*. 2012;78:2106–19.
21. Demirel B, Scherer P. The roles of acetotrophic and hydrogenotrophic methanogens during anaerobic conversion of biomass to methane: a review. *Rev Environ Sci Biotechnol*. 2008;7:173–90.
22. Ziganshin AM, Liebetreu J, Pröter J, Kleinstuber S. Microbial community structure and dynamics during anaerobic digestion of various agricultural waste materials. *Appl Microbiol Biotechnol*. 2013;97:5161–74.
23. Smith AM, Sharma D, Lappin-Scott H, Burton S, Huber DH. Microbial community structure of a pilot-scale thermophilic anaerobic digester treating poultry litter. *Appl Microbiol Biotechnol*. 2014;98:2321–34.
24. Hanreich A, Schimpf U, Zakrzewski M, Schlüter A, Benndorf D, Heyer R, et al. Metagenome and metaproteome analyses of microbial communities in mesophilic biogas-producing anaerobic batch fermentations indicate concerted plant carbohydrate degradation. *Syst Appl Microbiol*. 2013;36:330–8.
25. Luo J, Liang H, Yan L, Ma J, Yang Y, Li G. Microbial community structures in a closed raw water distribution system biofilm as revealed by 454-pyrosequencing analysis and the effect of microbial biofilm communities on raw water quality. *Bioresour Technol*. 2013;148:189–95.
26. Sun H, Shi B, Bai Y, Wang D. Bacterial community of biofilms developed under different water supply conditions in a distribution system. *Sci Total Environ*. 2014;472:99–107.
27. Li C, Motaleb A, Sal M, Goldstein SF, Charon NW. Spirochete periplasmic flagella and motility. *J Mol Microbiol Biotechnol*. 2000;2:345–54.
28. Kragelund C, Levantesi C, Borger A, Thelen K, Eikelboom D, Tandoi V, et al. Identity, abundance and ecophysiology of filamentous Chloroflexi species present in activated sludge treatment plants. *FEMS Microbiol Ecol*. 2007;59:671–82.
29. Björnsson L, Hugenholtz P, Tyson GW, Blackall LL, Hill R. Filamentous Chloroflexi (green non-sulfur bacteria) are abundant in wastewater treatment processes with biological nutrient. *Microbiology*. 2002;148(8):2309–18.
30. Wang ZH, Yang JQ, Zhang DJ, Zhou J, Zhang CD, Su XR, et al. Composition and structure of microbial communities associated with different domestic sewage outfalls. *Genet Mol Res*. 2014;13:7542–52.
31. Lee SH, Kang HJ, Lee YH, Lee TJ, Han K, Choi Y, et al. Monitoring bacterial community structure and variability in time scale in full-scale anaerobic digesters. *J Environ Monit*. 2012;14:1893–905.
32. Traversi D, Villa S, Aciri M, Pietrangeli B, Degan R, Gilli G. The role of different methanogen groups evaluated by Real-Time qPCR as high-efficiency bioindicators of wet anaerobic co-digestion of organic waste. *AMB Express*. 2011;1:28.
33. Wirth R, Kovács E, Maróti G, Bagi Z, Rákhely G, Kovács KL. Characterization of a biogas-producing microbial community by short-read next generation DNA sequencing. *Biotechnol Biofuels*. 2012;5:41.
34. St. Pierre B, Wright AD. Metagenomic analysis of methanogen populations in three full-scale mesophilic anaerobic manure digesters operated on dairy farms in Vermont, USA. *Bioresour Technol*. 2013;138:277–84.
35. Klocke M, Nettmann E, Bergmann I, Mundt K, Souidi K, Mumme J, et al. Characterization of the methanogenic Archaea within two-phase biogas reactor systems operated with plant biomass. *Syst Appl Microbiol*. 2008;31:190–205.
36. Zhao H, Li J, Li J, Yuan X, Piao R, Zhu W, et al. Organic loading rate shock impact on operation and microbial communities in different anaerobic fixed-bed reactors. *Bioresour Technol*. 2013;140:211–9.
37. Weiß S, Lebhuhn M, Andrade D, Zankel A, Cardinale M, Birner-Gruenberger R, et al. Activated zeolite—suitable carriers for microorganisms in anaerobic digestion processes? *Appl Microbiol Biotechnol*. 2013;97:3225–38.
38. Zhang D, Li J, Guo P, Li P, Suo Y, Wang X, et al. Dynamic transition of microbial communities in response to acidification in fixed-bed anaerobic baffled reactors (FABR) of two different flow directions. *Bioresour Technol*. 2011;102:4703–11.
39. Ariesyady HD, Ito T, Okabe S. Functional bacterial and archaeal community structures of major trophic groups in a full-scale anaerobic sludge digester. *Water Res*. 2007;41:1554–68.
40. Montero B, García-Morales JL, Sales D, Solera R. Evolution of microorganisms in thermophilic-dry anaerobic digestion. *Bioresour Technol*. 2008;99:3233–43.
41. Montero B, García-Morales JL, Sales D, Solera R. Analysis of methanogenic activity in a thermophilic-dry anaerobic reactor: use of fluorescent *in situ* hybridization. *Waste Manag*. 2009;29:1144–51.
42. Zahedi S, Sales D, Romero LI, Solera R. Optimisation of single-phase dry-thermophilic anaerobic digestion under high organic loading rates of industrial municipal solid waste: Population dynamics. *Bioresour Technol*. 2013;146:109–17.
43. Nakahira E, Ikemoto-Yamamoto R, Honda R, Ohtsuki S, Takano M, Suetsugu Y, et al. Effect of the addition of rice straw on microbial community in a sewage sludge digester. *Water Sci Technol*. 2014;70:819–27.
44. Li J, Zhang L, Ban Q, Jha AK, Xu Y. Diversity and distribution of methanogenic archaea in an anaerobic baffled reactor (ABR) treating sugar refinery wastewater. *J Microbiol Biotechnol*. 2013;23:137–43.
45. Shen P, Zhang J, Zhang J, Jiang C, Tang X, Li J, et al. Changes in microbial community structure in two anaerobic systems to treat bagasse spraying wastewater with and without addition of molasses alcohol wastewater. *Bioresour Technol*. 2013;131:333–40.
46. Kim J, Kim W, Lee C. Absolute dominance of hydrogenotrophic methanogens in full-scale anaerobic sewage sludge digesters. *J Environ Sci (China)*. 2013;25:2272–80.
47. German standard methods for the examination of water, wastewater and sludge. Wiley-VCH 2013, Weinheim, Germany
48. Klindworth A, Pruesse E, Schweer T, Peplies J, Quast C, Horn M, et al. Evaluation of general 16S ribosomal RNA gene PCR primers for classical and next-generation sequencing-based diversity studies. *Nucleic Acids Res*. 2013;41:e1.
49. Schloss PD, Westcott SL, Ryabin T, Hall JR, Hartmann M, Hollister EB, et al. Introducing MOTHUR: open-source, platform-independent, community-supported software for describing and comparing microbial communities. *Appl Environ Microbiol*. 2009;75:7537–41.

**Submit your next manuscript to BioMed Central
and take full advantage of:**

- Convenient online submission
- Thorough peer review
- No space constraints or color figure charges
- Immediate publication on acceptance
- Inclusion in PubMed, CAS, Scopus and Google Scholar
- Research which is freely available for redistribution

Submit your manuscript at
www.biomedcentral.com/submit



RESEARCH

Open Access



From grass to gas: microbiome dynamics of grass biomass acidification under mesophilic and thermophilic temperatures

Christian Abendroth^{1,2,3}, Claudia Simeonov³, Juli Peretó^{1,2,4,7}, Oreto Antúnez⁵, Raquel Gavidia⁵, Olaf Luschnig⁶ and Manuel Porcar^{1,2,7,8*}

Abstract

Background: Separating acidification and methanogenic steps in anaerobic digestion processes can help to optimize the process and contribute to producing valuable sub-products such as methane, hydrogen and organic acids. However, the full potential of this technology has not been fully explored yet. To assess the underlying fermentation process in more detail, a combination of high-throughput sequencing and proteomics on the acidification step of plant material (grass) at both mesophilic and thermophilic temperatures (37 and 55 °C, respectively) was applied for the first time.

Results: High-strength liquor from acidified grass biomass exhibited a low biodiversity, which differed greatly depending on temperature. It was dominated by Bacteroidetes and Firmicutes at 37 °C, and by Firmicutes and Proteobacteria at 55 °C. At the methane stage, *Methanosaeta*, *Methanomicrobium* and *Methanosarcina* proved to be highly sensitive to environmental changes as their abundance in the seed sludges dropped dramatically after transferring the seed sludges from the respective reactors into the experimental setup. Further, an increase in Actinobacteria coincided with reduced biogas production at the end of the experiment. Over 1700 proteins were quantified from the first cycle of acidification samples using label-free quantitative proteome analysis and searching protein databases. The most abundant proteins included an almost complete set of glycolytic enzymes indicating that the microbial population is basically engaged in the degradation and catabolism of sugars. Differences in protein abundances clearly separated samples into two clusters corresponding to culture temperature. More differentially expressed proteins were found under mesophilic (120) than thermophilic (5) conditions.

Conclusion: Our results are the first multi-omics characterisation of a two-stage biogas production system with separated acidification and suggest that screening approaches targeting specific taxa such as *Methanosaeta*, *Methanomicrobium* and *Methanosarcina* could be useful diagnostic tools as indicators of environmental changes such as temperature or oxidative stress or, as in the case of Actinobacteria, they could be used as a proxy of the gas production potential of anaerobic digesters. Metaproteome analyses only detected significant expression differences in mesophilic samples, whereas thermophilic samples showed more stable protein composition with an abundance of chaperones suggesting a role in protein stability under thermal stress.

Background

Anaerobic digestion is a promising technology for biofuel production, and has been the object of research for over

100 years [1, 2]. The anaerobic digestion process consists of four stages: hydrolysis, acidogenesis, acetogenesis and methanogenesis. During the first three stages, hydrogen and acetate are formed as intermediary products, which are then converted into methane and carbon dioxide during methanogenesis [3]. Countless works have been published characterizing those stages or comparing

*Correspondence: manuel.porcar@uv.es

⁸ Institute for Integrative Systems Biology (I2SysBio, Universitat de València-CSIC), Postal Code 22085, 46071 Paterna, València, Spain
Full list of author information is available at the end of the article

different substrates for co-digestion and reactor configurations. Furthermore, substantial efforts have been made in recent decades to shed light on the underlying microbial biocoenosis of anaerobic digestion processes. The first determinations of taxonomic profiles appeared in the 90 s [4, 5], when 16S-rDNA data from anaerobic sludges were investigated. More recently, high-throughput approaches like 16S-rDNA sequencing or metagenomics have been applied [2, 6–8], as well as proteome analyses [9, 10]. However, most of the aforementioned work focused on reactor configurations, where acidogenesis and methanogenesis occur, combined in the same reactor stage. It is well-known since the 80 s that the process can be split into multistage processes, in such a way that hydrolysis/acidogenesis occurs separately from acetogenesis/methanogenesis [11, 12]. Although it may be difficult to fully separate the underlying microbial processes (for example nitrogen-rich substrates seem to cause methanogenic contaminations in the acid-producing step [13]), improved biogas production has been reported using a separated setup. For example, in 1988 authors described a rumen-derived microbial community optimally fermenting cellulose in a separated acidification step [14]. Others report that some practices such as shock loading (high loads of substrate that cause accumulation of volatile fatty acids, VFA) increase hydrogen formation at pH < 6.5 [15]. As pH values between 4 and 6.5 are common during acidification [16–18] and methanogenesis is inhibited at either low pH or high VFA concentration [19], this renders hydrogen production in the acidification stage as a valuable sub-product in addition to the methane [20]. Additionally, a high concentration of acetic acid is known to improve chemical hydrolysis [21]. Even though hydrogen production in seed sludges with diverse microbiomes is highly unpredictable, a few previous reports have explored the possible production of hydrogen [22–24], by, for example, immobilization of hydrogen-producing bacteria [23, 24].

Separated acidification has been proposed as the best technology to produce organic acids like lactic, butyric and acetic acid, even though it is still complicated to extract organic acids from the fermentation process [25].

The benefits of separated acidification cannot be fully explored without a deeper knowledge of the underlying microbial communities. Currently, such knowledge is very fragmentary. For example, it is known that fermentation of 52.85 g/L of rice straw at 39.23 °C and pH 10.0 leads to an increase in the families Ruminococcaceae, Bacteroidaceae, Porphyromonadaceae and Lachnospiraceae [26]; or that the acidification of alginate correlates with high titres of *Bacteroides*- and *Clostridium*-related microorganisms [27]. Proteomics has been used to study standard, one-step digestion plants

without separated acidification [9, 10, 28], but there are no detailed proteomics studies of a separated acidification stage to date. In order to bridge this gap and to finely characterize one of the most important phases of the biogas production process, the dynamic behaviour of grass acidification processes at mesophilic and thermophilic temperatures (37 and 55 °C, respectively) was monitored through both proteomics and 16S-rDNA analysis. The efficient use of lignocellulosic biomass as a feedstock is an active research area of high interest [30]. In the present work grass was chosen because of its potential as a renewable energy source [29].

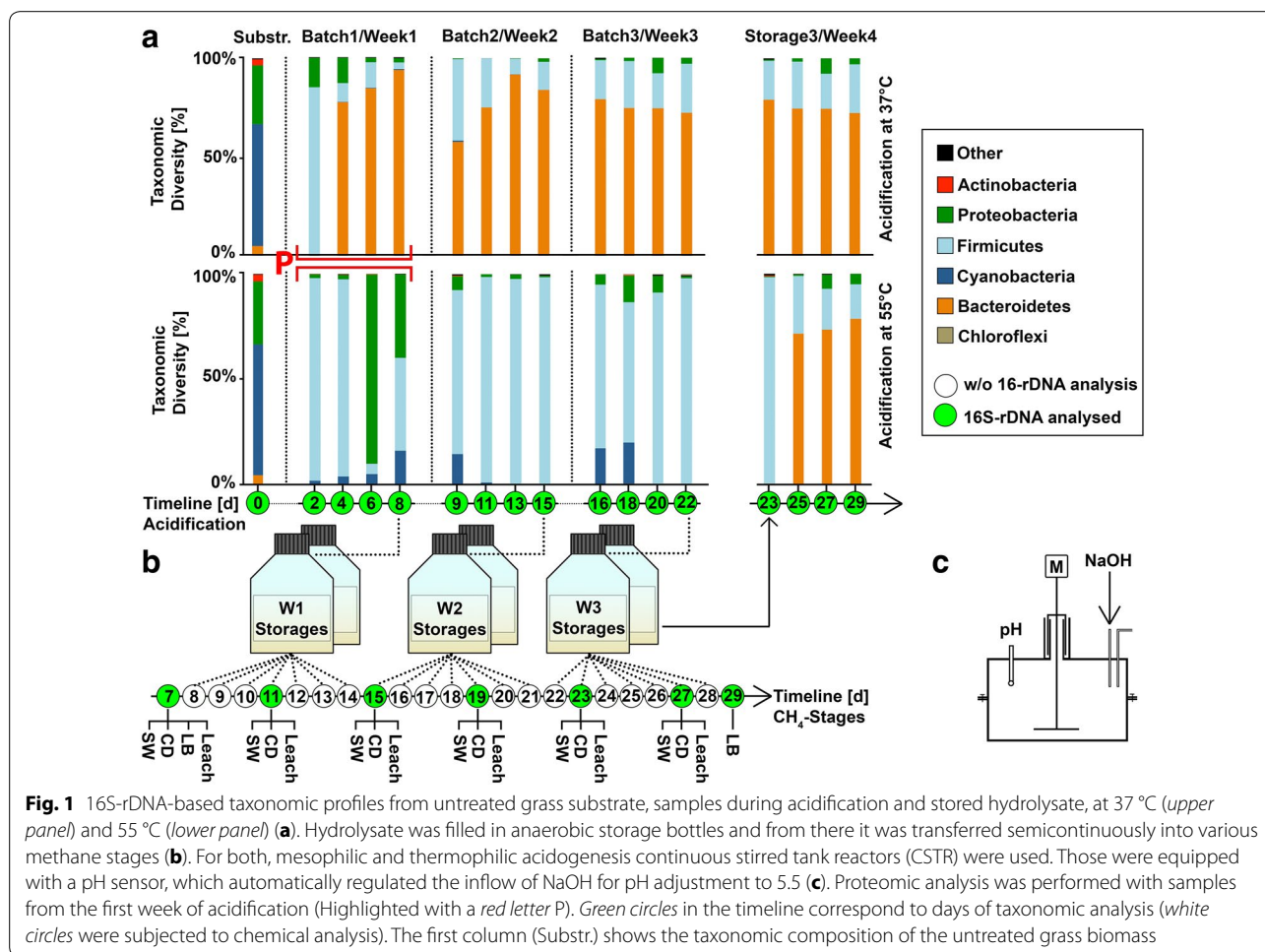
Results and discussion

16S-rDNA-based analysis on high-strength liquor from grass acidification

Mechanically ground mixed grass (Graminidae) was acidified in three subsequent batch reactions under anaerobic conditions at mesophilic and thermophilic temperatures (Fig. 1). pH was automatically adjusted to 5.5 to prevent it dropping below that value. Acidification occurred in tap water as a result of microbial activity. The second and third batch received 5% Inoculum from the previous batch. Samples for VFA analysis were taken daily and every two days for 16S-rDNA amplicon sequencing. The mixed grass microbiome was analysed prior to entering acidification reactors, and it proved rich in Cyanobacteria- and Proteobacteria-related taxa. Upon transference into the reactors, the taxonomic profile rapidly switched to the one dominated by members of the phylum Firmicutes. This happened under both mesophilic and thermophilic conditions (Fig. 1).

After just two days, hardly any Proteobacteria and Cyanobacteria remained. As often occurs with 16S-rDNA-based analyses of plant material, cyanobacteria-related sequences may correlate to plant chloroplasts. On day four, most of the Firmicutes were suppressed by Bacteroidetes at mesophilic temperatures, while the proportion of Firmicutes remained high at 55 °C. The acidification process was repeated three times in a row and Bacteroidetes were also the dominating phylum at mesophilic temperatures. At thermophile temperatures the dominant phylum was Firmicutes, although at two of the sampling points a strong but transitory shift towards Proteobacteria was observed (Fig. 1a). In the second and third week an inoculum from the previous stages was used; however, this hardly influenced the taxonomic profile, which was constantly dominated by Bacteroidetes.

Upon termination of each acidification cycle, the high-strength liquors produced were transferred into bottles filled with nitrogen and stored at room temperature thereafter (Fig. 1b). The microbial composition in the stored liquor was analysed (Fig. 1, right) and yielded no significant changes at mesophilic temperature. However,



a strong shift in the stored liquor originating from the thermophilic reaction was observed after incubation at room temperature (RT). After four days at RT, numbers of Bacteroidetes dramatically increased, yielding a stable taxonomic profile very similar to the one of the mesophilic acidification step. The microbial profile of the thermophilic samples upon RT storage was not accompanied by any changes in the concentration of chemical oxygen demand (COD) or VFA (Data not shown).

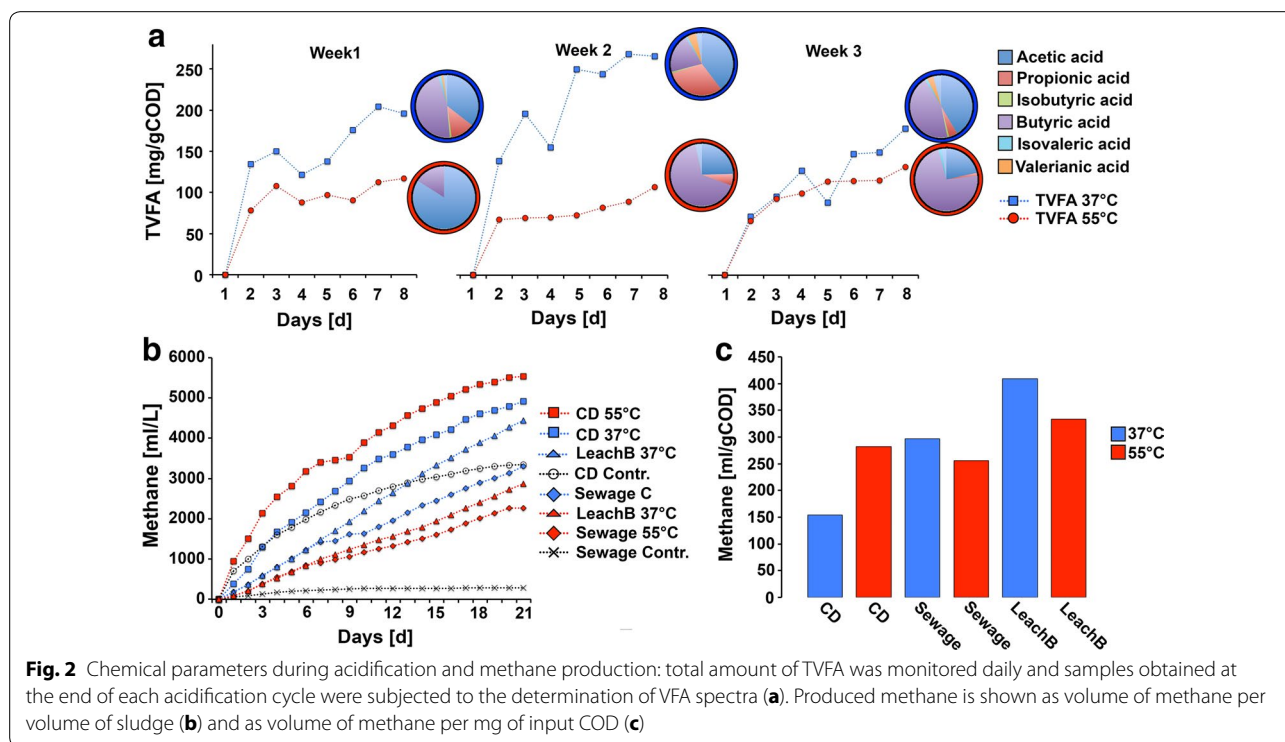
The results are in concordance with a previous work describing high titres of Bacteroidetes and Firmicutes during acidification of alginate under mesophilic conditions [24]. A microbiome dominated by Bacteroidetes and Firmicutes has also been reported for one-stage processes at mesophilic temperatures [9, 31, 32], but not for sewage sludge [7, 8].

There are no previous reports on the microbiome of acidification at thermophilic temperatures; however, a shift to Clostridia (Firmicutes) has been described for one-stage digesters [33, 34], similar to the increased titre of Firmicutes described in the present results.

Environmental parameters

Production of total volatile fatty acids (TVFAs) was more effective at mesophilic temperatures than at thermophilic ones (Fig. 2). With 200 mg TVFA per gram of input COD, the mesophilic stage yielded twice as many TVFAs as at thermophilic temperatures (Fig. 2a). At 37 °C, the relative amount of acetic acid and propionic acid were much higher than at 55 °C (Fig. 2b). By contrast, an accumulation of butyric acid was observed at thermophilic temperatures.

To the best of our knowledge, there are no previous reports comparing taxonomic profiles of mesophilic and thermophilic biogas acidification stages. There are reports, however, that thermophilic processes in one-stage digesters result in higher degradation efficiency compared to mesophilic ones [34–37]. Previous works have reported long incubation times for adaption of the biocoenosis to thermophile temperatures, ranging from several months [35] to up to one year [37]. Therefore, successful adaption to high temperatures and well-chosen seed sludge might be crucial for a separated acidification step.



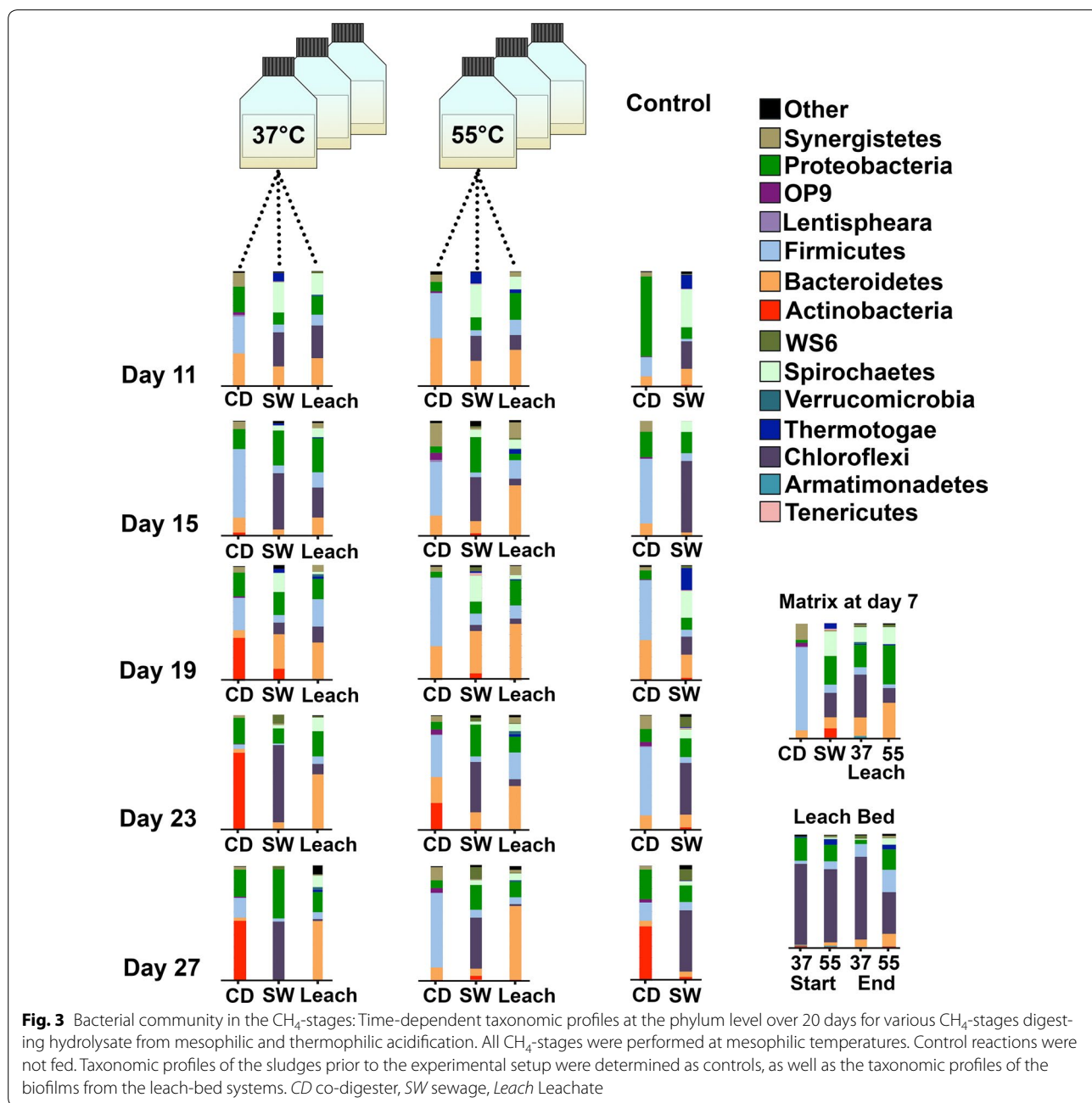
In concordance with the reduced acid production in the thermophilic acidification, two of the corresponding methane stages (leach bed and semicontinuous batch with sewage) yielded more methane per gram of input COD with thermophilic liquor than with mesophilic. (Fig. 2c). However, in the system containing seed sludge from a co-digester (CD), the yield from the thermophilic-treated liquor was higher than in the one receiving mesophilic liquor. This might be related to the higher total solids (TS) content, high heterogeneity and high gasification activity also causing very high gas yields in the negative control from the CD sludge (Fig. 2b). In concordance with a previous work [38], the liquefied COD from the produced high-strength liquor was efficiently transformed into methane, indicating no inhibitory effects.

Usage of the high-strength liquor produced

High-strength liquor was stored in bottles at RT upon production, which were always flushed with nitrogen after opening to keep anoxic conditions. The liquor was semicontinuously fed into various methane stages (Figs. 1b, 2, 3).

The used seed sludge from the co-digester was very rich in Firmicutes, Synergistetes and Bacteroidetes, while the seed sludge from the sewage plant (SW) consisted mainly of Proteobacteria, Bacteroidetes, Spirochaeta and Chloroflexi (Matrix at day 7, Fig. 3). Both findings are in concordance with our previous report on

several co-digester microbiomes [8]. The starting samples for the leach-bed systems (Matrix at day 7, Fig. 3) were taken 24 h after refilling the leach bed with sewage seed sludge. Compared to the original sewage, there was a dramatic decrease in Actinobacteria. This may be due to the high sensitivity of Actinobacteria to environmental changes, as sensitivity to environmental changes has been described for Actinobacteria in soil [39]. The two leach-bed systems were both rich in Chloroflexi, especially in the leach-bed biofilm (Fig. 3, Leach Bed). This is in concordance with other works describing high abundance of Chloroflexi in deep biofilm layers on building walls [40] and in the sediments of Winogradsky columns [41]. The input of the high-strength liquor, rich in Firmicutes and Bacteroidetes, did not result in an increase in those phyla in the sewage sludge batches or in the leach-bed systems (SW and Leach samples from Day 11 to Day 27, Fig. 3). Samples from both systems remained rich in Chloroflexi and Spirochaeta, even though they received a daily microbial input rich in Firmicutes and Bacteroidetes. This highlights the stability of the underlying biocoenosis and suggests the potential of separated acidification as an important step in preventing the occurrence of major microbial disturbances in the biocoenosis of the respective sewage digesters. For example, an additional thermophilic acidification stage could be included in co-digestion in sewage digesters in order to improve the robustness



of the active microbiome. The positive effect of co-digesting organic matter with sewage sludge (e.g. food waste or energy grass) on the reactor performance has recently been reported [42, 43]. Moreover, the application of leachate in sewage digestion has been proposed too [44]. Our results indicate that using liquefied grass biomass (after separation from solids) might be a promising method for co-digestion with sewage. Large amounts of unused grass biomass, could still be valorised [29]. Although there have been attempts to add grass biomass into sewage sludge for co-digestion [45],

co-digestion of liquefied grass biomass with sewage has not been demonstrated until now.

During the experiment, the lowered temperature in the storage bottle of the high-strength liquor at room temperature (Storage 3/Week 4, Fig. 1) resulted in a dramatically modified community composition of the thermophilic liquor after two days at RT. Thus, the transference of thermophilic high-strength liquor into a mesophilic sewage digester might destabilize the microbial community in the liquor and provide an advantage to the existing biocoenosis from the sewage digester. Using the

high-strength liquor for co-digestion prevented the entry of solids into the water treatment circle.

In the last days of the experiment, the sludge samples from the co-digester exhibited low levels of Firmicutes and Bacteroidetes, and high rates of Actinobacteria. This coincided with a reduction in the production of biogas (Fig. 2). Interestingly, we have previously reported a concurrence between increasing amounts of Actinobacteria and low methane production [8]. Occurrence of Actinobacteria in anaerobic digester plants has been reported repeatedly [46, 47]. Actinobacteria were described in previous works as important key players in the degradation of plant material in compost [48] with effective enzymes that can allow large-scale application for breakdown of cellulosic plant material [49]. This is not necessarily contradictory with our results, since Actinobacteria survival and its efficiency for degradation of plant material could vary greatly at different nutrient concentrations due to their sensitivity to environmental changes as mentioned before. Although further work is needed to confirm this link, it is tempting to propose the identification and quantification of microbial key players as a marker of process efficiency.

In the case of the leach-bed system, the last part of the experiment was characterized by higher amounts of Bacteroidetes in the liquid phase (Leach samples from Day 11 to Day 27, Fig. 3). It has to be stressed that the biofilm became denser during the experiment and thus a biofilm filtering effect could be responsible for the very clear supernatant observed at the end of the process, which might, in turn, have affected the microbial composition of the leachate.

Archaea were also detected through 16S-rDNA amplification and identification (Fig. 4). The genus *Methanoculleus* was the most abundant one in most of the samples. The co-digester sludge contained small amounts of *Methanobacterium* and *Methanosarcina*, as previously reported for the same plant [8] (Matrix at day 7, Fig. 4). However, upon transferring the sludge into the batch systems, a rapid shift was observed, in terms of an overwhelming abundance of *Methanoculleus* (CD, SW and Leach-Bed Samples at day 11, Fig. 4). This might be related to stress factors caused by the sludge transference (e.g. changing reactor conditions or short-time exposure to oxygen), and it could be hypothesized that *Methanoculleus* is more resistant to these changes. This is consistent with previous reports on the robustness of *Methanoculleus*, which is particularly resistant to inhibitors such as ammonia [50], phenol [51] or paraffin [52].

After eight days of incubation under constant conditions *Methanosaeta* and *Methanobacterium* started to recover in the batch reactions with the sewage seed sludge (Fig. 4), although no significant increases were

observed for the leach-bed system. However, *Methanosaeta* proved frequent in the biofilm from the leach bed, (Fig. 4, Leach Bed). The occurrence of *Methanosaeta* in biofilms has been reported previously [53, 54]. This result highlights the need for a separate analysis of leach-bed samples and associated biofilms. In the co-digesters, *Methanosarcina* were also recovered as of day 23 (CD samples at day 23–27, Fig. 4).

Proteomic analysis on the high-strength liquor produced

Proteins were extracted from the samples d2, d4, d6 and d8 from the first cycle of acidification. The proteome at mesophilic and thermophilic temperatures proved strikingly different in the previous SDS-PAGE analysis (Additional file 1: Figure S3). This observation was approved by a principal component aggregation (PCA) from mass spectroscopy raw data (peptide) analysis, where samples not only separated into two groups by temperature (X-axis, Fig. 5b), but also showed dynamic changes in time (Y-axis, Fig. 5b).

At the first stages, plant proteins were detected in the greatest amounts, as expected from the mixed grass biomass used in all assays. However, in line with increasing incubation time, the ratio between plants and bacteria shifted due to massive microbial growth and/or degradation of plant material at 37 °C (Fig. 5a). However at 55 °C, there was a constant plant:bacteria ratio in the protein abundance, indicating a decrease in the total microbial population.

An abundance of enzymes involved in carbohydrate metabolism and degradation in metaproteomes from both series of samples were identified using a protein database search for Bacteria and Archaea domains, although additionally diverse chaperones and heat-shock proteins (e.g. 10 and 60 kDa chaperonins, and GroEL) were overrepresented in the thermophilic samples (Additional file 2: Table S4). Among the most abundant proteins detected in all analysed samples, there was an almost complete set of glycolytic enzymes (glucose-6-phosphate isomerase, fructose-bisphosphate aldolase, triosephosphate isomerase, glyceraldehyde-3-phosphate dehydrogenase, phosphoglycerate kinase, enolase), as well as components of sugar transport systems (like the phosphotransferase system, PTS). These results indicate that the microbial population is basically engaged in the degradation and catabolism of sugars in the fermentative phase of short-chain acid production, an observation that is coherent with previous reports on the metaproteome [28] and metametabolome [55] of this kind of microbial communities.

Label-free quantitative proteome analysis was performed to determine differentially expressed proteins between mesophilic and thermophilic temperatures

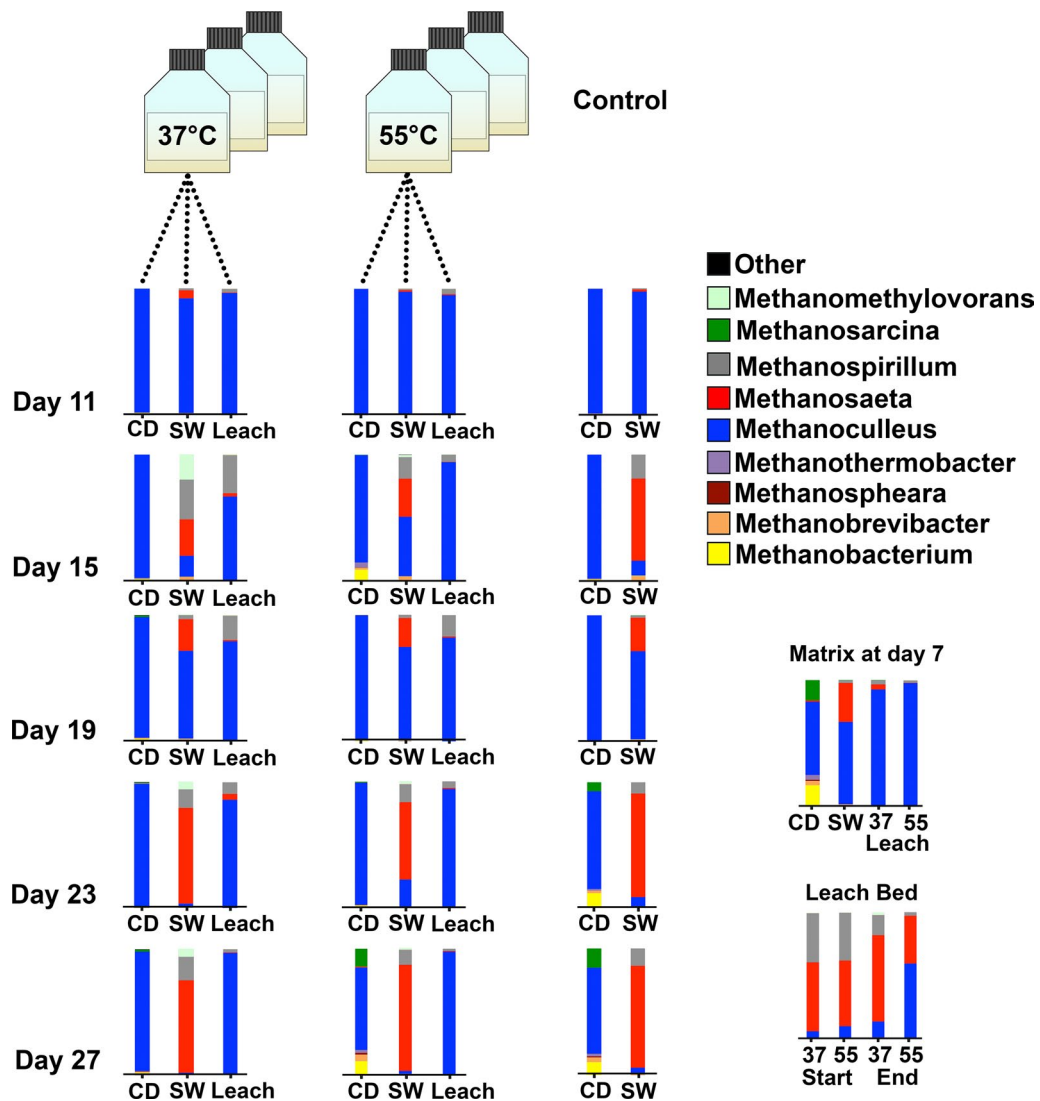


Fig. 4 Archaeal community in the CH₄-stages: Time-dependent community behaviour at the genus level over 20 days for various CH₄-stages digesting hydrolysate from mesophile and thermophile acidification. All CH₄-stage measurements were performed at mesophilic temperatures. CD co-digester, SW—sewage, Leach Leachate

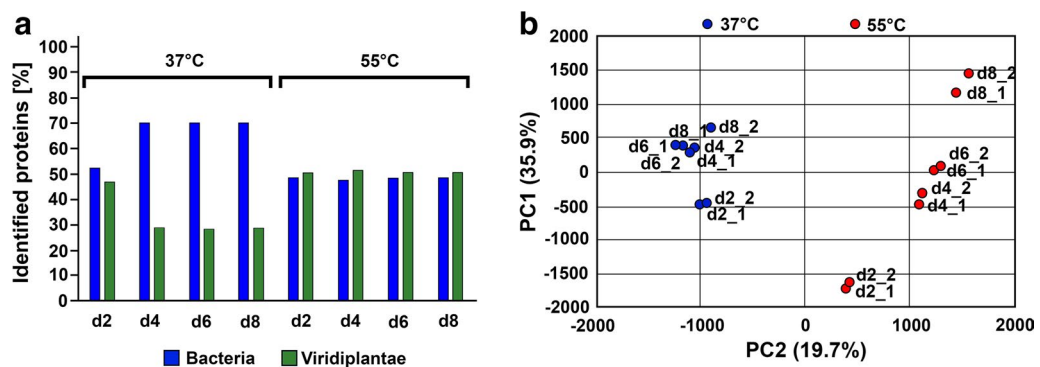


Fig. 5 Bacteria and Viridiplantae proteomic profile evolution in the first cycle of acidification (a); PCA aggrupation of quantified peptides at mass spectroscopy analysis (b)

(Additional file 3: Table S5). A total of 1731 proteins were quantified from samples d2, d4, d6 and d8 collected from the first cycle of acidification: 556 proteins increased and 176 decreased between mesophilic and thermophilic conditions (37 vs. 55 °C). Samples were compared using the Limma statistics software package. Differences in protein abundances clearly separated samples into two clusters corresponding to culture temperature, with the subset of proteins showing an increased expression that was richer at 37 than 55 °C (Fig. 6a). On comparing protein abundances during sampling time, 120 (out of 1731) proteins showed differential expression at 37 °C, whereas at 55 °C, the differentially expressed proteins were only 5 (out of 1731) (Fig. 6b). Remarkably, most differences were observed when comparing d2 and d4 samples, and d2 and d8 at mesophilic conditions, whereas at thermophilic conditions a small set of differential proteins was only detected when comparing samples d2 and d8 (Fig. 6b). Among the differentially expressed proteins at mesophilic conditions there is a notable representation of ribosomal proteins indicating a dynamic state of these microbial communities. The taxonomic profiles of metaproteome samples were in agreement with the presented metagenomic data.

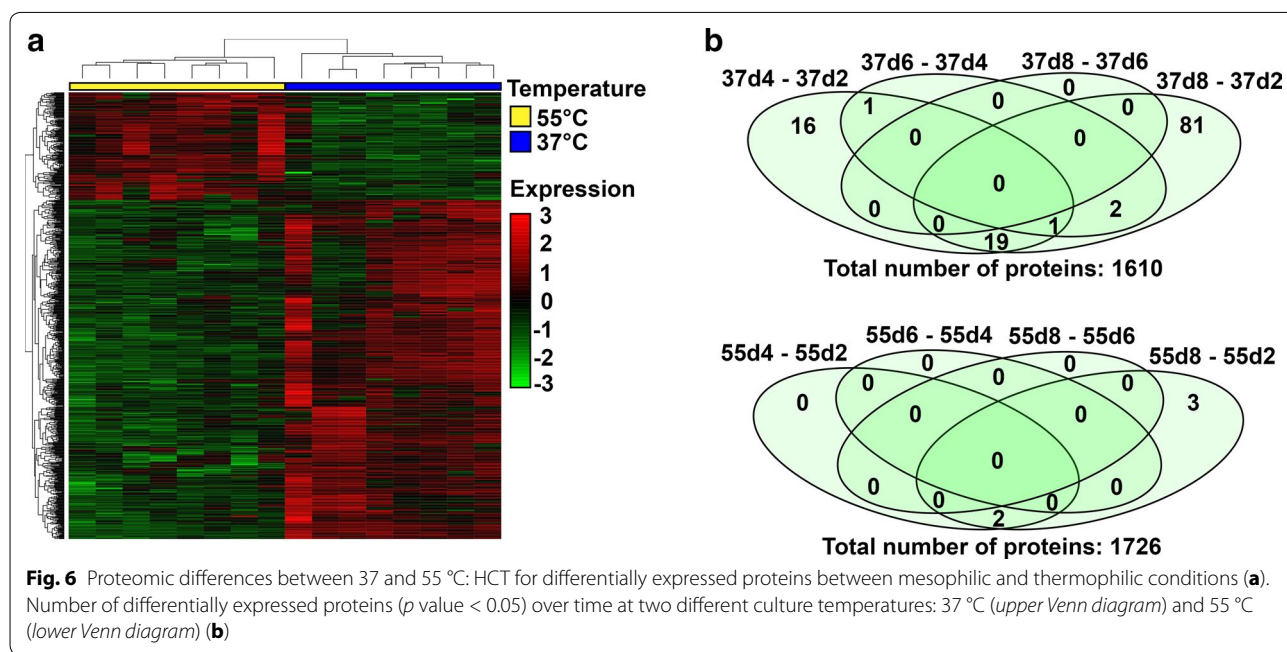
Among the differentially expressed proteins in d2 samples at 37 °C, noteworthy was the presence of several membrane transport systems from Firmicutes species involved in sugar uptake. These were the PTS HPr-related protein and the cellobiose-specific PTS IIB component, and the PTS phosphocarrier protein HPr. There was also an increase in haemolysin-type calcium-binding protein, with a predicted hydrolytic

activity on O-glycosyl compounds and a carbohydrate-binding domain (CBM) type 2 from an Alpha-proteobacterium in d2 samples. Previous studies on mesophilic biogas-producing, cellulolytic communities have indicated the abundance of sugar transporters and enzymes involved in polysaccharide degradation [9, 28, 56].

Conclusions

Plant biomass (a mix of grass) was acidified at mesophilic and thermophilic temperatures. The taxonomic communities in both cases proved very different, and consisted of Bacteroidetes and Firmicutes at 37 °C and Firmicutes and Proteobacteria at 55 °C. At the methane stage, *Methanosaeta*, *Methanomicrobium* and *Methanosarcina* proved highly sensitive to environmental changes whereas *Methanoculleus* proved to be very robust with all the seed sludges. At the end of the experiment, there was an increase in Actinobacteria in the semicontinuous batches containing co-digester seed sludge, which coincided with reduced biogas formation. Thus, Actinobacteria determination could be a useful prediction tool for biogas production.

Metaproteome analyses only detected significant expression differences in mesophilic samples, and collectively implied a dynamic microbial community engaged in polysaccharide demolition and sugar fermentation as remarkable metabolic activities during the acidification phase. Thermophilic samples showed more stable protein composition with an abundance of chaperones suggesting a role in protein stability under thermal stress.



Methods

Reactor performance

Acidification of grass was carried out in three sequential reactions, which were operated in parallel at 37 and 55 °C with a COD input concentration of 30 gO₂/L. Acidification occurred in tap water as a result of microbial activity. For the second and third cycle of acidification 5% inoculum was applied from the previous reactions. After separating the liquid phase from the solids manually using a sieve, the resulting high-strength liquor was stored under anaerobic conditions (nitrogen atmosphere) until further fermentation occurred in several methane stages (Fig. 1). Acidification was carried out in continuous stirred tank reactors with a total working volume of 5 L and equipped with a pH regulation system (BL 7916, Hanna Instruments, Germany) that stabilized the pH at 5.5 (Fig. 1).

The high-strength liquor was stored until usage in glass bottles at RT. To ensure anaerobic atmosphere, the bottles were nitrogen-purged and a gasbag (TECOBAG, TESSERAUX Spezialverpackungen GmbH, Germany) was connected to verify that no further gas production occurred.

High-strength liquor was digested in semicontinuous batch reactions, as well as two leach-bed systems. The setup of batch systems was carried out according to VDI 4630 [57]. Feeding was applied not only at the beginning of the experiment but semicontinuously by adding daily 33 mL/L day to the batch bottles, which corresponds to a solubilized COD of 0.51 gO₂ for the mesophilic stage and 0.39 gO₂/L for the thermophilic stage.

The leach-bed systems consisted of packed columns with 3 L working volumes. They were filled with 2 L of seed sludge and 485 g of bed packing (Hel-X-Füllkörper, Christian Stöhr GmbH&Co.KG, Germany) and were fed equally to the batch bottles with 33 mL/L*day. Gas production was quantified with a MilliGascounter (Ritter Apparatebau GmbH, Germany) and collected in a gasbag for further analysis (TECOBAG, TESSERAUX Spezialverpackungen GmbH, Germany).

In total, eight methane stages were set in place. Two leach-bed systems, three batch systems filled with low TS seed sludge (sewage) and three batch systems filled high TS seed sludge (CSTR, co-digester) (Additional file 4: Table S1 and Additional file 5: Table S2). The leach-bed systems were filled with sewage sludge and the leach bed contained a thick biofilm from previous experiments also performed with sewage. All methane stages were set as duplets in order to compare methanisation of liquor from acidification, at 37 and 55 °C. Control reactions without feeding were performed (Fig. 1).

Sampling and environmental chemical analysis

A mixture of grass species was collected from a backyard in Jena (Germany) and mechanically ground. Mechanical

treatment was performed using a conventional juicer (Angel Juicer 8500 s, Angel Co.LTD., Corea). After the mechanical treatment, grass juice and squashed solids were remixed and stored at -20 °C until use.

Sewage was collected from a water treatment plant in Jena (Jena). Sludge from a co-digester was collected from the continuous stirred tank reactor near the water treatment plant. Sludge samples and substrates were characterized by analysing TS and VS (Additional file 4: Table S1) and during the acid-producing step, the concentration of VFA and COD was monitored daily using conventional photometer-based assays (Nanocolor CSB15000 and Nanocolor organische Säuren 3000, Macherey-Nagel, Germany) (Fig. 2). At the end of each experiment, the VFA spectrum was determined at Eurofins Umwelt Ost GmbH, using a gas chromatograph (Shimadzu, Japan). A flame ionization detector was equipped with a DB.1701 column (Macherey-Nagel, Germany).

During methanisation of the high-strength liquor produced, the volume of biogas obtained was monitored daily, using a "COMBIMASS GA-m" gas measurement device (Binder, Germany), to determine the ratio of CO₂ and CH₄ (Fig. 2). Samples for DNA analysis were taken every two days for the acidification step and every four days for the methane stages. One milliliter of sample was mixed with 1 mL of pure ethanol and kept at -20 °C until required. Additional samples from the acidification stages were taken for proteomic approaches (20 mL per sample). Samples for proteomic analysis were stored at -70 °C until further analysis.

DNA extraction and amplification

To reduce the amount of humic acids and other inhibitors, samples were intensively washed: they were centrifuged at 20,000×g and resuspended in PBS buffer repeatedly until a clear supernatant was observed. DNA Extraction was performed using the PowerSoil DNA isolation KIT (Mo Bio Laboratories, USA). After a quality control on a 0.8% (w/v) agarose gel and quantification with the Nanodrop-1000 Spectrophotometer (Thermo Scientific, Wilmington, DE, USA), variable regions V1–V3 from the 16S-rDNA gene were amplified. For amplification of bacterial 16S-rDNA sequences the universal primers 28F (5'-GAG TTT GAT CNT GGC TCA G-3') and 519R (5'-GTN TTA CNG CGG CKG CTG-3') were used (Additional file 6: Table S6 and Additional file 7: Table S7). Archaea target sequences were amplified using the primers Arch349F (5'-GYG CAS CAG KCG MGA AW-3') and Ar9r (5'-CCC GCC AAT TCC TTT AAG TTTC-3') (Additional file 8: Table S8). Resulting amplicons had a length of 500 bp for bacteria and 578 bp for archaea [58]. For amplification, after initial denaturation at 95 °C for 5 min, 35 cycles of amplification (95 °C for 30 s, 54 °C for 30 s, and extension at 72 °C for 1 min) were

carried out. The reaction was completed with a 10-min elongation step at 72 °C.

DNA-sequencing and analysis

All DNA-sampled were quantified using the Qubit 2.0 Fluorometer (Invitrogen, Carlsbad, CA, USA). For bacteria and archaea, separate libraries were built. Approximately 100 ng of each sample was added applying the amplicon fusion method (Ion Plus Fragment Library Kit, MAN0006846, Life Technologies). For quantification, the Agilent 2100 Bioanalyzer (Agilent Technologies Inc, Palo Alto, CA, USA) was used. PCRs were carried out applying the Ion PGM Template OT2 400 kit as stated by the manufacturer (MAN0007218, Revision 3.0 Life Technologies). For the final sequencing step, an Ion 318 Chip v2 on a Personal Genome Machine (PGM) (IonTorrent™, Life Technologies) at Life Sequencing S.L. (Life Sequencing, Valencia, Spain) was used. Here the Ion PGM Sequencing 400 kit was applied, following the manufacturer's instructions (publication number MAN0007242, revision 2.0, Life Technologies).

After removing short (<100 bp) and low-quality (<q15) reads, resulting sequences were split and barcode sequences were trimmed. Final sequences were then analysed using Mothur [59]. Based on the k-mer algorithm, sequences were aligned to the 16S reference from the Greengenes database. In the case of eubacteria, assignments were performed at the phylum level. Assignments with a similarity percentage lower than 70% were not considered for further analysis. In case of archaea, amplicons were analysed at the genus level and the cut-off was set to 93%.

Protein extraction, identification and data analysis

Protein extraction was performed using the Novipure Soil Protein Extraction Kit (MO BIOS Laboratories Inc). Total protein extracts were precipitated with TCA (Trichloroacetic Acid) to clean total extracts, and pellets were dissolved with 100 µL of 8 M Urea, 0.5 M TEAB (Triethylammonium bicarbonate buffer). The protein concentration in the samples was determined using Qubit 2.0 Fluorometer (Invitrogen, Carlsbad, CA, USA). Then, 20 µg of each sample was digested as described in the following protocol. Cysteine residues were reduced by 2 mM DTT (DL-Dithiothreitol) in 50 mM ABC (Ammonium bicarbonate) at 60 °C for 20 min. Sulphydryl groups were alkylated with 5 mM IAM (iodoacetamide) in 50 mM ABC in the dark at room temperature for 30 min. IAM excess was neutralized with 10 mM DTT in 50 mM ABC, 30 min at room temperature. Each sample was subjected to trypsin digestion with 500 ng (100 ng/µL) of sequencing grade-modified trypsin (Promega) in 50 mM

ABC at 37 °C overnight. The reaction was stopped with TFA (trifluoroacetic acid) at a final concentration of 0.1%. Final peptide mixture was concentrated in a speed vacuum and suspended in 65 µL of 2% CAN, 0.1%TFA. Finally, 1.5 µg of each sample was used for protein identification by LC_MS/MS analysis and label-free differential expression analysis. For that 5 µL of each sample was loaded onto a trap column (NanoLC Column, 3 µm C18-CL, 75 µm × 15 cm; Eksigent) and desalted with 0.1% TFA at 3 µL/min during 10 min. The peptides were then loaded onto an analytical column (LC Column, 3 µm C18-CL, 75 µm × 12 cm, Nikkyo) equilibrated in 5% acetonitrile 0.1% FA (formic acid). Elution was carried out with a linear gradient from 5a35% B in A for 120 min. (A: 0.1% FA; B: ACN, 0.1% FA) at a flow rate of 300 nL/min. Peptides were analysed in a mass spectrometer nanoESI-qTOF (5600 TripleTOF, ABSCIEX).

Eluted peptides were ionized applying 2.8 kV to the spray emitter. Analysis was carried out in a data-dependent mode. Survey MS1 scans were acquired from 350–1250 m/z for 250 ms. The quadrupole resolution was set to 'UNIT' for MS2 experiments, which were acquired 100–1500 m/z for 50 ms in 'high sensitivity' mode. Following which switch criteria were used: charge: 2+ to 5+; minimum intensity; 70 counts per second (cps). Up to 25 ions were selected for fragmentation after each survey scan. Dynamic exclusion was set to 25 s.

ProteinPilot default parameters were used to generate peak list directly from 5600 TripleTOF wiff files. The Paragon algorithm of ProteinPilot v 4.5 was used to search Uniprot bacteria and Archaea protein database with the following parameters: trypsin specificity, cys-alkylation and the search effort set to through with FDR to multiple test correction.

To avoid using the same spectral evidence in more than one protein, the identified proteins were grouped based on MS/MS spectra by the ProteinPilot Pro group algorithm. The Peak View v1.1 (SCIEX) software was used to generate peptide and protein areas from ProteinPilot result files and to perform a multivariate data analysis.

Differential expression analysis was performed using the Limma package (<http://bioconductor.org/packages/limma/>), fitting a linear model using an appropriate design matrix. A contrast matrix was set to make comparisons of interest, in our case 37 versus 55 °C. For the contrast of interest the package computed fold changes and t-statistics. After fitting a linear model, the standard errors were moderated using an empirical Bayes method to obtain moderated t-statistics. The function top Table was used to present a list of the proteins most likely to be differentially expressed for a given contrast. FDR was used to adjust the *p* value for multiple testing.

Additional files

Additional file 1: Figure S3. SDS-PAGE displaying the protein profiles.

Additional file 2: Table S4. Mascot results.

Additional file 3: Table S5. Differentially expressed proteins.

Additional file 4: Table S1. Description of the used seed sludge.

Additional file 5: Table S2. Overview of reaction stages and reactor performance.

Additional file 6: Table S6. Number of sequences and mean length for bacteria from the acidification stages.

Additional file 7: Table S7. Number of reads and mean length of reads for bacteria from the methane stages.

Additional file 8: Table S8. Number of reads and mean length of reads for archaea from the methane stages.

Abbreviations

CD: co-digester (sludge from industrial CSTR); COD: chemical oxygen demand; CSTR: continuous stirred tank reactor; LB: leach bed; Leach: Leachate from leach-bed system; RT: room temperature; SW: sewage; TS: total solids; TVFA: total volatile fatty acids; VFA: volatile fatty acids.

Authors' contributions

CA, OL and MP designed the work. CS and CA performed the digestion experiments and sampling. CA extracted DNA and analysed 16S-rDNA amplicons. CS and CA performed chemical analyses. OA and JP performed proteomics. CA, JP and MP wrote the manuscript. All authors have read and approved the final version of the manuscript.

Author details

¹ Cavanilles Institute of Biodiversity and Evolutionary Biology, Universitat de València, C/ José Beltran 2, 46980 Paterna, Spain. ² Institute for Integrative Systems Biology (I2SysBio, Universitat de València-CSIC), C/ José Beltran 2, 46980 Paterna, Spain. ³ Robert Boyle Institut e.V., Im Steinfeld 10, 07751 Jena, Germany. ⁴ Departament de Bioquímica i Biologia Molecular, Universitat de València, Paterna, Spain. ⁵ Servei Central de Suport a la Investigació Experimental (SCSIE), Universitat de València-CSIC, Paterna, Spain. ⁶ Bio H2 Energy GmbH, Im Steinfeld 10, 07751 Jena, Germany. ⁷ Darwin Bioprospecting Excellence, S.L. Parc Científic Universitat de València, C/ Catedrático Agustín Escardino Benlloch, 9, 46980 Paterna, Valencia, Spain. ⁸ Institute for Integrative Systems Biology (I2SysBio, Universitat de València-CSIC), Postal Code 22085, 46071 Paterna, València, Spain.

Acknowledgements

We thank our students and traineeships Robert Förster, Justus Hardegen, Sonia Casani and Sandra Jörg for technical assistance. Further we thank Dr. Peter Miethe from the research centre for medical technology and biotechnology (FZMB) in Bad Langensalza for his suggestions regarding the title. We are grateful for funding of the work by the Federal Ministry of Economic Affairs and Energy in Germany (Funding Numbers FKZ03KB1 10A; 16KN041 331, KF21 12205SA4 and KF3400701SA4). Servei Central de Suport a la Investigació Experimental (SCSIE) from University of Valencia belongs to ProteoRed, PRB2-ISCIII, supported by grant PT13/0001, of the PE I+D+i 2013–2016, funded by ISCIII and FEDERPT13/0001.

Competing interests

The authors declare that they have no competing interests.

Publisher's Note

Springer Nature remains neutral with regard to jurisdictional claims in published maps and institutional affiliations.

Received: 3 April 2017 Accepted: 27 June 2017

Published online: 03 July 2017

References

- McCarty PL. The development of anaerobic treatment and its future. *Water Sci Technol.* 2001;44:149–56.
- Wirth R, Kovács E, Maróti G, Bagi Z, Rákhely G, Kovács KL. Characterization of a biogas-producing microbial community by short-read next generation DNA sequencing. *Biotechnol Biofuels.* 2012;5:41.
- Haarstrick A, Hempel DC, Ostermann L, Ahrens H, Dinkler D. Modelling of the biodegradation of organic matter in municipal landfills. *Waste Manag Res.* 2001;19:320–31.
- Ng A, Melvin WT, Hobson PN. Identification of anaerobic digester bacteria using a polymerase chain reaction method. *Bioresour Technol.* 1994;47:73–80.
- Godon JJ, Zumstein E, Dabert P, Habouzit F, Moletta R. Molecular microbial diversity of an anaerobic digester as determined by small-subunit rDNA sequence analysis. *Appl Environ Microbiol.* 1997;63:2802–13.
- Ritari J, Koskinen K, Hultman J, Kurolo JM, Kymäläinen M, Romantschuk M, Paulin L, Auvinen P. Molecular analysis of meso- and thermophilic microbiota associated with anaerobic biowaste degradation. *BMC Microbiol.* 2012;12:121.
- Sundberg C, Al-Soud WA, Larsson M, Alm E, Yekta SS, Svensson BH, et al. 454 pyrosequencing analyses of bacterial and archaeal richness in 21 full-scale biogas digesters. *FEMS Microbiol Ecol.* 2013;85:612–26.
- Abendroth C, Vilanova C, Günther T, Luschning O, Porcar M. Eubacteria and Archaea communities in seven mesophilic anaerobic digester plants. *Biotechnol Biofuels.* 2015;8:87. doi:10.1186/s13068-015-0271-6.
- Hanreich A, Schimpf U, Zakrzewski M, Schlüter A, Benndorf D, Heyer R, Rapp E, Pühler A, Reichl U, Klocke M. Metagenome and metaproteome analyses of microbial communities in mesophilic biogas-producing anaerobic batch fermentations indicate concerted plant carbohydrate degradation. *Syst Appl Microbiol.* 2013;36:330–8.
- Heyer R, Kohrs F, Benndorf D, Rapp E, Kausmann R, Heiermann M, Klocke M, Reichl U. Metaproteome analysis of the microbial communities in agricultural biogas plants. *N Biotechnol.* 2013;30:614–22.
- Baccay RA, Hashimoto AG. Acidogenic and methanogenic fermentation of causticized straw. *Biotechnol Bioeng.* 1984;26:885–91.
- Dinopoulou G, Rudd T, Lester JN. Anaerobic acidogenesis of a complex wastewater: I. The influence of operational parameters on reactor performance. *Biotechnol Bioeng.* 1988;5:958–68.
- Abendroth C, Wünsche E, Luschning O, Bürger C, Günther T. Producing high-strength liquor from mesophilic batch acidification of chicken manure. *Waste Manag Res.* 2015;33:291–4.
- Gijzen HJ, Zwart KB, Verhagen FJ, Vogels GP. High-Rate two-phase process for the anaerobic degradation of cellulose, employing rumen microorganisms for an efficient acidogenesis. *Biotechnol Bioeng.* 1988;31:418–25.
- Voolapalli RK, Stuckey DC. Hydrogen production in anaerobic reactors during shock loads—influence of formate production and H₂ kinetics. *Water Res.* 2001;35:1831–41.
- Hwang S, Lee Y, Yang K. Maximization of acetic acid production in partial acidogenesis of swine wastewater. *Biotechnol Bioeng.* 2001;75:521–9.
- Yu HQ, Fang HHP. Acidogenesis of dairy wastewater at various pH levels. *Water Sci Technol.* 2002;45:201–6.
- Yu HQ, Fang HHP. Acidogenesis of gelatin-rich wastewater in an upflow anaerobic reactor: influence of pH and temperature. *Water Res.* 2003;37:55–66.
- Demeyer D, Henderickx H, Van Nevel C. Influence of pH on fatty acid inhibition of methane production by mixed rumen bacteria. *Arch Int Physiol Biochim.* 1967;75:555–6.
- Dareioti MA, Kornaros M. Anaerobic mesophilic co-digestion of ensiled sorghum, cheese whey and liquid cow manure in a two-stage CSTR system: effect of hydraulic retention time. *Bioresour Technol.* 2014;175:553–62.
- Trzcinski AP, Stuckey DC. Contribution of acetic acid to the hydrolysis of lignocellulosic biomass under abiotic conditions. *Bioresour Technol.* 2015;185:441–4.
- Kumar G, Park JH, Sivagurunathan P, Lee SH, Park DH, Kim SH. Microbial responses to various process disturbances in a continuous hydrogen reactor fed with galactose. *J Biosci Bioeng.* 2017;123:216–22.
- Kumar G, Sivagurunathan P, Pugazhendhi A, Thi NBD, Zhen G, Kuppam C, Kadier A. A comprehensive overview on light independent fermentative hydrogen production from wastewater feedstock and possible integrative options. *Energy Convers Manag.* 2016;141:390–402.

24. Kumar G, Sivagurunathan P, Sen B, Kim SH, Lin CY. Mesophilic continuous fermentative hydrogen production from acid pretreated de-oiled jatropha waste hydrolysate using immobilized microorganisms. *Bioresour Technol.* 2017;240:137–43. doi:[10.1016/j.biortech.2017.03.059](https://doi.org/10.1016/j.biortech.2017.03.059).
25. Koutinas A, Kanellaki M, Bekatorou A, Kandyli A, Pissaridi K, Dima A, Boura K, Lappa K, Tsafrakidou P, Stergiou PY, Foukis A, Gkini OA, Papamichael EM. Economic evaluation of technology for a new generation biofuel production using wastes. *Bioresour Technol.* 2016;200:178–85.
26. Park GW, Seo C, Jung K, Chang HN, Kim YC. A comprehensive study on volatile fatty acids production from rice straw coupled with microbial community analysis. *Bioprocess Biosyst Eng.* 2015;38:1157–66.
27. Seon J, Lee T, Lee SC, Pham HD, Woo HC, Song M. Bacterial community structure in maximum volatile fatty acids production from alginate in acidogenesis. *Bioresour Technol.* 2014;157:22–7.
28. Kohrs F, Heyer R, Magnussen A, Benndorf D, Muth T, Behne A, Rapp E, Kausmann R, Heiermann M, Klocke M, Reichl U. Sample prefractionation with liquid isoelectric focusing enables in depth microbial metaproteome analysis of mesophilic and thermophilic biogas plants. *Anaerobe.* 2014;29:59–67.
29. Jungers JM, Fargione JE, Sheaffer CC, Wyse DL, Lehman C. Energy potential of biomass from conservation grasslands in Minnesota, USA. *PLoS ONE.* 2013. doi:[10.1371/journal.pone.0061209](https://doi.org/10.1371/journal.pone.0061209).
30. Sivagurunathan P, Kumar G, Mudhoo A, Rene ER, Saratale GD, Kobayashi T, Xu K, Kim SH, Kim DH. Fermentative hydrogen production using lignocellulose biomass: an overview of pre-treatment methods, inhibitor effects and detoxification experiences. *Renew Sust Energy Rev.* 2017;77:28–42.
31. Klocke M, Mähner T, Mundt K, Souidi K, Linke B. Microbial community analysis of a biogas producing completely stirred tank reactor fed continuously with fodder beet silage as mono-substrate. *Syst Appl Microbiol.* 2007;30:139–51.
32. Ziganshin AM, Liebetreu J, Pröter J, Kleinstüber S. Microbial community structure and dynamics during anaerobic digestion of various agricultural waste materials. *Appl Microbiol Biotechnol.* 2013;97:5161–74.
33. Moset V, Poulsen M, Wahid R, Højberg O, Møller HB. Mesophilic versus thermophilic anaerobic digestion of cattle manure: methane productivity and microbial ecology. *Microb Biotechnol.* 2015;8:787–800.
34. Ghasimi DSM, Tao Y, Kreuk M, Zandvoort MH, van Lier JB. Microbial population dynamics during long-term sludge adaptation of thermophilic and mesophilic sequencing batch digesters treating sewage fine sieved fraction at varying organic loading rates. *Biotechnol Biofuels.* 2015;8:171.
35. Kim M, Ahn YH, Speece RE. Comparative process stability and efficiency of anaerobic digestion; mesophilic vs. thermophilic. *Water Res.* 2002;36:4369–85.
36. Vindis P, Mursec B, Janzekovic M, Cus F. The impact of mesophilic and thermophilic anaerobic digestion on biogas production. *J Achiev Manuf Eng.* 2009;36:192–8.
37. Moset V, Poulsen M, Wahid R, Højberg O, Møller HB. Mesophilic versus thermophilic anaerobic digestion of cattle manure: methane productivity and microbial ecology. *Microb Biotechnol.* 2014;8:787–800.
38. McEniry J, Allen E, Murphy JD, O'Kiely P. Grass for biogas production: the impact of silage fermentation characteristics on methane yield in two contrasting biomethane potential test systems. *Renew Energy.* 2014;63:524–30.
39. Tang H, Shi X, Wang X, Hao H, Zhang XM, Zhang LP. Environmental controls over actinobacteria communities in ecological sensitive Yanshan mountains zone. *Front Microbiol.* 2016;7:343.
40. Kusumi A, Li X, Osuga Y, Kawashima A, Gu JD, Nasu M, Katayama Y. Bacterial communities in pigmented biofilms formed on the sandstone bas-relief walls of the Bayon Temple, Angkor Thom, Cambodia. *Microbes Environ.* 2013;28:422–31.
41. Esteban DJ, Hysa B, Bartow-McKenney C. Temporal and spatial distribution of the microbial community of Winogradsky columns. *PLoS ONE.* 2015. doi:[10.1371/journal.pone.0134588](https://doi.org/10.1371/journal.pone.0134588).
42. Prabhu MS, Mutnuri S. Anaerobic co-digestion of sewage sludge and food waste. *Waste Manag Res.* 2016;34:307–15.
43. Maragkaki AE, Fountoulakis M, Kyriakou A, Lasaridi K, Manios T. Boosting biogas production from sewage sludge by adding small amount of agro-industrial by-products and food waste residues. *Waste Manag.* 2017. doi:[10.1016/j.wasman.2017.04.024](https://doi.org/10.1016/j.wasman.2017.04.024).
44. Guven H, Akca MS, Iren E, Keles F, Ozturk I, Altinbas M. Co-digestion performance of organic fraction of municipal solid waste with leachate: preliminary studies. *Waste Manag.* 2017. doi:[10.1016/j.wasman.2017.04.039](https://doi.org/10.1016/j.wasman.2017.04.039).
45. Zhang M, Yang C, Jing Y, Li J. Effect of energy grass on methane production and heavy metal fractionation during anaerobic digestion of sewage sludge. *Waste Manag.* 2016;58:316–23.
46. Gannoun H, Omri I, Chouari R, Khelifi E, Keskes S, Godon JJ, Hamdi M, Sghir A, Bouallagui H. Microbial community structure associated with the high loading anaerobic codigestion of olive mill and abattoir wastewaters. *Bioresour Technol.* 2016;201:337–46.
47. Rui J, Li J, Zhang S, Yan X, Wang Y, Li X. The core populations and co-occurrence patterns of prokaryotic communities in household biogas digesters. *Biotechnol Biofuels.* 2015;8:158.
48. Wang C, Dong D, Wang H, Müller K, Qin Y, Wang H, Wu W. Metagenomic analysis of microbial consortia enriched from compost: new insights into the role of Actinobacteria in lignocellulose decomposition. *Biotechnol Biofuels.* 2016;9:22.
49. Lewin GR, Carlos C, Chevrette MG, Horn HA, McDonald BR, Stankey RJ, Fox BG, Currie CR. Evolution and ecology of actinobacteria and their bioenergy applications. *Annu Rev Microbiol.* 2016;70:235–54.
50. Poirier S, Desmond-Le Quémener E, Madigou C, Bouchez T, Chapleur O. Anaerobic digestion of biowaste under extreme ammonia concentration: identification of key microbial phylogenies. *Bioresour Technol.* 2016;207:92–101.
51. Poirier S, Bize A, Bureau C, Bouchez T, Chapleur O. Community shifts within anaerobic digestion microbiota facing phenol inhibition: towards early warning microbial indicators? *Water Res.* 2016;100:296–305.
52. Wawrik B, Marks CR, Davidova IA, McInerney MJ, Pruitt S, Duncan K, Sufita JM, Callaghan AV. Methanogenic paraffin degradation proceeds via alkane addition to fumarate by “Smithella” spp. mediated by a syntrophic coupling with hydrogenotrophic methanogens. *Environ Microbiol.* 2016;8:2604–19.
53. Auguet O, Pijuan M, Batista J, Borrego CM, Gutierrez O. Changes in microbial biofilm communities during colonization of sewer systems. *Appl Environ Microbiol.* 2015;81:7271–80.
54. Jo Y, Kim J, Hwang S, Lee C. Anaerobic treatment of rice winery wastewater in an upflow filter packed with steel slag under different hydraulic loading conditions. *Bioresour Technol.* 2015;193:53–61.
55. Yang D, Fan X, Shi X, Lian S, Qiao J, Guo R. Metabolomics reveals stage-specific metabolic pathways of microbial communities in two-stage anaerobic fermentation of corn-stalk. *Biotechnol Lett.* 2014;36:1461–8.
56. Lü F, Bize A, Guillot A, Monnet V, Madigou C, Chapleur O, Mazéas L, He P, Bouchez T. Metaproteomics of cellulose methanisation under thermophilic conditions reveals a surprisingly high proteolytic activity. *ISME J.* 2014;8:88–102.
57. VDI 4630 (2006) Fermentation of organic materials, characterisation of the substrate, sampling, collection of material data, fermentation tests. Düsseldorf: The Association of German Engineers (VDI).
58. Klindworth A, Pruesse E, Schweer T, Peplies J, Quast C, Horn M, et al. Evaluation of general 16S ribosomal RNA gene PCR primers for classical and next-generation sequencing-based diversity studies. *Nucleic Acids Res.* 2013;41:e1.
59. Schloss PD, Westcott SL, Ryabin T, Hall JR, Hartmann M, Hollister EB, et al. Introducing MOTHUR: open-source, platform-independent, community-supported software for describing and comparing microbial communities. *Appl Environ Microbiol.* 2009;75:7537–41.

Towards a Microbial Thermoelectric Cell

Raúl Rodríguez-Barreiro¹, Christian Abendroth¹, Cristina Vilanova¹, Andrés Moya^{1,2}, Manuel Porcar^{1,3*}

1 Cavanilles Institute of Biodiversity and Evolutionary Biology, Universitat de València, València, Spain, **2** Unidad Mixta de Investigación en Genómica y Salud, Centro Superior de Investigación en Salud Pública (CSISP), València, Spain, **3** Fundació General de la Universitat de València, València, Spain

Abstract

Microbial growth is an exothermic process. Biotechnological industries produce large amounts of heat, usually considered an undesirable by-product. In this work, we report the construction and characterization of the first microbial thermoelectric cell (MTC), in which the metabolic heat produced by a thermally insulated microbial culture is partially converted into electricity through a thermoelectric device optimized for low ΔT values. A temperature of 41°C and net electric voltage of around 250–600 mV was achieved with 1.7 L baker's yeast culture. This is the first time microbial metabolic energy has been converted into electricity with an *ad hoc* thermoelectric device. These results might contribute towards developing a novel strategy to harvest excess heat in the biotechnology industry, in processes such as ethanol fermentation, auto thermal aerobic digestion (ATAD) or bioremediation, which could be coupled with MTCs in a single unit to produce electricity as a valuable by-product of the primary biotechnological product. Additionally, we propose that small portable MTCs could be conceived and inoculated with suitable thermophilic or hyperthermophilic starter cultures and used for powering small electric devices.

Citation: Rodríguez-Barreiro R, Abendroth C, Vilanova C, Moya A, Porcar M (2013) Towards a Microbial Thermoelectric Cell. PLoS ONE 8(2): e56358. doi:10.1371/journal.pone.0056358

Editor: Chenyu Du, University of Nottingham, United Kingdom

Received: October 17, 2012; **Accepted:** January 14, 2013; **Published:** February 26, 2013

Copyright: © 2013 Rodríguez-Barreiro et al. This is an open-access article distributed under the terms of the Creative Commons Attribution License, which permits unrestricted use, distribution, and reproduction in any medium, provided the original author and source are credited.

Funding: Financial support was provided by grant Prometeo/2009/092 (Conselleria d'Educació, Generalitat Valenciana, Spain) to AM. The funders had no role in study design, data collection and analysis, decision to publish, or preparation of the manuscript.

Competing Interests: The authors have a patent describing the results they report on their article: The reference of the patent is P201200977 (application number for the Spanish Office of Patents and Trademarks, OEPM). The authors of the patent are the same of the manuscript submitted to PLOS ONE: Porcar, M; Rodríguez-Barreiro, R; Abendroth, C; Vilanova, C; and Moya, A. The complete title is "Dispositivo termoeléctrico microbiano y método asociado a dicho dispositivo" (Thermoelectric Microbial device and associated method). The authors have prepared the patent and the registration in collaboration with the Research Transfer Office (OTRI) of the University of Valencia (contact person, Marta Garcés: marta.garces@uv.es). The authors formally confirm that this patent does not alter the authors' adherence to all the PLOS ONE policies on sharing data and materials.

* E-mail: manuel.porcar@uv.es

Introduction

Both developed and fast growing developing countries exhibit steadily growing energy demands. Taking into account the limited nature of oil, coal and gas reservoirs, this could obviously lead to a shortage of standard (fossil) fuels in the relatively near future. The lack of sustainability of current fossil-centered energy strategies, as well as the recent extremely serious accident at Fukushima Daiichi power facility [1] have increased the concerns about the economic and environmental consequences of relying on these energy sources, leading to some dramatic shifts in energy policies, like in Germany [2]. It is widely accepted that massive fossil fuel consumption, which results in the production of nine billion metric tons of atmospheric carbon per year [3], is at least partially responsible for current global warming. Therefore, alternative non-fossil non-nuclear technologies are seen as promising, albeit not fully competitive. Among these, biomass-based energy has been suggested as one of the most promising technologies for renewable energy production [4,5]. Biomass from crops; urban, industrial or agricultural wastes; green algae, cyanobacteria or other microbial cultures, are renewable organic resources that are suitable for energy production in the form of biofuels (mainly, but not limited to, bioethanol and biodiesel), and electricity.

Besides lignocellulosic combustion-based power production, a biological system allowing direct conversion of biomass into electricity already exists: a broad range of organic substances can be oxidized by electrogenic bacteria, which transfer electrons to an

anode in a simple device known as a Microbial Fuel Cell (MFC). At the cathode, other useful products can be generated, including hydrogen, methane, and hydrogen peroxide [6,7,8]. The electric yield of MFCs has increased dramatically in recent years, mainly by increasing the ratio of the area of the electrodes/volume in the reactor, with best yields reaching up to 2–7 W/m². A moderate MFC unit, of about 1 L, can produce enough electricity to power a small propeller for more than one year [9]. However, MFCs seem to work better at small scales, as scaling-up faces important challenges [9].

Many bacterial species have been reported to display electroactive properties, including members of common genera such as *Clostridium*, *Pseudomonas*, *Geobacter* or *Shewanella*. A few eukaryotic microorganisms have been assayed for power production in MFCs. Baker's yeast *Saccharomyces cerevisiae* has proven able to transfer electrons to an anode in two independent studies [10,11] with moderate efficiency. In both reports, researchers found net voltage values of about 0.33 V for 1 L reactors.

To date MFCs are still the only direct method to microbiologically convert biomass into electricity. Nonetheless, there is possibly another non-fuel alternative. Since microbial growth is an exothermic process, it produces heat, which is a by-product that usually goes unnoticed in lab-scale cultures but which has a strong impact on the design and performance of industrial-scale microbial fermentations. Almost 90% of the heat produced in a microbial fermentation is reported to be metabolic heat; and almost all this heat is removed through forced heat exchange [12].

The thermoelectric or Peltier-Seebeck effect is the direct conversion of electric voltage to temperature differences (Peltier effect) and vice-versa (Seebeck effect). Theoretically, an electric current would be produced by coupling an exothermic microbial culture with an endothermic reaction –or, alternatively, a heat sink– through a thermoelectric cell. If the thermal energy from exothermic microbial cultures could be turned into electricity efficiently, power-producing devices could be designed and coupled to existing microbial reactors within a range of applications (alcoholic fermentations, bioremediation, waste treatment, autotrophic thermal aerobic digestion ATAD, etc.).

Here, we report the characterization of the first Microbial Thermoelectric Cell, a bioreactor specifically designed for power production through a completely different mechanism than that operating in MFCs: the thermoelectric effect. Our results might contribute to providing a new scenario for the future development of microbial-based cellular electricity facilities, which might be useful for local electric production and heat recycling in a wide range of biological processes.

Materials and Methods

Construction of the MTC

In order to implement a thermoelectric-based power generator, a reactor was designed able to i) sustain microbial growth; ii) remain thermally isolated on most of its surface; and iii) efficiently transfer heat through a relatively small area to a thermoelectric device. One of us (M. Porcar) had previously designed an LCC (Liquid Culture Calorimeter) for microbial growth, suitable for fine recordings of internal temperature changes through a thermocouple [13]. Based on the LCC, we conceived a Microbial Thermoelectric Cell (MTC hereon) to produce power from a microbial culture by the Peltier-Seebeck effect. Figure 1 shows the structure of the MTC. The core of the reactor is a 1.9 L glass container from a commercial vacuum flask. The flask was placed inside an expanded polystyrene (EPS) box and the gap filled with a polyurethane foam spray (Silicex Fischer, Fisher Ibérica, Tarra-gona, Spain). The box was then inserted into a second EPS isolation box. The upper part of the MTC was drilled and a copper bar (20 mm in diameter) inserted through the hole. The upper part of the copper bar was adapted in order to allow a TE-Power Probe thermal harvester (MicroPelt, Germany) to be screwed through a 1/4" Whitworth thread (DIN 2999, JIS B0203, ISO 7/1). TE-Power Probe is a prototype of an integrated proximity thermoharvester designed to replace primary batteries in wireless systems operating in duty cycle mode. The key element of the TE-Power Probe is the MPG-D751 thermogenerator, which produces electricity from a rather low gradient of temperature. The TE-Power Probe is originally designed to attach to a heat source in the shape of piping that carries a hot fluid, and heat is dissipated through an aluminum heat sink, with the resulting temperature gradient allowing power production by the MPG-D751 thermogenerator. In our experiments, temperature changes in different parts of the Probe were measured by PT-100 sensors. Since the TE-Power Probe is specifically designed to operate using natural convection to ambient air, we mounted it horizontally, as suggested by the manufacturer.

The two EPS isolation layers of the MTC were shaped so the round bottom of the vacuum flask would fit. The flask bottom was placed conveniently close (20 mm) to the bottom of the MTC in order to allow stirring by a magnetic stirrer. When recordings were to be taken, the MTC was first filled with 1.8 L of medium; a small magnet was added; the MTC was placed inside a standard laboratory magnetic stirrer set at low speed (600 rpm); the

inoculum was then added, and the copper bar with the screwed TE-Power Probe finally set in place. This configuration was modified for characterization purposes in some experiments, as described in sections 2.4 and 2.5.

Yeast Strains, Media and Culture Conditions

The following six diploid *S. cerevisiae* strains, from the wine industry or genetic modifications thereof, were used: EC118, L2056, 3aS2Δ, T73, D170, and TTRX2. All the strains were kindly provided by Prof. Emilia Matallana (IATA, Valencia, Spain). In order to assess their exothermic abilities, independent cultures were set in filter-sterilized YPD (20 g/L peptone, 10 g/L yeast extract, with 18% sugar), and the internal temperature of the cultures (grown overnight in non-isolated Erlenmeyer flasks) was continuously measured. Thermotolerance was assessed by growing the strains at 30, 37 and 41°C. After an overnight incubation under low stirring, the OD₆₀₀ of the six overnight cultures was measured.

For standard experiments after strain selection, the filter-sterilized 18% sucrose YPD was inoculated with 1:50 of an overnight yeast pre-culture grown at 30°C, and subjected to low stirring for 120 h.

Data Acquisition, Monitoring and Recording

The MTC was connected to a PC in order to record internal and external temperatures and the output current provided by the heat harvester TE-Power Probe (Fig. S1).

The internal temperature of the MTC was measured by a thin T-type thermocouple inserted into the microbial culture and connected to a PC through a data logger, as previously described [13]. Another thermocouple recording room temperature was also set in place. The thermocouples were connected to an acquisition card inserted on the data logger, which was connected via a GPIB cable to a PC with an acquisition software that one of us (R. Rodríguez-Barreiro) conceived specifically for this work (Fig. S1). The TE-Power Probe output was also connected to the PC, which yielded two additional temperature recordings by using two Pt-100 sensors (that of the cold and hot sides of the thermogenerator device) and the output voltage. The connections between the thermocouples and the data logger were performed on an ice-water mixture to take into account the unwanted background electric voltage, due to the junction of dissimilar metals in the thermocouple-data logger connection. Finally, a thermocouple was inserted inside the box containing the ice-water mixture in order to verify that the temperature of the datalogger-thermocouple connections was kept at 0°C.

Temperature records (and, when TE-Power Probe was connected, electric power) were taken every 6 minutes throughout the experiment.

Identification Assay to Estimate Broth Heat Capacity and Global Thermal Resistance of MTC

In order to estimate the heat capacity of the broth ($m \cdot C_p$) and the global thermal resistance (R_g), the MTC (without TE-Power Probe) was set up under the following conditions: first, an electrical resistance was placed inside the MTC to generate a controlled heat flow, as consequence of the Joule effect induced by an external voltage input through the resistance. Second, the MTC was loaded with room-temperature sterile broth with 1 g/L nipagine supplementation to avoid contamination by yeasts. Broth was subjected to continuous stirring and room temperature was kept constant. Throughout the experiment, broth and room temperatures and the power generated in the resistance were

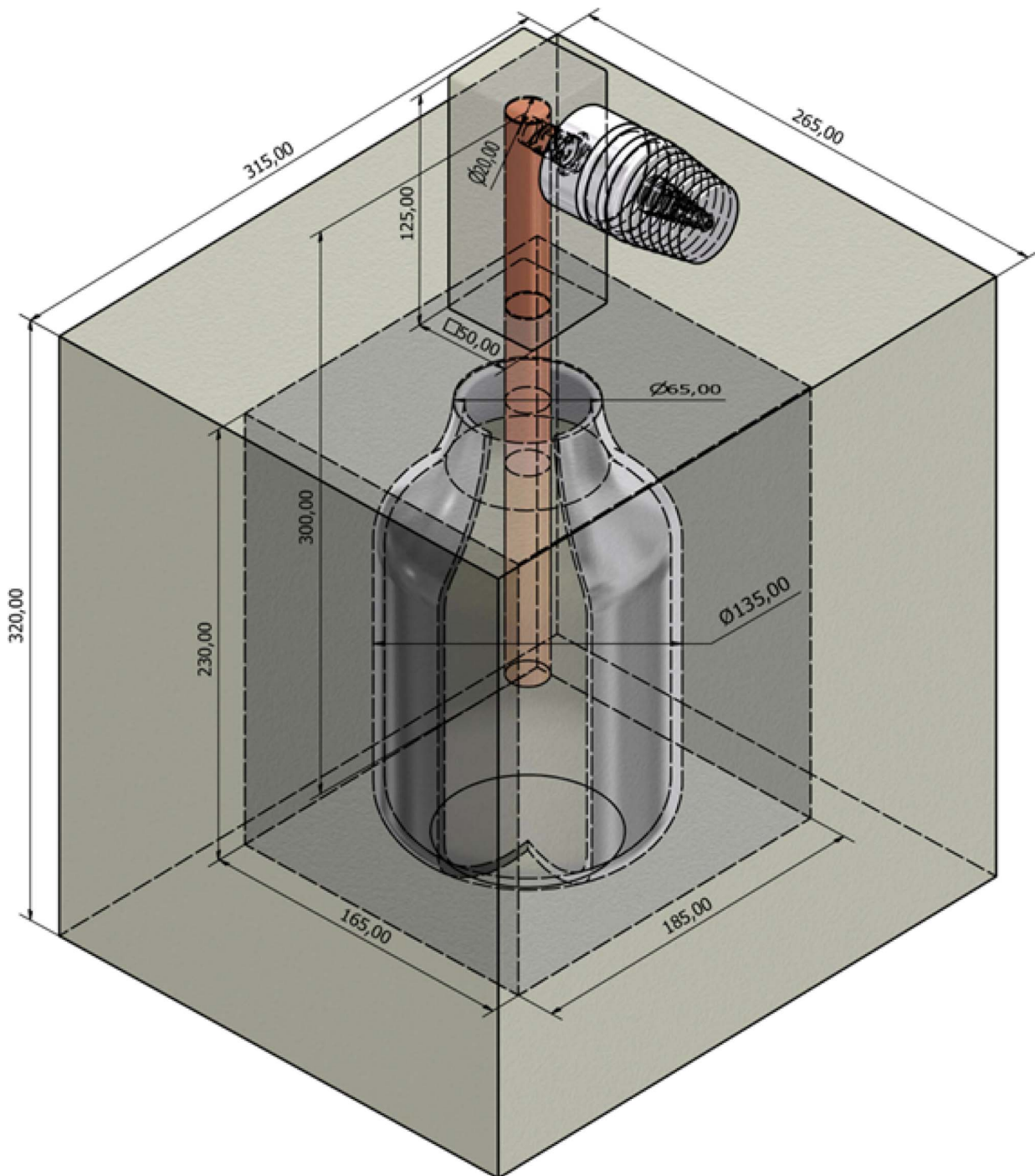


Figure 1. Schematic drawing of the Microbial Thermoelectric Cell (Auto-CAD). All dimensions are given in mm.
doi:10.1371/journal.pone.0056358.g001

continuously measured. To ensure the initial steady-state conditions (broth temperature equal to room temperature), the system was kept in the off mode for approximately 20 h before applying the input voltage.

Theory

The equation for the heat flow balance corresponding to the MTC we describe in this work can be stated as follows:

$$\sum \text{Heat accumulated} = \sum \text{Heat generated} - \sum \text{Heat lost} \quad (1)$$

Heat accumulated is a consequence of the variation in broth temperature. Since there is no forced cooling of the system, heat flow losses are due only to heat transfer from the culture to the

environment through both the MTC surface and the TE-Power Probe thermogenerator. For calibration purposes, we first set the MTC to generate a heat flow from an electric resistance placed inside the vacuum flask through the Joule effect. In standard experiments, heat flow was obtained from the metabolic heat as a consequence of microbial growth.

Therefore, the heat flow balance equation can be written for the MTC as follows (a definition of all the symbols used throughout the MTC modelling is available in Table 1):

$$\dot{Q}_{acc} = P_J + \dot{Q}_p - \dot{Q}_{env} - \dot{Q}_{Th} \quad (2)$$

Where Q_{acc} is the heat flow accumulated in the broth; P_J is the heat flow due to the Joule effect; Q_p is the heat flow due to microbial metabolism; Q_{env} is the heat flow loss through the MTC surface to

the environment; and Q_{Th} is the heat flow loss through the copper bar connected to the TE-Power Probe.

Accumulation Terms

Heat accumulation (Q_{acc}) in a particular body is determined by the variation in its temperature (dT_i/dt) and by its heat capacity ($m_i \cdot C_{pi}$). In the MTC, heat can be accumulated in the broth (subscript “b”), the vacuum flask (“v”) and the insulation walls (“w”), as follows:

$$\dot{Q}_{acc} = m_b \cdot C_{pb} \cdot \frac{dT_b}{dt} + m_v \cdot C_{pv} \cdot \frac{dT_v}{dt} + m_w \cdot C_{pw} \cdot \frac{dT_w}{dt} \quad (3)$$

The MTC is a very simple system with a single sensor to measure the temperature of the broth. Therefore, the equation can

Table 1. Nomenclature used in MTC modelling.

Symbol	Description (units)
α	Seebeck coefficient (V/K)
I	Electrical current (A)
$m \cdot C_p$	Whole system heat capacity (J/K)
$m_b \cdot C_{pb}$	Broth heat capacity (J/K)
$m_v \cdot C_{pv}$	Vacuum flask heat capacity (J/K)
$m_w \cdot C_{pw}$	Insulation walls heat capacity (J/K)
P_J	Electrical input power due to the Joule effect (W)
P_e	Electrical power generated (W)
Q_{acc}	Accumulated heat flow (W)
Q_C	Net heat flow released through the cold side of the thermogenerator (W)
Q_{env}	Heat flow released to the environment (W)
Q_H	Net heat flow absorbed through the hot side of the thermogenerator (W)
Q_j	Heat flow due to the Joule effect inside of the thermogenerator (W)
Q_p	Heat produced by microbial metabolism (W)
Q_{sC}	Heat flow produced in the cold side of the thermogenerator due to the Seebeck effect (W)
Q_{sH}	Heat flow produced in the hot side of the thermogenerator due to the Seebeck effect (W)
Q_t	Heat flow loss due to the natural thermal conduction established between both sides of the thermogenerator (W)
Q_{Th}	Heat flow absorbed from the broth through the copper bar (W)
R	Electrical resistance (Ω)
R_{Cu}	Thermal resistance of the copper bar (K/W)
R_g	Global thermal resistance of the MTC (K/W)
R_i	Internal electrical resistance of the thermogenerator (Ω)
R_{Load}	Electrical resistance connected between the terminals of the thermogenerator (Ω)
R_{Sk}	Thermal resistance of the heat sink (K/W)
R_{th}	Thermal resistance of the thermogenerator (K/W)
T_b	Broth temperature (K)
T_C	Temperature of the cold side of the thermogenerator (K)
T_{env}	Room temperature (K)
T_H	Temperature of the hot side of the thermogenerator (K)
ΔT_{th}	Difference of temperature between the hot and the cold sides of the thermogenerator (K)
T_v	Vacuum flask temperature (K)
T_w	Insulation walls temperature (K)
V_{ext}	Input voltage (V)
V_o	Voltage output in the terminals of the thermogenerator (V)

doi:10.1371/journal.pone.0056358.t001

be simplified:

$$\dot{Q}_{acc} \approx m \cdot C_p \cdot \frac{dT_b}{dt} \quad (4)$$

Where $m \cdot C_p$ represents the whole system heat capacity, deduced from the variation in culture temperature. This parameter can easily be determined under a simplified experimental configuration (described in 2.4) using the model equations described below (section 3.2).

Loss Terms (I): Heat Flow Loss to the Environment

Energy losses through the MTC walls can be due to the natural heat flow (Q_{env}) from the warm internal broth to the relatively cool environment. Since insulation materials in the MTC display low emissivity values, radiation losses can be neglected and Q_{env} can be expressed as follows:

$$\dot{Q}_{env} = \frac{1}{R_g} \cdot (T_b - T_{env}) \quad (5)$$

Where R_g represents the global thermal resistance of the MTC and T_b and T_{env} are the temperatures of the broth and the environment, respectively. This thermal resistance can be experimentally determined under the same conditions described for $m \cdot C_p$ (see 2.4 and 3.2).

Loss Terms (II): Heat Flow Loss Through the TE-Power Probe

The global heat flow through the copper bar (Q_{Th}) is the same than the heat flow absorbed by the hot side of the thermogenerator cell (Q_H) and is composed of: (i) a spontaneous flow due to the difference in temperature between the hot and cold sides of the thermogenerator cell, expressed as $(T_H - T_C)/R_{th}$; (ii) an induced heat flow as a consequence of the conversion of heat to electric power through the Seebeck effect. Then, the heat flow loss through the thermogenerator can be stated as follows [14]:

$$\dot{Q}_{Th} = \dot{Q}_H = \left(\frac{T_H - T_C}{R_{th}} \right) + \left(\alpha \cdot T_H \cdot I - \frac{1}{2} \cdot I^2 \cdot R_i \right) \quad (6)$$

Where $\alpha \cdot T_H \cdot I$ corresponds to heat absorbed by the thermogenerator due to the Seebeck effect, while the term $1/2 \cdot I^2 \cdot R_i$ corresponds to the heat produced as a consequence of the Joule effect, associated to the circulation of the electric current produced through the internal resistance of the thermogenerator. T_H and T_C represent the temperature of the hot and cold sides of the cell, whereas R_{th} and R_i correspond to its internal thermal and electrical resistance, respectively. α is the Seebeck coefficient of the thermogenerator and I is the electrical current obtained from the TE-Power Probe.

Generation Terms (I): Heat Flow Due to the Joule Effect

When an electrical resistance was placed inside the vacuum flask, a heat flow (P_J) was obtained as a consequence of applying an external voltage according to the Joule effect:

$$P_J = \frac{V_{ext}^2}{R} \quad (7)$$

Where V_{ext} is the input voltage and R is the electrical resistance.

Generation Terms (II): Heat Flow Due to Yeast Growth

When the electrical resistance was replaced by a yeast culture, the heat flow was generated as a consequence of the exothermic properties of yeast metabolism. This heat flow, represented as Q_p , was estimated for the different experimental configurations as described below (section 3.3).

Taking all the equations described above together, the general energy balance (Eq. 2) can be written as:

$$m \cdot C_p \cdot \frac{dT_b}{dt} = P_J + \dot{Q}_p - \frac{(T_b - T_{env})}{R_g} - \dot{Q}_{Th} \quad (8)$$

Model Equations for the Estimation of $m \cdot C_p$ and R_g

In order to calculate the global heat capacity and the global thermal resistance of the MTC ($m \cdot C_p$ and R_g , respectively), a simplified experimental set up was used, as explained in section 2.4. Briefly, heat flow was induced in the sterile broth by applying a constant input power through a resistance according to the Joule effect. In this experiment, room temperature was kept constant and the TE-Power Probe was not mounted on the MTC. Therefore, Q_{Th} and Q_p terms (corresponding to the TE-Power Probe and the yeast, respectively) from Eq. 8 are null, so it can be written as the following first-order EDO:

$$m \cdot C_p \cdot \frac{dT_b(t)}{dt} = P_J - \frac{T_b(t) - T_{env}}{R_g} \quad (9)$$

A first-order EDO is mathematically characterized by its gain and its time constant, which can be estimated manually or with a standard mathematical software from experimental data. In Eq. 9, the gain (R_g) and the time constant ($m \cdot C_p \cdot R_g$) were estimated from the experimental values of T_b and P_J .

Estimation of Heat Yield Due to Yeast Metabolism and Calculation of the Electrical Power Generated

Heat yield due to yeast metabolism (Q_p) was estimated from Eq. 8, where the term P_J is null since no electrical resistance was set up inside the flask:

$$\dot{Q}_p(t) = m \cdot C_p \cdot \frac{dT_b(t)}{dt} + \frac{T_b(t) - T_{env}(t)}{R_g} + \dot{Q}_{Th}(t) \quad (10)$$

In the assays where the TE-Power Probe was not included, the term Q_{Th} (the broth heat lost through the copper bar) is null, so Q_p was calculated from the experimental data of T_b and T_{env} using the estimations of $m \cdot C_p$ and R_g previously obtained.

When the TE-Power Probe was included, the metabolic heat yield was calculated from Eq. 10, along with the model equations for TE-Power Probe in order to estimate Q_{Th} (a detailed description of these equations and a schematic representation of associated heat flows is available in Appendix S2 and Fig. S2,

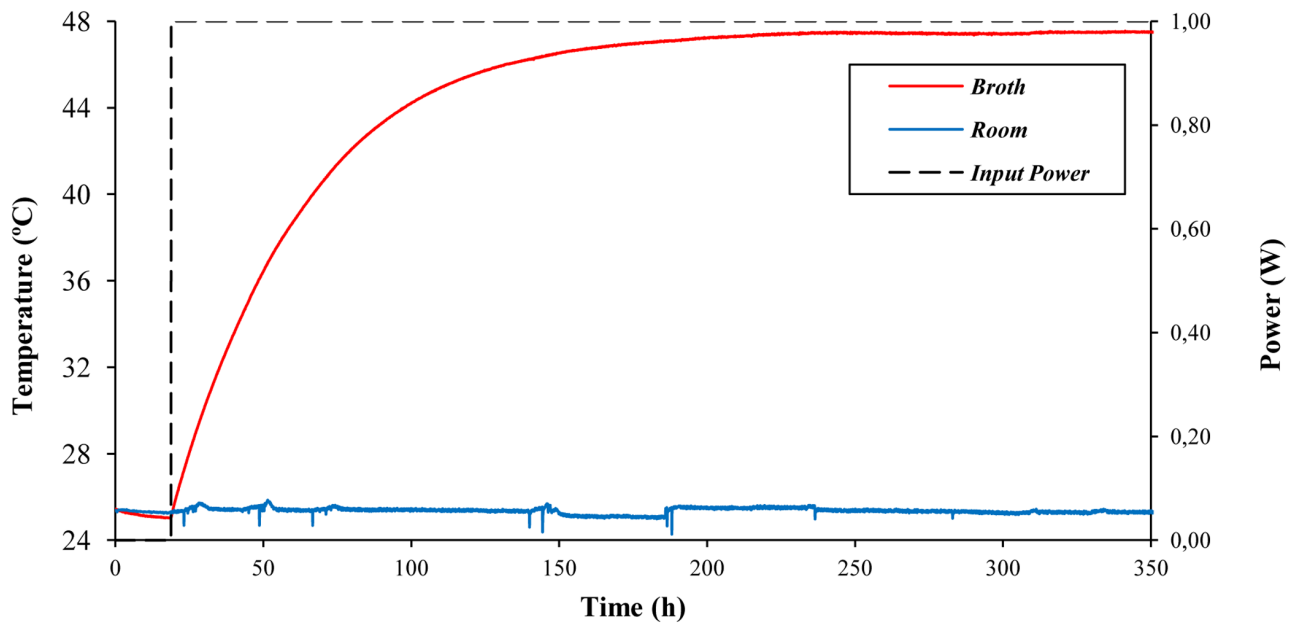


Figure 2. Time course of broth and room temperatures during the identification assay of broth heat capacity and global thermal resistance of the MTC. The experiment was carried out under the conditions described in section 2.4. Recordings of room temperature (blue), broth temperature (red) and input power (dashed line) were taken every 6 min. doi:10.1371/journal.pone.0056358.g002

respectively). These model equations are dependent on the electrical configuration used in the thermogenerator during the assays. When no load resistance was connected to the terminals of the thermogenerator (no electrical power was taken out), the following equation for TE-Probe was used (for a detailed version of this open-circuit model, see Appendix S1):

$$\dot{Q}_{Th}(t) = \frac{\Delta T_{th}(t)}{R_{Th}} \quad (11)$$

ΔT_{th} represents the difference of temperature between the hot and the cold side of the thermogenerator, whereas R_{th} is the thermal resistance of the thermogenerator.

Voltage output (V_o) of the terminals of the TE-Power Probe, which under this configuration is equal to the voltage generated in the Peltier cell, can be expressed as:

$$V_o(t) = \alpha \cdot \Delta T_{th}(t) \quad (12)$$

Being α the Seebeck coefficient.

Otherwise, when a load resistance was fitted to achieve the maximum power from the thermogenerator, Eq.11 was replaced by Eq.13 (deduced in the maximum-power model of Appendix S2):

$$\dot{Q}_{Th}(t) = \frac{\alpha^2 \cdot \Delta T_{th}(t)}{R_i} \cdot \left(\frac{T_H(t)}{2} - \frac{\Delta T_{th}(t)}{8} + \frac{R_i}{\alpha^2 \cdot R_{th}} \right) \quad (13)$$

Where R_i and R_{th} are the internal electrical and thermal resistance, respectively.

Under this configuration, voltage output (V_o) of the terminals of TE-Power Probe can be expressed as:

$$V_o(t) = \frac{\alpha \cdot \Delta T_{th}(t)}{2} \quad (14)$$

and the maximal power generated can be calculated as follows:

$$P_e(t) = \frac{V_o^2(t)}{R_i} \quad (15)$$

Results

Estimation of Broth Heat Capacity and Global Thermal Resistance of MTC

In order to characterize the thermal evolution of the MTC prior to the experiments with yeast cultures, an identification assay for $m \cdot C_p$ and R_g was set up as described in 2.4. The time course of broth and room temperature during the experiment is shown in Figure 2. From a steady-state, in which room and broth temperature were the same (25.5°C), a constant input power of 1 W was supplied, and the broth reached a final temperature of 47.5°C. The system gain (meaning the temperature increase divided by the input power) was 22 K/W, and the time constant (the time by which 63% of the temperature increase is reached) was 43.5 h. According to the model equations (see 3.2), the gain represents the global thermal resistance of the MTC, and the broth heat capacity can be obtained by dividing the time constant by the gain. Thus, our estimated values for R_g and $m \cdot C_p$ are 22 K/W and 7118 J/K, respectively.

When the mathematical software was used to estimate R_g and $m \cdot C_p$ from the same experimental data, similar values were

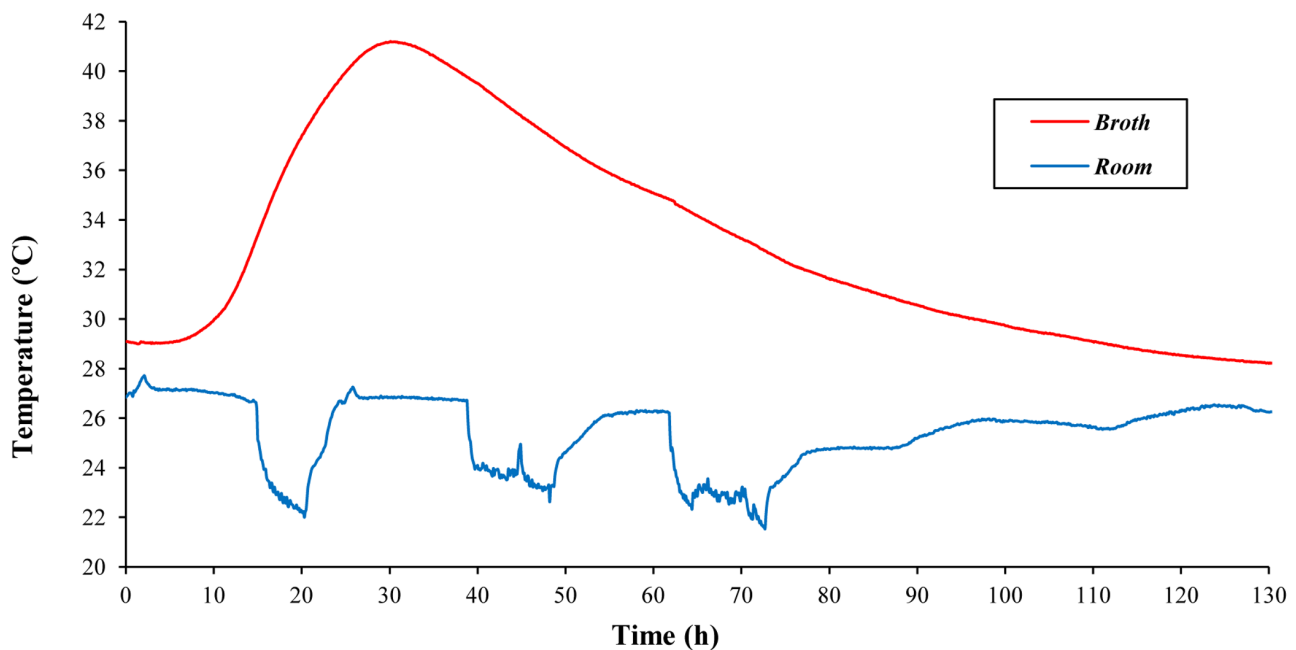


Figure 3. Typical performance of the MTC without TE-Power Probe. Experimental values of broth and room temperature (red and blue lines, respectively) are shown. doi:10.1371/journal.pone.0056358.g003

obtained ($R_g=22$ K/W and $m \cdot C_p=7100$ J/K) with a confidence level of 98.7%.

Strain Selection and MTC Performance

All yeast strains exhibited similar performance in terms of exothermic potential and resistance to high temperatures, with strain D170 displaying slightly higher thermoresistance (data not shown). This strain was thus selected for further studies. When yeast strain D170 was inoculated into a pre-warmed 18% sucrose YPD medium and grown in the MTC without the copper bar and the TE-Power Probe set in place, the internal temperature dropped slowly (about 1°C), stabilized and finally started to rise after 6–7 h. The temperature peaked after approximately 24 h and reached up to 41°C. Figure 3 shows a typical experiment in which the maximum temperature is around twelve degrees higher than the initial temperature of the culture. After the peak, the yeast culture temperatures started dropping and reached the initial temperature after about 70–90 h. Despite the abrupt changes (22°C–27°C) in room temperature as a consequence of switching the air conditioning on and off, the change in the internal temperature of the yeast culture was only mildly affected.

Estimation of Heat Yield Due to Yeast Growth

The heat yield due to yeast growth (Q_p) was estimated as described in section 3.3 for each experimental set up (Fig. 4). In all the experiments, the estimated evolution of Q_p peaked before broth temperature reached its maximum due to the high inertia of the broth ($m \cdot C_p$). In the assay carried out without TE-Power Probe (Fig. 4A), Q_p reached its maximum (1.96 W) after 20 h and remained above 0.2 W for 40 h. In an open-circuit configuration, maximum Q_p (almost 1.4 W) peaked after 10 h, reaching values above 0.2 W over 50 h (Fig. 4B). Maximum Q_p was obtained earlier in this case because a more concentrated inoculum was used, indicating that, as expected, there is a dependence between initial yeast concentration and time until Q_p maximum. Finally,

under a load-resistance configuration, Q_p peaked (with a value of almost 1.5 W) after 20 h (as in the experiment without TE-Power Probe, in which the same initial yeast concentration was used), producing more than 0.2 W for 50 h (Fig. 4C). Our data show that when the TE-Power Probe was inserted, lower Q_p values were estimated from experimental data. In accordance, total energy generated by yeast metabolism, calculated as the area below the curve of Q_p , was higher in the experiment carried out without the TE-Power Probe (194,7 kJ) in comparison with those configurations in which it was included (144,4 and 145,4 kJ for the open-circuit and the load-resistance set up, respectively). This might be due to the effect of the copper bar on effective broth stirring, which might be lower and therefore affect yeast growth.

Electricity Production with the MTC

Under the MTC insulation conditions assayed, the metabolic heat produced by strain D170 was partially transformed into electricity through the TE-Power Probe thermal harvester. When the TE-Power Probe was mounted in the yeast-culturing MTC under open circuit conditions, the internal temperature of the culture increased up to about 35°C and remained higher than 32°C for about 54 h (Fig. 5A). Under these conditions, electric voltage yielded around 250 mV (net value) for a two-day period, with significant, lower room temperature-associated peaks of about 350–600 net mV (Fig. 5A). The same experiment was performed under load resistance conditions (330 Ω , the same as that for the MPG-D751 thermogenerator) and produced an internal temperature peak of about 32°C, with the culture being hotter than room temperature (which was constant in this experiment) for a period of 110 h (Fig. 5B). Under these conditions, a maximum of 290 mV were obtained on the electrical load resistance, corresponding to around 580 mV generated in the Peltier cell (Eq. 15). The maximum power obtained, corresponding to the maximum ΔT values, reached around 255 μ W (net value).

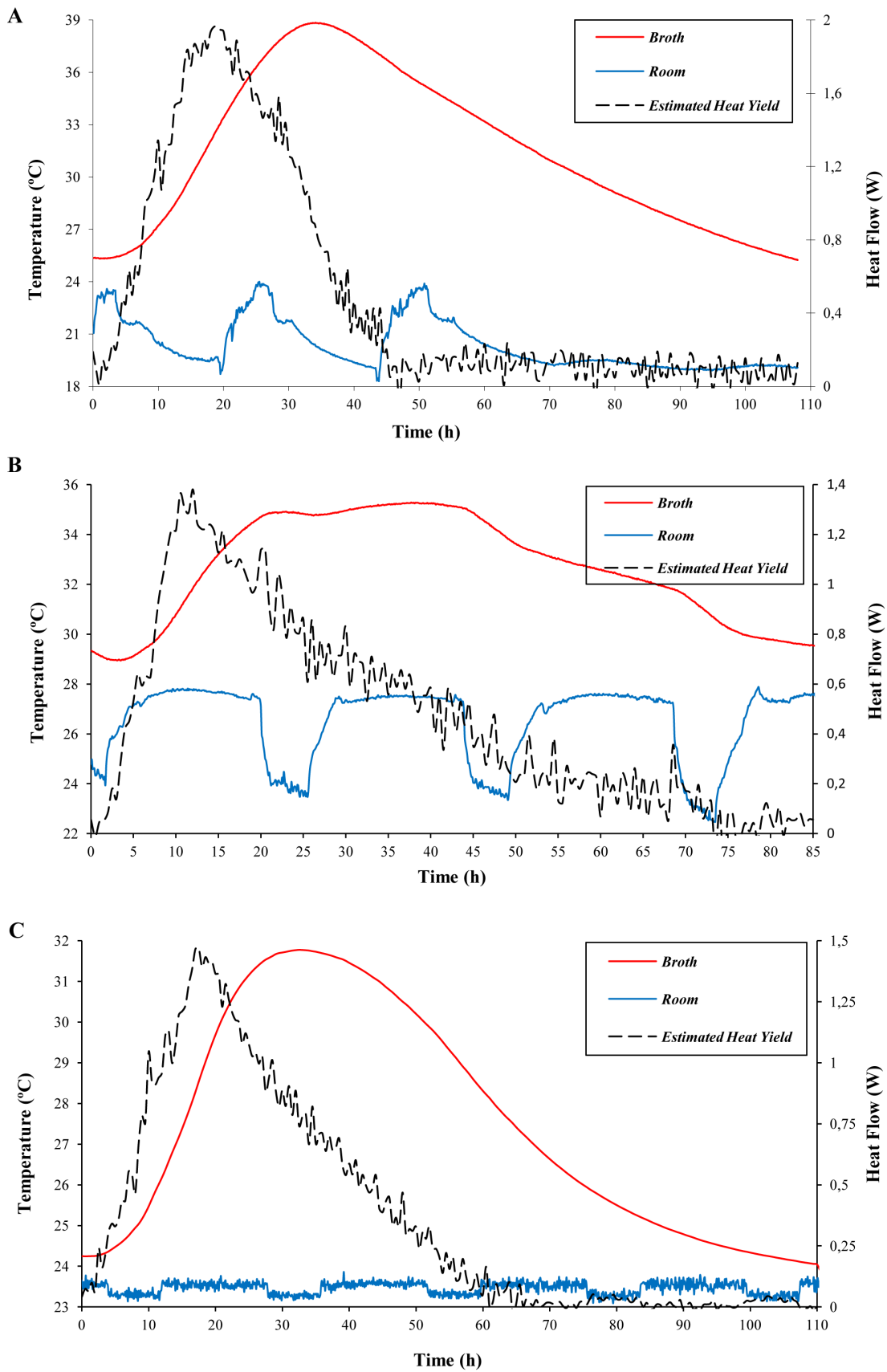


Figure 4. Time course of broth and room temperatures and heat yield due to yeast growth for different MTC configurations: without TE-Power Probe (A), open-circuit (B) and load-resistance (C). Experimental values of broth and room temperature (red and blue lines, respectively) were recorded every 6 min. Heat yield (dashed line) was estimated for each configuration as described in section 3.3. doi:10.1371/journal.pone.0056358.g004

The energy conversion yield was calculated for this latter experiment as the total electrical power generated (33.1 J) divided by the total heat energy produced by the yeasts (147.44 kJ, as calculated from the estimated heat yield represented in Fig. 4C). The resulting value, 0.022%, was low, as expected from the poor efficiency of heat-harvesting devices such as the TE-Power Probe. Notwithstanding, it allowed the production of significant amounts of electrical power from relatively moderate values of ΔT .

Discussion

The results presented here clearly indicate that the exothermic nature of microbial growth can be exploited when transformed into significant electric voltage. We have designed and constructed the first Microbial Thermoelectric Cell, which consists of a simple, thermally insulated reactor, with a small heat exchange surface on which a thermoelectric prototype thermal harvester, equipped with a MPG-D751 thermogenerator device (TE-Power Probe) is mounted. The chosen thermogenerator is optimum for relatively high efficiencies in electric production at low ΔT values, such as

those existing between an insulated yeast culture (41°C, under our conditions) and room temperatures. With a medium size MTC (smaller than two liters), we typically obtained 150–600 mV. These values are similar to those obtained with yeast-based MFCs for which net voltage values of about 0.33 V for 1 L reactors have been reported [10,11]. It is noteworthy that MFCs and MTCs work on a totally different basis –albeit theoretically compatible– as MFCs produce electricity from direct microbial-mediated electron transfer from organic matter oxidation to an anode; whereas the MTC partially transforms metabolic thermal energy into electricity by the Seebeck effect. As it is also the case for MFCs, MTCs could be combined with other microbial processes. Baker's yeast *S. cerevisiae* was used for our MTC due to its well-known exothermic growth under a range of different conditions. Indeed, any other microbial culture resulting in important heat production, such as ethanolic fermentation (beer, bread, wine, biofuels), auto thermal aerobic digestion (ATAD) or hydrocarbon-polluted soil bioremediation and bioaugmentation, could be coupled with MTCs into a single unit, with electricity production

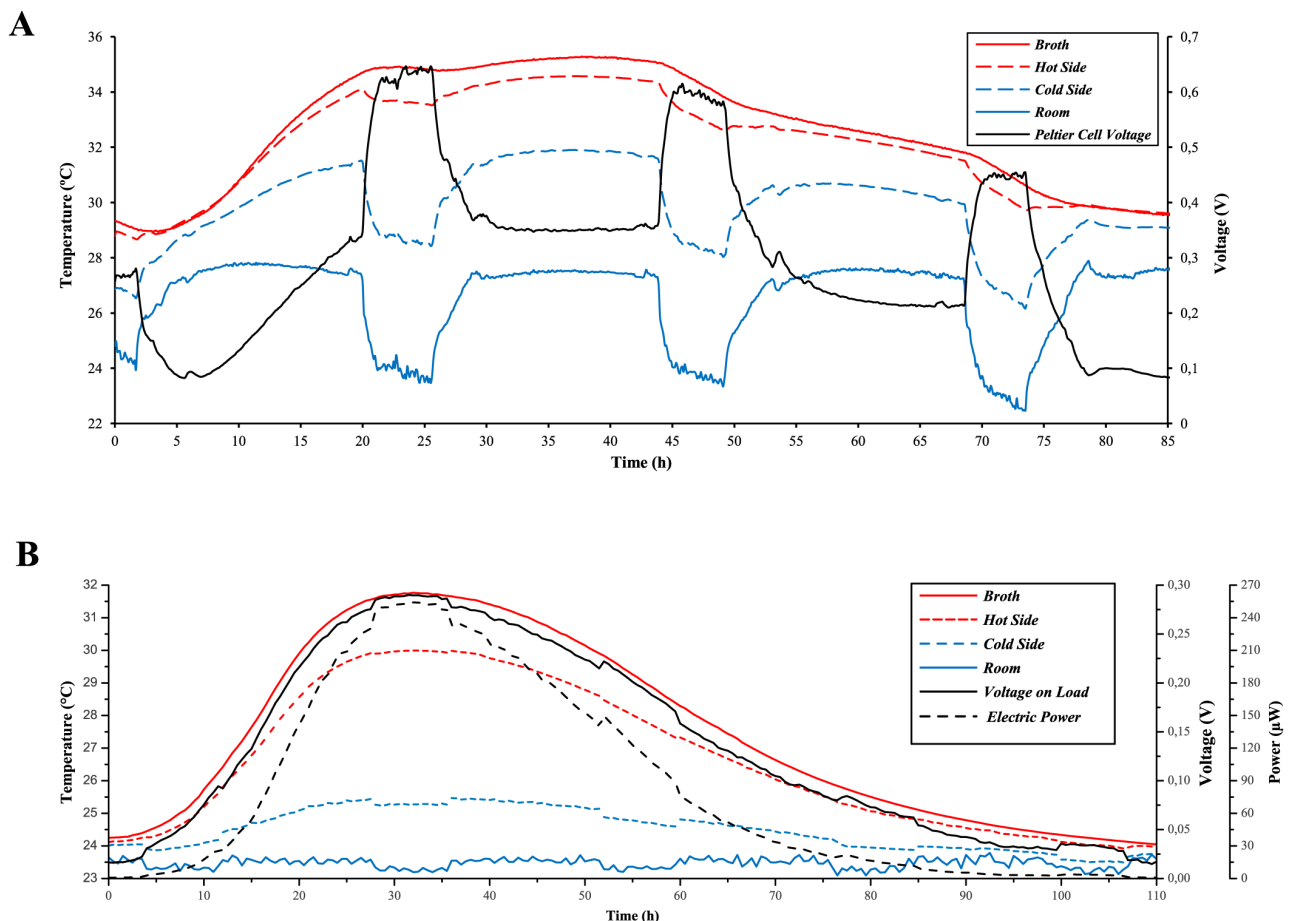


Figure 5. Electricity production by MTC under open-circuit (A) and load-resistance (B) configurations. The experimental temperature values of broth (red), room (blue), and thermogenerator hot and cold sides (red and blue dashed lines, respectively) are shown along with the evolution of voltage and power output (black continuous and dashed lines, respectively). doi:10.1371/journal.pone.0056358.g005

as a valuable sub-product of the main biotechnological purpose. In fact, metabolic heat is often seen in industry as an undesirable sub-product of large-scale microbial fermentations, and cooling facilities are often needed in order to maintain an optimum broth temperature [12,15]. The conversion, albeit partial, of this heat into electricity would both help to control internal temperatures in biotechnological processes and contribute to energy savings by cogeneration. Interestingly, our results suggest that heat production through metabolic growth and heat flow through a thermogenerator can be tuned in such a way that no energy is needed to heat the broth up for microbial growth nor to cool it down in order to avoid excessive temperatures, known to abruptly stop the fermentation process.

It seems reasonable to predict that, in addition to yeast, other cultures might be suitable as heat producers in an MTC. For example, naturally-occurring thermophilic and hyperthermophilic bacteria, such as *Bacillus coagulans*, *Bacillus licheniformis* or many *Geobacillus spp.* strains, many of which can be isolated from extreme environments such as deep oil wells and the optimal growth of which is 50–60°C. Additionally, these bacteria are reported as able to heat their own culture up to 50–55°C [16]. The perfect candidate for MTC should meet the following criteria: (i) thermoresistant; (ii) strong exothermic ability; (iii) rapid and easy growth; and (iv) an ability to grow and degrade high concentrations of carbon sources.

In the MTC we designed, the “cold side” of the system was an aluminum heatsink. In order to optimize electricity yield by increasing ΔT , a biological cooling system could theoretically be implemented, rather than simple convection-driven heat loss. In fact, methanogenic archaea have been reported to exhibit endothermic growth [7]. Although it is uncertain whether endothermia is a result of particular growth or of heat loss due to gas evaporation from the culture, the fact is that these microorganisms could be combined with those producing heat through a thermoelectric element in order to increase electricity production. These archaea have optimal growth at temperatures of around 37°C, and this implies that the whole system should be finely tuned in order to regulate heat transfer across the thermoelectric element, allowing optimal microbial growth while maintaining as high a ΔT as possible.

The surface:volume ratio of microbial fermentors is a critical factor affecting heat loss to the environment and thus internal temperature of the culture. Although standard lab-scale microbial cultures produce heat, most of it is lost to environment due to high surface to volume ratio, resulting in the absence of any noticeable increase in internal temperature. However, large, production-scale bioreactors have been characterized thermodynamically and proved to work nearly adiabatically due to much lower surface to volume ratio compared to laboratory-scale non-insulated bioreactors [12]. The results presented here, together with previous reports on medium-scale liquid culture calorimeters [13], demonstrate that relatively small liquid cultures can also work almost adiabatically, provided proper insulation is provided and significant autothermal growth can be achieved. This implies that small portable MTCs for electricity production could be envisaged, since most of the metabolic heat from microbial growth can be stored inside the MTC. These small thermoelectric cells could theoretically be used to power small electric devices. However, in order for MTCs to display higher electric yields, optimization of the thermoelectric elements should take place. Indeed, only 0.5–8% of the total heat flow is usually transformed into electricity through the thermoelectric plates. Interestingly, only 12% of the maximum theoretical efficiency is achieved in the best thermoelectric devices today [17], so there is still room for

significant improvement in the optimization of this technology. There has been a dramatic increase in research into high efficiency thermoelectric devices in recent decades, with reports of significant improvements in ZT values, design optimization, and development of alternative materials. As proposed by [17], “TE solid-state heat engines could well play a crucial role in addressing some of the sustainability issues we face today”.

Other heat harvesting methods, such as absorption heat transformers or organic Rankine cycle, have been reported previously [18,19]. However, these systems are space-consuming and involve mobile parts that require continuous maintenance. In contrast with these, solid-state thermoelectric systems are small, require almost no maintenance, and display high adaptability to a range of industrial designs [17].

In conclusion, this is the first report of microbial metabolic energy being converted into electricity with an *ad hoc* thermoelectric device, i.e., the Microbial Thermoelectric Cell. Our results show that even small volumes of broth are able to exhibit significant autothermal performance and produce electricity when properly insulated and set in such a way that heat exchange is minimized over the whole surface, except the small area on which a (prototype) thermal harvester is mounted. Although the electric power we obtained was rather low, this work may contribute towards a novel strategy to harvest excess heat produced by the biotechnology industry, particularly if ongoing research into thermoelectric materials and design finally yields high efficiency thermoelectric devices.

Supporting Information

Figure S1 Schematic drawing of MTC data-recording system. Dashed lines represent thermocouple connections measuring the temperature of the broth (T_b), the temperature of the hot and cold sides of the thermogenerator (T_H and T_C , respectively), and the room temperature (T_{env}); whereas continuous lines represent voltage measurements corresponding to the thermogenerator (V_{th}) and the electrical resistance (V_r). (TIF)

Figure S2 Schematic drawing of heat flows and resistances within the thermogenerator cell. Symbols used are in accordance with the nomenclature summarized in Table 1. (TIF)

Appendix S1 Thermogenerator cell (MPG-D751) general equations. (DOCX)

Appendix S2 TE-Power Probe model description. (DOCX)

Acknowledgments

We are very grateful to Emilia Matallana, for kindly supplying yeast strains, Julián Heredero, for his fine work manufacturing the copper bar, to Ruslan Klymenko for assistance with Figure 1 and to Fabiola Barraclough for correction of the English text.

The technology described in this work has been found by us to hold not only for scientific publication, but also for patenting (Application number P201200977 at Spanish Office of Patents and Trademarks, OEPM).

Author Contributions

Conceived and designed the experiments: RRB CA CV MP. Performed the experiments: RRB CA CV MP. Analyzed the data: RRB CA CV AM MP. Contributed reagents/materials/analysis tools: AM. Wrote the paper: RRB CV AM MP.

References

- Dauer LT, Zanzonico P, Tuttle RM, Quinn DM, Strauss HW (2011) The Japanese tsunami and resulting nuclear emergency at the Fukushima Daiichi power facility: technical, radiologic, and response perspectives. *J Nucl Med* 52 (9): 1423–1432.
- Gross M (2011) Energy U-turn in Germany. *Curr Biol* 21 (10): 379–381.
- Lehmann J (2007) A handful of carbon. *Nature* 447: 143–144.
- Kim D, Chang IS (2009) Electricity generation from synthesis gas by microbial processes: CO fermentation to microbial fuel cell technology. *Bioresour Technol* 100: 4527–4530.
- Song C (2002) Fuel processing for low-temperature and high-temperature fuel cells: Challenges, and opportunities for sustainable development in the 21st century. *Catal Today* 77 (1): 17–49.
- Cheng S, Xing D, Call DF, Logan BE (2009) Direct biological conversion of electrons into methane by electromethanogenesis. *Environ Sci Technol* 43 (10): 3953–3958.
- Liu H, Grot S, Logan BE (2005) Electrochemically assisted microbial production of hydrogen from acetate. *Environ Sci Technol* 39 (11): 4317–4320.
- Rozendal RA, Hamelers HVM, Euverink GJW, Metz SJ, Buisman CJN (2006) Principle and perspectives of hydrogen production through biocatalyzed electrolysis. *Int J Hydrogen Energy* 31 (12): 1632–1640.
- Logan BE (2010) Scaling up microbial fuel cells and other bioelectrochemical systems. *Appl Microbiol Biotechnol* 85(6): 1665–71.
- Gunawardena A, Fernando S, To F (2008) Performance of a yeast-mediated biological fuel cell. *Int J Mol Sci* 9(10): 1893–1907.
- Ducommun R, Favre MF, Carrard D, Fischer F (2010) Outward electron transfer by *Saccharomyces cerevisiae* monitored with a bi-cathodic microbial fuel cell-type activity sensor. *Yeast* 27 (3): 139–148.
- Türker M (2004) Development of biocalorimetry as a technique for process monitoring and control in technical scale fermentations. *Thermochim Acta* 419 (1): 73–81.
- Delás J, Notari M, Forés J, Pechuan J, Porcar M, et al. (2009) Yeast cultures with UCPI uncoupling activity as a heating device. *N Biotechnol* 26 (6): 300–306.
- Linykin S, Ben-Yaakov S (2007) Modeling and analysis of thermoelectric modules. *IEEE Trans Ind Appl* 43 (2): 505–512.
- von Stockar U, van der Wielen LAM (1997) Thermodynamics in biochemical engineering. *J Biotechnol* 59 (1): 25–37.
- Ungwuanyi JO, Harvey LM, McNeil B (2008) Diversity of thermophilic populations during thermophilic aerobic digestion of potato peel slurry. *J Appl Microbiol* 104 (1): 79–90.
- Bell LE (2008) Cooling, heating, generating power, and recovering waste heat with thermoelectric systems. *Science* 321 (5895): 1457–1461.
- Larjola J (1995) Electricity from industrial waste heat using high-speed organic Rankine cycle (ORC). *Int J Prod Econ* 41 (1): 227–235.
- Saidur R, Rezaei M, Muzammil WK, Hassan MH, Paria S, et al. (2012) Technologies to recover exhaust heat from internal combustion engines. *Renew Sust Energ Rev* 16: 5649–5659.

Producing high-strength liquor from mesophilic batch acidification of chicken manure

Christian Abendroth^{1,2}, Erik Wünsche¹, Olaf Luschnig^{1,3}, Christoph Bürger¹ and Thomas Günther⁴

Abstract

This report describes the results from anaerobic batch acidification of chicken manure as a mono-substrate studied under mesophilic conditions. The manure was diluted with tap water to prevent methane formation during acidification and to improve mixing conditions by reducing fluid viscosity; no anaerobic digester sludge has been added as an inoculum. Highest acidification rates were measured at concentrations of 10 gVSL⁻¹ and 20 gVSL⁻¹; the pH value remained high (pH 6.9–7.9) throughout the test duration and unexpected fast methane formation was observed in every single batch. At substrate concentrations of 10 gVSL⁻¹ there was a remarkable methane formation representing a value of 82% of the respective biochemical methane potential of chicken manure. Increasing substrate concentrations did not suppress methane formation but impaired acid production. Consequently, the liquor cannot be stored over longer periods but should immediately be used in a digestion process.

Keywords

Chicken manure, acidification, biogas, anaerobic digestion, two-stage digestion, high-strength liquor

Introduction

During our research we investigated the batch acidification of chicken manure (CM) with the aim of producing a strong liquor containing high concentrations of volatile fatty acids (VFA) as a substrate for anaerobic digesters. CM is an interesting substrate for anaerobic digestion. With chicken farming being one of the most intensive operations in agriculture (Abouelenien et al., 2009), large amounts of CM with a considerable biogas potential are locally available. The manure is known for its high nitrogen content and the fermentation of CM has been described as difficult (Abouelenien et al., 2009). Therefore, Abouelenien et al. (2010) suggested ammonia removal to improve digestion conditions. Nonetheless, the toxicity of ammonia derived from CM, in reality, prevents the use of CM for digestion. Several recent publications, including Niu et al. (2013) and Fotidis et al. (2014), are dealing with this problem. Other authors, Safley et al. (1985), Webb and Hawkes (1985) and Bujoczek et al. (2000), have described in detail the digestion process of CM. They reported that the anaerobic digestion of CM is difficult at higher loadings of total solids (TS) (higher than 10% TS) and that an optimal concentration range is between 4% and 10% influent TS feed concentration. Webb and Hawkes (1985) suggested the optimisation based on a two-stage process. Current works from Fu and Holtzapfel (2011), Liu et al. (2012), Yan et al. (2014) or Jie et al. (2014) give insight into the optimisation of acidification conditions in anaerobic digestion (AD) and the advantage of separately controlled acidification processes.

Although our work includes research into the two-stage process, the main focus is on the acidification step with CM as a mono-substrate. The key objective of this research was to produce high-strength liquor, rich in VFA by maximising the solubilisation of nutrients and production of VFA in a separately operated batch acidification step.

Material and methods

Substrate

CM was collected from a local poultry farm near Jena/Thuringia (Germany). The fresh CM, as described in Table 1, was dried at 40°C in an oven with forced ventilation, ground in a ball mill, sieved through a 1 mm screen and thoroughly mixed to provide a homogeneous substrate. The drying procedure led to a 6.8% reduction of total nitrogen as compared with the fresh manure owing to ammonia losses. Table 1 shows substrate characteristics of the CM.

¹Bio H2 Energy GmbH, Jena, Germany

²Cavanilles Institute of Biodiversity and Evolutionary Biology, Universidad de Valencia, Spain

³BioEnergie Verbund e.V., Jena, Germany

⁴Eurofins Umwelt Ost GmbH, Jena, Germany

Corresponding author:

Christian Abendroth, Bio H2 Energy GmbH, Im Steinfeld 10, 07751 Jena, Germany.

Email: christian_abendroth@gmx.de

Table 1. Chemical characteristics of dried CM (mean \pm standard deviation).

Parameter chicken manure	Unit	Dried
Total solids (TS)	% (W/W)	95.6 \pm 3.2
Volatile solids (VS)	% TS	69.4 \pm 0.9
Chemical oxygen demand (total COD)	mg g ⁻¹ TS	893 \pm 45
Total organic carbon (TOC)	% TS	36.3 \pm 4.7
Total nitrogen (TN)	% TS	5.5 \pm 1.5
Ammonia nitrogen (NH ₄ -N)	% TS	0.52 \pm 0.002
Total phosphorus	% TS	1.48 \pm 0.4
pH (CaCl ₂ -extract)	—	6.8 \pm 0.11

The biochemical methane potential (BMP) of CM was measured in batch experiments at 37 °C and over 21 days in accordance with the German standard method of VDI4630 (2006). The final methane yield was 200 LCH₄/kg VS (corresponding to 56% methanisation of initially added chemical oxygen demand (COD)).

Batch experiments

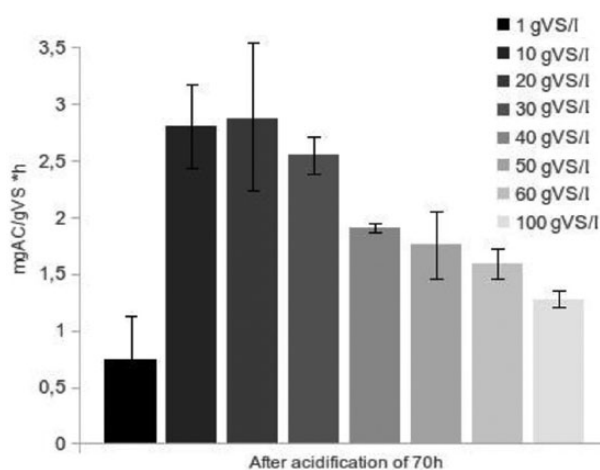
Initial tests included short-term acidification experiments, which have been performed in 0.5L SIMAX-bottles (duration between 4 to 5 days). Substrate concentrations were set up at 10, 20, 30, 40, 50, 60 and 100 gVSL⁻¹. Corresponding amounts of CM were suspended in 0.5L of tap water stirred by a magnetic stirrer and heated to 37 °C. The bottles were then flushed with nitrogen to ensure anaerobic conditions. Each bottle had been connected to an eudiometer (liquid displacement system) for measurement of biogas formation.

Investigations into the long-term conditions for acidification formed the second part of our research. The experimental procedure was similar to the short-term batch acidification, but with an extended incubation time of 41 days. The CM was again suspended in tap water with initial substrate concentrations of 10, 20 and 40 gVSL⁻¹. The first acidification batches were set up without the addition of inoculation sludge, but this was changed for later batches, where we added 100 ml of the suspension from the previous batch (total volume 500 ml). Sampling occurred every 3 or 4 days through the bottle sampling port.

To ensure constant and accurate sampling conditions, gas and liquid samples were taken from two identical sets of bottles, one set for gas sampling and the other set for liquid sampling. This approach of sampling was chosen to avoid withdrawal of nutrients that could affect gas production rates. Biogas samples were taken from the eudiometers with a gas tight syringe and transferred into headspace vials displacing the barrier solution (saturated saline solution; pH2).

Analytical methods

The wet samples were dried overnight at 105 °C (TS). Volatile solids (VS) content was estimated as the loss of ignition by dry

**Figure 1.** Characterisation of the acidogenesis: Acid-production (TVFA) per hour under conditions of different concentrations of VS. TVFA are given as acetic acid equivalent (AC).

matter combustion at 525 °C. For all pH measurements, a pH-meter (WTW, Germany) with a glass electrode (Schott/Germany) was used.

The concentration of individual volatile fatty acids (acetate, propionate, butyrate, isobutyrate, valerate, isovalerate and caproate) was determined by gas chromatography with a Shimadzu gas chromatograph/flame ionisation detector and equipped with a DB-1701 column (Macherey-Nagel, Germany). For determination of soluble COD, the samples were passed through a 0.45- μ m-pore-size membrane filter. The COD of the filtrate was determined using a COD-Spectroquant test kit (Merck, Germany) and a digital photometer SQ 118 (Merck, Germany). Gas composition (CH₄, CO₂) was analysed with a Combimass GA-m (Bender, Germany) multi-gas monitor.

Results and discussion

Optimal CM concentration during acidification

The amount of total volatile fatty acids (TVFA) produced from dry CM was optimised in a first acidification step. Several initial substrate concentrations were investigated (Figure 1). Optimal acid production occurred at concentrations of between 10 gVSL⁻¹ and 20 gVSL⁻¹. The rate of acid formation decreases substantially at low concentrations. CM-concentrations around 10 gVSL⁻¹ show a four times higher acidification rate than the initial CM-concentration of 1 gVSL⁻¹ (a decrease from 2.8 mgTVFAgVS⁻¹*h for the 10 gVSL⁻¹ to 0.75 mgTVFAgVS⁻¹*h for the 1 gVSL⁻¹). At higher concentrations than 20 gVSL⁻¹, the acidification rate decreases successively and drops to 1.28 mgTVFAgVS⁻¹*h at a concentration of 100 gVSL⁻¹.

Although unexpected, we observed already during the first days methane formation. Therefore the methane formation during batch acidification was investigated in more detail in subsequent experiments.

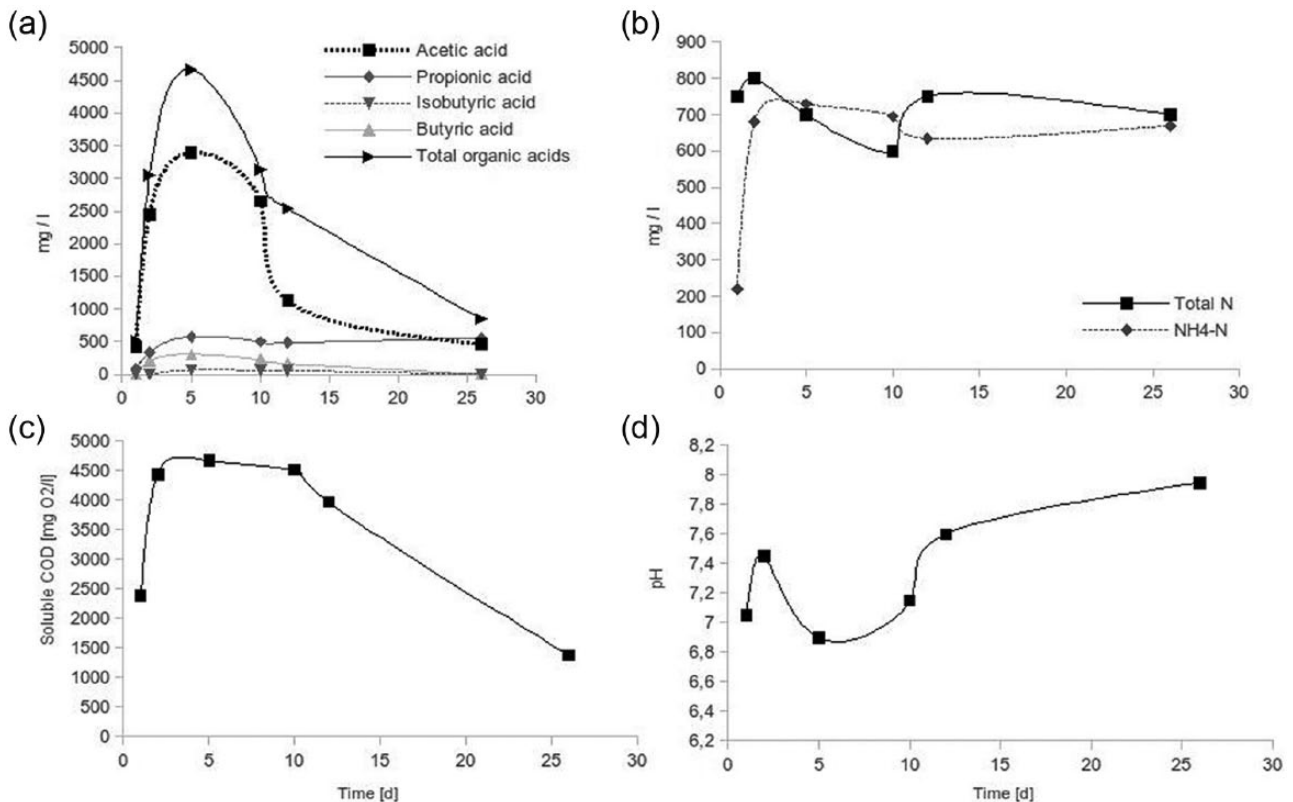


Figure 2. Long-term batch digestion of CM at an initial concentration of 10 g L⁻¹ VS. (a) Acid production, (b) total nitrogen and NH₄-N, (c) solubilised COD and (d) pH value.

Characterisation of the produced VFA-liquor

During long-term batch experiments, the hydrolysis and acidification of CM were investigated at a concentration of 10 g VS L⁻¹ (equivalent to 12870 mg L⁻¹ of COD). CM was rapidly degraded to VFA under anaerobic conditions. Maximum TVFA concentration (4663 mg L⁻¹) was achieved at Day 4–5, indicating an acidification efficiency of 46% of COD (Figure 2(a)). Acetic acid was the predominant VFA species (3400 mg L⁻¹) followed by comparably low concentrations of propionate and butyrate (<500 mg L⁻¹). The maximum TVFA concentration coincided with the peak of soluble COD (4680 mg L⁻¹) (Figure 2(c)). In total, 36.4% of the initially added COD was solubilised. Another parameter monitored was the reduction of organic nitrogen to ammonium (NH₄-N) (Figure 2(b)). The conversion took place within the first 3–5 days, with the final concentration close to total-N concentration in the feed. These data indicate a rapid and nearly complete degradation of organic nitrogen into soluble NH₄-N. This opens the possibility for a subsequent ammonia removal from the digestate prior to full methanisation.

In spite of intense VFA formation from CM, the pH of the batches did not drop below pH 6.9 (Figure 2(d)). The stabilisation of pH in a neutral range can give rise to methanogenic

activity counteracting the accumulation of VFA. Hence, after 5 days TVFA and soluble COD decreased slowly, reaching values as low as a third of the respective maximum value (Figure 2(a) and (c)) at Day 26. It has been concluded that methane formation was the cause for VFA reduction.

Methane formation during acidification

Gas production during batch CM acidification started at Day 2, followed by a short lag-phase until Day 5, indicating a diauxic growth curve (Figure 3). At a concentration of 10 g VS L⁻¹ the continued anaerobic incubation of batches led to continuous production of methane starting on Day 2 and accelerating on Day 6. On Day 41, a cumulative methane production of 189 L CH₄/kg VS was measured. These values approximate the BMP of 200 L CH₄/kg VS. The results indicate that under the chosen conditions of CM batch acidification, a significant methane production will occur. The early appearance of methane during the acidification process interferes with VFA accumulation and is expected to prevent a temporary storage of the liquor rich in VFA at ambient temperatures. Additional attempts to stabilise TVFA-accumulation and to suppress methane formation failed. Using tap water instead of anaerobic digester sludge (ADS) for inoculation of batches was not sufficient to inhibit methane formation. Higher CM-concentrations led to impaired acidification

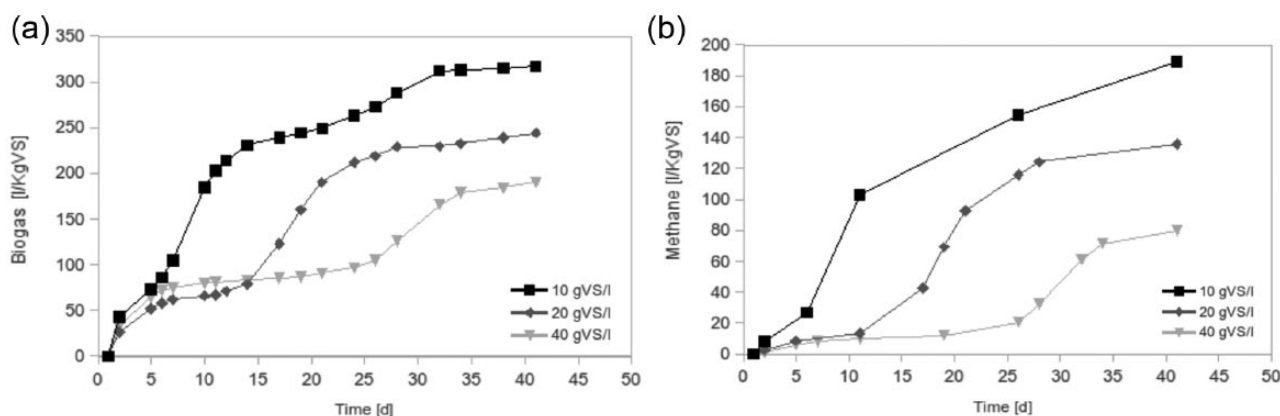


Figure 3. Analysis of the gas-production during batch-acidogenesis: (a) biogas formed per kgVS; (b) methane formed per kgVS.

and a delayed gas production, but did neither prevent methane formation. This is consistent with the observation of Bujoczek et al. (2000), who described 40 days of lag phase for digestion of undiluted CM. We concluded that elevated buffer capacity (ammonium and carbonate buffer systems) led to pH stabilisation of the liquid phase with values above pH 7, and these conditions were sufficient to maintain methanogenic activity in the VFA-liquor.

Conclusions

The results from our trials show optimal substrate concentration for CM batch acidification between 10 and 20 gVSL⁻¹ with an maximum acidification rate of 2.8 mgTVFA gVS⁻¹h (acidification yields of 47%). The highest TVFA accumulation in the liquid phase corresponds to 450 mgVFA gVS⁻¹. A rapid hydrolysis of CM into soluble products is indicated by peaks in soluble COD, TVFA and the complete conversion of organic nitrogen into ammonia-N at Day 5. However, after Day 5, soluble COD and TVFA decrease significantly, accompanied by increasing methane formation, leading to consumption of VFA by methanogens. After 41 days, most of the CM is consumed for biogas formation. The approach to produce VFA-liquor from CM in an anaerobic batch process was successful with respect to rapid hydrolysis and acidification, and the use of an ADS-free process. However, the system failed in stabilising the accumulated VFA in the liquid phase and preventing methanogenic conditions. Therefore, the liquor should immediately be used in a digestion process.

Acknowledgements

We thank Manfred Schmid and Ursula Kepp for proofreading of the article and William Than SP (SP Multitech Malaysia) for the collaboration and regular access to his CM fed two-stage plant.

Declaration of conflicting interests

The authors declare that there is no conflict of interest.

Funding

This work was supported by a grant of the German Federal Ministry of Economics and Technology [ProInno II, grant VP2531901ST9 / ZIM, grant 16KN017626].

References

- Abouelenien F, Nakashimada Y and Nishio N (2009) Dry mesophilic fermentation of chicken manure for production of methane by repeated batch culture. *Journal of Bioscience and Bioengineering* 107: 293–295.
- Abouelenien F, Fujiwara W, Namba Y, et al. (2010) Improved methane fermentation of chicken manure via ammonia removal by biogas recycle. *Bioresource Technology* 101: 6368–6373.
- Bujoczek G, Oleszkiewicz J, Sparling R, et al. (2000) High solid anaerobic digestion of chicken manure. *Journal of Agricultural Engineering Research* 76: 51–60.
- Fotidis IA, Kougias PG, Zaganas ID, et al. (2014) Inoculum and zeolite synergistic effect on anaerobic digestion of poultry manure. *Environmental Technology* 35: 1219–1225.
- Fu Z and Holtzapple MT (2011) Anaerobic thermophilic fermentation for carboxylic acid production from in-storage air-lime-treated sugarcane bagasse. *Applied Microbiology and Biotechnology* 90: 1669–1679.
- Jie W, Peng Y, Ren N, et al. (2014) Volatile fatty acids (VFAs) accumulation and microbial community structure of excess sludge (ES) at different pHs. *Bioresource Technology* 152: 124–129.
- Liu H, Wang J, Liu X, et al. (2012) Acidogenic fermentation of proteinaceous sewage sludge: Effect of pH. *Water Research* 46: 799–807.
- Niu Q, Qiao W, Qiang H, et al. (2013) Mesophilic methane fermentation of chicken manure at a wide range of ammonia concentration: Stability, inhibition and recovery. *Bioresource Technology* 137: 358–367.
- Safley LM, Vetter RL, Smith D (1985) Managing a poultry manure anaerobic digester. In: *Proceedings of the Fifth International Symposium on Agricultural Wastes, Agricultural Waste Utilization and Management*, Chicago, IL, 16–17 December, pp 491–499. St. Joseph, MI: ASAE Publication.
- VDI 4630 (2006) Fermentation of organic materials, characterisation of the substrate, sampling, collection of material data, fermentation tests. Düsseldorf, Germany: The Association of German Engineers (VDI).
- Webb AR and Hawkes FR (1985) The anaerobic digestion of poultry manure: Variation of gas yield with influent concentration and ammonium-nitrogen levels. *Agricultural Wastes* 14: 135–156.
- Yan BH, Selvam A and Wong JW (2014) Application of rumen microbes to enhance food waste hydrolysis in acidogenic leach-bed reactors. *Bioresource Technology* 168: 64–71.



Contents lists available at ScienceDirect

Bioresource Technology

journal homepage: www.elsevier.com/locate/biortech

Short Communication

Microbial communities involved in biogas production exhibit high resilience to heat shocks

Christian Abendroth^{a,b}, Sarah Hahnke^c, Claudia Simeonov^b, Michael Klocke^c,
Sonia Casani-Miravalls^d, Patrice Ramm^c, Christoph Bürger^d, Olaf Luschnig^d, Manuel Porcar^{a,e,*}

^a Institute for Integrative Systems Biology (I²SysBio), Paterna, Valencia, Spain

^b Robert Boyle Institut e.V., Jena, Germany

^c Leibniz Institute for Agricultural Engineering and Bioeconomy (ATB), Bioengineering, Potsdam, Germany

^d Bio H2 Umwelt GmbH, Jena, Germany

^e Darwin Bioprospecting Excellence, S.L. Parc Científic Universitat de Valencia, Paterna, Valencia, Spain

ARTICLE INFO

Keywords:

Anaerobic digestion
Two-phase digestion
Two-stage digestion
Acidification
16S-rRNA gene sequencing
Thermal stress

ABSTRACT

We report here the impact of heat-shock treatments (55 and 70 °C) on the biogas production within the acidification stage of a two-stage reactor system for anaerobic digestion and biomethanation of grass. The microbiome proved both taxonomically and functionally very robust, since heat shocks caused minor community shifts compared to the controls, and biogas yield was not decreased. The strongest impact on the microbial profile was observed with a combination of heat shock and low pH. Since no transient reduction of microbial diversity occurred after the shock, biogas keyplayers, but also potential pathogens, survived the treatment. All along the experiment, the heat-resistant bacterial profile consisted mainly of Firmicutes, Bacteroidetes and Proteobacteria. *Bacteroides* and *Acholeplasma* were reduced after heat shocks. An increase was observed for *Aminobacterium*. Our results prove the stability to thermal stresses of the microbial communities involved in acidification, and the resilience in biogas production irrespectively of the thermal treatment.

1. Introduction

Anaerobic digestion is a highly sophisticated process that consists of four phases: hydrolysis, acidogenesis, acetogenesis, and methanogenesis (Haarstrick et al., 2001). In practice, all four stages are usually combined in a single reaction vessel, denominated as Completely or Continuously Stirred Tank Reactor (CSTR). However, several reports demonstrated the advantages of separating the degradation process into two stages optimized each either for acidification or methane-production (Baccay and Hashimoto, 1984; Dinopoulou et al., 1988; Gijzen et al., 1988; Abendroth et al., 2015a). In the first stage, biopolymers are degraded into monomers such as different volatile short-chain fatty acids (VFAs). In the second stage, produced acids are converted into methane and carbon dioxide. A separated acidification stage is especially interesting, as it allows the production of valuable intermediates or by-products, such as VFAs (Koutinas et al., 2016) and molecular hydrogen (Voolapalli and Stuckey, 2001). In addition, having the acidification stage as a separate sub-system allows using substrates such as silages with high content of solids and high organic loading rates.

Besides biological pre-treatments, physical, chemical and physico-chemical methods are also used. All of them can make the biomass accessible to microbial enzymes and, hence, yield higher amounts of fermentable sugars (Mood et al., 2013). Thermal pre-treatments, which require high amounts of energy, can successfully increase the accessibility of lignocellulose, but temperatures as high as 200–300 °C have been reported to be required (Yan et al., 2009). However, recent studies suggest that lower temperatures such as 120 °C (Ennouria et al., 2016) or even 70 °C (Gonzales-Fernandez et al., 2012) can already significantly improve biomass degradability. In fact, a recent study reports improved hydrogen production from digesters with granular sludge after a mild heat-shock treatment (Alibardi et al., 2012).

Stable reactor performance has been reported even for hyperthermophilic digestion conditions up to at least 65 °C (Rademacher et al., 2012; Algapani et al., 2016). At those temperatures, microorganisms require very long adaptation times (Moset et al., 2014). Besides thermal tolerance, anaerobic microbiomes tend to be robust and adaptable to extreme conditions, including high ammonia levels (Abendroth et al., 2015a; Tian et al., 2017) or high salinity (Vrieze

* Corresponding author at: Institute for Integrative Systems Biology (I²SysBio), Paterna, Valencia, Spain.
E-mail address: manuel.porcar@uv.es (M. Porcar).

<https://doi.org/10.1016/j.biortech.2017.10.093>

Received 15 September 2017; Received in revised form 25 October 2017; Accepted 28 October 2017
0960-8524/ © 2017 Elsevier Ltd. All rights reserved.

et al., 2016).

To reduce energetic demand and costs, and to avoid long adaptation times compared to long thermophilic processes, we aimed at exploring a new method for biogas production based on the application of mild thermal shocks throughout the process. The question we raised was whether acidifying microbiomes that are adjusted to mesophilic conditions, might tolerate short, hyperthermophilic heat shocks, and which would be the effect on the efficiency of the process. With the aim of combining thermal and biological pre-treatments, we constructed a two-stage two-phase system, heated the first stage cyclically up to 55 °C and 70 °C and investigated the impact of this treatment on the microbial community dynamics applying culture-dependent and cultivation-independent approaches. As substrate of choice, grass biomass was chosen because of its high potential as renewable energy source (Jungers et al., 2013), and because of its suitability for two-stage digestion (Abendroth et al., 2017).

2. Material and methods

2.1. Fermentation conditions

Digestion experiments were performed in two two-stage two-phase biogas reactor systems designed *ad hoc* for this work (Fig. 1). One two-

stage system was used to investigate the impact of heat-shocks and a second one was used as a control system. The first stage of each system was used for acidification, and the second stage was used for subsequent methane formation. Additionally, each of the methane stages was filled with 1.58 kg of bed packing (Christian Stöhr, Germany). At the beginning of the experiment, each methane stage received 11.75 L of sewage seed sludge, and each acidification stage received 8 L of sewage sludge as inoculum. During acidification, fresh untreated grass biomass (Graminidae) consisting of 30.4% total solids (TS), with 84.2% volatile solids (VS) of TS and a chemical oxygen demand (COD) of 260 mgO₂/g was used as solid phase. For every batch cycle, 96.2 gL⁻¹ of grass VS were filled into a cylindrical sieve, which was located in the first stage for acidification to retain the solid phase during the percolation process. Leachate was percolated on the fixed grass bed to produce high-strength liquor, which was collected after every batch cycle of acidification. To keep the pH constantly at 6.0 or 6.8, a pH-regulation system was used for each acidification stage (BL 7916, Hanna Instruments, Germany). Collected liquor was stored under anoxic conditions at 4 °C and fed semi-continuously and manually into the methane stages. Each methane stage received daily approximately 100 gCOD (8.5 gCOD L⁻¹). Digestate from the methane stages was stored under anoxic conditions at 4 °C and was used as leachate for the set-up of new acidification cycles (Fig. 2). Produced gas from all stages was collected in gasbags (Tecobag, Tesseraux, Germany) and analysed with the Combimass Measurement device (Binder, Germany). Two multistage systems were performed in parallel and at mesophilic temperature (37 °C). The produced high strength liquor from the acidification stage from the first system was regularly exposed to heat shocks.

2.2. Heat shocks and sampling

An overview about heat shock regimes is given in Fig. 2. Heat shocks were applied manually transferring the leachate into an incubator, where the leachate was heated up to 55 °C. After the core of the biomass reached that temperature, the liquor was further incubated for 30 min and then refilled into the two-phase acidification stage. During the first 21 days, only one heat shock with 55 °C was carried out per week. From day 22 until day 42, the heat-shock temperature was increased to 70 °C, performed similarly, and three heat shocks were applied for each acidification cycle (Fig. 2). Between experimental day 21 and 2, there was a technical break in operation for two weeks.

A second, identical multistage system was used as control without heat shocks (further referred as control system). Samples for 16S-rRNA gene-amplicon high-throughput analysis were taken every second and seventh day of each acidification cycle (Figs. 2 and 4). Additionally, at day 36, directly after a 70 °C heat shock, a sample for 16S-rRNA gene full length sequencing was taken, as well as a sample for microbial culturing at day 37.

2.3. Chemical and microbial process analysis

Analysis of chemical parameters was performed as previously described (Abendroth et al., 2015b). Extraction of DNA, primer nucleotide sequences for bacteria, 16S-rRNA gene amplification, high-throughput amplicon sequencing with IonTorrent, and sequence analysis was performed as described by Abendroth et al. (2017). At day 36 of the experiment, the acidification stage from the heat-shock system was analysed through full length sequencing of the 16S-rRNA gene and anaerobic culturing approaches. Cloning and library construction was performed as described by Rademacher et al. (2012).

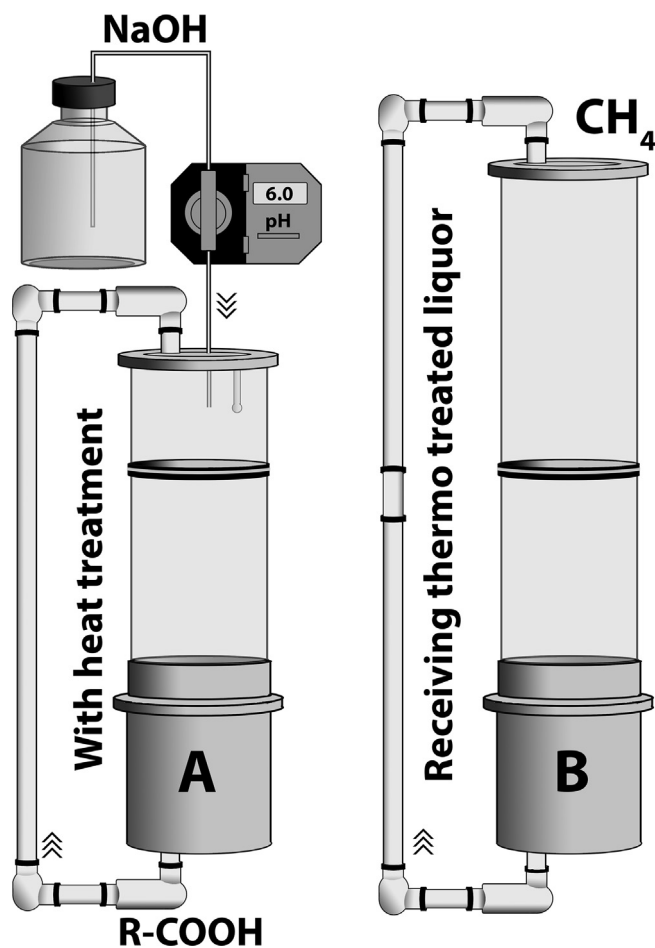


Fig. 1. Experimental set-up: Reactor set-up consisting of a hydrolytic/acidogenic stage (A) and a methanogenic stage (B). Feeding of the methanogenic stage with the liquid phase from the hydrolytic/acidogenic stage and heat-treatment was performed manually on a daily basis. Two reactor systems were built, further referred as heat-shock system and control system.

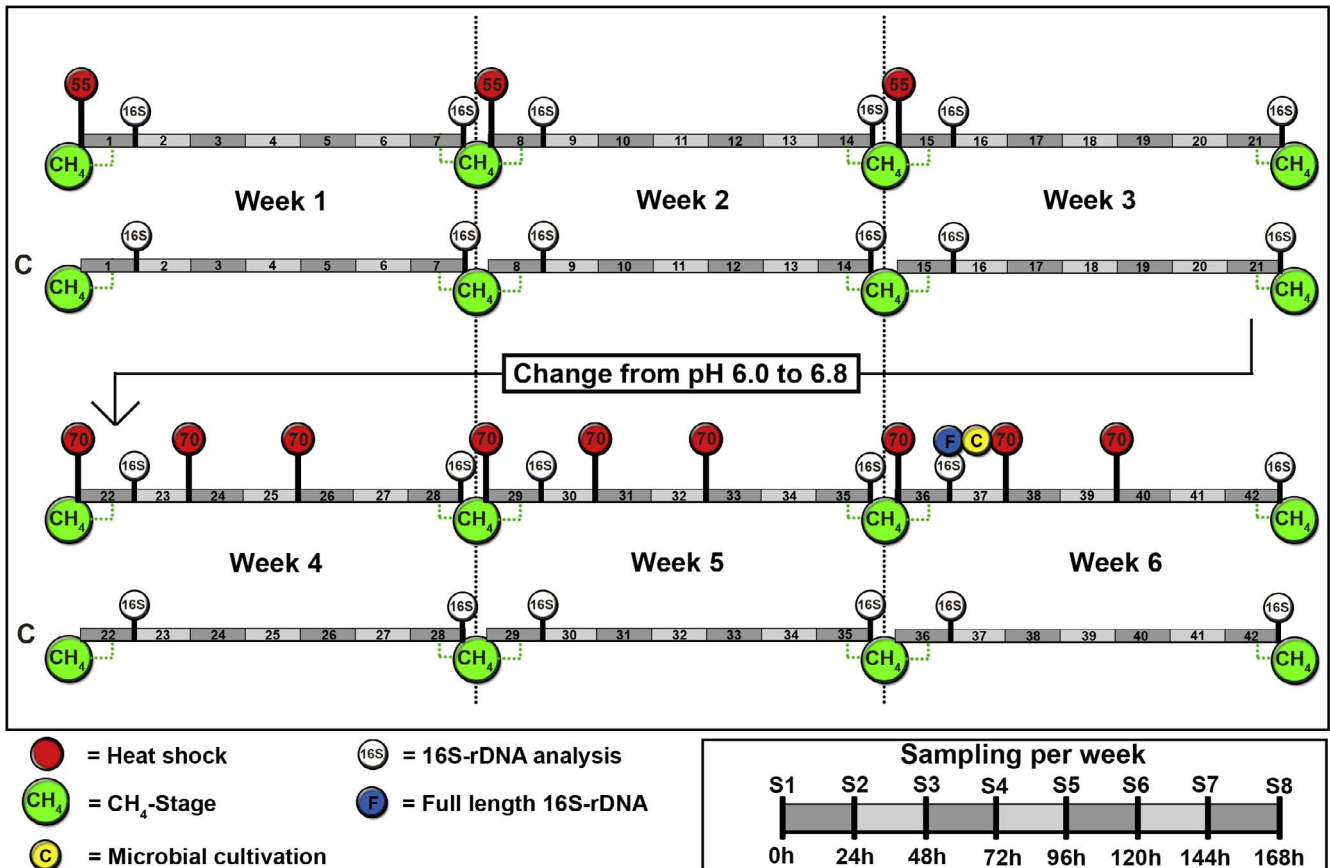


Fig. 2. Experimental timeline: Acidification occurred in six cycles of one week each. Experimental week 3 and experimental week 4 were separated by a two-weeks interval. Green circles indicate the collection of liquor and the subsequent feeding into the methane stages. Collected digestates from the methane stages were used for setting up new acidification cycles. (For interpretation of the references to colour in this figure legend, the reader is referred to the web version of this article.)

2.4. Isolation of microbial strains

To isolate different bacteria, cultivation was performed under anoxic conditions on Reinforced Clostridial Agar (Oxoid Ltd.) and on modified DSMZ medium No. 350 (*Cellulomonas fermentans* medium). In contrast to the DSMZ medium 350 (DSMZ 2007), the modified medium contained (per liter) 2.0 g yeast extract, 0.5 g cellobiose, 2.0 g soluble starch, 1.0 g methyl cellulose and 15.0 g agar; the pH of the medium was 6.9. After autoclaving 10 mL L⁻¹ vitamin solution was added according to DSMZ medium 141 (DSMZ 2017). The reactor sample was diluted 10¹, 10⁴ and 10⁶ fold in anoxic Ringer's solution and aliquots of the dilutions were streaked on pre-reduced agar plates. After incubation at 37 °C in an anaerobic chamber single colonies were re-streaked until purification was achieved. A loop full of colonies of the isolates were suspended in 50 µL molecular biological grade water and cells were lysed by consecutive freezing and thawing. Amplification and subsequent sequencing of the nearly full-length 16S rRNA gene of the strains was carried out using the primers 27F and 1492R as described by Hahnke et al. (2014).

3. Results and discussion

3.1. Impact of heat-shocks on process performance

After applying heat shocks on the acidification stage, almost no differences of chemical parameters were observed between the heat-shock

system and the control system (Fig. 3). Solubilisation of chemical oxygen demand and production of total volatile fatty acids (TVFA) were monitored daily and found to reach similar values in both the heat-shock system and the control system (Fig. 3A). Additionally, similar volumes of methane from the produced high-strength liquor were produced (Fig. 3B). During the first three weeks, when 55 °C heat shocks were applied, 29.1 ± 11.4 gCOD L⁻¹ and 15.9 ± 5.6 gTVFA L⁻¹ were produced. The respective control showed 35.6 ± 6.8 gCOD L⁻¹ and 20.5 ± 3.7 gTVFA L⁻¹. In the following three weeks, where heat shocks were more frequently applied and at a higher temperature (70 °C), concentrations of 26.9 ± 2.7 gCOD L⁻¹ and 18.9 ± 0.8 gTVFA L⁻¹ were measured. The corresponding control samples yielded 28.4 ± 5.7 gCOD L⁻¹ and 19.6 ± 0.2 gTVFA L⁻¹. Even though the degradation efficiency was not detectably improved, no process inhibition was found either. At week 2 the heat-shock system and the control system showed both a higher COD compared to the other weeks. Very likely this is due to heterogeneity of the used substrate.

The high conversion of solubilized COD indicates that methanation was not inhibited in both methane stages (heat shock system and control system) (Fig. 3B). The produced amount of methane per g of solubilized COD was in both methane stages slightly above the theoretical maximum of 350 mL gCOD⁻¹ due to small particles that remained in the collected high strength liquor from the acidification.

In addition and in comparison to the control system, we observed in the heat-shock system a reduced methane formation in the acidification

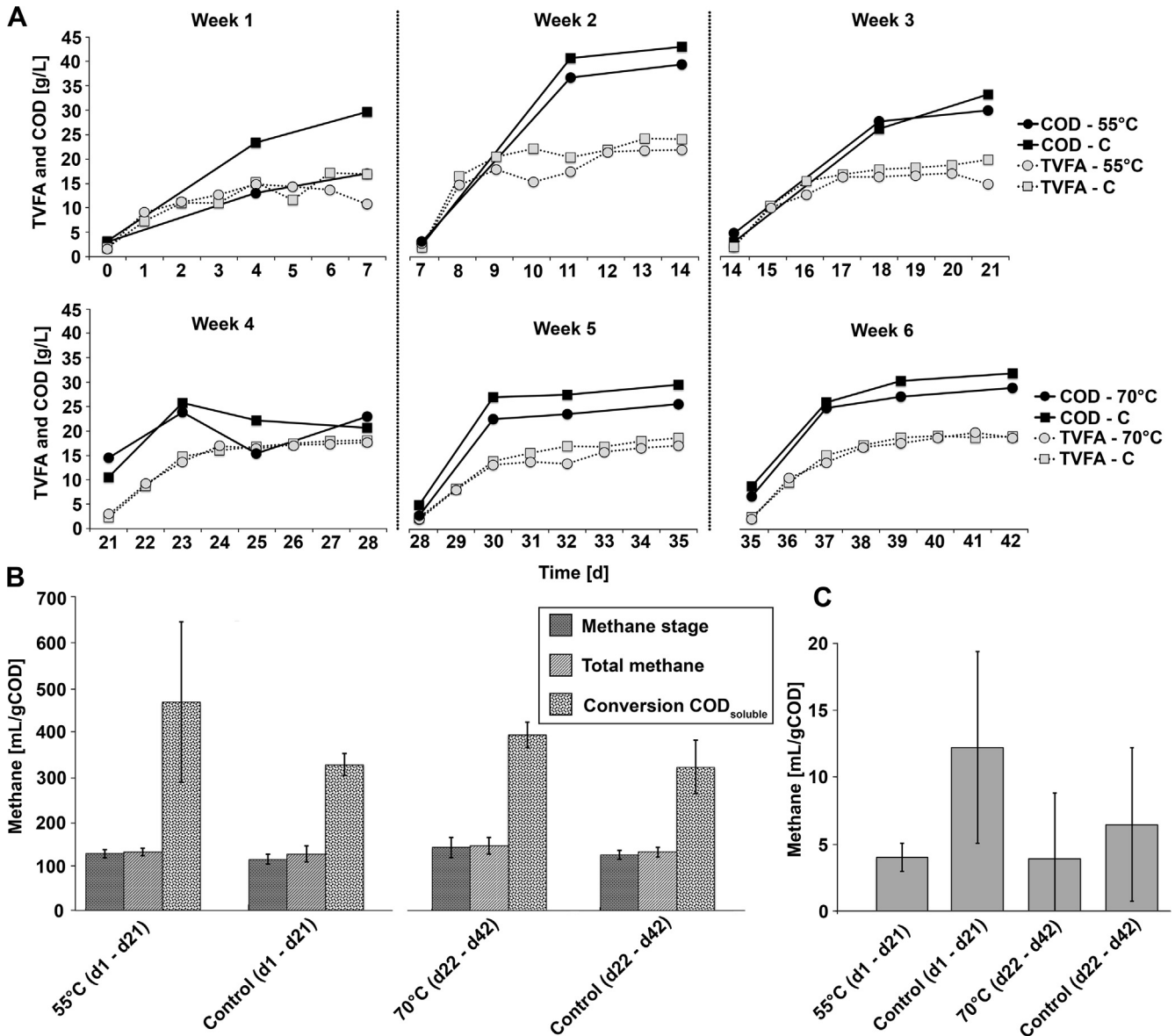


Fig. 3. Chemical analysis: Produced total volatile fatty acids (TVFA) and solubilized chemical oxygen demand (COD) are given for both the heat-shock system and the control system (A). Produced methane as well as conversion efficiency of solubilized COD for acidification and methane stages is summarized for different time intervals: d1–d21, day 1–21; d22–d42, day 22–42 (B). The methane production from the acidification stage is shown in (C). Gas volume is given as a mean value for the total gas formation per week (for each batch cycle). Standard deviations were calculated with the mean value from experimental week 1–3 and experimental week 4–6.

stage subjected to heat shocks. Compared to the methane stage, only low levels of methane were formed in the acidification stage of both reactor systems. In the acidification stage with 55 °C heat shocks, 67% less methane was formed than in the un-heated control. In the experiment with 70 °C, it was 40% less methane compared to the control (Fig. 3C).

Therefore, the reduction of methanogenic contaminations from the seed sludge in the acidification stage associated to heat treatments could help to separate acidification from methanation more efficiently in order to prevent loss of methane.

3.2. Post heat-shock transient microbial community

For each acidification cycle, samples for 16S-rRNA high throughput sequencing were taken at the second and last day (Figs. 2 and 4). On the phylum level, all sequences showed a profile mainly consisting of Firmicutes, Bacteroidetes and Proteobacteria (Fig. 4). This is in concordance with our previous studies on microbiomes from seven

anaerobic digester plants in Germany, and acidification of grass biomass (Abendroth et al., 2015a,b, 2017). During experimental weeks 1–3 Proteobacteria were especially enriched, whereas Bacteroidetes tended to decrease in the control non-shocked reactor. The high abundance of Proteobacteria is in concordance with a study published by Weerasekara et al. (2016), where Proteobacteria increased in frequency in wastewater due to acidic conditions. In our experiment, by changing the pH to 6.8 (experimental week 4–6) the amount of Proteobacteria was dramatically reduced and, in the heat shocked system the phylum Bacteroidetes recovered. This indicates a high microbial redundancy, as the change of dominating microbial groups showed no negative effects on the degradability of the used grass biomass.

On genus level, *Bacteroides*, *Prevotella*, *Enterococcus*, *Clostridium* and *Pseudomonas* were abundant during experimental weeks 1–3. Raising the pH to 6.8 at day 21 was associated with a dramatic shift in the microbial composition, consisting mainly of *Bacteroides*, *Streptococcus*, *Aminobacterium*, *Clostridium* and *Tissierella* (Fig. 4). The fact that even three shocks per cycle at 70 °C did not cause permanent shifts in the

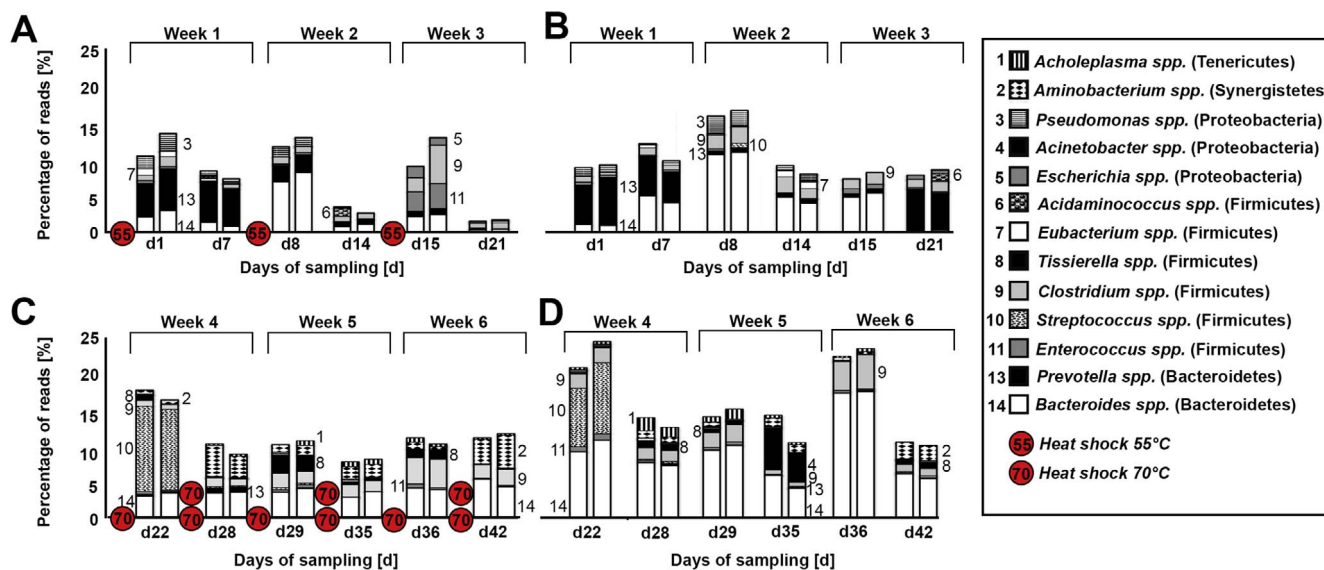


Fig. 4. Microbiome composition of heat-shocked samples. Microbial composition is given as a percentage of all analysed bacterial sequences. Sequences were classified on the genus level. Values for samples from the experiment with 55 °C heat shocks are shown in A; and C corresponds to the 70 °C heat shocks. Values for samples from the control system without heat shocks are shown in B and D. All samples were analysed as duplicates.

microbial composition, but only transient modifications indicates that the mesophilic microbiomes from anaerobic digesters exhibit high resilience against heat shocks, while being more sensitive to pH changes.

Interestingly, many sequences remained unclassified on the genus level (Fig. 4). This is in accordance with other studies on biogas facilities, e.g., based on previous study on NGS (Maus et al., 2016), where also many unclassified species were detected.

3.3. Heat shocks and pathogens

Microbial culturing as well as culture-independent 16S-rDNA full-length sequencing was used to assess microbiota on species level (Fig. 2). Surprisingly, many opportunistic pathogenic species listed with risk level 2 in the TRBA (technical rules for biological working materials, 2004) were detected, namely *Bacteroides ovatus*, *Bacteroides thetaiotaomicron*, *Bacteroides uniformis*, *Citrobacter werkmanii*, *Enterococcus gallinarum*, *Globicatella sulfidifaciens*, *Streptococcus lutetiensis*, *Corynebacterium freneyi*, *Escherichia hermannii*, *Lactococcus garvieae*, or *Proteus mirabilis*. The application of sewage sludge as seed sludge might explain the occurrence of detected pathogens mentioned before, as sewage is well known for its content of pathogenic bacteria (Arthurson, 2008). The fact that corresponding genera were observed in high abundance (Fig. 4) also implies a high abundance of these pathogens. In conclusion, abundant heat treatments at 70 °C were not sufficient to suppress potential pathogenic genera.

4. Conclusions

The response of microbial populations present in mesophilic acidification stages to short heat cycles was investigated. The studied microbiomes proved very robust, since the same amount of methane was produced in heat-shocked samples compared to the control ones. Heat-shocks caused only minor, transient community shifts and the strongest impact on the microbiome was observed with a combination of heat shock and low pH. Potential pathogenic genera remained abundant; and several pathogens were still found after the heat treatment. Our results can be the first step towards future approaches combining microbial-driven acidification and thermal treatments as a new pretreatment methodology.

Acknowledgements

We thank our student Justus Hardegen for technical assistance. Further, we are grateful for funding of the work by the German Federal Ministry of Economic Affairs and Energy (grant no. KF 2050830SA4, KF 3400701SA4, KF 2112205SA4 and 03KB110A). SH and MK thank Kerstin Mundt for the excellent technical assistance.

Appendix A. Supplementary data

Supplementary data associated with this article can be found, in the online version, at <http://dx.doi.org/10.1016/j.biortech.2017.10.093>.

References

- Abendroth, C., Wünsche, E., Luschig, O., Bürger, C., Günther, T., 2015a. Producing high-strength liquor from mesophilic batch acidification of chicken manure. *Waste Manage. Res.* 33, 291–294.
- Abendroth, C., Vilanova, C., Günther, T., Luschig, O., Porcar, M., 2015b. Eubacteria and Archaea communities in seven mesophile anaerobic digester plants. *Biotechnol. Biofuels* 8, 87.
- Abendroth, C., Simeonov, C., Peretó, J., Antúnez, O., Gavidia, R., Luschig, O., Porcar, M., 2017. From grass to gas: microbiome dynamics of grass biomass acidification under mesophilic and thermophilic temperatures. *Biotechnol. Biofuels* 10, 171.
- Algapani, D.E., Qiao, W., Su, M., di Pumo, F., Wandera, S.M., Adani, F., Dong, R., 2016. Bio-hydrolysis and bio-hydrogen production from food waste by thermophilic and hyperthermophilic anaerobic process. *Bioresour. Technol.* 216, 768–777.
- Alibardi, L., Favaro, L., Lavagnolo, M.C., Basaglia, M., Casella, S., 2012. Effects of heat treatment on microbial communities of granular sludge for biological hydrogen production. *Water Sci. Technol.* 66, 1483–1490.
- Arthurson, V., 2008. Proper sanitization of sewage sludge: a critical issue for a sustainable society. *Appl. Environ. Microbiol.* 74, 5267–5275.
- Baccay, R.A., Hashimoto, A.G., 1984. Acidogenic and methanogenic fermentation of causticized straw. *Biotechnol. Bioeng.* 26, 885–891.
- Dinopoulou, G., Rudd, T., Lester, J.N., 1988. Anaerobic acidogenesis of a complex wastewater: I. The influence of operational parameters on reactor performance. *Biotechnol. Bioeng.* 5, 958–968.
- Ennouria, H., Miladia, B., Diaz, S.Z., Güelfoc, L.A.F., Solera, R., Hamdi, M., Bouallagui, H., 2016. Effect of thermal pretreatment on the biogas production and microbial communities balance during anaerobic digestion of urban and industrial waste activated sludge. *Bioresour. Technol.* 214, 184–191.
- Gijzen, H.J., Zwart, K.B., Verhagen, F.J., Vogels, G.P., 1988. High-rate two-phase process for the anaerobic degradation of cellulose, employing rumen microorganisms for an efficient acidogenesis. *Biotechnol. Bioeng.* 31, 418–425.
- Gonzales-Fernandez, C., Sialve, B., Bernet, N., Steyer, J.P., 2012. Thermal pretreatment to improve methane production of *Scenedesmus* biomass. *Biomass Bioenergy* 40, 105–111.

- Haarstrick, A., Hempel, D.C., Ostermann, L., Ahrens, H., Dinkler, D., 2001. Modelling of the biodegradation of organic matter in municipal landfills. *Waste Manage. Res.* 19, 320–331.
- Hahnke, S., Striesow, J., Elvert, M., Mollar, X., Klocke, M., 2014. *Clostridium bornimense* sp. nov., isolated from a mesophilic, two-phase, laboratory-scale biogas reactor. *Int. J. Syst. Evol. Microbiol.* 64, 2792–2797.
- Jungers, J.M., Fargione, J.E., Sheaffer, C.C., Wyse, D.L., Lehman, C., 2013. Energy potential of biomass from conservation grasslands in Minnesota USA. *PLoS One* 8 (4), e61209.
- Koutinas, A., Kanellaki, M., Bekatorou, A., Kandylis, A., Pissaridi, K., Dima, A., Boura, K., Lappa, K., Tsafrakidou, P., Stergiou, P.Y., Foukis, A., Gkini, O.A., Papamichael, E.M., 2016. Economic evaluation of technology for a new generation biofuel production using wastes. *Bioresour. Technol.* 200, 178–185.
- Maus, I., Koeck, D.E., Cibis, K.G., Hahnke, S., Kim, Y.S., Langer, T., Kreubel, J., Erhard, M., Bremges, A., Off, S., Stolze, Y., Jaenicke, S., Goesmann, A., Sczyrba, A., Scherer, P., König, H., Schwarz, W.H., Zverlov, V.V., Liebl, W., Pühler, A., Schlüter, A., Klocke, M., 2016. Unraveling the microbiome of a thermophilic biogas plant by metagenome and metatranscriptome analysis complemented by characterization of bacterial and archaeal isolates. *Biotechnol. Biofuels* 9, 171.
- Mood, S.H., Golfeshan, A.H., Tabatabaei, M., Jouzani, G.S., Najafi, G.H., Gholami, M., Ardjmand, M., 2013. Lignocellulosic biomass to bioethanol, a comprehensive review with a focus on pretreatment. *Renew. Sustain. Energy Rev.* 27, 77–93.
- Moset, V., Poulsen, M., Wahid, R., Højberg, O., Møller, H.B., 2014. Mesophilic versus thermophilic anaerobic digestion of cattle manure: methane productivity and microbial ecology. *Microb. Biotechnol.* 8, 787–800.
- Rademacher, A., Nolte, C., Schönberg, M., Klocke, M., 2012. Temperature increases from 55 to 75 °C in a two-phase biogas reactor result in fundamental alterations within the bacterial and archaeal community structure. *Appl. Microbiol. Biotechnol.* 96, 565–576.
- Tian, H., Fotidis, I.A., Mancini, E., Angelidaki, I., 2017. Different cultivation methods to acclimatise ammonia-tolerant methanogenic consortia. *Bioresour. Technol.* 232, 1–9.
- Voolapalli, R.K., Stuckey, D.C., 2001. Hydrogen production in anaerobic reactors during shock loads – influence of formate production and H₂ kinetics. *Water Res.* 35, 1831–1841.
- Yan, W., Acharjee, T.C., Coronella, C.J., Vasquez, V.R., 2009. Thermal pretreatment of lignocellulosic biomass. *Environ. Prog. Sustain.* 28, 435–440.
- Vrieze, J.D., Christiaens, M.E.R., Walraedt, D., Devooght, A., Ijaz, U.Z., Boona, N., 2016. Microbial community redundancy in anaerobic digestion drives process recovery after salinity exposure. *Water Res.* 111, 109–117.
- Weerasekara, A.W., Jenkins, S., Abbott, L.K., Waite, I., McGrath, J.W., Larma, I., Eroglu, E., Donnell, O.A., Whiteley, A.S., 2016. Microbial phylogenetic and functional responses within acidified wastewater communities exhibiting enhanced phosphate uptake. *Bioresour. Technol.* 220, 55–61.



Complete Genome Sequence of a New *Firmicutes* Species Isolated from Anaerobic Biomass Hydrolysis

Christian Abendroth,^{a,b,c} Sarah Hahnke,^d Francisco M. Codoñer,^e Michael Klocke,^d Olaf Luschning,^f Manuel Porcar^{a,b,g}

Cavanilles Institute of Biodiversity and Evolutionary Biology, Universitat de València, Paterna, Valencia, Spain^a; Institute for Integrative Systems Biology (I2SysBio), Paterna, Valencia, Spain^b; Robert Boyle Institut eV, Jena, Germany^c; Leibniz Institute for Agricultural Engineering and Bioeconomy (ATB), Bioengineering, Potsdam, Germany^d; Lifesequencing SL, Paterna, Valencia, Spain^e; Bio H2 Umwelt GmbH, Jena, Germany^f; Darwin Bioprospecting Excellence, Paterna, Valencia, Spain^g

ABSTRACT A new *Firmicutes* isolate, strain HV4-6-A5C, was obtained from the hydrolysis stage of a mesophilic and anaerobic two-stage lab-scale leach-bed system for biomethanation of fresh grass. It is assumed that the bacterial isolate contributes to plant biomass degradation. Here, we report a draft annotated genome sequence of this organism.

Degrading bacteria, most of them isolated from soil, play relevant roles in the turnover of different types of material, such as petrol (1), pollutants (2), metal (3), and cellulose (4, 5). In the case of plant biomass degradation in biogas reactors, such microorganisms play an important role in making hardly accessible polymeric carbon sources available for other organisms for the production of biogas.

In this study, we present the genome sequence of a new *Firmicutes* isolate, strain HV4-6-A5C, which has a putative role in the microbial metabolic network for plant biomass degradation. This strain was isolated from a lab-scale leach-bed biogas reactor system, which was operated at 37°C with fresh grass as the sole substrate. Isolation was performed on reinforced clostridial agar (Oxoid Ltd.) after the diluted hydrolysate was reincubated with microcrystalline cellulose as the sole carbon source.

We applied a massive genome-sequencing approach using the Illumina NextSeq 500 platform. A Nextera XT library with a mean insert size of 350 nucleotides (nt) was constructed and sequenced with a combination of 150-bp paired-end (PE) reads. A total of 29.2 million PE sequences, with a mean length of 149.85 nt, were obtained. Sequences were filtered by quality, and a total of 29.15 million PE sequences with a Q value higher than 20 (mean Q, 33.17) were included in the assembly. The sequences were assembled with SPAdes version 3.10.1 (6) using default parameters and a *k*-mer value that provided us with the lowest number of contigs, the longest contig, the largest N_{50} value, and the highest percentage of clean sequences. With a *k*-mer value of 77, a total of 106 contigs were obtained. The total size of the genome was approximately 3.3 Mb, with an estimated GC content of 33.43%, a longest contig size of 276,895 bp, and an N_{50} value of 113,179 bp.

The assembled genome sequences were annotated using the Prokka version 1.11 annotation pipeline (7), which involved predicting tRNAs, rRNAs, mRNAs, and signal peptides in the sequences using Aragorn, RNAmmer, Prodigal, and SignalP, respectively (8–11).

The genome contains 5,376 elements, of which 5,311 are open reading frames (ORFs) (2,723 canonical and 2,588 noncanonical) and 65 are encoded structural RNAs (sRNAs)—i.e., 5 ORFs for rRNAs and 60 ORFs for tRNAs.

Received 31 May 2017 Accepted 19 July 2017 Published 5 October 2017

Citation Abendroth C, Hahnke S, Codoñer FM, Klocke M, Luschning O, Porcar M. 2017. Complete genome sequence of a new *Firmicutes* species isolated from anaerobic biomass hydrolysis. *Genome Announc* 5:e00686-17. <https://doi.org/10.1128/genomeA.00686-17>.

Copyright © 2017 Abendroth et al. This is an open-access article distributed under the terms of the [Creative Commons Attribution 4.0 International license](https://creativecommons.org/licenses/by/4.0/).

Address correspondence to Manuel Porcar, manuel.porcar@uv.es.

Using BLAST, we compared the contigs with all genome sequences available in the database. According to the PCOP (12) and the AAI (13), the genome can be classified as a species belonging to the genus *Clostridium*. Based on the average nucleotide sequence identity (ANI) (14), the closest related species is *Sporanaerobacter acetigenes*, showing an identity of only 71.13%, which indicates that the novel strain represents a new species within the phylum *Firmicutes*.

Accession number(s). The microbial strain reported here has been deposited at DSMZ with the deposit number DSM 104144. The results of the whole-genome project have been deposited at DDBJ/EMBL/GenBank under the accession no. [FXVB02000001](https://doi.org/10.1093/nar/gkh152) to [FXVB02000106](https://doi.org/10.1093/nar/gkm160). The version described here is the first draft version.

ACKNOWLEDGMENT

We are grateful for the funding provided by the German Federal Ministry of Economic Affairs and Energy (grant no. KF 2050830SA4, KF 3400701SA4, and KF 2112205SA4).

REFERENCES

- Pérez-Hernández I, Ochoa-Gaona S, Adams RH, Rivera-Cruz MC, Pérez-Hernández V, Jarquín-Sánchez A, Geissen V, Martínez-Zurimendi P. 2017. Growth of four tropical tree species in petroleum-contaminated soil and effects of crude oil contamination. *Environ Sci Pollut Res Int* 24: 1769–1783. <https://doi.org/10.1007/s11356-016-7877-5>.
- McCormick ML, Adriaens P. 2004. Carbon tetrachloride transformation on the surface of nanoscale biogenic magnetite particles. *Environ Sci Technol* 38:1045–1053. <https://doi.org/10.1021/es030487m>.
- Kip N, van Veen JA. 2015. The dual role of microbes in corrosion. *ISME J* 9:542–551. <https://doi.org/10.1038/ismej.2014.169>.
- Singh N, Mathur AS, Tuli DK, Gupta RP, Barrow CJ, Puri M. 2017. Cellulosic ethanol production via consolidated bioprocessing by a novel thermophilic anaerobic bacterium isolated from a Himalayan hot spring. *Bio-technol Biofuels* 10:73. <https://doi.org/10.1186/s13068-017-0756-6>.
- Poszytek K, Cieczkowska M, Skłodowska A, Drewniak L. 2016. Microbial consortium with high cellulolytic activity (MCHCA) for enhanced biogas production. *Front Microbiol* 7:324. <https://doi.org/10.3389/fmicb.2016.00324>.
- Bankevich A, Nurk S, Antipov D, Gurevich AA, Dvorkin M, Kulikov AS, Lesin VM, Nikolenko SI, Pham S, Pribelski AD, Pyshkin AV, Sirotkin AV, Vyahhi N, Tesler G, Alekseyev MA, Pevzner PA. 2012. SPAdes: a new genome assembly algorithm and its applications to single-cell sequencing. *J Comput Biol* 19:455–477. <https://doi.org/10.1089/cmb.2012.0021>.
- Seemann T. 2014. Prokka: rapid prokaryotic genome annotation. *Bioinformatics* 30:2068–2069. <https://doi.org/10.1093/bioinformatics/btu153>.
- Laslett D, Canback B. 2004. ARAGORN, a program to detect tRNA genes and tmRNA genes in nucleotide sequences. *Nucleic Acids Res* 32:11–16. <https://doi.org/10.1093/nar/gkh152>.
- Lagesen K, Hallin P, Rødland EA, Staerfeldt HH, Rognes T, Ussery DW. 2007. RNAmmer: consistent and rapid annotation of ribosomal RNA genes. *Nucleic Acids Res* 35:3100–3108. <https://doi.org/10.1093/nar/gkm160>.
- Hyatt D, Chen GL, Locascio PF, Land ML, Larimer FW, Hauser LJ. 2010. Prodigal: prokaryotic gene recognition and translation initiation site identification. *BMC Bioinformatics* 11:119. <https://doi.org/10.1186/1471-2105-11-119>.
- Petersen TN, Brunak S, von Heijne G, Nielsen H. 2011. SignalP 4.0: discriminating signal peptides from transmembrane regions. *Nat Methods* 8:785–786. <https://doi.org/10.1038/nmeth.1701>.
- Qin QL, Xie BB, Zhang XY, Chen XL, Zhou BC, Zhou J, Oren A, Zhang YZ. 2014. A proposed genus boundary for the prokaryotes based on genomic insights. *J Bacteriol* 196:2210–2215. <https://doi.org/10.1128/JB.01688-14>.
- Rodríguez-R LM, Konstantinidis KT. 2014. Bypassing cultivation to identify bacterial species. *Microbe* 9:111–118. <https://doi.org/10.1128/microbe.9.111.1>.
- Richter M, Rosselló-Móra R. 2009. Shifting the genomic gold standard for the prokaryotic species definition. *Proc Natl Acad Sci U S A* 106: 19126–19131. <https://doi.org/10.1073/pnas.0906412106>.

Warm and wet: robust lipase-producing bacteria from the indoor environment

Kristie Tanner¹, Christian Abendroth^{1,2}, and Manuel Porcar^{1,3*}

[†]Both authors contributed equally to this work

¹ Institute for Integrative Systems Biology (I2SysBio, University of Valencia-CSIC)

² Robert Boyle Institute e.V., Im Steinfeld 10, 07751 Jena, Germany

³ Darwin Bioprospecting Excellence, S.L. Parc Científic Universitat de Valencia C/ Catedrático Agustín Escardino Benlloch, 9

*Corresponding author:

E-mail: manuel.porcar@uv.es (MP)

Lipases are key biocatalysts with important biotechnological applications. With the aim of isolating robust lipolytic microbial strains, we have analyzed the bacterial communities inhabiting two domestic extreme environments: a thermophilic sauna and a dishwasher filter. Scanning electron microscopy revealed biofilm-forming and scattered microorganisms in the sauna and dishwasher sample, respectively. A culture-independent approach based on 16S rRNA analysis indicated a high abundance of Proteobacteria in the sauna sample; and, a large amount of Proteobacteria, Firmicutes, Cyanobacteria and Actinobacteria in the dishwasher filter. With a culture-dependent approach, we isolated 48 bacterial strains, screened their lipolytic activities on media with tributyrin as the main carbon source, and finally selected five isolates for further characterization. These strains, all of them identified as members of the genus *Bacillus*, displayed optimum lipolytic peaks at pH 6.5 and with 1-2% NaCl, and the activity proved very robust at a wide range of pH (up to 11.5) and added NaCl concentrations (up to 4%). The thermal, pH and salt robustness of the selected isolates is a valuable attribute for these strains, which are promising as highly tolerant biodegradants. To our knowledge, this is the first report regarding the isolation from an indoor environment of *Bacillus* strains with a high potential for industry.

Introduction

In the past decade, research programs on indoor environments have resulted in an increasing data matrix of taxonomic and ecological interest [1, 2]. Attention has especially been paid to frequently used domestic places that are, on many occasions, overgrown with potential pathogenic bacteria, like in the recently described coffee-machine or refrigerator bacteriomes [3, 4]. It is important to stress that indoor environments mimic natural, often extreme, environments. For example, refrigerators are almost as cold as tundra and thus rich in cold-adapted bacteria, whereas sun-exposed artificial flat surfaces, such as solar panels, are home of a rich desert-like biocenosis [5]. Therefore, bioprospecting nearby indoor extreme environments is a poorly explored but yet promising screening strategy that might yield bacterial strains with new or improved biotechnological applications.

Indeed, and besides the obvious medical implications, another reason to further investigate indoor microbiomes is the search of enzymes with high industrial significance, especially as novel biocatalysts [6]. A very well known (natural) precedent is the discovery of the extremophile bacterium *Thermus aquaticus* [7], whose thermoresistant Taq polymerase allowed the revolutionary development of Polymerase Chain Reaction in the last decades of the 20th century.

Within the current repertoire of available enzymes, esterases are particularly suitable for industrial processes, since they are stable in organic solvents and can freely reverse the enzymatic reaction from hydrolysis to synthesis [8]. Lipases have also been highlighted as key biocatalysts for biotechnological applications, such as the production of new biopolymeric materials and biodiesel, or the synthesis of fine chemicals like therapeutics, agrochemicals, cosmetics and flavors [9]. Their stereoselective properties make them able to recognize enantiomers and enantiotopic groups, while many other enzymes for hydrolysis are just capable of metabolizing one antipode of the specific substrate [10].

Environments with extreme and/or oscillating temperatures are of special interest, due to the opportunity of finding esterases that are active at wide intervals of temperature and that can thus be used under a range of industrial conditions, such as those present in dishwashers or washing machines. A new and promising esterase has recently been discovered in the thermophilic bacterium *Thermogutta terrifontis*. This enzyme retains up to 95% of its activity after incubation for 1h at 80°C [11]. A cold-active and solvent-tolerant lipase from *Stenotrophomonas maltophilia* has also been reported, with retention of 57% of its activity at 5°C and more than 50% of its activity in pure organic solvents [12]. More examples of extremophilic enzymes with industrial potential include thermoalkalophilic esterases from *Geobacillus* sp., which have all proven active at high temperature (65°C) and at pH of up to 10 [13]; or a cold-adapted esterase from *Pseudoalteromonas arctica*, which still retained 50% of its activity at the freezing point of water [14].

Upon discovery, extremophile enzymes can often be further optimized to improve their industrial use, as it was the case for the thermal stability and activity in the cold-adapted lipase B from *Candida antarctica* through chemical linking of

amino groups of the lipase to oxidized polysaccharides using reducing agents [15].

Bioprospecting indoor extreme environments could yield new lipolytic microbial strains harbouring previously uncharacterized esterases and other enzymes. In the present work, we have focused on the microbial communities inhabiting two high-temperature, domestic environments: a thermophilic sauna and a dishwasher. We have isolated 48 bacterial strains, many of them lipase-producing bacteria. Furthermore, we have characterized five of them, displaying robust lipase activities with promising biotechnological applications.

Material and Methods

2.1. Sampling

Environmental samples were taken from a sauna and from a dishwasher. The sauna, set at a temperature of approximately 45°C and with 100% relative humidity, is a publicly-owned facility located in a communal swimming pool in Valencia (Spain) and therefore did not require specific permission for the sampling. A biofilm-like mass below the aluminium bench of the sauna was collected in a sterile 50 mL Falcon tube and was stored at -20 °C until required. The dishwasher sample was collected from the filter of a domestic Siemens dishwasher (property of one of the co-authors of this work, MP), Model sm6p1s. The sample was obtained by scratching the inner surface of the filter with a sterile bladder and the resulting biomass was kept at -20 °C until required.

2.2. Scanning electron microscopy

Biomass samples were fixed on a 0.2 µm membrane filter (Merck Millipore Ltd, Tullagreen, Cork, Ireland) using paraformaldehyde 2% - glutaraldehyde 2.5%. A volume of 5 ml was pressed two times through the filter. The filter was washed with Milli-Q water (Merck Millipore Ltd, Tullagreen, Cork, Ireland) and then dehydrated in ethanol (gradually increasing concentration). Dehydrated samples were placed in microporous capsules of 30 µm in pore size (Ted Pella Inc.) and immersed in absolute ethanol. Critical point drying was performed in an Autosamdri 814 (Tousimis). Once dried, samples were placed on SEM stubs by means of silver conducting paint TAAB S269. Stubs were examined under a scanning electron microscope Hitachi S-4100.

2.3. 16S-rDNA analyses with Ion Torrent

DNA was retrieved from sauna and dishwasher samples using the PowerSoil DNA Isolation Kit (MO BIO Laboratories, USA). DNA quality was analyzed using a Nanodrop-1000 Spectrophotometer (Thermo Scientific, Wilmington, DE, USA). A 500 bp long fragment from the hypervariable 16S-rDNA regions V1 – V3 was amplified using the universal primers 28F (5' -GAG TTT GAT CNT GGC TCA G-3') and 519R (5' -GTN TTA CNG CCG CKG CTG-3'). The quality of the resulting amplicons was checked on a 0,8% (w/v) agarose gel. Amplicons were precipitated with 3M potassium acetate and isopropanol. Sequencing libraries were constructed using 100 ng of the DNA pool and performing the amplicon fusion method (Ion Plus Fragment Library Kit, MAN0006846, Life Technologies). Both libraries (Sauna and Dishwasher) were quantified with the Agilent2100 Bioanalyzer (Agilent Technologies Inc, Palo Alto, CA, USA) prior to clonal amplification. Emulsion PCRs were carried out with the Ion PGM Template OT2 400 kit as described following the user guide provided by the manufacturer (MAN0007218,

Revision 3.0 Life Technologies). Libraries were sequenced in an Ion 318 Chip v2 on a Personal Genome Machine (PGM) (Ion-Torrent™, Life Technologies) at Life Sequencing S.L. (Life Sequencing, Valencia, Spain), using the Ion PGM Sequencing 400 kit and following the manufacturer's protocol (publication number MAN0007242, revision 2.0, Life Technologies). Short reads (<100bp) and low quality reads (<q15) were removed upon sequencing at the sequencing center. Resulting sequences were analyzed by phylotyping with the MOTHUR software [16]. Amplicons were aligned to the 16S-reference from the Greengenes database. Classification was performed using the k-mer algorithm. Assignments with a similarity percentage lower than 80% were discarded.

2.4. Isolation of microbial strains

Lysogenic broth (LB) and Reasoner's 2A (R2A) agar [17] media were used for bacterial culturing. Samples were suspended in PBS-buffer, vortexed, spread on LB and R2A plates and incubated at 37 °C and 55 °C for one day. Thermophilic and thermo-resistant strains were picked, grown in liquid culture and stored in 20 % Glycerol at -70 °C.

2.5. Lipolytic Activity and microbial identification

Tributyryl-containing medium is frequently used when screening for lipase-producing microorganisms [18,19], as the degradation of this compound generates clear halos around the lipolytic colonies in the otherwise turbid medium. Samples (1 µL) from the cryo-preserved strains were directly spotted on minimal medium [20], which contained tributyrin (10 mL/L) as main carbon source. Incubations were performed at 4 °C, 20 °C, 37 °C, 46 °C and 55 °C. After 5 days of incubation, the diameter of the halos around lipase-producing strains was measured.

2.6. 16S rRNA sequencing of selected strains

Hypervariable 16S-rDNA regions V1 – V3 of the selected strains were amplified by colony PCR using 28F and 519R primers and sequenced with the Sanger method by the Sequencing Service of the University of Valencia (Spain). This allowed the identification of the five selected isolates at a genus level. In order to identify the isolates at a species level, further *Bacillus* spp. primers were used to amplify: the TU elongation factor (tufGPF and tufGPR) [21], a group-specific 16S rRNA region (B-K1/F and B-K1/R1) [22], an endoglucanase gene (ENIF and EN1R) [23] and a glycosyltransferase (Ba-G206F and Ba-G1013R) [24]. The resulting sequences were manually edited using Pregap4 (Staden Package, 2002) to eliminate low-quality base calls. The final sequence for each isolate was compared to sequence databases using the NCBI BLAST tool.

2.7. Lipolytic assays varying pH and salt conditions

Lipase production of the five selected strains was tested on solid minimal medium supplemented with tributyrin (10 mL/L), adjusted to a range of pH (6.5, 8, 9.5 and 11.5), and with or without additional 4 % NaCl. Two microliters of each strain were spotted on each combination of pH and salt media and incubated at 4, 20, 37, 46 or 55 °C for 5 days. After incubation, the diameters of the halos were measured.

In order to determine the optimal conditions for the lipase production of the five selected strains, two microliters of each strain were spotted on additional combinations of pH and salt (pH 6.5, 8, 9.5 and 11.5; NaCl 0, 1, 2, 3 and 4 %). The plates were

incubated for five days at 37 °C. The assay was performed in triplicate.

3. Results and Discussion

3.1. Scanning Electron Microscopy

The samples obtained from a wet sauna and a dishwasher filter proved rich in microorganisms, as deduced by observation under SEM (Fig 1). In the sauna sample, microorganisms were mostly present in the form of a very dense biofilm almost totally embedded in a smooth matrix, very likely made of EPS (Fig 1A); whereas the dishwasher filter sample consisted mainly of food debris with scattered microorganisms (Fig 1B).

3.2. 16S-rDNA analyses with Ion Torrent

The taxonomic diversity of the two samples was determined by high throughput-sequencing, performed as described in Materials and Methods, and resulted in very different taxonomic profiles of both samples (Fig 1C and 1D). Proteobacteria were overwhelmingly abundant in the sauna sample, accounting for more than 90 % of the reads (Fig 1C). Of those, alpha-, beta- and gamma-proteobacteria were present at similar frequencies,

each accounting for more than 20 % of the assigned sequences. Minor taxa with frequencies of 1-5% included Bacteroidetes, Actinobacteria and Acidobacteria. The dishwasher filter was characterized by large amounts of Proteobacteria, Firmicutes (Bacilli, most of them), Cyanobacteria and Actinobacteria; and very low amounts of other taxa (Fig 1D).

These results are consistent with previous reports on these two extreme environments. Lee *et al.* [25] characterized the bacterial community contaminating the floor of a hot and dry sauna, which proved rich in Firmicutes, Gamma-proteobacteria and Beta-proteobacteria. Another report by Kim *et al.* [26] of a 64°C dry sauna revealed a population with Firmicutes, Gamma-proteobacteria, Beta-proteobacteria and Deinococci as the most frequent taxa. As mentioned above, our samples were rich Beta- and Gammaproteobacteria, although we also detected Alpha-proteobacteria, which was absent in the works by Kim *et al.* [25] and Lee *et al.* [26]. Reciprocally, we did not detect Firmicutes or Deinococci with our 16S rRNA analysis, while both taxa were found by those two previous reports. Concerning the dishwasher samples, a previous report by Savage *et al.* [27] characterized, among other household surfaces, the bacteria present in the dishwasher rinse reservoir. According to that

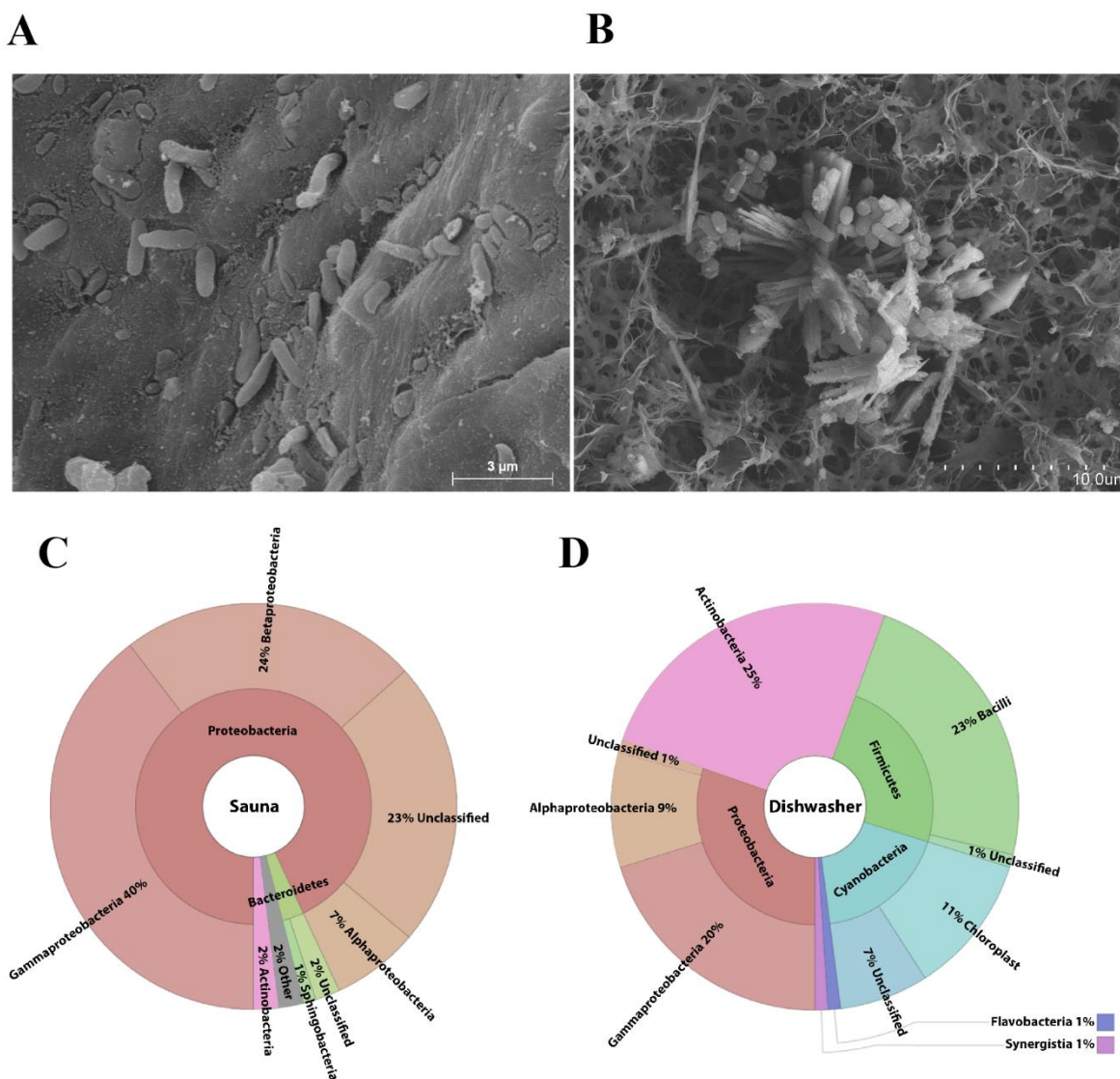


Fig 1. Scanning electron micrographs from the sauna (A) and the dishwasher (B) samples; taxonomic diversity estimated by 16Sr amplicon sequencing of sauna (C) and dishwasher (D). The sauna (C) sample was especially rich in Proteobacteria; whereas the dishwasher filter (D) also contained high amounts of Firmicutes, Cyanobacteria and Actinobacteria

previous report, bacterial population in the dishwasher consists of Proteobacteria, Firmicutes, Cyanobacteria and Actinobacteria, which corresponds to the taxonomic profile we found in the dishwasher filter. Nevertheless, Euryarcheota and Bacteroidetes that were found in the rinse reservoir [27] were not detected in the filter in the present work.

3.3. Culturing strains and lipolytic activity screening

Bacterial colonies randomly selected among those with a strong growth on LB and R2A plates were re-streaked to yield a collection of strains, and lipase production was screened after growth for five days in tributyrin-containing media, as described in materials and methods. Lipase production of all the strains is shown in Fig 2A. Most of the strains (72 and 79 % of the sauna and dishwasher strains, respectively) displayed some level of lipolytic activity. In general, sauna strains were able to produce lipases within a broader range of temperature, including, in two cases, values as high as 46 °C and as low as 4 °C. At least in these cases, though, lipases are not only produced, but are fully functional at extreme temperatures as deduced by this assay. In contrast, strains from the dishwasher displayed lipolytic activity within a smaller range of temperatures, in most cases only around 37 °C within the tested range. Interestingly, lipolytic activity, as deduced by haloes diameter, was maximum at 46 °C in several sauna strains, although no strains produced detectable lipolysis at 55 °C.

On the basis of this first screening for lipolytic activities, five strains were selected for further assays. Those included the strains with the broadest temperature activity range: S22 and S23, both active in all temperatures tested except at 55 °C; and D3, D11 and D18, the three dishwasher samples active at both 20 °C and 37 °C. In order to assess the potential of these five strains for biotechnological purposes (in terms of lipase production under extreme environmental conditions), they were taxonomically identified and subjected to a stress test under a range of temperatures and pH conditions, performed in minimum media with and without 4% added salt. Lipase activity were tested under different temperatures, NaCl and pH conditions, and results are shown in Fig 2B. Again, sauna samples exhibited a broad range of thermal stability, with medium to large halos at pH values mildly acid to moderately alkaline (6.5-9.5) and even in the presence of 4 % NaCl (pH 8 and 9.5). Interestingly, very alkaline (11.5) conditions, combined with high salt contents correlated with an increased thermal range of lipase production and activity for both S22 and S23, which increased from 20 °C up to 46 °C. In general, though, salt addition yielded smaller haloes at any temperature compared to standard media.

Regarding the strains we isolated from the dishwasher filter, assays performed with minimum media (without salt) adjusted to a wide range of pH values and incubated at different temperatures revealed the alkaliphily of their lipolytic abilities, both in terms of thermal broad range at alkaline pH values, and intensity of the activity as deduced by haloes sizes (Fig 2B). Addition of NaCl to the media resulted in smaller haloes and, at least for pH values of 8-9.5, in a narrower thermal activity range. In the three dishwasher strains, the combination of 4 % added NaCl and high (11.5) pH resulted in an altered thermal range of activity. At least in one case (D11) addition of 4 % NaCl partially restored the lack of activity observed with no added salt and at a pH of 11.5.

Sequencing of a16S rRNA gene fragment allowed identification of all five isolates as *Bacillus* sp. Further sequencing of the TU elongation factor (*tufGP* primers) and the group-specific 16S rRNA region (BK-1 primers) revealed D11 strain as *Bacillus megaterium* (with 99 and 100 % identity, respectively); and S22/S23 strains as *Bacillus pumilus* (with 100 and 99 % identity in the case of *tufGP* and BK-1 primers, respectively). D3 was not completely identified, and remains as *Bacillus* sp., possibly *B. subtilis*, *B. amyloliquefaciens*, *B. methylotrophicus* or *B. velenzensis*. D18 was identified as *B. cereus/B. thuringiensis*.

3.4. Robustness of the selected isolates in varying pH and salt conditions

In order to characterize the robustness of lipolytic activity of the five selected strains under alkaline and/or high salinity conditions, the strains were tested on combined pH and salt contents conditions, at 37 °C. Lipolytic activity results are shown in Fig 3.

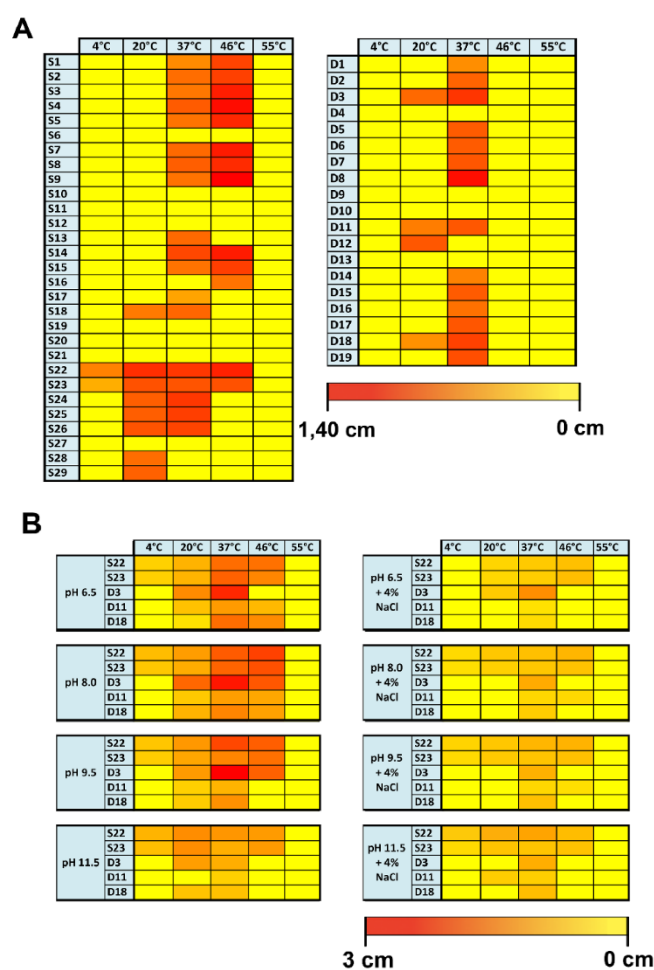


Fig 2. Heatmaps of lipolytic activity. (A) Isolates from the sauna and from the dishwasher contained mainly strains with lipolytic activity. Strains from the sauna exposed lipolytic activity within a broader range of temperature. Sauna samples with the widest range of temperature were S22 and S23. In the dishwasher most samples showed lipolytic activity at 37 °C and only sample D3, D11 and D18 had lipolytic activity at two tested temperatures. (B) Heatmap of lipolytic activity of selected strains from sauna (S22, S23) and dishwasher (D3, D11, D18) under different pH (6.5, 8, 9.5, 11.5) and temperature conditions (4, 20, 37, 46 and 55°C) in minimal medium or minimal medium with 4 % NaCl.

In general, all strains displayed a very robust lipase activity under different salt and pH conditions when grown at 37 °C, as deduced by the relatively flat 3D profile (Fig 3), although halo diameters generally decreased towards extreme salt values (0% and 4% NaCl). Specifically, D11 and D18 (Fig 3D and 3E, respectively) were the most robust lipase producers, followed by S22 and S23 (Fig 3A and 3B, respectively). In contrast, D3 (Fig 3C) was the least robust strain, with variations in activity depending on pH conditions and an even higher salt-dependent variation: lipolytic activity ranged from undetectable in very alkaline conditions to very large (2.45 cm) haloes at pH 6.5 with 1% NaCl.

Aside from the robustness observed, the five selected strains displayed clear optimum peaks at pH 6.5 with 2% NaCl for S22 and S23; and with 1% NaCl for D3, D11 and D18. D3 displayed the highest lipolytic activity under optimum conditions, with halo diameters of up to 2.45 cm, followed by S22 and S23, both with diameters of up to 1.35 and 1.40 cm, respectively. Strains D11 and D18 displayed the lowest lipolytic activity, with maximum halos of 0.76 and 1.17, respectively.

Bacillus sp. have been previously reported to produce thermostable lipases [28, 29, 30, 31]. Regarding the *Bacillus* species that we have isolated and identified in the present work, they are known to produce thermo-resistant lipases, some of them stable at very low or very high pH values. For example,

thermostable lipases can be found in *B. megaterium* (a monoacylglycerol lipase and a carboxylesterase, Uniprot accession number: A0A0H4RCB5 and G2RXU5). Furthermore, a thermostable extracellular lipase has been described for this species, which is capable of retaining 100 % of its activity at 50 °C, and becomes stimulated in the presence of acetone, DMSO, isopropanol and several reducing agents [32]. On the other hand, there are several thermostable lipases known for the *B. cereus* group (Uniprot accession number: A0A0B5NXJ9; A0A090YL00; A0A0A0WM49) and for the *B. subtilis* group [33, 34]. *Bacillus pumilus* is well-known for its thermostable lipases, as many reports describe lipase fully or partially functional at high temperatures [35, 36, 37, 38, 39], including a lipase that is able to resist temperatures up to 100 °C [36]. Even lipases that are functional at both high temperatures and high or low pH values have been described [37, 38]. Finally, *B. pumilus*, has been identified as the most efficient lipolytic enzymes producer out of 65 strains analysed in a previous report [39]. In fact, in our experiments, isolates S22 and S23 were among the three strains with the highest lipolytic activity, and both of these were identified as *B. pumilus*.

In summary, we have identified from domestic environments several *Bacillus* spp. which are strong producers of robust lipolytic enzymes, and this is in concordance with the

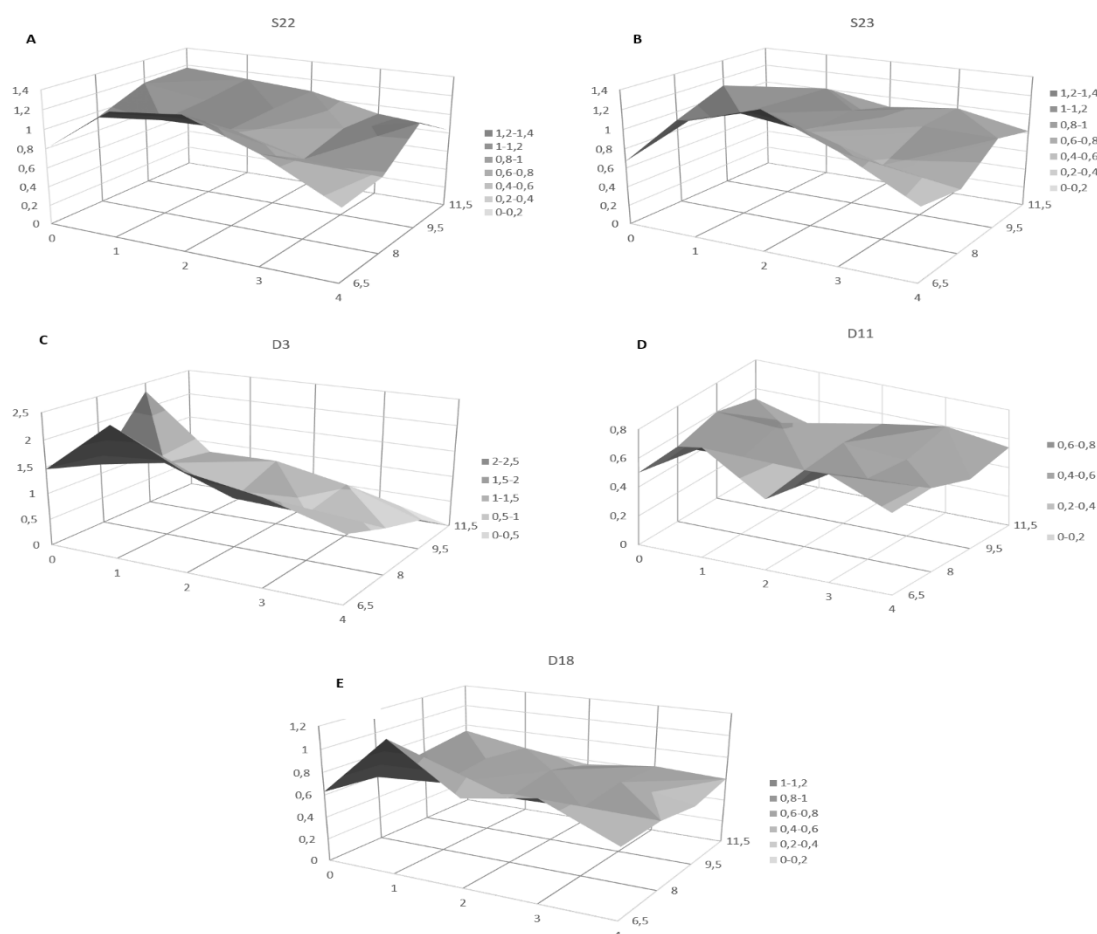


Fig 3. Surface graphs of lipolytic activities of the five selected strains (S22, S23, D3, D11 and D18) under different pH (6.5, 8, 9.5 and 11.5) and NaCl (0, 1, 2, 3 and 4%) conditions. Diameter of the lipolysis haloes (cm) is represented in the Y axis, whereas salt and pH conditions are represented in the X and Z axis, respectively. Halo sizes are in grey to dark grey as indicated at the bottom of each graph.

literature on strains of this genus isolated from other environments. It has to be highlighted that, in our assays, the lipases corresponding to the isolated strains showed high activity at wide ranges of pH (6.5 – 11.5), temperature (4°C - 46 °C) and salt (up to 4 % NaCl), and that all measurements were performed in-situ within their host organisms. Therefore, not only the bacteria are able to produce lipases under these conditions, but also these lipases are perfectly functional. Further tests of the lipase extracts will shed light on the robustness of the lipolytic activity itself, without the limitations caused by the bacterial production.

Our results suggest that the isolated strains may be used as robust chassis for lipase production, and these lipases may be used in the industry as robust bio-detergents. As described in the works mentioned above, especially *B. pumilus* seems to be of interest, since it shows a very strong lipolytic activity and since it adapts, according to our data, most efficiently to different conditions of pH, salt and temperature. This is especially interesting, since we found no previous description of *Bacillus* lipases, which work efficient in wide range of pH, salt and temperature at the same time. The present work shows for the first time the potential of domestic environments as a source of *Bacillus* strains with potential biotechnological applications.

4. Conclusions

The present work is the first screening of extreme indoor environments specifically aiming at the identification of biotechnological relevant bacterial strains able to produce robust enzymes, in our case, robust lipases. Our results reveal that such domestic environments are promising sources for the identification of robust enzymatic activities, as we have managed to isolate five strains with stable lipolytic activity under a wide range of temperature, salt and pH conditions. These metabolic capabilities can be especially useful as components of robust bio-detergents. Furthermore, this work might be the first step of a new view on the human-associated indoor microbiome, focused on ecological aspects and on biotechnological applications.

Acknowledgements

We thank C. Vilanova and X. Baixeras for assistance with electron microscopy. Further the authors are indebted to E. L. James for inspiring us to choose the title for the present work.

References

1. Kelley ST, Gilbert JA. Studying the microbiology of the indoor environment. *Genome Biol.* 2013;14: 202.
2. Adams RI, Bateman AC, Bik HM, Meadow JF. Microbiota of the indoor environment: a meta-analysis. *Microbiome* 2015;3: 49.
3. Vilanova C, Iglesias A, Porcar M. The coffee-machine bacteriome: biodiversity and colonisation of the wasted coffee tray leach. *Sci Rep.* 2015;5: doi: 101038/srep17163.
4. Jackson V, Blair IS, McDowell DA, Kennedy J, Bolton DJ. The incidence of significant foodborne pathogens in domestic refrigerators. *Food Control* 2007;18: 346–351.
5. Dorado-Morales P, Vilanova C, Perete J, CodoCod FM, RamtC, PePorcar M. A highly diverse, desert-like microbial biocenosis on solar panels in a Mediterranean city. *Sci Rep.* 2016;6: 29235.
6. Antranikian G, Vorgias CE, Bertoldo C. Extreme environments as a resource for microorganisms and novel biocatalysts. *Adv Biochem Eng Biot.* 2005;96: 219–262.
7. Brock TD, Freeze H. *Thermosus aquaticus* gen. n. and sp. N., a nonsporulating extreme thermophile. *J Bacteriol.* 1969;98: 289–297.
8. Littlechild JA. Enzymes from extreme environments and their industrial applications. *Front Bioeng and Biotechnol.* 2015;3: 161.
9. Jaeger KE, Eggert T. Lipases for biotechnology. *Curr Opin Biotech.* 2002;13: 390–397.
10. Rogalska E, Nury S, Douchet I, Verger R. Microbial lipases: structures, function and industrial applications. *Biochem Soc T.* 1997;25: 161–164.
11. Sayer C, Isupov MN, Bonch-Osmolovskaya E, Littlechild JA. Structural studies of a thermophilic esterase from a new *Planctomycetes* species, *Thermogutta terrifontis*. *FEBS J.* 2015;282: 2846–2857.
12. Li M, Yang L, Xu G, Wu J. Screening, purification and characterization of a novel cold-active and organic solvent-tolerant lipase from *Stenotrophomonas maltophilia* CGMCC 4254. *Bioresource Technol.* 2013;148: 114–120.
13. Tekedar HC, Sanli-Mohamed G. Molecular cloning, over expression and characterization of thermoalkalophilic esterases isolated from *Geobacillus* sp. *Extremophiles* 2011;2: 203–211.
14. Al Khudary R, Venkatachalam R, Katzer M, Elleuche S, Antranikian G. A cold-adapted esterase of a novel marine isolate, *Pseudoalteromonas arctica*: gene cloning, enzyme purification and characterization. *Extremophiles* 2010;3: 273–285.
15. Siddiqui KS, Cavicchioli R. Improved thermal stability and activity in the cold-adapted lipase B from *Candida antarctica* following chemical modification with oxidized polysaccharides. *Extremophiles* 2005;6: 471–476.
16. Schloss PD, Westcott SL, Ryabin T, Hall JR, Hartmann M, Hollister EB, et al. Introducing MOTHUR: open-source, platform-independent, community-supported software for describing and comparing microbial communities. *Appl Environ Microbiol.* 2009;75: 7537–7541.
17. Reasoner DJ, Geldreich EE. A new medium for the enumeration and subculture of bacteria from potable water. *Appl Environ Microbiol.* 1985;49(1): 1–7.
18. Mobarak-Qamsari E, Kasra-Kermanshahi R, Moosavi-nejad Z. Isolation and identification of a novel, lipase-producing bacterium, *Pseudomonas aeruginosa* KM110. *Iran J Microbiol.* 2011;3(2): 92–98.
19. Kumar D, Kumar L, Nagar S, Raina C, Parshad R, Gupta VK. Screening, isolation and production of lipase/esterase producing *Bacillus* sp. Strain DVL2 and its potential evaluation in esterification and resolution reactions. *Arch Appl Sci Res.* 2012;4(4): 1763–1770.
20. Vilanova C, Marín M, Baixeras J, Latorre A, Porcar M. Selecting microbial strains from pine tree resin: biotechnological applications from a terpene world. *PLoS One* 2014;9(6): e100740.
21. Caamaño-Antelo S, Fernández-No IC, Böhme K, Ezzat-Alnakip M, Quintela-Balujá M, Barros-Velázquez J, et al. Genetic discrimination of foodborn pathogenic

- and spoliage *Bacillus* spp. Based on three housekeeping genes. Food Microbiol. 2015;46: 288-298.
22. Wu XY, Walker MJ, Homitzky M, Chin J. Development of a group-specific PCR combined with ARDRA for the identification of *Bacillus* species of environmental significance. J Microbiol Methods. 2006;64: 107-119.
 23. Ashe S, Maji UJ, Sen R, Mohanty S, Maiti NK. Specific oligonucleotide primers for detection of endoglucanase positive *Bacillus subtilis* by PCR. Biotech. 2014;4: 461 – 465.
 24. Kim W, Kim JY, Cho SL, Nam SW, Shin JW, Kim YS, et al. Glycosyltransferase – a specific marker for the discrimination of *Bacillus anthracis* from the *Bacillus cereus* group. J Med Microbiol. 2008;57: 279–286.
 25. Lee JY, Park DH. Characterization of bacterial community contaminating floor of a hot and dry sauna. J Bacteriol Virol 2012;42(4): 313-320.
 26. Kim BS, Seo JR, Park DH. Variation and characterization of bacterial communities contaminating two saunas operated at 64 °C and 72 °C. Journal of bacteriology and virology 2013;43(3): 195-203.
 27. Savage AM, Hills J, Driscoll K, Fergus DJ, Grunden AM, Dunn RR. Microbial diversity of extreme habitats in human homes. PeerJ 4:e2376; DOI 10.7717/peerj.2376
 28. Shariff FM, Rahman RN, Basri M, Salleh AB. A newly isolated thermostable lipase from *Bacillus* sp. Int J Mol Sci. 2011;12: 2917 – 2934.
 29. Sivaramakrishnan R1, Muthukumar K. Isolation of thermo-stable and solvent-tolerant *Bacillus* sp. lipase for the production of biodiesel. Appl Biochem Biotechnol. 2012;166: 1095 – 1111.
 30. Bora L, Bora M. Optimization of extracellular thermophilic highly alkaline lipase from thermophilic *Bacillus* sp isolated from hot spring of Arunachal Pradesh, India, Braz J Microbiol. 2012;43: 30 – 42.
 31. Surendhiran D, Sirajunnisa AR, Vijay M. An alternative method for production of microalgal biodiesel using novel *Bacillus* lipase. 3 Biotech. 2015;5: 715 – 725.
 32. Sekhon A, Dahiya N, Tiwari RP, Hoondal GS. Properties of a thermostable extracellular lipase from *Bacillus megaterium* AKG-1. J Basic Microbiol. 2005;45: 147-54.
 33. Iqbal SA, Rehman A. Characterization of Lipase from *Bacillus subtilis* I-4 and Its Potential Use in Oil Contaminated Wastewater, Braz. arch. biol. technol. 2015;58: 789 – 797.
 34. Senthilkumar B, Meshachpaul D, Sethumadhavan R, Rajasekaran R. Selection of effective and highly thermostable *Bacillus subtilis* lipase A template as an industrial biocatalyst-A modern computational approach. Front. Biol. 2015;10: 508 – 519.
 35. Akbulut N, Tuzlakoglu Öztürk M, Pijning T, İşsever Öztürk S, Gümüşel F. Improved activity and thermostability of *Bacillus pumilus* lipase by directed evolution. J Biotechnol. 2012;164: 123 – 129.
 36. Laachari F, Bergadi F, Sayari A, Elabed S, Mohammed I, Harchali H, Ibnsouda SK. Biochemical characterization of a new thermostable lipase from *Bacillus pumilus* strain. Turk J Biochem. 2015;40(1): 8-14.
 37. Ma J, Ma Y, Wei W, Wei DZ. In vivo functional expression of an extracellular Ca²⁺-independent *Bacillus pumilus* lipase in *Bacillus subtilis* WB800N. Annals of Microbiology 2015;65: 1973 – 1983.
 38. Kumar R, Sharma A, Kumar A, Singh D. Lipase from *Bacillus pumilus* RK31: Production, Purification and Some Properties. World Appl Sci J. 2012;16: 940 – 948.
 39. Kalapatapu VP, Battina R, Iska BR. Isolation and identification of lipase producing *Bacillus pumilus* GN9. GJRA 2016;doi 10.15373/22778160.

S1 Data. Sequences obtained from high-throughput 16S rRNA sequencing of the DNA isolated from the sauna sample.

S2 Data. Sequences obtained from high-throughput 16S rRNA sequencing of the DNA isolated from the dishwasher sample.

Both available under request.

Appendix B

Supplementary material

Eubacteria and archaea communities in seven mesophilic anaerobic digester plants in Germany

Christian Abendroth^{1,2}, Cristina Vilanova¹, Thomas Günther³, Olaf Luschning^{2,4},
Manuel Porcar*^{1,5}

¹Cavanilles Institute of Biodiversity and Evolutionary Biology, Universitat de València, 46020 Valencia, Spain. ²Bio H2 Energy GmbH, Im Steinfeld 10, 07751 Jena, Germany. ³Eurofins Umwelt Ost GmbH, Löbstedter Straße 78, 07749 Jena, Germany. ⁴BioEnergie Verbund e.V., Im Steinfeld 10, 07751 Jena, Germany. ⁵Fundació General de la Universitat de València, València, Spain.

Additional file 1: Table S1. Chemical environmental parameters of analyzed sludge samples and volume and composition of produced biogas (w/o VFA, error $\pm 10\%$).

Additional file 2: Figure S1. Principal component analysis (PCA) performed on the chemical environmental parameters measured for all samples. Data were normalized, and two components explaining nearly 90 % of the total variance were used for plotting.

Additional file 3: Table S2. Content of VFA in the sampled reactors (error $\pm 10\%$).

Additional file 4: Table S3. Sequencing statistics.

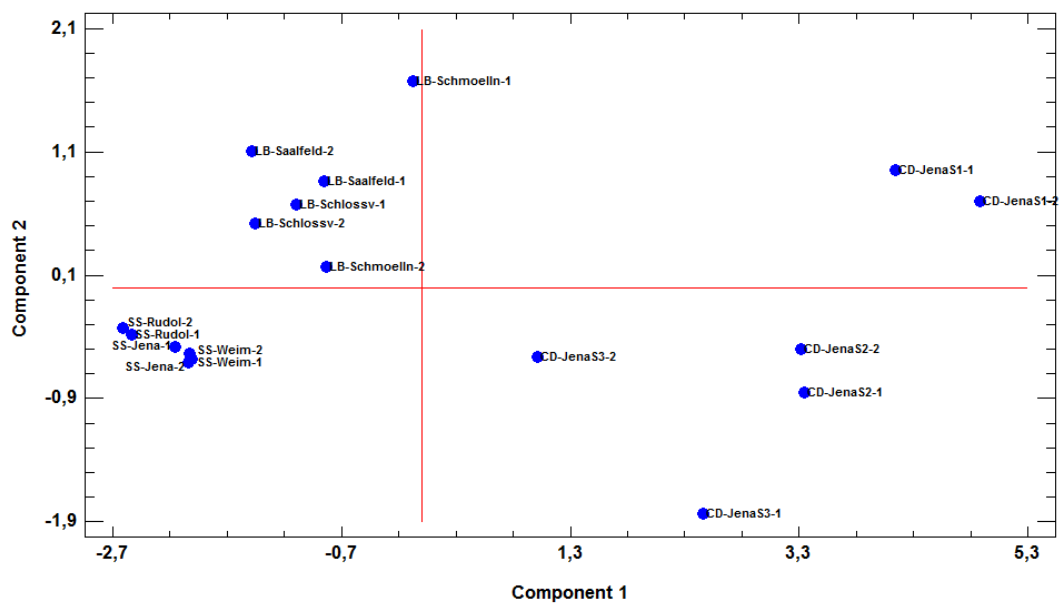


Figure S1 - Principal component analysis (PCA) performed on the chemical environmental parameters measured for all samples. Data were normalized, and two components explaining nearly 90 % of the total variance were used for plotting.

Table S2. Content of VFA in the sampled reactors (error \pm 10%).

	TVFA (mg/L)	Acetic acid (mg/L)	Propionic acid (mg/L)	Isobutyric acid (mg/L)	Isovaleric acid (mg/L)
LB-Schmoelln-1	2.010.00	1.300.00	710.00	0.00	0.00
LB-Schmoelln-2	747.00	690.00	57.00	0.00	0.00
CD-JenaS1-1	3.500.00	930.00	1.900.00	310.00	360.00
CD-JenaS1-2	2.670.00	870.00	1.500.00	0.00	300.00
CD-JenaS2-1	780.00	560.00	57.00	53.00	110.00
CD-JenaS2-2	880.00	710.00	60.00	0.00	110.00
CD-JenaS3-1	79.00	0.00	0.00	0.00	0.00
CD-JenaS3-2	490.00	490.00	0.00	0.00	0.00
SS-Jena-1	0.00	0.00	0.00	0.00	0.00
SS-Jena-2	0.00	0.00	0.00	0.00	0.00
SS-Weim-1	0.00	0.00	0.00	0.00	0.00
SS-Weim-2	0.00	0.00	0.00	0.00	0.00
LB-Schlossv-1	300.00	0.00	0.00	0.00	0.00
LB-Schlossv-2	0.00	0.00	0.00	0.00	0.00
SS-Rudol-1	0.00	0.00	0.00	0.00	0.00
SS-Rudol-2	0.00	0.00	0.00	0.00	0.00
LB-Saalfeld-1	385.00	320.00	65.00	0.00	0.00
LB-Saalfeld-2	1.170.00	990.00	180.00	0.00	0.00

Table S3. Sequencing statistics.

	Number of Sequences Analyzed for Archaea (bp)	Average Length (bp)	Number of Sequences Analyzed for Bacteria (bp)	Average-Length (bp)
CD-Jena-S1-1A	9.511	552	25.526	527
CD-Jena-S1-1B	124.529		19.867	531
CD-Jena-S1-1C	8.088	501	28.422	532
CD-Jena-S1-2A	7.926	510	18.945	528
CD-Jena-S1-2B	10.375	501	32.839	531
CD-Jena-S1-2C	6.394	507	11.600	531
CD-Jena-S2-1A	15.546	541	6.243	539
CD-Jena-S2-1B	17.978	541	8.116	535
CD-Jena-S2-1C	8.907	508	8.173	532
CD-Jena-S2-2A	4.805	546	5.163	529
CD-Jena-S2-2B	2.045	482	12.872	529
CD-Jena-S2-2C	3.441	429	22.541	526
CD-Jena-S3-1A	-	-	36.139	526
CD-Jena-S3-1B	-	-	27.249	528
CD-Jena-S3-1C	-	-	8.324	518
CD-Jena-S3-2A	-	-	22.862	514
CD-Jena-S3-1B	-	-	8.381	514
CD-Jena-S3-1C	-	-	17.793	509
LB-Schmölln-1A	21.242	557	16.672	536
LB-Schmölln-1B	19.990	558	7.762	533
LB-Schmölln-1C	17.612	555	27.439	535
LB-Schmölln-2A	17.584	523	15.029	531
LB-Schmölln-2B	10.498	495	8.353	537
LB-Schmölln-2C	102.404	516	16.529	528
LB-Saalfeld-1A	26.082	561	23.180	527
LB-Saalfeld-1B	25.638	531	14.301	524
LB-Saalfeld-1C	24.703	539	42.882	520
LB-Saalfeld-2A	14.798	511	13.249	518
LB-Saalfeld-2B	11.503	484	12.262	514
LB-Saalfeld-2C	12.981	506	9.960	517
LB-Schlossv-1A	39.907	559	6.854	527
LB-Schlossv-1B	26.575	553	9.935	520
LB-Schlossv-1C	33.577	553	16.253	526
LB-Schlossv-2A	34.187	490	6.924	520
LB-Schlossv-2B	31.977	511	4.385	519
LB-Schlossv-2C	20.777	540	7.217	518
SS-Jena-1A	40.233	565	36.609	528
SS-Jena-1B	36.122	570	11.314	533
SS-Jena-1C	36.576	565	46.963	532
SS-Jena-2A	34.107	556	12.209	532
SS-Jena-2B	22.293	562	15.127	534
SS-Jena-2C	24.756	558	29.519	535
SS-Weim-1A	39.883	573	15.591	545
SS-Weim-1B	36.285	571	31.944	532
SS-Weim-1C	45.212	567	29.564	529
SS-Weim-2A	24.457	551	17.480	529
SS-Weim-2B	28.348	560	8.166	521
SS-Weim-2C	16.001	560	15.722	526
SS-Rudol-1A	35.503	573	11.792	534
SS-Rudol-1B	29.760	562	14.161	520
SS-Rudol-1C	25.978	571	28.028	531
SS-Rudol-2A	46.357	561	12.047	526
SS-Rudol-2B	44.304	560	33.660	524
SS-Rudol-2C	16.501	553	16.562	530

From grass to gas: microbiome dynamics of grass biomass acidification under mesophilic and thermophilic temperatures

Christian Abendroth^{1,2,3}, Claudia Simeonov³, Juli Peretó^{1,2,4,7}, Oreto Antúnez⁵, Raquel Gavidia⁵, Olaf Luschnig⁶, Manuel Porcar^{*1,2,7,8}

¹Cavanilles Institute of Biodiversity and Evolutionary Biology, Universitat de València, C/ José Beltran 2, 46980 Paterna, Spain. ²Institute for Integrative Systems Biology (I2SysBio, Universitat de València-CSIC), C/ José Beltran 2, 46980 Paterna, Spain. ³ Robert Boyle Institut e.V., Im Steinfeld 10, 07751 Jena, Germany. ⁴Departament de Bioquímica i Biologia Molecular, Universitat de València, Paterna, Spain. ⁵Servei Central de Suport a la Investigació Experimental (SCSIE), Universitat de València-CSIC, Paterna, Spain. ⁶Bio H2 Energy GmbH, Im Steinfeld 10, 07751 Jena, Germany. ⁷Darwin Bioprospecting Excellence, S.L. Parc Científic Universitat de València, C/ Catedrático Agustín Escardino Benlloch, 9, 46980 Paterna, València, Spain. ⁸Institute for Integrative Systems Biology (I2SysBio, Universitat de València-CSIC), Postal Code 22085, 46071 Paterna, València, Spain.

Additional file 1: Figure S3. SDS-PAGE displaying the protein profiles.

Additional file 2: Table S4. Mascot results. Online available:

<https://biotechnologyforbiofuels.biomedcentral.com/articles/10.1186/s13068-017-0859-0>

Additional file 3: Table S5. Differentially expressed proteins. Online available:

<https://biotechnologyforbiofuels.biomedcentral.com/articles/10.1186/s13068-017-0859-0>

Additional file 4: Table S1. Description of the used seed sludge.

Additional file 5: Table S2. Overview of reaction stages and reactor performance.

Additional file 6: Table S6. Number of sequences and mean length for bacteria from the acidification stages.

Additional file 7: Table S7. Number of reads and mean length of reads for bacteria from the methane stages.

Additional file 8: Table S8. Number of reads and mean length of reads for archaea from the methane stages.

Tab. S1: Description of the used seed sludge

Stage of the experiment	Type of seed sludge	Origin of seed sludge	Input at the original plant	Plant configuration
Digestion of high strength liquor in high-TS sludge	High-TS sludge from a plug flow digester (17% TS)	Two-stage digester from Jena (vertical plug flow and CSTR)	Farm manure, Livestock Farming waste, Silage	HRT: 87 days Produced gas: 1.2 m ³ /m ³ × day OLR: 3.0 kg × VS/m ³ × day Stage 1 (plug flow): 790 m ³ Stage 2 (CSTR): 2000 m ³ Stage 3 (Digestate): 3800 m ³
Digestion of high strength liquor in low-TS sludge	Low-TS sludge from a sewage digester (4% TS)	Digester from the sewage plant in Jena (CSTR)	Municipal sewage sludge	HRT: 21 days Produced gas: 0.6 m ³ /m ³ × day OLR: 1.8 kg × VS/m ³ × day Single stage process (2 reactors) Digester volume: 2 × 2000 m ³
Digestion of high strength liquor in a leach-bed system	Low-TS sludge from a sewage digester (4% TS) Fully overgrown solids for a packed bed	Digester from the sewage plant in Jena (CSTR)	Municipal sewage sludge	HRT: 21 days Produced gas: 0.6 m ³ /m ³ × day OLR: 1.8 kg × VS/m ³ × day Single stage process (2 reactors) Digester volume: 2 × 2000 m ³

Tab. S2: Overview of reaction stages and reactor performance

	Experiment 1	Experiment 2
Acidification stages	<p>Temperature = 37°C; pH 5.5 (NaOH-regulated); CSTR (Batch); Incubation per cycle = 7day; Volume = 5L; Input = 30 gO₂/L; No seed sludge; Duration: 3 × 7days; 5% inoculum (from previous batch cycle)</p>	<p>Temperature = 55°C; pH 5.5 (NaOH-regulated); CSTR (Batch); Incubation per cycle = 7day; Volume = 5L; Input = 30 gO₂/L; No seed sludge; Duration: 3 × 7days; 5% inoculum (from previous batch cycle)</p>
Methane stage 1	<p>Seed sludge: Industrial codigester (CSTR);</p> <p>Temperature = 37°C; Substrate = Mesophilic liquor; Input: 33 ml/day (0.51 gO₂/L×day); Semi-continuous Batch; 1L bottles (horizontal shaking) No pH regulation</p>	<p>Seed sludge: Industrial codigester (CSTR);</p> <p>Temperature = 37°C; Substrate = Thermophilic liquor; Input: 33 ml/day (0.39 gO₂/L×day); Semi-continuous Batch; 1L bottles (horizontal shaking); No pH regulation</p>
Methane stage 2	<p>Seed sludge: Sewage sludge</p> <p>Temperature = 37°C; Substrate = Mesophilic liquor; Input: 33 ml/day (0.51 gO₂/L×day); Semi-continuous Batch; 1L bottles (horizontal shaking) No pH regulation</p>	<p>Seed sludge: Sewage sludge</p> <p>Temperature = 37°C; Substrate = Mesophilic liquor; Input: 33 ml/day (0.37 gO₂/L×day); Semi-continuous Batch; 1L bottles (horizontal shaking) No pH regulation</p>
Methane stage 3	<p>Seed sludge: Sewage sludge</p> <p>Temperature = 37°C; Substrate = Mesophilic liquor; Input: 33 ml/day (0.51 gO₂/L×day); Semi-continuous Batch; Volume = 3L Leach bed (Hel-X-Füllkörper); Continuous leach circulation; No pH regulation</p>	<p>Seed sludge: Sewage sludge</p> <p>Temperature = 37°C; Substrate = Mesophilic liquor; Input: 33 ml/day (0.37 gO₂/L×day); Semi-continuous Batch; Volume = 3L Leach bed (Hel-X-Füllkörper); Continuous leach circulation; No pH regulation</p>

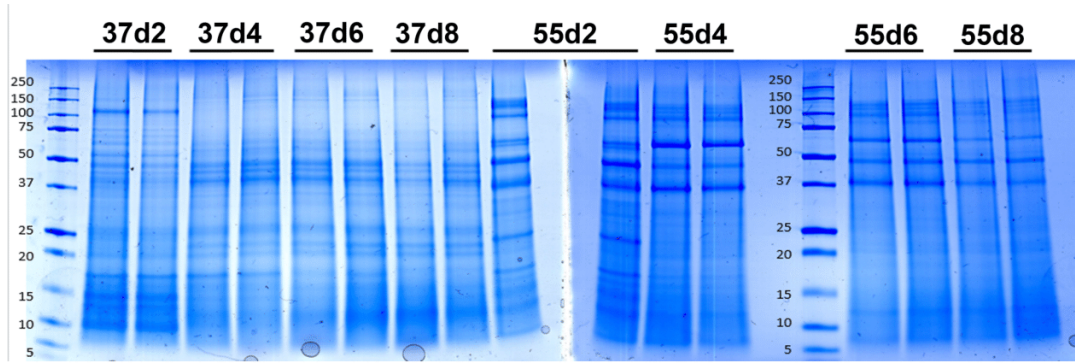


Figure S3 - SDS-page: Blue-Coomassie stained gel showing protein extraction from several samples. Molecular weights are given to the left in kDa (10 μ g per lane).

Tab. S6: Number of sequences and mean length for bacterial reads from the acidification stages

Name of sample	Reads	Mean length
Grass - Substrate	9,195	410
Acidification W1-37-d2	1,871	305
Acidification W1-55-d2	3,566	369
Acidification W1-37-d4	8,565	350
Acidification W1-55-d4	2,820	323
Acidification W1-37-d6	35,180	368
Acidification W1-37-d8	842	377
Acidification W1-55-d8	2,124	298
Acidification W2-37-d2	1,390	327
Acidification W2-55-d2	3,901	327
Acidification W2-37-d4	1,101	370
Acidification W2-55-d4	788	453
Acidification W2-37-d6	3,058	392
Acidification W2-55-d6	1,265	395
Acidification W2-37-d8	595	395
Acidification W2-55-d8	1,824	377
Acidification W3-37-d2	4,088	383
Acidification W3-55-d2	5,309	376
Acidification W3-37-d4	1,086	336
Acidification W3-55-d4	4,476	339
Acidification W3-37-d6	3,044	398
Acidification W3-55-d6	1,917	447
Acidification W3-37-d8	253,369	308
Acidification W3-55-d8	1,018	427
Acidification W3-RT37-d2	1,660	415
Acidification W3-RT55-d2	1,439	376
Acidification W3-RT37-d4	788	373
Acidification W3-RT55-d4	24,697	446
Acidification W3-RT37-d6	1,359	389
Acidification W3-RT55-d6	1,772	388
Acidification W3-RT37-d8	577	383
Acidification W3-RT55-d8	1,043	413

Tab. S7: Number of reads and mean length of reads for bacteria from the methane stages

Name of sample	Reads	Mean length
C-Euco-d0	864	365
37-Euco-d4	1,768	408
55-Euco-d4	1,405	398
C-Euco-d4	521	410
37-Euco-d8	883	401
55-Euco-d8	4,545	341
C-Euco-d8	764	391
37-Euco-d12	1,842	390
55-Euco-d12	1,485	409
C-Euco-d12	981	402
37-Euco-d16	1,155	379
55-Euco-d16	1,089	412
C-Euco-d16	1,614	377
37-Euco-d20	2,263	380
55-Euco-d20	2,083	371
C-Euco-d20	2,825	371
C-SW-d0	602	421
37-SW-d4	2,624	422
55-SW-d4	2,910	431
C-SW-d4	1,931	418
37-SW-d8	1,636	424
55-SW-d8	1,732	420
C-SW-d8	577	420
37-SW-d12	1,776	376
55-SW-d12	33,005	373
C-SW-d12	822	433
37-SW-d16	444	405
55-SW-d16	1,079	410
C-SW-d16	64,878	354
37-SW-d20	2,982	309
55-SW-d20	23,503	326
C-SW-d20	17,184	358
Biofilm-Start-37	1,403	383
Biofilm-Start-55	2,566	405
Biofilm-End-37	710	400
Biofilm-End-55	16,395	409
Leach-37-d0	959	396
Leach-55-d0	724	396
Leach-37-d4	2,259	409
Leach-55-d4	1,797	383
Leach-37-d8	1,338	405
Leach-55-d8	4,205	417
Leach-37-d12	503	414
Leach-55-d12	19,397	453
Leach-37-d16	947	413
Leach-55-d16	12,437	414
Leach-37-d20	55,342	356
Leach-55-d20	1,268	396
L1A-55-d6	2,594	416

Tab. S8: Number of reads and mean length of reads for archaea from the methane stages

Name of sample	Reads	Mean length
C-Euco-d0	4,121	173 bp
37-Euco-d4	16,665	396 bp
55-Euco-d4	9,291	341 bp
C-Euco-d4	8,886	260 bp
37-Euco-d8	11,629	226 bp
55-Euco-d8	4,106	315 bp
C-Euco-d8	11,771	131 bp
37-Euco-d12	11,322	302 bp
55-Euco-d12	10,613	409 bp
C-Euco-d12	10,138	380 bp
37-Euco-d16	35,098	228 bp
55-Euco-d16	15,843	383 bp
C-Euco-d16	1,891	207 bp
37-Euco-d20	27,677	301 bp
55-Euco-d20	1,511	225 bp
C-Euco-d20	15,812	227 bp
C-SW-d0	20,431	255 bp
37-SW-d4	51,179	218 bp
55-SW-d4	19,73	395 bp
C-SW-d4	17,777	300 bp
37-SW-d8	26,646	418 bp
55-SW-d8	21,654	274 bp
C-SW-d8	14,833	319 bp
37-SW-d12	27,206	418 bp
55-SW-d12	15,998	368 bp
C-SW-d12	25,793	377 bp
37-SW-d16	11,178	294 bp
55-SW-d16	53,94	159 bp
C-SW-d16	40,778	200 bp
37-SW-d20	39,236	291 bp
55-SW-d20	58,3	331 bp
C-SW-d20	27,957	422 bp
Biofilm-Start-37	17,929	400 bp
Biofilm-Start-55	10,851	444 bp
Biofilm-End-37	9,000	456 bp
Biofilm-End-55	30,565	292 bp
Leach-37-d0	19,021	283 bp
Leach-55-d0	17,221	283 bp
Leach-37-d4	10,17	372 bp
Leach-55-d4	10,688	275 bp
Leach-37-d8	27,395	346 bp
Leach-55-d8	40,587	271 bp
Leach-37-d12	12,174	310 bp
Leach-55-d12	23,277	237 bp
Leach-37-d16	198	379 bp
Leach-55-d16	16,404	374 bp
Leach-37-d20	15,678	407 bp
Leach-55-d20	20,677	318 bp

Towards a Microbial Thermoelectric Cell

Raúl Rodríguez-Barreiro¹, Christian Abendroth¹, Cristina Vilanova¹, Andre's Moya^{1,2}, Manuel Porcar^{1,3*}

¹Cavanilles Institute of Biodiversity and Evolutive Biology, Universitat de València, València, Spain

²Unidad Mixta de Investigación en Genómica y Salud, Centro Superior de Investigación en Salud Pública (CSISP), València, Spain

³Fundació General de la Universitat de València, València, Spain

Additional file 1: Appendix S1. Thermogenerator cell (MPG-D751) general equations.

Additional file 2: Appendix S2. TE-Power Probe model description.

Additional file 3: Figure S1. Schematic drawing of MTC data-recording system.

Additional file 4: Figure S2. Schematic drawing of heat flows and resistances within the thermogenerator cell.

Appendix S1. Thermogenerator cell (MPG-D751) general equations

According to the first law of thermodynamics, the equations for a thermogenerator cell (for a schematic representation, see Fig. S2) are defined as follows [14]:

$$\dot{Q}_H(t) = \dot{Q}_{sH}(t) - \frac{\dot{Q}_j(t)}{2} + \dot{Q}_i(t) = \alpha \cdot T_H(t) \cdot I(t) - \frac{1}{2} \cdot I^2(t) \cdot R_i + \left(\frac{T_H(t) - T_C(t)}{R_{th}} \right) \quad (\text{S1.1})$$

$$\dot{Q}_C(t) = \dot{Q}_{sC}(t) + \frac{\dot{Q}_j(t)}{2} + \dot{Q}_i(t) = \alpha \cdot T_C(t) \cdot I(t) + \frac{1}{2} \cdot I^2(t) \cdot R_i + \left(\frac{T_H(t) - T_C(t)}{R_{th}} \right) \quad (\text{S1.2})$$

$$P_e(t) = \dot{Q}_H(t) - \dot{Q}_C(t) = \alpha \cdot (T_H(t) - T_C(t)) \cdot I(t) - I^2(t) \cdot R_i = I^2(t) \cdot R_{Load} \quad (\text{S1.3})$$

Where Q_H and Q_C are the net heat flows (absorbed and released, respectively) through the hot and cold sides of the thermogenerator; Q_{sH} and Q_{sC} are the heat flows produced in the hot and cold sides of the cell due to the Seebeck effect (being α the Seebeck coefficient, and T_H and T_C the temperature of the hot and cold sides of the thermogenerator). Q_j is the heat flow generated due to the Joule effect when the current (I) goes through the internal resistance (R_i). This heat flow is equally distributed in both sides of the thermogenerator. Q_i represents heat flow loss due to natural thermal conduction (being R_{th} the thermal resistance) occurring between both sides of the cell, which are at a different temperature. P_e represents the electrical power production on a load resistance (R_{load}).

In order to obtain the maximum electrical power, the load resistance must be equal to the internal resistance of the thermogenerator. Thus, the electrical current of this circuit configuration is:

$$I = \frac{\alpha \cdot \Delta T_{th}(t)}{2 \cdot R_i} \quad (\text{S1.4})$$

Where ΔT_{th} represents the difference in temperature between the hot and the cold side of the thermogenerator.

On the other hand, under an open-circuit configuration I is null, so there is no electrical power production, and both Q_H and Q_C are equal to Q_i .

Appendix S2. TE-Power Probe model description

The definition of I for maximal power acquisition, Eq. S1.4 in Appendix S1, was taken into account to define a simple thermal model, in which every thermal resistance of the TE-Power Probe is considered (Fig. S2). The equations modeling TE-Power Probe performance are:

$$\dot{Q}_{Th}(t) = \dot{Q}_H(t) = \frac{\alpha^2 \cdot \Delta T_{th}(t)}{R_i} \cdot \left(\frac{T_H(t)}{2} - \frac{\Delta T_{th}(t)}{8} + \frac{R_i}{\alpha^2 \cdot R_{th}} \right) \quad (S2.1)$$

$$\dot{Q}_C(t) = \frac{\alpha^2 \cdot \Delta T_{th}(t)}{R_i} \cdot \left(\frac{T_C(t)}{2} + \frac{\Delta T_{th}(t)}{8} + \frac{R_i}{\alpha^2 \cdot R_{th}} \right) \quad (S2.2)$$

$$V_O(t) = \frac{\alpha \cdot \Delta T_{th}(t)}{2} \quad (S2.3)$$

$$P_e^{\max}(t) = \frac{(\alpha \cdot \Delta T_{th}(t))^2}{4 \cdot R_i} \quad (S2.4)$$

$$T_H(t) = T_b(t) - \dot{Q}_H(t) \cdot R_{Cu} \quad (S2.5)$$

$$T_C(t) = T_{env}(t) + \dot{Q}_C(t) \cdot R_{Sk} \quad (S2.6)$$

Where V_o is the output voltage and ΔT_{th} represents the difference in temperature between the hot and the cold side of the thermogenerator; R_{Cu} is the thermal resistance of the copper bar connecting the broth (at a temperature T_b) and the hot side of the cell (at a temperature T_H); and R_{Sk} is the thermal resistance found between the cold side of the thermogenerator (T_C) and the environment (considering room temperature T_{env}).

Under an open-circuit configuration the model equations can be written as follows:

$$\dot{Q}_{Th}(t) = \dot{Q}_H(t) = \dot{Q}_C(t) = \left(\frac{T_H(t) - T_C(t)}{R_{th}} \right) \quad (S2.7)$$

$$V_O(t) = \alpha \cdot \Delta T_{th}(t) \quad (S2.8)$$

$$T_H(t) = T_b(t) - \dot{Q}_H(t) \cdot R_{Cu} \quad (S2.9)$$

$$T_C(t) = T_{env}(t) + \dot{Q}_H(t) \cdot R_{Sk} \quad (S2.10)$$

Where there is no electrical power production.

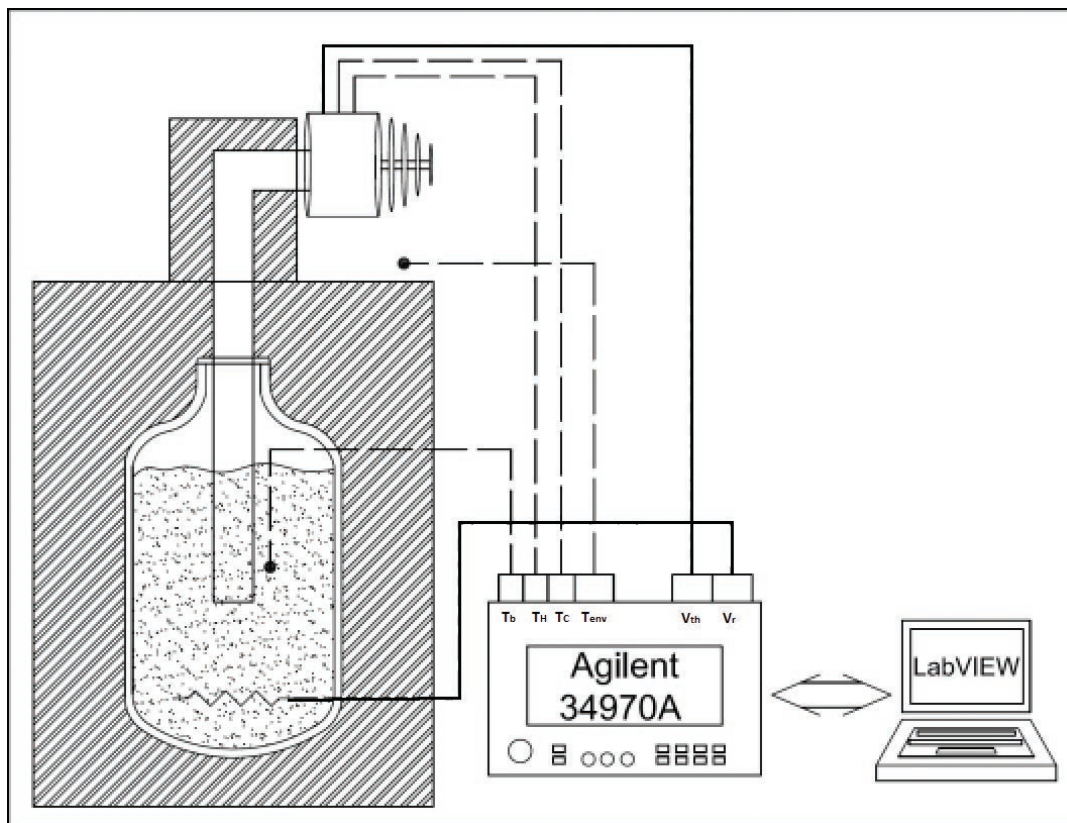


Figure S1 - Schematic drawing of MTC data-recording system. Dashed lines represent thermocouple connections measuring the temperature of the broth (T_b), the temperature of the hot and cold sides of the thermogenerator (T_H and T_C , respectively), and the room temperature (T_{env}); whereas continuous lines represent voltage measurements corresponding to the thermogenerator (V_{th}) and the electrical resistance (V_r).

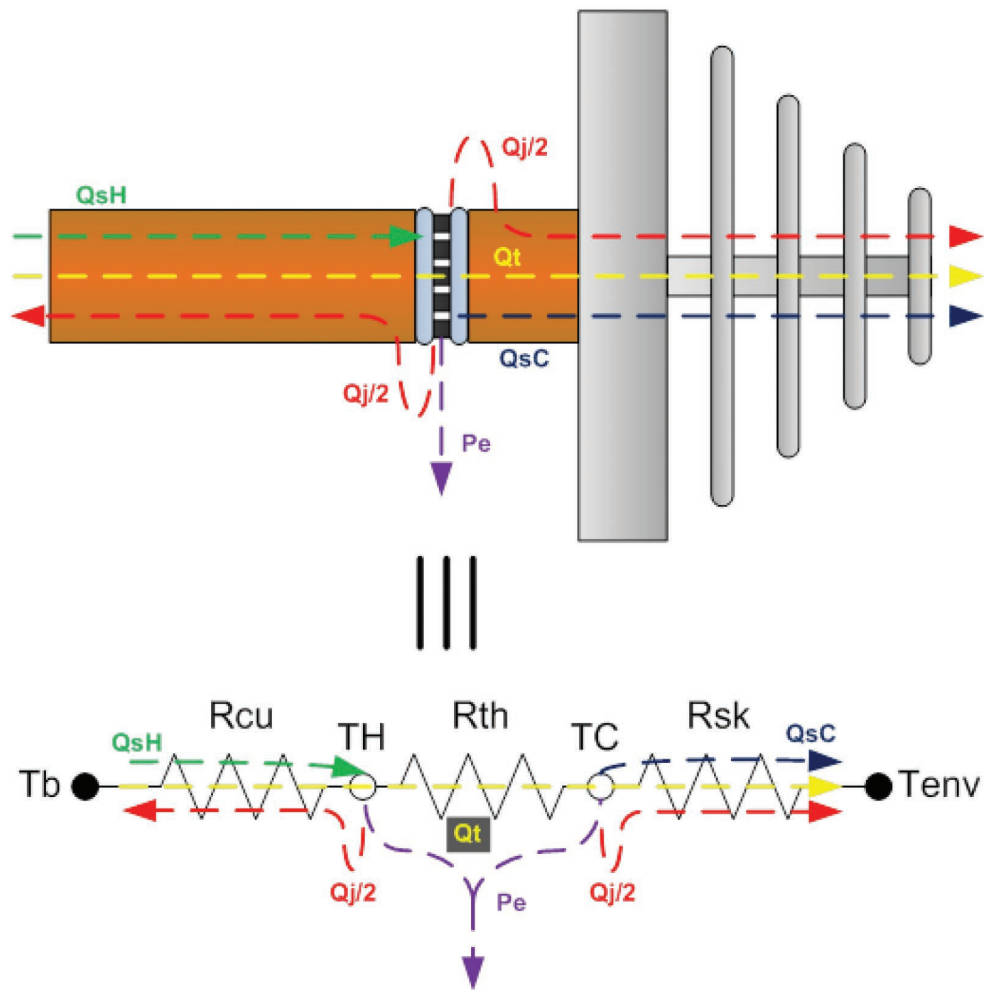


Figure S2 - Schematic drawing of heat flows and resistances within the thermogenerator cell. Symbols used are in accordance with the nomenclature summarized in Table 2.



- (51) Clasificación Internacional de Patentes:
H01M 8/16 (2006.01)
- (21) Número de la solicitud internacional:
PCT/ES2013/000212
- (22) Fecha de presentación internacional:
27 de septiembre de 2013 (27.09.2013)
- (25) Idioma de presentación: español
- (26) Idioma de publicación: español
- (30) Datos relativos a la prioridad:
P201200977
28 de septiembre de 2012 (28.09.2012) ES
- (71) Solicitante: UNIVERSITAT DE VALENCIA [ES/ES];
Av. Blasco Ibáñez, 13, E-46010 Valencia (ES).
- (72) Inventores: PORCAR MIRALLES, Manuel; Universitat de Valencia, Av. Blasco Ibáñez, 13, E-46010 Valencia (ES). RODRÍGUEZ BARREIRO, Raúl; Universitat de Valencia, Av. Blasco Ibáñez, 13, E-46010 Valencia (ES). VILANOVA SERRADOR, Cristina; Universitat de Valencia, Av. Blasco Ibáñez, 13, E-46010 Valencia (ES). ABENDROTH, Christian; Universitat de Valencia, Av. Blasco Ibáñez, 13, E-46010 Valencia (ES). MOYA

SIMARRO, Andrés; Universitat de Valencia, Av. Blasco Ibáñez, 13, E-46010 Valencia (ES). ALCAINA ACOSTA, José Joaquín; Universitat de Valencia, Av. Blasco Ibáñez, 13, E-46010 Valencia (ES).

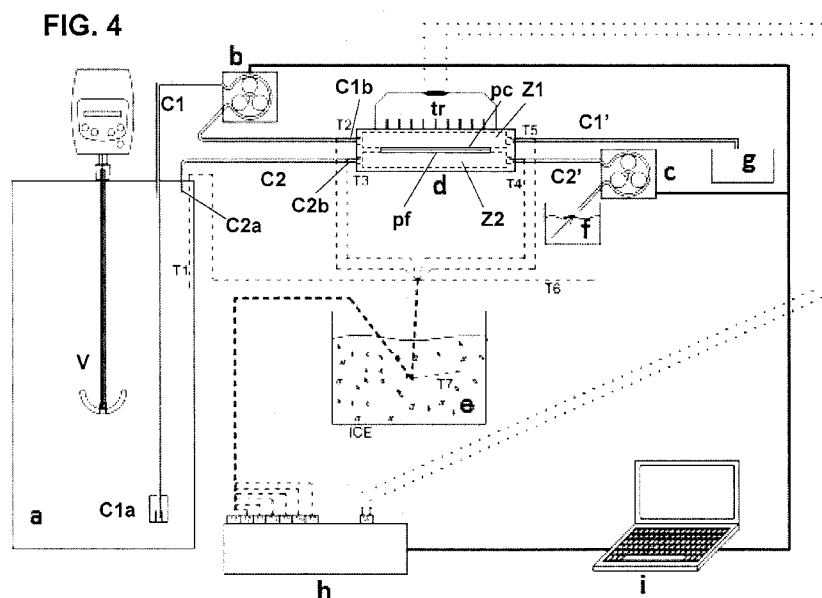
- (74) Mandatario: TORNER LASALLE, Elisabet; Gran Via de les Corts Catalanes, 669 bis, 1r. 2a., E-08013 Barcelona (ES).
- (81) Estados designados (a menos que se indique otra cosa, para toda clase de protección nacional admisible): AE, AG, AL, AM, AO, AT, AU, AZ, BA, BB, BG, BH, BN, BR, BW, BY, BZ, CA, CH, CL, CN, CO, CR, CU, CZ, DE, DK, DM, DO, DZ, EC, EE, EG, ES, FI, GB, GD, GE, GH, GM, GT, HN, HR, HU, ID, IL, IN, IS, JP, KE, KG, KN, KP, KR, KZ, LA, LC, LK, LR, LS, LT, LU, LY, MA, MD, ME, MG, MK, MN, MW, MX, MY, MZ, NA, NG, NI, NO, NZ, OM, PA, PE, PG, PH, PL, PT, QA, RO, RS, RU, RW, SA, SC, SD, SE, SG, SK, SL, SM, ST, SV, SY, TH, TJ, TM, TN, TR, TT, TZ, UA, UG, US, UZ, VC, VN, ZA, ZM, ZW.

- (84) Estados designados (a menos que se indique otra cosa, para toda clase de protección regional admisible): ARIPO (BW, GH, GM, KE, LR, LS, MW, MZ, NA, RW, SD, SL, SZ, TZ, UG, ZM, ZW), euroasiática (AM, AZ,

[Continúa en la página siguiente]

(54) Title: MICROBIAL THERMOELECTRIC DEVICE AND ASSOCIATED METHOD

(54) Título : DISPOSITIVO TERMOELÉCTRICO MICROBIANO Y MÉTODO ASOCIADO A DICHO DISPOSITIVO



(57) Abstract: The invention concerns a device and a method for generating electrical energy from microbiological cultures. More specifically, the invention concerns a device and an associated method for obtaining electrical energy from thermal energy produced in metabolic reactions, the device comprising a reactor configured to accommodate a microbiological culture, a thermally insulating means disposed as reactor cover, and a thermoelectric conversion means. The invention also enables the temperature of the microbiological culture to be controlled in a continuous fermentation process.

(57) Resumen:

[Continúa en la página siguiente]

WO 2014/049181 A1

Microbial communities involved in biogas production exhibit high resilience to heat shocks

Christian Abendroth*^{1,2}, Sarah Hahnke³, Claudia Simeonov², Michael Klocke³,
Sonia Casani Miravalls⁴, Patrice Ramm³, Christoph Bürger⁴, Olaf Luschnig⁴,
Manuel Porcar*^{1,5}

¹Institute for Integrative Systems Biology (I2SysBio), Paterna, Valencia, Spain

²Robert Boyle Institut e.V., Jena, Germany

³Leibniz Institute for Agricultural Engineering and Bioeconomy (ATB),
Bioengineering, Potsdam, Germany

⁴Bio H2 Energy GmbH, Jena, Germany

⁵Darwin Bioprospecting Excellence, S.L. Parc Científic Universitat de Valencia,
Paterna, Valencia, Spain

Additional file 1: Figure S1. Microbiome composition of heat-shocked samples.

Additional file 2: Table S2. Number of sequences and mean length for bacteria from the acidification stages.

Additional file 3: Table S3. Percentage of bacterial reads that can be classified on class and genus level.

Additional file 4: Table S4. Identified microbial isolates.

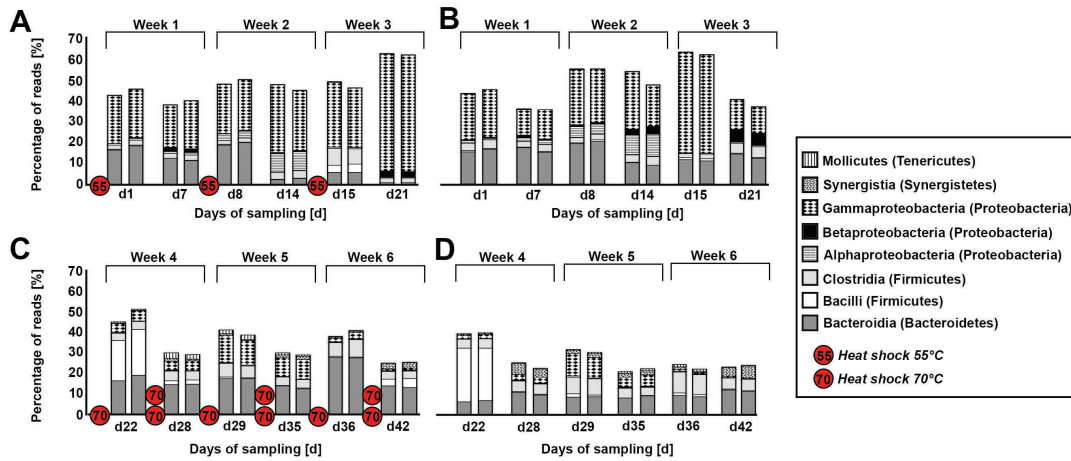


Figure S1 - Microbiome composition of heat-shocked samples. Microbial composition is given as a percentage of all analysed bacterial sequences. Sequences were classified on the class level. Values for samples from the experiment with 55°C heat shocks are shown in A; and C corresponds to the 70°C heat shocks. Values for samples from the control system without heat shocks are shown in B and D. All samples were analysed as duplicates.

Tab. S2: Number of sequences and mean length for bacteria from the acidification stages

Name of sample	Reads	Mean length
55_W1_d2_1	14687	416.81
55_W1_d2_2	12443	425.897
55_W1_d7_1	8378	427.981
55_W1_d7_2	11045	427.253
55_W2_d2_1	16713	433.586
55_W2_d2_2	41941	434.986
55_W2_d7_1	20063	426.696
55_W2_d7_2	4014	433.529
55_W3_d2_1	7144	431.301
55_W3_d2_2	17168	422.04
55_W3_d7_1	23719	472.801
55_W3_d7_2	12905	460.459
C55_W1_d2_1	17875	423.359
C55_W1_d2_2	5445	410.648
C55_W1_d7_1	16871	452.825
C55_W1_d7_2	1076	444.721
C55_W2_d2_1	20715	437.42
C55_W2_d2_2	4115	443.536
C55_W2_d7_1	3526	436.289
C55_W2_d7_2	50543	436.819
C55_W3_d2_1	5106	460.342
C55_W3_d2_2	4702	444.726
C55_W3_d7_1	8931	430.297
C55_W3_d7_2	30696	427.292
70_W1_d2_1	34948	423.14
70_W1_d2_2	16278	413.072
70_W1_d7_1	13919	456.985
70_W1_d7_2	9846	455.488
70_W2_d2_1	3181	457.661
70_W2_d2_2	10782	428.338
70_W2_d7_1	6016	452.81
70_W2_d7_2	4447	466.635
70_W3_d2_1	20547	433.893
70_W3_d2_2	3181	455.8
70_W3_d7_1	12976	463.001
70_W3_d7_2	5594	458.582
C70_W1_d2_1	28840	411.848
C70_W1_d2_2	16894	435.465
C70_W1_d7_1	8547	467.907
C70_W1_d7_2	73378	449.583
C70_W2_d2_1	4321	464.129
C70_W2_d2_2	5967	466.088
C70_W2_d7_1	47190	422.634
C70_W2_d7_2	13207	436.796
C70_W3_d2_1	29617	466.096
C70_W3_d2_2	4212	463.12
C70_W3_d7_1	17109	471.47
C70_W3_d7_2	12644	470.041

Tab. S3: Percentage of bacterial reads that can be classified on class and genus level.

Name of sample	Class percentage of bacterial reads [%]	Genus percentage of bacterial reads [%]
55_W1_d2_1	56	11
55_W1_d2_2	53	14
55_W1_d7_1	61	9
55_W1_d7_2	59	9
55_W2_d2_1	51	13
55_W2_d2_2	49	14
55_W2_d7_1	52	4
55_W2_d7_2	55	4
55_W3_d2_1	50	10
55_W3_d2_2	52	14
55_W3_d7_1	37	2
55_W3_d7_2	37	2
C55_W1_d2_1	58	10
C55_W1_d2_2	56	10
C55_W1_d7_1	65	14
C55_W1_d7_2	65	12
C55_W2_d2_1	45	18
C55_W2_d2_2	46	18
C55_W2_d7_1	47	11
C55_W2_d7_2	54	10
C55_W3_d2_1	39	8
C55_W3_d2_2	39	9
C55_W3_d7_1	61	9
C55_W3_d7_2	64	9
70_W1_d2_1	56	21
70_W1_d2_2	50	25
70_W1_d7_1	71	15
70_W1_d7_2	72	13
70_W2_d2_1	59	15
70_W2_d2_2	62	16
70_W2_d7_1	71	15
70_W2_d7_2	72	11
70_W3_d2_1	63	23
70_W3_d2_2	60	24
70_W3_d7_1	75	12
70_W3_d7_2	75	11
C70_W1_d2_1	62	18
C70_W1_d2_2	62	17
C70_W1_d7_1	75	11
C70_W1_d7_2	78	9
C70_W2_d2_1	69	10
C70_W2_d2_2	70	11
C70_W2_d7_1	79	8
C70_W2_d7_2	78	9
C70_W3_d2_1	76	12
C70_W3_d2_2	78	11
C70_W3_d7_1	77	12
C70_W3_d7_2	76	12

Tab. S4: 16S-rRNA clone library and bacterial isolates (Pathogens are highlighted in red)

Name	Completeness (%)	Top-hit taxon	RG	Top-hit strain	Similarity (%)	Top-hit taxonomy
16S-rRNA Clone Library: Clones with at least 98,65% similarity to valid species names						
>Clone 52363_Consensus	100	Alkalibaculum bacchi	1	CP11(T)	98,98	Bacteria;Firmicutes;Clostridia;Clostridiales;Eubacteriaceae;Alkalibaculum
>Clone 52441_Consensus	100	Amphibacillus xylanus	1	NBRC 15112(T)	99,73	Bacteria;Firmicutes;Bacilli;Bacillales;Bacillaceae;Amphibacillus
>Clone 52469_Consensus	100	Bacteroides ovatus	2	ATCC 8483(T)	98,9	Bacteria;Bacteroidetes;Bacteroidia;Bacteroidales;Bacteroidaceae;Bacteroides
>Clone 52445_Consensus	100	Bacteroides ovatus	2	ATCC 8483(T)	98,96	Bacteria;Bacteroidetes;Bacteroidia;Bacteroidales;Bacteroidaceae;Bacteroides
>Clone 52385_Consensus	100	Bacteroides ovatus	2	ATCC 8483(T)	98,83	Bacteria;Bacteroidetes;Bacteroidia;Bacteroidales;Bacteroidaceae;Bacteroides
>Clone 52376_Consensus	100	Bacteroides ovatus	2	ATCC 8483(T)	99,59	Bacteria;Bacteroidetes;Bacteroidia;Bacteroidales;Bacteroidaceae;Bacteroides
>Clone 52409_Consensus	100	Bacteroides thetaiotaomicron	2	VPI-5482(T)	99,24	Bacteria;Bacteroidetes;Bacteroidia;Bacteroidales;Bacteroidaceae;Bacteroides
>Clone 52495_Consensus	100	Bacteroides uniformis	2	ATCC 8492(T)	99,72	Bacteria;Bacteroidetes;Bacteroidia;Bacteroidales;Bacteroidaceae;Bacteroides
>Clone 52464_Consensus	100	Bacteroides uniformis	2	ATCC 8492(T)	99,65	Bacteria;Bacteroidetes;Bacteroidia;Bacteroidales;Bacteroidaceae;Bacteroides
>Clone 52443_Consensus	100	Bacteroides uniformis	2	ATCC 8492(T)	99,79	Bacteria;Bacteroidetes;Bacteroidia;Bacteroidales;Bacteroidaceae;Bacteroides
>Clone 52425_Consensus	100	Bacteroides uniformis	2	ATCC 8492(T)	99,86	Bacteria;Bacteroidetes;Bacteroidia;Bacteroidales;Bacteroidaceae;Bacteroides
>Clone 52422_Consensus	100	Bacteroides uniformis	2	ATCC 8492(T)	99,59	Bacteria;Bacteroidetes;Bacteroidia;Bacteroidales;Bacteroidaceae;Bacteroides
>Clone 52408_Consensus	100	Bacteroides uniformis	2	ATCC 8492(T)	99,59	Bacteria;Bacteroidetes;Bacteroidia;Bacteroidales;Bacteroidaceae;Bacteroides
>Clone	100	Bacteroides	2	ATCC 8492(T)	99,72	Bacteria;Bacteroidetes;Bacteroidia;Bacteroidales;Bacteroidaceae;Bacteroides

52387_Consensus			uniformis				oidaceae;Bacteroides
>Clone 52367_Consensus	100	2	Bacteroides uniformis	ATCC 8492(T)	99,72	Bacteria;Bacteroidetes;Bacteroidia;Bacteroidales;Bacteroidaceae;Bacteroides	
>Clone 52358_Consensus	100	2	Bacteroides uniformis	ATCC 8492(T)	99,72	Bacteria;Bacteroidetes;Bacteroidia;Bacteroidales;Bacteroidaceae;Bacteroides	
>Clone 52493_Consensus	100	1+	Bacteroides vulgatus	ATCC 8482(T)	99,59	Bacteria;Bacteroidetes;Bacteroidia;Bacteroidales;Bacteroidaceae;Bacteroides	
>Clone 52406_Consensus	100	1	Bacteroides xyliansolvensis	XB1A(T)	98,68	Bacteria;Bacteroidetes;Bacteroidia;Bacteroidales;Bacteroidaceae;Bacteroides	
>Clone 52471_Consensus	100	2	Citrobacter werkmanii	NBRC 105721(T)	99,59	Bacteria;Proteobacteria;Gammaproteobacteria;Enterobacteriales;Enterobacteriaceae;Citrobacter	
>Clone 52478_Consensus	100	1	Clostridium isatidis	WV6(T)	98,72	Bacteria;Firmicutes;Clostridia;Clostridiales;Clostridiaceae;Clostridium	
>Clone 52449_Consensus	100	1	Clostridium isatidis	WV6(T)	98,72	Bacteria;Firmicutes;Clostridia;Clostridiales;Clostridiaceae;Clostridium	
>Clone 52447_Consensus	100	1	Clostridium isatidis	WV6(T)	98,72	Bacteria;Firmicutes;Clostridia;Clostridiales;Clostridiaceae;Clostridium	
>Clone 52399_Consensus	100	1	Clostridium isatidis	WV6(T)	98,72	Bacteria;Firmicutes;Clostridia;Clostridiales;Clostridiaceae;Clostridium	
>Clone 52394_Consensus	100	1	Clostridium isatidis	WV6(T)	98,72	Bacteria;Firmicutes;Clostridia;Clostridiales;Clostridiaceae;Clostridium	
>Clone 52418_Consensus	100	1	Clostridium pasculi	DSM 10365(T)	99,58	Bacteria;Firmicutes;Clostridia;Clostridiales;Clostridiaceae;Clostridium	
>Clone 52405_Consensus	100	1+	Clostridium sartagoforme	DSM 1292(T)	99,79	Bacteria;Firmicutes;Clostridia;Clostridiales;Clostridiaceae;Clostridium	
>Clone 52455_Consensus	100	1	Desulfovibrio legallii	H1(T)	99,58	Bacteria;Proteobacteria;Deltaproteobacteria;Desulfovibrionales;Desulfovibrionaceae;Desulfovibrio	
>Clone 52470_Consensus	100	1	Enterococcus asini	ATCC 700915(T)	99,8	Bacteria;Firmicutes;Bacilli;Lactobacillales;Enterococcaeae;Enterococcus	
>Clone 52436_Consensus	100	1	Enterococcus asini	ATCC 700915(T)	99,8	Bacteria;Firmicutes;Bacilli;Lactobacillales;Enterococcaeae;Enterococcus	
>Clone 52412_Consensus	100	1+	Enterococcus cecorum	DSM 20682(T)	99,73	Bacteria;Firmicutes;Bacilli;Lactobacillales;Enterococcaeae;Enterococcus	
>Clone 52463_Consensus	100	2 ht	Enterococcus gallinarum	NBRC 100675(T)	99,8	Bacteria;Firmicutes;Bacilli;Lactobacillales;Enterococcaeae;Enterococcus	

>Clone 52480_Consensus	100	Fermentimonas caenicola	-	ING2-E5B(T)	99,93	Bacteria;Bacteroidetes;Bacteroidia;Bacteroidales;Porphyromonadaceae;Fermentimonas
>Clone 52459_Consensus	100	Fermentimonas caenicola	-	ING2-E5B(T)	99,93	Bacteria;Bacteroidetes;Bacteroidia;Bacteroidales;Porphyromonadaceae;Fermentimonas
>Clone 52448_Consensus	100	Fermentimonas caenicola	-	ING2-E5B(T)	99,73	Bacteria;Bacteroidetes;Bacteroidia;Bacteroidales;Porphyromonadaceae;Fermentimonas
>Clone 52431_Consensus	100	Fermentimonas caenicola	-	ING2-E5B(T)	98,97	Bacteria;Bacteroidetes;Bacteroidia;Bacteroidales;Porphyromonadaceae;Fermentimonas
>Clone 52427_Consensus	100	Fermentimonas caenicola	-	ING2-E5B(T)	99,04	Bacteria;Bacteroidetes;Bacteroidia;Bacteroidales;Porphyromonadaceae;Fermentimonas
>Clone 52370_Consensus	100	Fermentimonas caenicola	-	ING2-E5B(T)	99,59	Bacteria;Bacteroidetes;Bacteroidia;Bacteroidales;Porphyromonadaceae;Fermentimonas
>Clone 52489_Consensus	100	Globicatella sulfidifaciens	2t	LMG 188441(T)	99,45	Bacteria;Firmicutes;Bacilli;Lactobacillales;Aerococcaceae;Globicatella
>Clone 52511_Consensus	53,7	Methanobacterium palustre	1	DSM 3108(T)	98,98	Archaea;Euryarchaeota;Methanobacteria;Methanobacteriales;Methanobacteriaceae;Methanobacterium
>Clone 52322_Consensus	54,9	Methanobrevibacter boviskoreani	1	JH1(T)	100	Archaea;Euryarchaeota;Methanobacteria;Methanobacteriales;Methanobacteriaceae;Methanobrevibacter
>Clone 52317_Consensus	53,8	Methanosacta concilii	1	GP-6(T)	99,62	Archaea;Euryarchaeota;Methanomicrobia;Methanosarcinales;Methanosactaceae;Methanosacta
>Clone 52522_Consensus	53,8	Methanosarcina mazei	1	S-6(T)	99,12	Archaea;Euryarchaeota;Methanomicrobia;Methanosarcinales;Methanosarcinaceae;Methanosarcina
>Clone 52500_Consensus	53,8	Methanosarcina mazei	1	S-6(T)	100	Archaea;Euryarchaeota;Methanomicrobia;Methanosarcinales;Methanosarcinaceae;Methanosarcina
>Clone 52337_Consensus	53,8	Methanosarcina mazei	1	S-6(T)	99,75	Archaea;Euryarchaeota;Methanomicrobia;Methanosarcinales;Methanosarcinaceae;Methanosarcina
>Clone 52315_Consensus	53,8	Methanosarcina mazei	1	S-6(T)	99,87	Archaea;Euryarchaeota;Methanomicrobia;Methanosarcinales;Methanosarcinaceae;Methanosarcina
>Clone 52294_Consensus	53,8	Methanosarcina mazei	1	S-6(T)	99,75	Archaea;Euryarchaeota;Methanomicrobia;Methanosarcinales;Methanosarcinaceae;Methanosarcina
>Clone 52283_Consensus	53,8	Methanosarcina mazei	1	S-6(T)	99,87	Archaea;Euryarchaeota;Methanomicrobia;Methanosarcinales;Methanosarcinaceae;Methanosarcina
>Clone 52379_Consensus	100	Paracoccus solventivorans	1	DSM 6637(T)	98,91	Bacteria;Proteobacteria;Alphaproteobacteria;Rhodobacterales;Rhodobacteraceae;Paracoccus

>Clone 52462_Consensus	100	Proteiniaclicu m ruminis	1	D3RC-2(T)	99,24	Bacteria;Firmicutes;Clostridia;Clostridiales;Clostridiaceae;Proteiniaclicum
>Clone 52424_Consensus	100	Sphaerochaeta associata	-	GLS2(T)	99,86	Bacteria;Spirochaetes;Spirochaetes_c;Spirochaetales;Spirochaetales;Sphaerochaeta
>Clone 52373_Consensus	100	Sphaerochaeta associata	-	GLS2(T)	99,73	Bacteria;Spirochaetes;Spirochaetes_c;Spirochaetales;Spirochaetales;Sphaerochaeta
>Clone 52372_Consensus	100	Streptococcus lutetiensis	2	CIP 106849(T)	99,86	Bacteria;Firmicutes;Bacilli;Lactobacillales;Streptococaceae;Streptococcus
>Clone 52434_Consensus	100	Vagococcus acidifermentans	1	AC-1(T)	99,72	Bacteria;Firmicutes;Bacilli;Lactobacillales;Enterococaceae;Vagococcus
Bacterial Isolates: Isolates with at least 98,65% similarity to valid species names						
>A4-10	91.8	Corynebacteriu m freneyi	2	ISPB 6695110(T)	99,17	Bacteria;Actinobacteria;Actinobacteria_c;Corynebacteriales;Corynebacteriaceae;Corynebacterium
>A4-6	90.5	Enterococcus asini	1	ATCC 700915(T)	99,78	Bacteria;Firmicutes;Bacilli;Lactobacillales;Enterococaceae;Enterococcus
>B6-2	93.7	Enterococcus gallinarum	2 ht	NBRC 100675(T)	99,86	Bacteria;Firmicutes;Bacilli;Lactobacillales;Enterococaceae;Enterococcus
>A4-6	91.6	Enterococcus mundtii	1+	DSM 4838(T)	99,93	Bacteria;Firmicutes;Bacilli;Lactobacillales;Enterococaceae;Enterococcus
>A4-8	93.5	Escherichia hermannii	2	GTC 347(T)	99,85	Bacteria;Proteobacteria;Gammaproteobacteria;Enterobacteriales;Enterobacteriaceae;Escherichia
>A4-2	93	Escherichia marmotae	-	HT073016(T)	99,41	Bacteria;Proteobacteria;Gammaproteobacteria;Enterobacteriales;Enterobacteriaceae;Escherichia
>B1-4	94.2	Lactococcus garvieae subsp. garvieae	2 ht	ATCC 49156(T)	100	Bacteria;Firmicutes;Bacilli;Lactobacillales;Streptococaceae;Lactococcus;Lactococcus garvieae
>B4-7	93,2	Proteus mirabilis	2 ht	ATCC 29906(T)	100	Bacteria;Proteobacteria;Gammaproteobacteria;Enterobacteriales;Enterobacteriaceae;Proteus
>A4-9	93,1	Pseudomonas formosensis	1	CC-CY503(T)	100	Bacteria;Proteobacteria;Gammaproteobacteria;Pseudomonadales;Pseudomonadaceae;Pseudomonas

Warm and wet: robust lipase-producing bacteria from the indoor environment

Kristie Tanner^{†1}, Christian Abendroth^{†1,2}, Manuel Porcar^{*1,5}

¹Institute for Integrative Systems Biology (I2SysBio, Universitat de València-CSIC), 46020 València, Spain. ²Robert Boyle Institute e.V., Im Steinfeld 10, 07751 Jena, Germany ³Darwin Bioprospecting Excellence, S.L. Parc Científic Universitat de València C/ Catedrático Agustín Escardino Benlloch, 9

16S-rRNA amplicons: Sequences were submitted to NCBI and can be accessed online:

<http://www.ncbi.nlm.nih.gov/biosample/7606431>

<http://www.ncbi.nlm.nih.gov/biosample/7606432>

Appendix C

Metrics

6

Number of indexed publications

14

Highest number of citations

18

Highest altmetric score

4629

Highest number of accesses

4

Q1-articles

5.7

Highest impact factor

TABLE. C1: Metrics of published articles (According to the information from the respective journal homepages)

Publication	Article Aceses	Citations	Altmetric Score
Publication1	3,690	14	5
Publication2	977	0	7
Publication3	4,629	2	3
Publication4	27	2	1
Publication5	-	-	-
Publication6	-	-	-
Publication7	696	-	18

TABLE. C2: Impact factors 2016 (<https://jcr.incites.thomsonreuters.com>).

Journal	Impact Factor
Bioresource Technology	5.651
Biotechnology for Biofuels	5.203
PLoS ONE	2.806
Waste Management & Research	1.803
Genome Announcements	-
BioRxiv	-